The assessment of proton MRS as a biomarker for Huntington disease

Thesis submitted for the degree of

Doctor of Medicine (Research)

Aaron Sturrock

UCL

Institute of Neurology

2014

I dedicate this work to the loving memory of my mother,

Anita Sturrock (22nd May 1949 – 19th July 2011),

whom was, and remains, my inspiration.

Declaration statement

I, Aaron Sturrock, confirm that the work presented in this thesis is my own. Where information has been derived from other sources, I confirm that this has been indicated in the thesis and acknowledgements.

Aaron Sturrock

Abstract

The development of effective therapies for Huntington disease will require the identification of reproducible and objective markers of disease progression and abrogation. Magnetic Resonance Spectroscopy (MRS), a method of measuring brain metabolism within a specified region of interest, has shown potential as one such biomarker modality.

Presented is work that demonstrates that putaminal MRS is an important biomarker modality, specifically in the context of clinical trials. At all time-points N-acetyl aspartate (NAA) and total NAA (tNAA), neuronal integrity markers, were lower in early manifest HD than control subjects. tNAA was consistently lower in pre-manifest HD than Controls. The gliosis marker, myo-inositol (mI), was robustly elevated in Early HD. Metabolites showed no longitudinal change for any group over 24 months. While motor assessments were better longitudinal measures of disease progression, the robustness of tNAA permitted development of a model in which this metabolite is an outcome measure for future clinical trials. Thus, if one were to test a therapeutic with efficacy to partially normalise tNAA based on the difference between Control vs. Early HD, around 350 or 52 subjects (split between two treatment arms) would be required depending on whether 20% or 50% normalization of tNAA levels are expected.

Brain metabolites most consistently correlated with disease burden but less so with motor phenotype. Direct and indirect evaluations of gliosis markers in

biosamples were performed based on spectroscopic findings, and these suggested significant biomarker potential for the oxidation product lipid peroxidase (LPO).

MRS demonstrates robust and consistent group metabolite differences in HD-affected individuals that correlate with disease burden. This modality has potential utility as an outcome measure for future therapeutic trials in HD, and furthermore may be useful in identifying novel biosample markers of disease.

Contents

Figures

Tables

Problem and Aims

Huntington Disease (HD) is the most common inherited neurodegenerative condition. While there is, at present, no disease-modifying treatment for this uniformly fatal disease, identifying such an agent is the intensifying focus of the work of many, international, research groups. In this search, one potential advantage over other neurodegenerative conditions is the ability to predict the development of disease in asymptomatic individuals through predictive genetic testing. This offers the theoretical possibility of halting pathophysiological processes before the outward manifestation of disease.

However, the ability to identify a disease-modifying agent will depend upon the identification of a readily quantifiable biological marker able to measure progression and abrogation of the disease process. This situation is made more difficult by the multi-faceted nature of this disease, since HD evolves as a complex phenotype comprising motor, cognitive, behavioural and psychiatric components that can vary from individual to individual. The absence of definitive, quantitative, and objective measures against which to assess therapeutic efficacy requires studies to be longer and involve more participants to be appropriately powered. The delineation of appropriate biomarkers has been the focus of a number of multicenter, longitudinal observational studies of HD.

A number of imaging modalities have been, and continue to be investigated for their biomarker potential including volumetric MRI, Positron Emission

Tomography (PET), functional MRI (fMRI), and Diffusion Tractographic Imaging (DTI). One putative imaging marker, Proton Magnetic Resonance Spectroscopy (MRS) has been evaluated in smaller cohorts, with mixed results. Yet this modality offers a number of advantages over other modalities. Since it is a metabolite measure, it can conceivably measure biochemical changes at the molecular level, when neurons are still relatively intact, with significant tissue loss yet to occur. Thus, while the utility of MRS as an HD biomarker is unclear, its delineation is of great importance not least because the *in vivo* quantification of brain metabolites may also elucidate additional, biosample correlates that may be easily and peripherally measurable, for example in blood or CSF. In view of this, MRS will form the focus of study in this thesis. Clearly the development of a biomarker measure that displays a clear relationship with physical or motor dysfunction has clear advantages, in terms of a clinically meaningful correlate for metabolite alteration. Hence, this association will be evaluated among the experiments described here.

In order to adequately power therapeutic trials in HD, it is vital that any metabolite measure is robust and reliably measurable with low variance. Lower variance in metabolite estimations maximises effect size, in turn reducing the subject numbers sampled in order to demonstrate efficacy of a medication and hence trial cost and duration. In this thesis, the cross-sectional and longitudinal biomarker sensitivity of MRS will be considered together with an assessment of the likely most useful metabolites to take forward into clinical trials.

Aims

To investigate the potential value of brain metabolites, readily measurable by Proton MRS, as measures of disease progression and therapeutic efficacy in HD by;

1. Examining the role of Proton MRS as a cross-sectional and longitudinal biomarker for HD using higher, 3T, field strengths.
2. Using MRS to assess the association between brain metabolites and both disease burden and robust measures of clinical motor phenotypic progression.
3. Estimating the number of subjects necessary to detect disease-modification in future therapeutic trials of candidate drugs, using brain metabolites as a marker of disease state.
4. Using MRS to attempt to identify novel peripheral biosample biomarker candidates.

1 Biomarkers in Huntington disease

1.1 Introduction

Huntington disease (HD) is a dominantly inherited disorder that results from a CAG trinucleotide expansion within the huntingtin (*HTT)* gene. With a prevalence of around 3-7/100,000 among Western populations, it is the most common hereditary neurodegenerative disorder. Both genders are equally affected and age at clinical diagnosis is usually in the fourth to fifth decades. As an autosomal dominant disorder, there is a 50% risk of inheritance for each child of an affected individual. Following identification of the HD gene locus on the short arm of chromosome 4, and linkage to a DNA marker in 1983 (Gusella et al. 1983), linkage analysis permitted the practice of predictive testing, or the testing of an asymptomatic individual for the presence of the abnormal gene. This was an entirely novel endeavour in medicine. The subsequent elucidation of the causative gene defect in 1993 (Huntington Disease Collaborative Research Group 1993), has since refined confirmatory and predictive testing making it more efficient and economical, but also allowing pre-implantation genetic testing.

'Pre-symptomatic', or 'asymptomatic' individuals, often referred to as 'pre-manifest HD' individuals, will develop subtle, progressive deficits; both clinical and pathophysiological, which accumulate and portend the diagnosis of HD. The clinical disease is often characterised as the triad of movement disorder, dementia, and behavioural or psychiatric disturbance, although the degree to which each of

these aspects manifests varies greatly between individuals. HD has a devastating impact on individuals and multiple generations within families. It affects all arenas of life from the loss of financial and functional independence to uncertainty for the future and guilt associated with potential genetic transmission. The progressive disability is associated with significant personal and socioeconomic burdens for both individual and healthcare services. Sadly, death usually occurs around 15 to 18 years after diagnosis in adult cases, often secondary to sepsis, and there is no therapeutic agent that has been shown to modify the disease course.

A major obstacle to the development of an effective therapy with which to abrogate the disease course is the lack of a reliable, validated biological marker and hence the ability to objectively track progression and abrogation of the disease process. The clinically multi-faceted, phenotypically heterogeneous, and sometimes unpredictably evolving nature of the disease challenge the identification of a simple linear clinical measure of progression. Nevertheless many clinical measures especially cognitive and motor measures are the subject of ongoing scrutiny, and some have shown significant biomarker potential (Paulsen et al. 2008, Tabrizi et al. 2012). “Wet” biomarkers, the measure of metabolites in biological samples overcome issues pertaining to phenotypic variability, examiner/reporter biases and a number of metabolites have shown great promise but these are also subject to other confounders including concomitant medication usage, issues pertaining to reproducibility, circadian rhythm and comorbidity. The third major biomarker modality - imaging biomarkers - while not without their

limitations may represent the most sensitive measures of disease progression in HD (Tabrizi et al. 2012).

Magnetic Resonance Imaging (MRI) is a powerful and reproducible biomarker tool that harnesses the properties of hydrogen containing molecules within tissues to identify pathological change. Most commonly it is used in volumetric quantification of HD related brain atrophy, but other biomarker roles exist including Magnetic Resonance Spectroscopy (MRS). MRS has been relatively under-examined as an HD biomarker, with only a few reported studies and generally with limited subject numbers. Yet MRS offers benefits unrealized with volumetric and other imaging measures, including the ability to indirectly measure subcellular pathophysiological changes *in vivo*. Since such change can be demonstrated in the grossly normal HD brain at post mortem (Vonsattel et al. 1998), MRS conceivably offers unique insight into initial changes in the HD brain. In support of this, spectroscopic changes have been reported at an early stage in the pre-manifest HD brain (Sanchez-Pernaute et al. 1999, Gomez-Anson et al. 2007). However subsequent studies with methodological differences have failed to reproduce these findings, casting uncertainty over the future use of this modality (Reynolds et al. 2005, van Oostrom et al. 2007). In this thesis all three of the major biomarker classes will be investigated with a view to assessing the biomarker role for MRS in HD, and the potential insights into novel putative markers that it might provide.

In the first two chapters the disease, its presentation, and pathogenesis will firstly

be considered in some detail. Since all three biomarker modalities will be relevant to this thesis, the field of HD biomarkers – clinical, biological and imaging - will then be comprehensively reviewed to examine their relative importance to defining clinical outcomes for therapeutic trials and provide a context for the investigations presented herein.

1.2 Huntington disease

1.2.1 Historical background

Although the first documented description of an inherited cause for chorea was in 1832, chorea had been identified as a potential manifestation of neurological disease in the early 16th Century (Hayden 1981). Despite the publication of earlier case reports in several languages, it was George Huntington's accurate and insightful description in 1872, which led to widespread recognition of the inherited chorea that now bears his name (Huntington 1872). Since that time a number of notable milestones have marked the progress of our understanding of this disorder including the mapping of the chromosomal localization of the Huntington disease (HD) mutation in 1983, identification in 1993 of the causative HTT gene mutation (Huntington's Disease Collaborative Research Group 1993) and the generation of the first transgenic HD mouse models in the late 1990s. Regardless of this evolution in our knowledge, many fundamental questions regarding HD pathogenesis remain unclear and an effective disease modifying therapy is yet to be identified for this devastating disorder.

1.2.2 The genetic basis of HD

HD is an autosomal dominant, progressive neurodegenerative disorder caused by an expanded trinucleotide CAG sequence in exon 1 of the huntingtin gene (*HTT*) encoding a stretch of glutamines in the huntingtin protein. It is expressed with nearly full penetrance. The protein huntingtin is ubiquitously expressed in most tissues, however, the polyglutamine repeat expansion in HD leads to relatively

selective neuronal cell death in the striatum and cortex. There is currently no known cure for this devastating neurodegenerative disease that is characterised by the development of progressive motor dysfunction, cognitive decline, and psychiatric disturbances (Huntington 1872, Nance 1998, Sturrock & Leavitt, 2010). CAG repeat length inversely correlates with age of disease onset in HD (Langbehn et al. 2004, Langbehn et al. 2010). Disease onset is most commonly around the mid-40's, although along with the rate of progression, and severity of clinical features, this can vary markedly between individuals. The clinical diagnosis of HD is usually made based on the presence of an otherwise unexplained extrapyramidal movement disorder in an at-risk individual.

1.2.3 Prevalence of HD

Among populations of European descent the prevalence of HD is between about 3 and 7 cases per 100 000 (Bates et al. 2002) and may remain relatively stable between generations (Pearson et al. 1955, Reed et al. 1958, Folstein et al. 1987). The prevalence of disease is lower in Chinese and black African populations and among the Japanese the prevalence is estimated at below 0.38 cases/100,000 population (Bates et al. 2002). Interestingly, the rare HD phenocopy Huntington Disease-Like 2 or HDL-2 has a prevalence comparable to HD among black South Africans (Kraus et al. 2002, Magazi et al. 2008). Certain higher prevalence HD populations have also been identified in which disease prevalence exceeds 15/100 000. One explanation for differential population prevalence is a founder effect seen in small geographically isolated regions, for example among the inhabitants of the

Lake Maracaibo region of Venezuela (Wexler et al. 2004). Alternatively, certain alleles predisposing to disease in successive generations may be more prevalent among certain ethnic groups (Warby et al. 2009, Fisher & Hayden, 2013).

1.3 Clinical features of HD

The clinical features of HD usually comprise some variation on the triad of movement disorder, cognitive dysfunction, and psychiatric or behavioural disturbance. The nature of each of these features, and their severity can vary markedly between individuals. Traditionally the clinical diagnosis of HD has rested on the confirmation by neurologic examination of an otherwise unexplained extrapyramidal movement disorder in an individual with a family history of HD or HD genetic diagnosis. The motor phenotype is usually assessed in manifest HD using the motor component of the Unified Huntington Disease Rating Scale (UHDRS-99). The UHDRS is a widely used clinical and research tool developed by the Huntington Study Group (HSG) for the measurement of the motor, cognitive, psychiatric, and functional performance in HD (Huntington Study Group, 1999). For clinical research purposes, the confirmation of HD diagnosis generally needs to be made with 99% certainty by an experienced HD clinician, in an individual who has tested positive for the causative *HTT* gene defect. It should be noted that in addition to the classic triad, a number of other clinical features have been described in HD and these will also be considered.

1.3.1 Pre-manifest HD

There is now incontrovertible evidence that subtle or ‘‘soft’’ motor, cognitive and psychiatric disturbances occur many years before the onset of clinically diagnosable HD (Penney et al. 1990, Paulsen et al. 2008, Tabrizi et al. 2009). While these individuals are often described as pre-symptomatic or pre-manifest, it has been proposed that ‘‘pre-diagnostic HD’’ may be a more appropriate term, given that among these gene-carriers will be those with the presence of subtle clinical features, those that have clinical features consistent with a diagnosis, but have not yet been diagnosed, in addition to genuinely asymptomatic individuals (Walker 2007). In the pre-manifest period, the appearance of ‘‘soft’’ motor, cognitive, and psychiatric or behavioral abnormalities may first attract the attention of a spouse or work colleagues rather than the affected individual. Potential issues may include altered executive function, or psychomotor processing leading to slower work performance. The spouse may notice an increase in fidgetiness or ‘‘twitches.’’ At clinical examination common findings in pre-manifest HD individuals may include mild oculomotor abnormalities, including increased saccadic latency. Minimal chorea or subtle hyperkinetic movements may also be an intermittent feature, often distally in the limbs. The motor features insidiously worsen until eventually the phenotype is sufficient to make the diagnosis.

1.3.2 Motor phenotype in HD

The HD motor phenotype in HD can be separated into involuntary and voluntary movement disorders (Nance 1998). The involuntary movement disorder usually

follows a biphasic pattern. Initial hyperkinetic movements first increase before gradually diminishing as bradykinesia and rigidity begin to predominate, eventually leading to severe hypokinesia and a rigid-akinetic state. Chorea, from the Greek ‘‘to dance,’’ refers to the rapid, jerky movements of limbs, trunk, and face that characterizes the hyperkinetic HD movement disorder in the majority of cases. Chorea is common in early HD and generally worsens in the mid-stages of disease. For most, as the disease progresses rigidity becomes more pronounced and often choreiform movements wane. Impairments in voluntary movement are also inexorably progressive. Manifesting as ataxia initially, mobility is progressively lost ultimately leaving the individual non-ambulatory. Slow and jerky ocular pursuit and increased saccadic latency eventually progress to a complete supranuclear gaze palsy (Quinn & Schrag, 1998). Deteriorating dysarthria and dysphagia reflect both impaired voluntary control, and worsening involuntary bucco-oro-lingual movements. Deficits in fine motor control first noticed as mild handwriting impairments, deteriorate to a point where the individual has minimal volitional control over limb movements.

1.3.3 Cognitive phenotype in HD

Prior to clinical diagnosis, it is not unusual for individuals to manifest modest cognitive deficits. These may be reported by the individual, despite the absence of any noticeable abnormality on global clinical cognitive measures. The nature of the progressive cognitive disorder in HD is ‘‘frontal-subcortical’’ and emerges early in the disease. This subcortical dementia, impairs both procedural memory and

visuospatial memory, although it appears that memory recall rather than memory storage that is primarily affected (Butters et al. 1985). Attention and concentration are affected early, leading to easy distractability (Pillon et al. 1991). Executive dysfunction in HD is also manifest through impaired behavioural regulation, organisational ability and judgement with individuals often lacking awareness of their disabilities. Cognitive deficits are progressive in HD—yet certain cognitive domains, for example those related to language function, are preserved until late in the disease course with dysarthria and later mutism being responsible for the speech disorder in HD.

1.3.4 Psychiatric phenotype in HD

The psychiatric manifestations of HD are the most variable aspect of the HD clinical phenotype. Depression, irritability, and impulsivity are the most common psychiatric features, but psychiatric presentations may be protean. Obsessive-compulsive and aggressive behaviours, psychosis, mania, anxiety, suicide and substance abuse can also occur. Individuals with pre-manifest HD both near and far from predicted disease onset exhibit a greater prevalence of subtle psychiatric disturbances than controls (Duff et al. 2007). These alterations fall below thresholds for clinical diagnosis but include increased scores on scales of depression, obsessive–compulsiveness, anxiety, and psychoticism. Interestingly, these subclinical features may be present among individuals more than 10 years from predicted disease onset (Duff et al. 2007). A significant concern in HD, major depression may have a lifetime prevalence of up to 40%, whereas the prevalence

of subsyndromal depression is probably higher at around 35% to 60% (Shiwach et al. 1994, Craufurd et al. 2001, Paulsen et al. 2001). In addition to developing the biological substrate for depression, individuals with HD find themselves coping with a number of situational stressors that can only exacerbate the mood disorder. Fear for the future, loss of employment, and altered family dynamics and relationships are all real concerns for the individual.

1.3.5 Other clinical features of HD

HD is associated with a number of other, poorly understood, clinical manifestations. Weight loss is a common feature in the later stages of HD. It occurs despite an increased appetite and higher calorific intake than controls (Morales et al. 1989) and while the hyperkinetic movement disorder in HD likely contributes (Pratley et al. 2000), metabolic profiling has identified a pro-catabolic phenotype in these patients (Underwood et al. 2006). Further support for a negative energy balance in HD is suggested by the demonstration of high levels of orexigenic hormones and low levels of the adipocyte hormone leptin in HD affected individuals (Popovic et al. 2004), a pattern that is recognized in catabolic states. Following the identification of testicular degeneration in transgenic HD mice (Leavitt et al. 2001), reduction in germ cells and abnormal seminiferous tubule morphology was identified in patients with HD and appears to be a toxic effect of mutant huntingtin (Van Raamsdonk et al. 2007). This phenotype likely develops later in life, since male fertility is unaffected in HD (Mastromauro et al. 1989). Sleep disturbances have been reported in advanced HD and include fragmentation

of sleep and reversal of the sleep-wake cycle (Hansotia et al. 1985, Morton et al. 2005). It is unclear as to the etiology of these disturbances but in transgenic HD mice alterations in hypothalamic orexin neurons correlates with narcoleptic episodes (Petersen et al. 2005).

1.3.6 Clinical disease progression in HD

As already discussed, individuals carrying the causative HD gene mutation will eventually make a transition from being completely asymptomatic to a period in which ‘‘soft’’ motor, psychiatric, and cognitive symptoms emerge. This pre-manifest stage involves insidious progression of soft signs and symptoms over a prolonged period of time that eventually culminates in the development of clinically diagnosable HD. The diagnosis of an HD motor phenotype (with 99% confidence) does not rest on the presence of a specific motor symptom or sign but rather a constellation of motor features. The average age of disease onset is between 35 and 44 years (Bates et al. 2002), but the clinical diagnosis has been made in infancy and in individuals as old as 90 years (Dennhardt & LeDoux, 2010). However, there is some variation in disease duration with some families exhibiting a slower rate of disease progression and longer survival. In advanced stages of HD, the individual is usually akinetic, mute, and fully dependent. The cause of death is recognisable infection in about 45% of cases, with ‘‘nonspecific’’ causes in a further 41% (Nance & Sanders 1996). Pneumonia may be responsible for around 25% of deaths in HD (National Huntington Research Roster 1998).

1.4 Pathophysiology in HD

1.4.1 The pathology of HD

Pathologically, a selective pattern of brain atrophy and neurodegeneration is observed in HD. The cardinal HD feature is early neostriatal atrophy. The neostriatum comprises the caudate and putamen, but of these structures the caudate is preferentially affected (Vonsattel et al. 1985). As the disease progresses, the atrophy becomes less selective with the whole brain ultimately appearing atrophic and brain weight reduced by up to 300g (Mann et al. 1993). Although neurodegeneration becomes less specific with disease progression, the cerebellum remains relatively invulnerable to mutant huntingtin-mediated neuronal damage (Vonsattel et al. 1998). Vonsattel and colleagues developed a widely used scale for the grading of striatal neuropathology in HD. The scale consists of 5 grades from 0 (no gross pathological abnormality) to 4 (severe pathology) and correlates strongly with physical disability at death (Vonsattel et al. 1985). Further attempted correlations between pathology and phenotype have inevitably been impacted by the relative paucity of pre-manifest and early HD cases undergoing postmortem. Imaging advances have recently helped mitigate this gap in our knowledge. Imaging studies suggest that as early as 15 years prior to the onset of a motor diagnosis, there is already evidence of striatal, cortical, thalamic, and white matter atrophy on magnetic resonance imaging (MRI) (Rosas et al. 2005, Paulsen et al. 2010) suggesting that in addition to the neostriatum, a number of brain regions are also particularly vulnerable early in the disease course. Imaging has also revealed

insights into genotype-pathology correlations. A recent Voxel-Based Morphometry (VBM) study in adults showed that increased CAG-repeat length was associated with more extensive striatal and extrastriatal atrophy after controlling for age in pre-manifest and early HD gene carriers (Henley et al. 2009).

Neuropathologic studies have suggested that neuronal loss within the neostriatum at the microscopic level, occurs early, and may predate the development of gross striatal atrophy. Indeed, 30 to 40% loss of caudate neurons may have occurred in the macroscopically normal brain. Loss of caudate neurons occurs in a dorsocaudal to rostroventral gradient, with the most rostral part of the caudate exhibiting the least neuronal loss (Vonsattel et al. 1985).

Neuronal loss in HD is relatively selective for the most abundant striatal cell type: the medium-spiny neuron (MSN). These cells comprise 2 subpopulations: MSN expressing γ-aminobutyric acid (GABA) and enkephalin and those expressing GABA and substance P (Kowall et al. 1987). Both cell types independently play a role in the biphasic motor phenotype associated with classical adult HD, (Reiner et al. 1988, Albin et al. 1990, Richfield et al. 1995, Sapp et al. 1995) whereas by contrast most striatal interneuron populations remain relatively preserved (Ferrante et al. 1980, Dawbarn et al. 1985, Ferrante et al. 1987).

1.4.2 Pathophysiology of HD

Identification of macroaggregates of the mutant huntingtin protein in nuclear and cytoplasmic inclusions in the first transgenic mouse models led to the suggestion that pathogenesis in HD was directly attributable to these neuronal intranuclear inclusions (NIIs) (Davies et al. 1997). However, the pathogenic role of these aggregates is now debated. Saudou's group showed that suppressing inclusion formation resulted in increased mutant huntingtin-induced cell death (Saudou et al. 1998). Furthermore, in single neuron cultures expressing mutant huntingtin, NIIs were shown not to be sufficient, or required, to cause cell death and may actually prolong cell survival (Arrasate et al. 2004).

The suggestion that mutant huntingtin may exert pleiotropic effects on multiple putative pathogenic mechanisms in HD has been a major research theme in HD (Aronin et al. 1999). Deficient transcription of genes involved in synaptic transmission, signal transduction, and calcium homeostasis have been identified in HD mice (Cha et al. 1999, Cha 2000, Luthi-Carter et al. 2000). Of particular note is the altered transcription of genes participating in N-methyl-D-aspartate receptor (NMDAR) signalling within the vulnerable population of striatal neurons in HD, which carries implications for the heightened sensitivity to NMDA receptor mediated toxicity associated with HD (Zucker et al. 2005). Axonal transport may also be defective in HD, with evidence supporting the altered trafficking of mitochondria potentially leading to impaired energy metabolism (Trushina et al. 2004).

McGeer and McGeer and Coyle and Schwarcz first suggested a role for excitotoxicity in HD pathogenesis after demonstrating selective neuronal degeneration following intrastriatal injection of kainic acid in rats (McGeer & McGeer 1976, Coyle & Schwarcz 1976). Subsequently, direct intrastriatal quinolinic acid (QA) injection in animal models was demonstrated to selectively activate NMDARs and generate an HD-specific pattern of neurodegeneration. Neurodegeneration in these models specifically targeted striatal MSN while preserving interneuron's (Beale et al. 1986, Sanberg et al. 1989, Hantraye et al. 1990, Ferrante et al. 1993). In rodents, 3-nitropropionic acid, an inhibitor of mitochondrial function, produced a similar neurodegenerative pattern that could be abrogated by pretreatment with an NMDAR antagonist (Beale et al. 1993, Greene et al. 1993). This strongly suggested that mitochondrial dysfunction may sensitize cells to NMDAR-mediated neuronal death. The concept of ''indirect excitotoxicity'' thus emerged (Albin et al. 1992, Beale et al. 1995, Peschanski et al. 2004). This theory suggests that at physiological levels of NMDAR activation, partially impaired energy metabolism may be sufficient to trigger excitotoxic cell death. Specifically, mitochondrial defects may provoke abnormal activation of NMDAR-associated calcium channels (Albin et al. 1992, Beale et al. 1995, Peschanski et al. 2004).

A dynamic, biphasic pattern of excitotoxic vulnerability in HD transgenic mice has been identified. Prior to development of an HD phenotype, during initiating disease

stages, mice exhibited heightened vulnerability to QA, whereas older, symptomatic mice had developed resistance to excitotoxic stress (Graham et al. 2009). Importantly, this dynamic excitotoxicity may necessitate varied therapeutic HD approaches depending on disease stage (Graham et al. 2009).

Mitochondria may play a role in aberrant excitotoxic pathways central to HD pathogenesis. *N*-methyl-D-aspartate receptor activation is associated with excessive increases in intracellular calcium (Cepeda et al. 2001, Zeron et al. 2002). Mitochondrial buffering of calcium alters the electrochemical gradient involved in adenosine triphosphate (ATP) production, impairing energy metabolism. Furthermore, the uptake of supraphysiological quantities of calcium ions may induce the mitochondrial permeability transition (mPT) pore, leading to release of mitochondrial contents and triggering the apoptotic death program (Beale 2005, Fernandes et al. 2007). Of note, mitochondria from human HD lymphoblasts exhibit an impaired buffering ability and a lower threshold for calcium-induced mPT formation (Panov et al. 2002). A further mitochondrial insult has been identified. The direct binding of expanded huntingtin protein to the outer mitochondrial membrane has been demonstrated and may directly stimulate mPT pore opening (Panov et al. 2002, Choo et al. 2004). Overall, a significant amount of evidence supports excitotoxicity and mitochondrial dysfunction as integral pathogenic mechanisms in HD. The early involvement of these mechanisms in the disease course suggests their primary roles in HD pathogenesis (Zeron et al. 2002, Panov et al. 2002).

The development of transgenic HD mice led to the observation that mice expressing N-terminal fragments of the transgene exhibited a more aggressive phenotype than full-length transgenic models (Mangiarini et al. 1996, Hodgson et al. 1999, Slow et al. 2003, Goldberg et al. 1996). This observation supported a previously demonstrated role for caspase-mediated cleavage of mutant huntingtin, which suggested a role for proteolytic cleavage in the generation of pathogenic N-terminal mutant huntingtin fragments that are potentially critical to neurodegeneration in HD (Goldberg et al. 1996). Indeed, mutation at the caspase 6 cleavage site in huntingtin prevented the development of neuropathology in mice carrying the full-length expanded human *HTT* transgene, suggesting that caspase-cleavage-mediated generation of an N-terminal expanded huntingtin fragment is a critical pathogenic step and may be a critical initiating event in the development of HD.

1.5 Biomarkers in HD

Due to the complexity of the HD clinical phenotype; the diversity of associated clinical features and the relatively slow progression of the disease, commonly used HD clinical rating scales such as the Unified Huntington's Disease Rating Scale (UHDRS) are subjective, often insensitive to subtle changes over short periods of time, and are potentially susceptible to bias and intra- and inter-rater variability (Henley et al. 2005). The relative absence of definitive, quantitative, and objective clinical trial measures or endpoints that follow disease progression in HD necessitates more protracted therapeutic studies and the involvement of greater subject numbers in order to be sufficiently powered. The identification of objective and quantitative biological markers (biomarkers) that can eventually be validated as clinical trial endpoints and are able to objectively determine disease onset and disease progression in early or even pre-manifest disease, will greatly facilitate the identification of new therapies that are able to alter disease course in HD.

Biomarkers can provide both trait (presence of the disease) and state (severity of the disease) information. Unlike many other neurological diseases, for example Parkinson's or Alzheimer's disease, there exists an excellent 'trait' biomarker for HD; the genetic test, which identifies individuals carrying the HD gene, signifying that they currently display or will predictably go on to display the clinical manifestations of the disease. However reliable 'state' biomarkers for HD; biologic measures sensitive enough to monitor the state of the disease in terms of overall progression, are lacking (Figure 1-1).

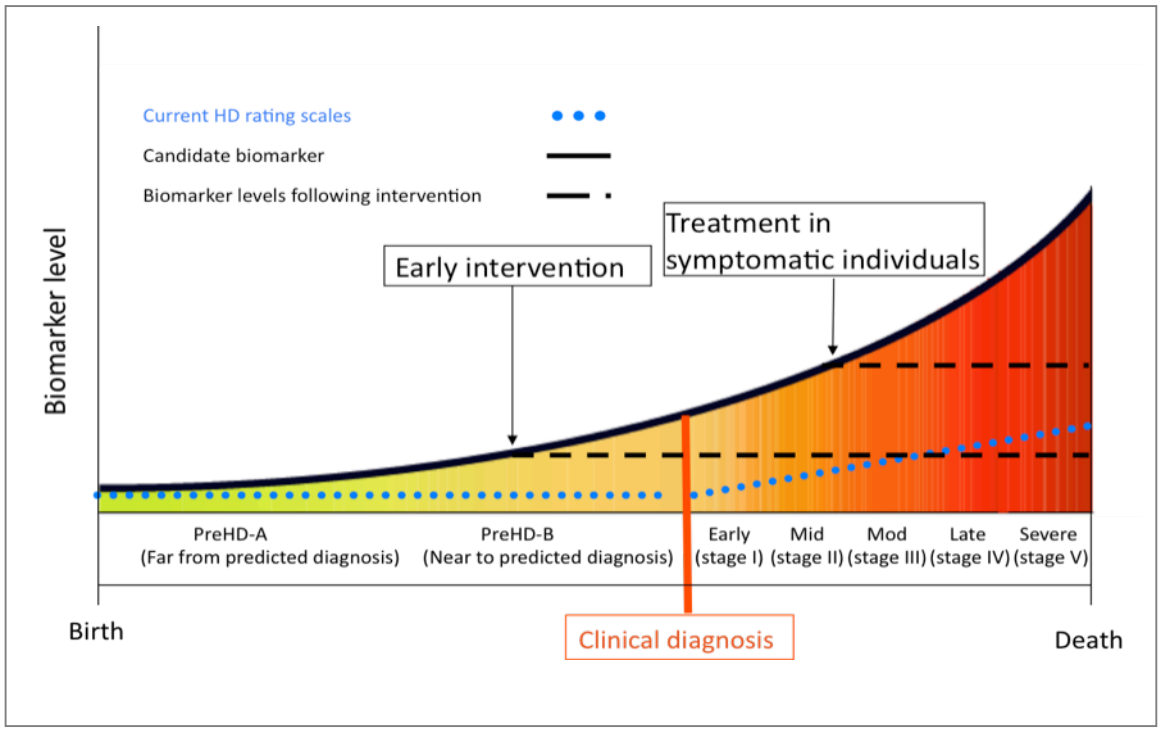

Figure 1-1 The ideal biomarker

1.5.1 The ideal 'state' biomarker

An ideal 'state' biomarker candidate should be readily quantifiable and reproducible. The biomarker measure should correlate reliably with disease progression. Additionally, the candidate biomarker should have low variability in the control population and not be affected by unrelated co-morbidities (Henley et al. 2005). Due to variability in the clinical phenotype of HD and potential confounding by environmental and pharmacological factors, it seems possible that a combination of different biomarkers may eventually be the most effective way to track HD progression and evaluate potential therapies. HD biomarker research includes both focused small scale studies of specific modalities and much larger

longitudinal observational studies such as PREDICT-HD (Paulsen et al. 2006) and TRACK-HD (Tabrizi et al. 2009), which aim to identify objective markers of disease progression using a range of experimental methodologies in large cohorts of pre-manifest gene carriers and HD patients.

1.5.2 The special case of identifying biomarkers in pre-manifest HD

The advent of predictive genetic testing has made it possible to identify and study expanded *HTT* gene carriers prior to disease onset. This has provided a unique window of opportunity, potentially decades, in which to study early mechanisms of the disease. The ability to identify individuals prior to disease onset makes a future in which HD progression is arrested before symptoms begin a possibility, though much work is still required.

To aid research within this population, attempts have been made to scale individuals using mathematical predictions of disease progression. For example, the disease burden score (DBS), a measure suggested to reflect the impact severity, or toxic load of the mutated HTT protein. Calculated using the formula [(CAG – 35.5) x age])(Penney et al. 1997), DBS is based on post mortem correlations between the degree of striatal atrophy, age at death and CAG length, where 35.5 was found to be the minimum repeat length for atrophy to be observed. Additionally, a number of models have been employed to estimate the years until onset in gene carriers, based on age and CAG length (see Langbehn et al. 2010 for review). However the potential confounds of using mathematical models to scale

subjects, particularly in cross sectional studies should be noted. Although one of the most frequently cited models (Langbehn et al. 2008), has recently been strengthened using longitudinal data from the PREDICT-HD study (Langbehn et al. 2010), the omission of genetic and environmental factors from the calculations, such as the age of onset in family members which may assist in the accuracy of predictions (Ranen et al. 1995), suggests a more conservative approach should be used. More specifically, for example, citing the probability of onset within 5 years rather than estimated years until onset. However such calculations do not provide any insight into the physiological processes nor clinical deterioration occurring in individuals leading to clinical diagnosis, emphasizing the need for measures to track changes and symptom development during this period.

1.6 Clinical biomarkers for HD

Clinical biomarkers refer to standardised clinical tests and rating scales that permit measurement of progression within different facets of the HD phenotype such as cognitive and motor function. They are generally inexpensive, usually simple to perform, readily applicable across assessment sites and rarely require sophisticated testing apparatus. Furthermore, they can provide neurobiological insights into, and better characterisation of, phenotypic variability in HD. The evaluation of predominantly clinical HD biomarkers is the focus of a number of large, multi-national, longitudinal observational studies in HD including: PREDICT-HD (n>1000), TRACK-HD (n=366), COHORT (n≈5000) and REGISTRY (n>7200) (Paulsen et al. 2006, Tabrizi et al. 2009, HSG website, EHDN network website). The ongoing Enroll-HD study is the largest natural history study in HD to date, and includes the merged subject pools of the COHORT and REGISTRY studies, as well as additional subjects from Central and South America (CHDI website).

The PREDICT-HD study is currently following the largest reported pre-manifest HD cohort in an attempt to identify biological predictors of disease onset and progression. Scrutiny of the full PREDICT-HD standardised cognitive battery, comprising 51 tasks, has led to the recognition of measures of psychomotor processing, emotion recognition and working memory as the most sensitive cognitive differentiators of pre-manifest individuals according to predicted time to disease onset (Stout et al. 2011). These tasks have formed the template for cognitive evaluation in subsequent studies, such as TRACK-HD (Paulsen et al. 2006,

Tabrizi et al. 2009). Cognitive tasks have now shown the ability to discriminate between controls, presymptomatic and manifest HD subjects in cross-sectional study (Johnson et al. 2007, Solomon et al. 2007, Tabrizi et al. 2009). Cross-sectional data from PREDICT-HD has identified consistent non-linear patterns of deteriorating motor and cognitive task performance beginning between ten to twenty years before predicted disease onset (Paulsen et al. 2008). Furthermore, positive correlations between deteriorating motor, cognitive and subclinical psychopathology scores were also found in this cohort (Paulsen et al. 2006, Duff et al. 2007). Longitudinal data at 24 months indicate that while a number of cognitive measures show significant decline in early HD compared to controls, only the indirect circle-tracing and negative emotion recognition tasks demonstrated significant change in pre-manifest individuals (Tabrizi et al. 2011) and thus longitudinal sensitivity of this group of tests may be a limitation of these particular analyses compared to other clinical biomarker modalities.

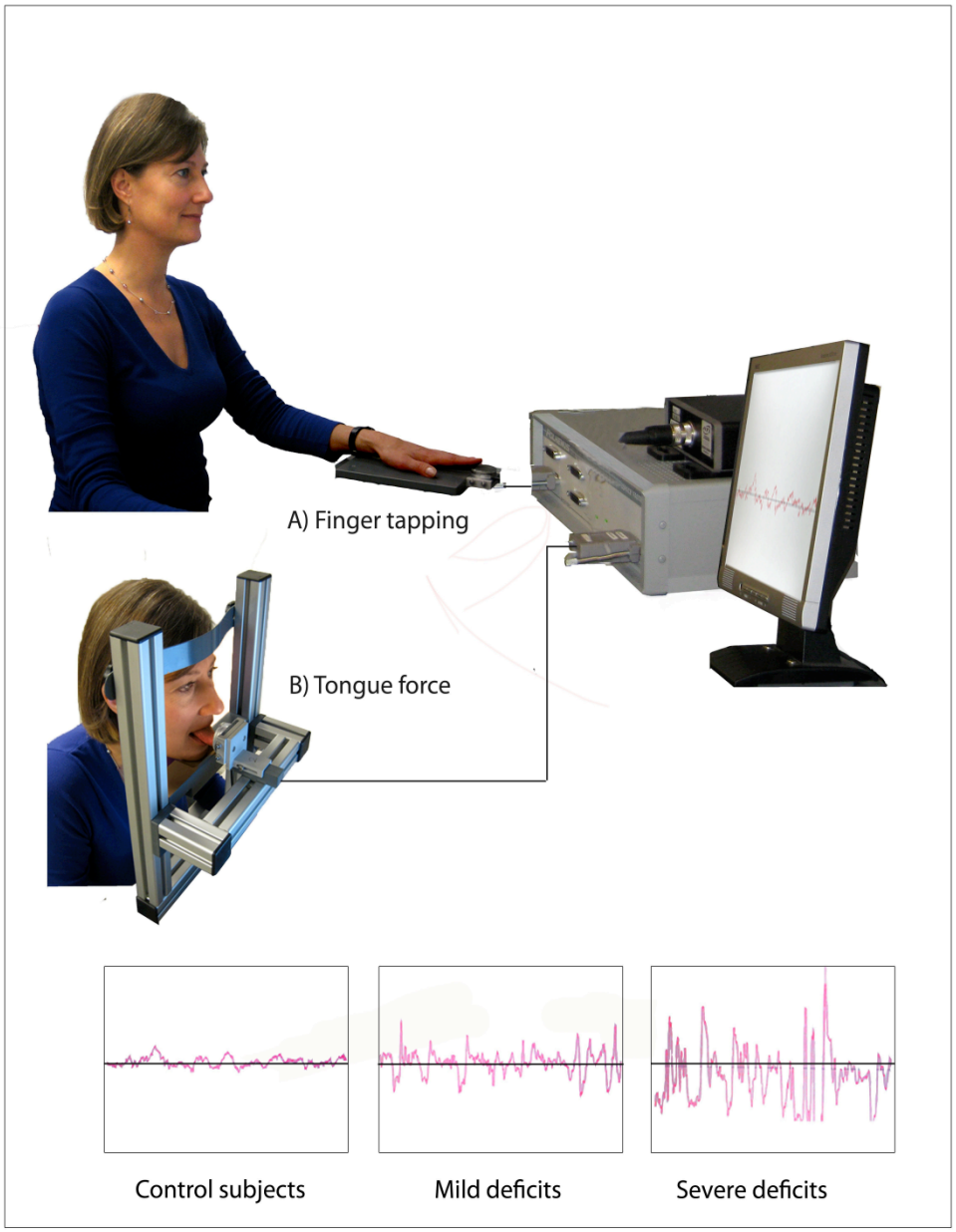

Figure 1-2 Quantitative Motor (QMotor) tasks. A) digitomotography (finger tapping tasks), B) glossomotography (tongue pressure tasks).

A unique aspect of TRACK-HD has been the adaptation of tasks comprising the motor section of the standard UHDRS assessment (such as tongue control, posturography and finger tapping) and their employment in an objective

quantitative motor battery that uses novel modular laboratory equipment (Figure 1-2). In cross-sectional analyses, these quantitative motor assessments have demonstrated excellent clinical sensitivity to differentiate subjects according to disease stage in the TRACK-HD study (Tabrizi et al. 2009, Reilmann et al. 2010, Bechtel et al. 2010). However, of quantitative motor evaluations, only the chorea position index showed significant change in both early manifest and pre-manifest groups vs. controls over one year. Over a longer, 24 months duration additional measures; speeded digitomotographic tasks and grip force variability were also able to identify phenotypic progression in pre-manifest HD subgroups in addition to among Early HD subgroups (Tabrizi et al. 2011, Tabrizi et al. 2012).

Confirmation of cognitive, motor and neuropsychiatric abnormalities in pre-manifest individuals (Paulsen et al. 2006, Duff et al. 2007, Paulsen et al. 2008, Tabrizi et al. 2009) reinforce the concept that the prodromal period, in which individuals maintain functional capacity despite the onset of neuronal dysfunction, represents the optimal window of opportunity in which to initiate disease-modifying therapy. Further longitudinal results from these studies of pre-manifest and early manifest disease are awaited with enthusiasm, and will be crucial to further clarifying the most sensitive measures of disease progression.

As phenotypic, rather than neuroimaging or biochemical measures, the progression or arrest of clinical endpoints in therapeutic trials have obvious functional implications for the individual. However, clinical biomarkers are not

without limitations. As such, they may exhibit limited ability to differentiate symptomatic improvement from modification of the disease course (Henley et al. 2005). A number of clinical measures are also self-reported for example, some behavioural/psychiatric and functional assessments, meaning that they are susceptible to reporter bias. Further, clinical biomarkers rarely provide basic insights into the underlying disease pathogenesis and the biological mechanisms underpinning phenotypic variability and disease progression; highlighting the need for additional non-clinical biomarker modalities. Notably, over 24 months neither cognitive nor quantitative motor markers of disease progression were as sensitive as corresponding structural imaging biomarker modalities, particularly to detect longitudinal change in pre-manifest HD (Tabrizi et al. 2011).

1.7 Biochemical biomarkers for HD

Another approach to biomarker identification involves the quantification of metabolites isolated from body fluid samples. The use of cerebrospinal fluid (CSF) for HD research is of great appeal due to its high concentration of brain specific proteins (Fang et al. 2009). However, the invasive lumbar puncture procedures required for sample collection make it less appealing in a wider clinical setting. Blood sampling is common in biomarker research, and has been used to identify abnormalities in both centrally and peripherally derived compounds. Studies of serum or plasma are among the most frequent due to the ease with which relatively large volumes can be obtained and the range of established analytical techniques available. However other blood components such as platelets, which have been suggested to resemble central neurons (Reilmann et al. 1994), leukocytes, erythrocytes, and the buffy coat have also been investigated as potentially exploitable biomarker resources. Despite the ease with which urine and saliva samples can be obtained, and their potential promise as marker resources, research using these materials has been very limited.

Biochemical biomarker studies generally comprise both: 1) candidate studies, involving the assay of pre-specified metabolites based on earlier experimental findings or hypotheses, and 2) non-hypothesis based exploratory studies, involving simultaneous measurement of large numbers of biochemicals in the hope of identifying a consistent abnormality are discussed below, with emphasis placed on potential markers of HD that may correlate with disease progression. Table 1-1

provides an overview of potential biochemical HD biomarkers studied in human subjects to date.

Category affected	**Biomarker candidate**
Endocrine function, metabolism and weight regulation	HPA axis (CRH, ACTH, Cortisol) HPG axis (GnRH, LH, FSH, testosterone, estrogen) GH, Ghrelin, leptin , CART, Orexin, Vasopressin,IGF-1 **Branch chain amino acids** Plasma: (Mochel et al. 2007)^{P,*}(Mochel et al 2011)^{P,*} Serum: (Underwood et al. 2006)
Immune response	TNF a, s100b, CRP, neopterin **IL-4,5, 6,8,10, 12, 23** Plasma: (Bjorkvist et al. 2008)$^{P,\#}$ (Dalrymple et al. 2007)$^{P,\#}$ **Clusterin** Plasma and CSF: (Dalrymple et al. 2007) $^{P,\#}$
Oxidative stress and antioxidants	8-OHdG, MDA, LPO, Lactate, kynurenines GPx, Cu/Zn-SOD, Uric acid, Creatine kinase
Homeostatic control and neuronal survival	TGF b, Adenosine A_{2A} receptors,AEA, FAAH **24hydroxycholesterol** Plasma: (Leoni et al. 2008) $^{P,\wedge,+}$ **Brain derived neurotrophic factor** Serum: (Ciammola et al. 2007)* (Squitieri et al. 2009) **Neurofilament** CSF: (Constantinescu et al. 2009)~
Neurotransmitter systems	Dopamine, Acetylcholine, GABA, Glutamate

Table 1-1 Summary of published HD biochemical biomarker candidates.

Previously studied compounds are classified into six general categories (endocrine function, metabolism and weight regulation; immune response; oxidative stress and antioxidants; homeostatic control and neuronal survival, and neurotransmitter systems) according to their association with system dysfunction in HD patients. The most promising candidates are shown in bold, with references displayed in brackets. NB. P= Study included pre-manifest subjects; # = difference found between subjects grouped according to UHDRS total functioning capacity (TFC) score; symbols indicate correlation found with * UHDRS motor scores, ~ TFC scores, ^ degree of

caudate atrophy , + probability of disease onset within 5 years in pre-manifest subjects. Abbreviations: HPA: hypothalamic pituitary adrenal, HPG: hypothalamic gonadal, GnRH: gonadotrophic releasing hormone, LH: Luteinizing hormone, FSH: follicle stimulating hormone, GH: Growth hormone, CART: cocaine and amphetamine regulated transcript, IGF: insulin likegrowth factor, TNF-α: tumour necrosis factor alpha, s100b: calcium binding protein s100b, CRP: c-reactive protein, IL: interleukin, CSF:cerebrospinal fluid, 8-OHdG: 8-hydroxydeoxyguanosine, MDA: malondialdehyde, LPO: lipid peroxidase, GPx : glutathione peroxidase, Cu/Zn SOD: copper zinc superoxidase, TGF-β : transforming growth factor beta, AEA: N-arachidonylethanolamine, FAAH: fatty acid amide hydrolase, GABA: gamma-amino butyric acid.

1.7.1 Endocrine function, metabolism and weight control

Often the discovery of disrupted organ or homeostatic systems in HD has been accompanied by the identification of novel, potential biomarkers. As such, reports of increased anxiety, stress and depression, led to study of the hypothalamic-pituitary-adrenal (HPA) axis, and findings of increased levels of cortisol and adrenocorticotropic hormone (ACTH) in HD plasma (Heuser et al. 1991, Saleh et al. 2009), serum(Leblhuber et al. 1995), and urine (Bjorkvist et al. 2006). In this case, other groups have failed to replicate these initial findings (Markianos et al 2007, Mochel et al. 2007). Investigations in the hypothalamic-pituitary-gonadal axis (HPG) have shown decreased plasma testosterone in male patients that inversely correlate with disease severity and degree of dementia (Markianos et al. 2005). However, other investigators failed to find any difference in plasma testosterone, luteinizing hormone (LH) or follicle stimulating hormone (FSH) in males (Saleh et al. 2009, Lavin et al. 1981), or androgen levels in females (Markianos et al. 2007).

Although endocrine function may be disrupted in HD, conflicting data regarding many of the implicated hormones has prevented their usage as biomarkers at this time.

Similarly, increased weight loss and alterations in metabolic state have fuelled research into mechanisms controlling such systems, presenting potential candidates such as leptin, growth hormone (GH), ghrelin, orexin, cocaine and amphetamine regulated transcript (CART), and branch chain amino acids (BCAA). Again, the evidence regarding many of these putative biomarkers is discrepant. Decreased leptin was reported in HD plasma (Popovic et al. 2004, Mochel et al. 2007), but not CSF (Popovic et al. 2004), although other groups reported finding normal plasma leptin levels in HD (Aziz et al. 2009a). Increased plasma levels of ghrelin (Popovic et al. 2004), and GH, associated with decreased UHDRS TFC and independence scores (Saleh et al. 2009) have been reported though (Popovic et al. 2004) contradicting reports of CSF (Popovic et al. 2004) and plasma (Murri et al. 1980, Aziz et al. 2009b) levels comparable to controls also appear in the literature. Insulin like growth factor (IGF-1), which is dependent on GH for secretion, has also been investigated. However, direct quantification of plasma IGF-1 has given variable results, with both reductions, negatively correlated with UHDRS scores (Mochel et al. 2007), and elevations, correlating with motor, functional and cognitive decline (Saleh et al. 2009) reported. Suggestions of a resistance to IGF-1in HD patients (Aziz et al. 2011), supported in part by findings of a decrease in levels of the IGF binding complex may help to explain such findings, however

further investigation is required. (Dalrymple et al. 2007, Mochel et al. 2007, Saleh et al. 2009). Levels of CART were elevated in HD CSF (Bjorkvist et al. 2006) though interestingly CSF levels of orexin, a biochemical involved in the sleep wake cycle that is thought to be disrupted in HD, were normal (Bjorkvist et al. 2006, Gaus et al. 2005, Meier et al. 2005). BCAA such as valine and leucine, have been found at decreased levels in plasma (Mochel et al. 2007, Mochel et al. 2011) and serum (Underwood et al. 2006) with differences seen between control, pre-manifest, and diagnosed HD patients, and were shown to correlate with weight loss, and negatively correlate with UHDRS scores and CAG repeat length. Despite dysregulation of weight control and normal metabolism in HD, contrasting or highly variable findings from many implicated metabolites limit their potential as state biomarkers. However, certain endocrine and metabolic markers, such as BCAA demonstrate promise and warrant further, longitudinal evaluation.

1.7.2 Oxidative stress and antioxidants

Mitochondrial dysfunction, impaired metabolism and increased oxidative stress, have been strongly implicated in the pathogenesis of HD (Browne et al. 1999, Stoy et al. 2005, Browne & Beale 2006, Chen et al. 2007, Klepac et al. 2007, Duran et al. 2010). Increased levels of 8-hydroxy-2-deoxyguanosine (8OHdG), an indicator of oxidative DNA injury, has been observed in HD serum (Hersch et al. 2006) and leukocytes (Chen et al. 2007) but longitudinal analyses are needed and are currently underway in HD samples from TRACK-HD. More recent data from the PREDICT-HD study has now suggested that blood measures of this marker may be

able to differentiate pre-manifest individuals by duration to disease onset, and that annualized rate of increase metabolite is greatest among those closest to predicted onset of disease (Long et al. 2012). Similarly, HD associated elevations of plasma lipid peroxide (Klepac et al. 2007, Duran et al. 2010), 4-hydroxynoneal (Stoy et al. 2005) and malondialdehyde (MDA) (Browne et al. 1999, Stoy et al. 2005); the latter of which correlated with UHDRS motor scores (Chen et al. 2007), also support a pathogenic role for oxidative stress in HD. While increased levels of iron and the iron transport protein ferritin, have been linked to oxidative stress in other neurodegenerative diseases (Rivera-Manci et al. 2010), normal serum iron despite significantly lower ferritin concentrations has been reported in HD serum (Bonilla et al. 1991). Oxidative stress generated by metabolites from the kynurenine pathway of tryptophan degradation have also been implicated in HD (see Schwarcz et al. 2009 for review), however a lack of consistency in peripheral measurements, and the complex interactions between these metabolites has limited their biomarker utility to date. Several antioxidant metabolites have demonstrated promise as biomarker candidates, with decreased glutathione peroxidase (Gpx), and copper/zinc superoxide dismutase (Cu/Zn-SOD) levels in red blood cells (Chen et al. 2007). Interestingly, higher levels of serum uric acid, a scavenger of oxygen free radicals, were associated with slower HD progression (Auinger et al. 2009).

1.7.3 Immune response

Investigations of key immune system components in HD have identified elevated cytokine levels, including the interleukins IL-4, IL-6, IL-8, IL-10, IL-23, tumour

necrosis factor alpha (TNF-α), and clusterin (Dalrymple et al. 2007, Bjorkqvist et al. 2008, Forrest et al. 2009) in the HD brain at autopsy and in plasma samples. IL-6, IL-8, and clusterin strongly correlated with both disease progression and corresponding CSF measurements. Combinations of different cytokines were found to be most effective for distinguishing between disease states (Bjorkqvist et al. 2008, Wild et al. 2008). Most strikingly, IL-6 was elevated in pre-manifest subjects at an average of 16 years from predicted phenoconversion (Bjorkqvist et al. 2008), the earliest biochemical abnormality identified in HD gene carriers. Although S-100 calcium binding protein b (S-100b) levels were normal, increased serum C-reactive protein (CRP) and neopterin (Stoy et al. 2005) provide further support for an inflammatory component in HD pathogenesis. These immunologically-active metabolites while offering potential as biomarkers, may be readily confounded by either infectious or inflammatory comorbidities, which is especially a concern given the increased incidence of sepsis in later disease stages (Dubinsky 2005, Andrich et al. 2009). The observed inflammatory profile differences between control subjects and gene carriers prior to clinical onset warrants further investigation particularly in the pre-manifest population.

1.7.4 Neurochemicals

The brain-specific oxidation of cholesterol to 24S-hydoxycholesterol (24OHC), is crucial for CNS development and function and may be disrupted in HD (reviewed by Katsuno et al. 2009). Decreased plasma 24OHC has been demonstrated in diagnosed and pre-manifest subjects and shown to correlate with caudate atrophy

and probability of motor onset (Leoni et al. 2008). The ability of 24OHC to effectively differentiate control and pre-manifest subjects suggests great biomarker potential and merits future examination.

The susceptibility of HD striatal neurons to atrophy has been linked to depletion of brain derived neurotrophic factor (BDNF) and transforming growth factor beta (TGF-beta). Both are essential for neuronal survival (Zuccato et al. 2007, Battaglia et al. 2010). Decreased serum TGF-beta, a cytokine with a potentially neuroprotective role in the brain, has been observed in pre-manifest, but not manifest HD subjects (Battaglia et al. 2010), limiting its potential utility as an HD biomarker at this time. Serum BDNF reductions in plasma were of great interest in the HD field, following demonstration of their association with increased CAG length and deteriorating cognitive and motor scores (Ciammola et al. 2007, Squitieri et al. 2009) , though validation of findings from other research groups is required. Adenosine A_{2A} receptors, which modulate the expression of BDNF in neurons (Potenza et al. 2007), appear to be altered in HD, with elevated platelet levels in pre-manifest (Varani et al. 2003) and symptomatic subjects. Furthermore, correlations between A_{2A} binding affinity, age of onset and CAG length (Maglione et al. 2005, Maglione et al. 2006) suggested excellent biomarker potential. However, in a recent large-scale well-controlled study, although elevated compared to controls, all gene carriers showed similar levels regardless of disease state (Varani et al. 2007).

Levels of N-arachidonolyethanolamine (AEA), the endogenous ligand of the cannabinoid receptor type 1 (CB1) in lymphocytes, were six times higher in HD subjects, though no difference in binding affinity between control, pre-manifest or symptomatic subjects was observed (Battista et al. 2007). Discrepancies in AEA levels may be due to variations in the metabolising enzyme, fatty acid amide hydrolase (FAAH), which was significantly decreased in all HD gene carriers including pre-manifest subjects (Battista et al. 2007). However, observations that FAAH does not vary with symptom severity, hints to an immediate effect of mutant huntingtin, suggesting that quantification may not be useful for biomarker purposes. Neurofilament proteins (NFL), released by dysfunctional and dying neurons to aid in nerve conduction have also been implicated with elevations seen in HD CSF, correlating with age and total functional capacity (TFC) (Constantinescu et al. 2009), yet no differences were found in plasma NFL levels (Wild et al. 2007).

A number of early HD studies aimed to investigate neurotransmitter systems through CSF measurements. However, interpretation of such studies, including work on the cholinergic and GABAergic systems has also been confounded by conflicting results, and possible methodological problems making it difficult to draw specific conclusions. Decreased CSF levels of glutamate have been reported (Kim et al. 1980) while others have shown levels to be comparable to controls in CSF, serum (Nicoli et al. 1993), plasma and platelets (Reilmann et al. 1994). Another excitatory amino acid, aspartate, was elevated in platelets, decreased in plasma (Reilmann et al. 1994), though normal in CSF and serum (Nicoli et al.

1993). Interestingly, plasma activity of aspartate and glutamate aminopeptidase was decreased in both symptomatic and pre-manifest subjects (Duran et al. 2010) and their future study may be valuable. Measurements of homovanillic acid (HVA) and prolactin (PRL), indicators of dopaminergic transmission and turnover have, similarly, yielded mixed results in HD. Reduced HVA has been reported in the CSF (Cunha et al. 1981, Garcia Ruiz et al. 1995), with one study suggesting a correlation between CSF HVA levels and duration of illness (Stahl et al. 1986), however, other studies report levels comparable to controls (Kurlan et al. 1988). Interestingly, plasma HVA (pHVA) was normal in early and moderate stage HD patients, but increased in severely affected subjects, correlating with disease severity (Markianos et al. 2009). Early investigations tended to suggest increased PRL levels in HD patients, however, more recent studies report levels comparable to controls when the effects of neuroleptic medication were taken into account (Markianos et al. 2009). Although dopaminergic signaling may be affected centrally in HD, highly variable results in peripheral body fluids limit the biomarker prospects of these biochemicals.

1.7.5 Novel approaches

Genomic profiling has also been utilized in the search for disease biomarkers, however only a very limited number studies have been performed, Analysing mRNA expression in peripheral blood samples, Borovecki and colleagues (Borovecki et al. 2005) reported 322 transcripts that were significantly altered in HD patients, from this a panel of the 12 was constructed which was able to

distinguish control, pre-manifest and symptomatic subjects. However, follow up studies (Runne et al. 2007, Lovrecic et al. 2009) have been unable to replicate such findings. Additionally, a highly sensitive assay technique known as Forster resonance energy transfer (FRET) has been developed to quantify concentrations of soluble mutant HTT in brain, plasma and CSF samples (Weiss et al. 2009). Such a technique offers great hope for tracking specific HTT-lowering therapeutic approaches and disease progression, however large scale human studies are required to determine the full potential of this assay in the clinical setting.

2 Neuroimaging in HD

As biomarker modalities, neuroimaging techniques are appealing for a number of reasons. These techniques have demonstrated sensitivity to detect altered structure or physiology within the pre-manifest and early HD brain, in some instances many years prior to disease onset. They also have practical advantages; they are generally non-invasive, quality control may be performed in parallel with data acquisition, the data generated is reproducible, can be duplicated, and can be transferred over long distances almost instantaneously and without loss of integrity. Neuroimaging biomarker modalities used in HD studies include structural imaging, functional imaging and metabolic imaging measures and are discussed below.

2.1 Structural imaging

2.1.1 Volumetric imaging

An early focus of structural imaging in HD patients was atrophy of the striatum (caudate nucleus and putamen), which has been shown to correlate with age of disease onset, CAG repeat length (Aylward et al. 1997) and motor dysfunction (Harris et al. 1992, Scahill et al. 2013). Strikingly, striatal atrophy has been reported in subjects 15-20 years from predicted disease onset (Harris et al. 1999, Aylward et al. 2004) with a pattern of rapid, almost linear, striatal tissue loss over time in individuals between 20 and 5 years from predicted onset (Paulsen et al.

2008). Additionally, significant atrophy has been identified in the cerebral white matter (WM) of pre-manifest subjects compared to gene negative controls, even 15 years prior to predicted disease-onset (Paulsen et al. 2010). After stratifying for CAG repeat length and age, a lower baseline striatal, grey matter (GM) and WM volume was also significant, and associated with greater likelihood of progression to clinically manifest disease over the next 1 to 4 years (Aylward et al. 2012, Tabrizi et al. 2013). Substantial loss of diffuse WM in HD patients has been correlated with declining cognitive and motor performance (Hobbs et al. 2010). Interestingly, in pre-manifest HD, the finding that WM volume loss correlates with motor and neuropsychological performance almost as well as striatal atrophy has supported the suggestion that combined structural imaging measurements may be most appropriate for biomarker purposes (Paulsen et al. 2010).

Cortical volume loss has also been described in HD, and suggests that individual variability in regional cortical volume loss may play a role in explaining phenotypic variability (Rosas et al. 2008). Magnetic Resonance Imaging (MRI) measured pre-manifest cortical changes are less clear, with some studies identifying minimal, regionally selective cortical thinning (Thieben et al. 2002, Kipps et al. 2005) and others demonstrating widespread atrophy (Rosas et al. 2005, Nopoulos et al. 2007). These discrepancies may, in part, result from use of different image processing techniques and small study sizes. Ultimately, regionally selective patterns of cortical degeneration in different individuals may limit the versatility of total cortical volume measures as an HD biomarker.

One major obstacle to the development of structural imaging as effective clinical trial endpoints has been a relative paucity of longitudinal compared to cross-sectional imaging studies. While cross-sectional studies have identified structural change in HD, they have a limited role in deriving useful therapeutic endpoints since, as previously discussed, their "snapshot" comparison of pre-manifest and manifest individuals effectively encompasses a considerable period of neurodegeneration (Tabrizi et al. 2011). Cross-sectional effects are therefore larger and represent less realistic therapeutic endpoints than longitudinal effects. Mitigating these issues several longitudinal studies yielded reasonably similar annualized atrophy rates. Thus caudate atrophy rates of 1.1-2.4% per year and 2.9-4.9% per year and putaminal atrophy rates of around 2.3% per year and 4.5% per year have been reported among prodromal and early symptomatic individuals respectively compared to controls (Aylward et al. 2000, Hobbs et al. 2009, Tabrizi et al. 2011).

A large longitudinal biomarker study (pre-manifest; n=116, early HD; n=114) reported significantly increased pre-manifest and early HD total brain volume atrophy rates (-0.2% per year all pre-manifest HD vs. -0.6% per year early HD) compared to controls, but were not significantly different for the pre-manifest subgroup >10.8 years from predicted diagnosis. WM atrophy rates were also increased in all Pre-manifest HD and Early HD groups (including those >10.8 years from diagnosis) (Tabrizi et al. 2011). Furthermore, at 24 months of follow-up white matter and caudate atrophy rates remained two of the strongest measures of

disease progression (Tabrizi et al. 2012). Consequently, powerful longitudinal effect sizes for varied brain regions in pre-manifest and early HD have been demonstrated through structural MRI and may help prioritize their validation as therapeutic endpoints (Aylward et al. 2010, Tabrizi et al. 2011, Tabrizi et al. 2012). Such potential biomarkers include: total brain, striatal, caudate, putamen, cerebral white matter and ventricular volumes. All have been proposed as potential biomarkers in cross-sectional studies, can be objectively measured and correlate with measures of disease progression. Despite their extensive observational study, structural imaging measures remain to be comprehensively assessed, and validated, in therapeutic trials. See Figure 2-1 for an example of volumetric imaging.

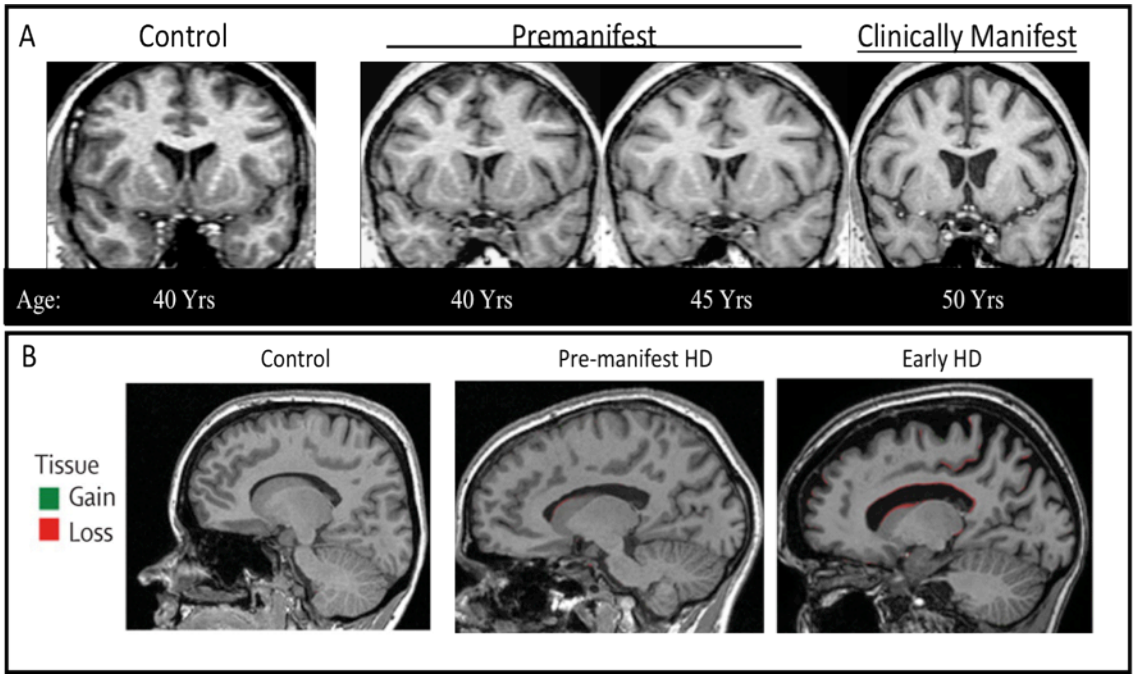

Figure 2-1 Atrophy in the HD brain. A. Shows coronal images from control and the same pre-manifest individual during the transition to symptomatic disease over 10 years. Over this duration a progressive atrophy of the striatum, whole brain and white matter is evident and accompanied by increased lateral ventricle sizes. Images courtesy of Prof. Elizabeth Aylward. B. Shows the brain boundary shift integral (BBSI) a quantification of whole-brain volume change estimated through measurement of shift at the brain–CSF boundary over 12 months within each subject group. 3B is from the TRACK-HD 12 month follow up (Tabrizi et al. 2011).

In selecting therapeutic endpoints, consideration should be given to differential atrophy rates. Variable atrophy rates have been demonstrated for some regions including globus pallidus within different pre-manifest stages (far, mid, near to predicted disease onset) (Aylward et al. 2010) likely necessitating stringent group

stratification to avoid confounding data. Structural imaging data is susceptible to confounding factors that limit inter-study comparisons including technical differences and, in pre-manifest studies, differences in prediction of disease onset method. Hence disparate reports of atrophy onset in striatal structures at around 11 (caudate) years and 15-20 years (striatum) from predicted clinical onset may partly reflect different models of disease onset prediction (Ranen et al. 1995, Langbehn et al. 2004, Aylward et al. 2004, Paulsen et al. 2008). The standardization of practices in imaging, and indeed all biomarker modalities, will assist their development as therapeutic endpoints. It is conceivable that very early structural changes in pre-manifest HD, may indicate the presence of neurodevelopmental anomalies in HD. In a large pre-manifest HD cohort imaging recently identified significantly smaller intracranial volumes (-4%), suggesting impaired maximal brain growth, in pre-manifest males than controls-a finding that did not reach significance in females (Nopoulos et al. 2011). The validity of this finding remains to be confirmed, and will need to be replicated in additional studies.

2.1.2 Diffusion Tensor Imaging (DTI)

An MRI modality known as Diffusion Tensor Imaging (DTI), which provides information regarding principal neuronal fibre orientation and allows patterns of white matter connectivity and disruption to be inferred, is also being investigated in HD. DTI has been used to differentiate presymptomatic individuals from controls, and to measure longitudinal sensitivity to WM degeneration. However,

uncertainty regarding the specificity and sensitivity of the measurements, and their correlation with histological changes, raises methodological problems and the true biomarker utility of DTI remains to be determined (Kloppel et al. 2009). Studies such as a recent report (within a large TRACK-HD sub-cohort) demonstrating both altered WM connections of sensorimotor cortex in both manifest and pre-manifest HD and their correlation with phenotypic deterioration and estimates of probability to disease onset (Dumas et al. 2011) will assist the full appreciation of DTI's biomarker role.

2.1.3 Brain iron imaging

The deposition of iron in the basal ganglia has been identified in HD and other neurodegenerative conditions at post-mortem (Dexter et al. 1991) and *in vivo* in manifest HD individuals using T2 MR relaxometry (Bartzokis et al. 1999, Vymazal et al. 2007). T2-weighted imaging has demonstrated more numerous hypointensities, indicators of iron deposition, in pre-manifest HD individuals than controls that correlated with motor dysfunction, longer CAG repeat length and a greater probability of developing symptoms within 5 years suggesting biomarker potential for such studies (Jurgens et al. 2010). Various aetiologies for iron deposition have been proposed including altered axonal transport and consequences related to possible myelin breakdown (Vymazal et al. 2007, Bartzokis et al. 2007), yet it remains to be determined whether iron deposition reflects a cause of neurodegeneration or epi-phenomenon. Nevertheless imaging-

based iron studies in HD remain an interesting and potentially valuable biomarker approach.

In summary, sensitivity to early neurodegenerative processes, ability to track with phenotypic measures, and a wealth of existing volumetric imaging data make structural neuroimaging measures, collectively, prime candidates for biomarker validation as potential endpoints in future interventional trials.

2.2 Functional imaging measures in HD

2.2.1 Introduction

Neurodegeneration in HD is likely preceded by significant neuronal dysfunction. Therefore techniques, such as functional MRI (fMRI), positron emission tomography (PET) and Magnetic Resonance Spectroscopy (MRS), which measure functional and metabolic changes in brain tissue may have the potential to identify neuronal physiological disturbances prior to macroscopic tissue loss. These bioimaging modalities offer theoretical advantages for monitoring very early disease progression and may be more likely to measure processes that are reversible by therapeutic agents.

2.2.2 Functional MRI (fMRI)

fMRI studies, measuring haemodynamic response to neural activation, have identified both reduced and enhanced cortical activation in HD patients during cognitive tasks - disparity that may be both task and region specific (Georgiou-Karistianis 2009). Surprisingly, fMRI showed enhanced activation in selective cortical regions, despite normal cognitive performance among subjects estimated to be far from predicted disease onset (see Georgiou-Karistianis 2009 for review). One possible explanation for this fMRI finding would be increased cortical recruitment as a compensatory response to primary striatal or cortical dysfunction. Hyperactivation may, alternatively, indicate early abnormalities in cellular processes representing direct pathogenic effects of mutant huntingtin protein (Paulsen et al. 2004). Interestingly, these activation patterns may provide

evidence of neuronal dysfunction preceding even the earliest HD phenotypes (Georgiou-Karistianis 2009). Further to this, fMRI findings have led to the suggestion that pre-manifest HD may be divided into (at least) two parts; a very early phase with predominant up regulation of processes followed by a later phase predominated by deficits in functional evaluations and physiological processes, possibly suggesting differential pathological mechanisms (Saft et al. 2008). The presence of altered function in pre-manifest disease is also supported by the finding of regionally reduced connectivity on fMRI during challenge of the default-mode network function, a network which is activated when the brain is not engaged in a cognitive task (Wolf et al. 2012). At present, however, temporal patterns of activation still require clarification through further longitudinal study.

Blood oxygen level dependence (BOLD) functional connectivity studies in HD have correlated activity between different cortical regions, suggestive of regional interactions, during specific cognitive tasks. These studies help characterise neurobiological correlates of HD, suggesting pathophysiological roles for cortico-striatal and even striatal-sparing fronto-parietal circuits in HD (Thiruvady et al. 2007). One ongoing obstacle to the adoption of fMRI as a biomarker in HD is uncertainty regarding the true functional and physiological significance of the altered fMRI activation patterns in this disorder.

2.2.3 Positron Emission Tomography (PET)

Another functional imaging technique; PET, which measures positron emissions from a radionuclide tracer attached to an intravenously introduced biologically active molecule, has been used to evaluate glucose uptake and dopaminergic signalling as potential disease markers in HD. Striatal glucose hypometabolism and regional reductions in cortical glucose utilisation have been identified in HD patients (Kuwert et al. 1990, Ciarmello et al. 2006). Furthermore, deficient caudate and regional cortical metabolism correlated with cognitive task performance (Berent et al. 1988, Kuwert et al. 1990), while striatal hypometabolism was associated with motor deficits and reduced functional capacity (Young et al. 1986, Kuwert et al. 1990). In diagnosed and pre-manifest gene carriers, longitudinal PET imaging revealed a similar pattern of deteriorating striatal metabolism that becomes more striking in manifest individuals (Harris et al 1992, Ciarmello et al. 2006).

Investigations of dopaminergic systems, specifically D1 and D2 receptors, which are highly expressed in vulnerable medium spiny neurons, have found reduced receptor densities and activity in the striatum, correlating with disease duration, impaired cognitive performance in multiple domains (Berent et al. 1988, Backman et al. 1997) and motor deterioration (Backman et al. 1997, Pavese et al. 2003). Furthermore, longitudinal evaluation in early stage HD identified progressive D2 receptor loss within striatum, temporal and frontal cortex (Pavese et al. 2003), while in pre-manifest subjects, declining striatal dopamine receptor binding

correlated with proximity to disease onset (Harris et al 1992, Ciarmello et al. 2006).

A further longitudinal study evaluating [11C]-raclopride and [18F]-fluorodeoxyglucose PET (FDG-PET) imaging in pre-manifest individuals identified a progressive decline in striatal D2 receptor binding associated with alterations in an HD-related metabolic network and regional metabolism. Notably, although striatal metabolism was impaired throughout the study, thalamic metabolism was increased at baseline and the HD-related metabolic covariance pattern also increased early in the study. These elevations were suggested to represent compensatory metabolism during a period of early neuronal loss and their reversal was associated with the advent of symptom onset (Feigin et al. 2007). In a cross-sectional comparison of raclopride PET binding potential (RAC-BP) in pre-manifest HD with FDG-PET and striatal MRI volumes, RAC-BP was reduced in 50% of subjects (and correlated with increases in the product of CAG repeat length and age), while striatal volume and FDG-PET was normal in 88% and 67% of subjects. The authors suggested therefore that D2 receptor availability measured by RAC-BP is the most sensitive indicator of neuronal impairment in pre-manifest HD (van Oostrom et al. 2005). These studies demonstrate the potential value of PET imaging as a biomarker modality in pre-manifest HD.

Yet the realization of functional imaging as an HD biomarker will require further larger-scale, longitudinal studies of pre-manifest subjects. Such studies may be

strengthened, as evidenced here, by implementing suggestions for future parallel evaluation of multi-modal imaging biomarkers (eg. fMRI, structural MRI, DTI), permitting a direct comparison of relative technique sensitivities in HD (Georgiou-Karistianis 2009).

2.3 Magnetic Resonance Spectroscopy (MRS) and its biomarker role in HD

2.3.1 Introduction

Magnetic Resonance Spectroscopy (MRS) permits the measurement of brain metabolites at the cellular level *in vivo*, providing unique insight into ongoing pathological processes. Used as both a clinical and biomarker research modality, it offers insight into brain pathologies, their progress and potentially abrogation.

MRS can be performed with ^{31}P-MRS, but also fluorine, carbon and sodium isotopes, however it is 'proton' or '^{1}H-MRS' that is most widely used due to its high sensitivity and relative abundance (almost 100 % available in the human brain). In this work, MRS will refer to ^{1}H-MRS only. For some time MRS was limited due to insensitivity related to poor field strength, and signal-to-noise ratios (SNRs) necessitating sampling with large voxels. This is being revisited with the advent of 3T and 7T scanners, the development of even more powerful magnets, with ever increasing SNRs. These higher sensitivities permit metabolite estimations in smaller voxels of interest - an important step in ensuring intra-voxel tissue homogeneity and in enabling the analysis of small, specified neuronal structures.

2.3.2 The basis of MRS: Larmor frequency, signal multiplicity and the PPM Scale

The Larmor frequency tells of the frequency with which nuclei will resonate or spin, in a field strength B0, based on the isotope's specific natural gyromagnetic ratio.

$$f=\gamma B_0$$

However this equation is based on a nucleus in isolation, unaffected by neighbouring nuclei. In nature, the nuclei will be influenced by nearby small magnetic fields generated by electrons within, for example, adjacent chemical bonds. These secondary fields will have effect in a direction opposing the main field and hence a shielding effect, causing the nucleus to resonate at a different, lower frequency. This is known as the *screening constant* which is characteristic for a given nucleus in a given situation and is responsible for the different spectral patterns seen in MRS. In addition to these screening effects, the magnetic fields generated by neighbouring nuclei spins also have an impact on a given nucleus. These interactions are described as coupling interactions or *J*-coupling. It is this phenomenon that is responsible for the signal multiplicity, or characteristic double peak seen with lactate due to interactions between CH3 and the C-H portions (Hajek & Dezortova 2008).

To display spectra, the PPM scale is favoured over a frequency display because firstly, there is no absolute zero that can be generated using any naturally occuring material, and secondly because overall frequency will depend on the strength of the main field B_0 and therefore subject to different peak positioning depending on field strength.

As an alternative the 'chemical shift', measured in parts per million (PPM), is used. *In vitro*, this measurement is straightforward; the chemical shift of the substance of interest (mixed into a solution) δ_{cs} can be calculated by measuring the frequency of that substance relative to the frequency of a reference and calculated as:

$$\delta_{cs} = \frac{f_s - f_{ref}}{f_{ref} \times 10^{-6}}$$

In vivo, a similar but alternative calculation is used which depends upon the calculation of an offset which can then be applied to other metabolites, based on the knowledge of the chemical shift of a metabolite standard N-Acetylaspartate (NAA), the measured frequency of the substance (f_s in this case NAA at 2.01ppm), and the frequency of the transmitter ($f_{transmitter}$):

$$\delta_{cs} = \frac{f_s}{f_{transmitter} \times 10^{-6}} + \text{Offset}$$

By avoiding a field dependent frequency display, each peak can be identified at a fixed and characteristic PPM defined position on the spectrum regardless of B_0 (Drost et al. 2002).

2.3.3 MRS acquisition techniques

An initial anatomical MR scan is performed, that is used to inform voxel placement. This must be done carefully in studies of neurodegeneration within a specific atrophied brain region. Either single voxel spectroscopy (SVS) or large volume Magnetic Resonance Spectroscopic Imaging (MRSI) can be performed. In the latter the volume is divided by grid into multiple voxels each of which is analysed concomitantly to produce a spectrum. This latter technique therefore, identifies spectral variation over a larger region of anatomical interest, and can therefore be useful for defining, for example physiological tumour boundaries. A water suppression sequence is then applied, usually either CHESS or WET (Haase et al. 1985, Ogg et al. 1994), to enable appreciation of the smaller metabolite concentrations (compared to water). This step is discussed in further detail below.

MRS, in addition to the main field magnet (B_0), employs gradient coils orientated in three planes to stipulate a three-dimensional Voxel of Interest (VOI), from which the MRS evaluation is required. These coils have minute switching times of milliseconds and exert very small mT field strengths (van der Graaf 2010).

The gradient coils, with their gradients in the x, y, and z axes are combined with each of the three pulses produced by a selected SVS acquisition technique (one of two) to enable signal generation and acquisition from a single slice, oblong VOI, delineated as the overlap of the three gradient fields. Figure 2-2 illustrates slice selection in a single plane. The two main SVS acquisition techniques are STEAM

and PRESS. Point-resolved spectroscopy (PRESS) and Stimulated echo acquisition mode (STEAM) both utilize three RF pulses. In PRESS a 90° excitation pulse is followed by two 180° refocusing pulses that result in the generation of a second echo. STEAM, instead uses three separate 90° pulses, to generate a stimulated echo (Figure 2-2) (Drost et al. 2002, van der Graaf 2010).

The major disadvantage of the PRESS technique is the longer duration of the 180° pulses compared to the 90° pulses, prolonging TE compared to STEAM and exacerbating chemical shift displacement artifacts (see below). The major disadvantage of STEAM however, is the generation of a stimulated echo, which has only about 50% SNR of the PRESS technique (due to the 90° rather than 180° pulses used). For this reason, STEAM is often used where precise voxel selection is required with short TE, while PRESS is for most purposes, the most widely used technique (Drost et al. 2002, van der Graaf 2010).

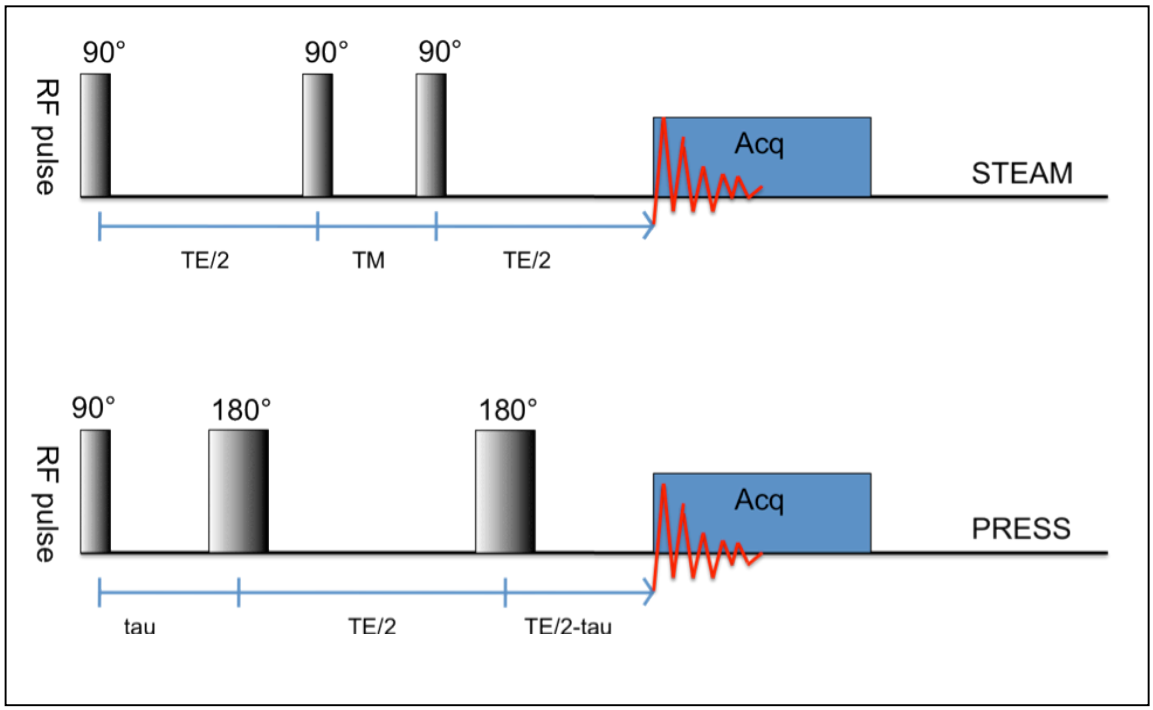

Figure 2-2 STEAM and PRESS Sequences. TM refers to mixing time in STEAM, and tau to the time between the first and second pulses in PRESS. Of note the three pulses are all applied in three planes.

2.3.4 MRSI

As already stated MRSI can provide simultaneous spectrums from multiple small voxels to provide information regarding larger spatial distributions of metabolite or neurophysiological abnormality. MRSI uses phase encoding gradients to provide spatial localization. MRSI employs either of the SVS acquisition techniques (STEAM or PRESS) to provide MRS data. In addition to the usual steps required for MRS, MRSI requires a phase encoding step that is usually applied after the application of the combined RF excitation with gradient for slice selection. The phase encoding gradients can be applied in 1,2 or 3 dimensions to sample the *k*-space. The *k*-space

is an area in which data collected from the signal, both in terms of frequency and its precise spatial origin, are stored (Westbrook 2009, van der Graaf 2010).

Importantly, the number of partitions or voxels acquired in a required MRSI field of view or FOV (and hence spatial resolution) is proportional to the number of phase encoding steps. Therefore time costs can become an issue since the duration for traditional MRSI will be equal to the product of the required phase encoding steps and the TR. Since the duration for phase encoding may exceed the duration required for optimal SNR, this can be a significant problem, and may be exacerbated when large FOVs and high-resolution images (with greater numbers of phase encoding steps) are required. To minimize the impact of time constraints on MRSI imaging quality a number of novel techniques including turbo-MRSI (using multiple spin echoes),multi-slice MRSI and parallel acquisitions have been developed (Bertholdo et al. www.ajnr.org/site/fellows/file/MRS-chapter-Castillo.pdf).

2.3.5 Single Voxel Spectroscopy vs MRSI

There are relative advantages and disadvantages to both SVS and MRSI methods. SVS is associated with some major advantages over MRSI methods. Figure 2-3 demonstrates both SVS and CSI sample spectra.

1. Quantitation time: SVS requires a comparatively shorter quantification time because MRSI requires a greater degree of phase encoding (a spatial

resolution phase) than does single voxel spectroscopy, since it involves the interrogation of larger volumes of interest, and provides anatomical mapping of spectral patterns. MRSI assessments can become prolonged if multiple phase encoding steps are required, for example when assessing larger higher resolution volumes. One method to reduce this is reduction of the Field of View (FOV).

2. Shimming issues: SVS also involves higher quality shimming. With MRSI shimming is performed for the entire volume rather than separate voxels as for SVS, the quality of the shim is impaired. Since shimming is used to improve main field homogeneity, it is important for increasing SNR and narrowing peak widths, ie. improving sensitivity and spectral resolution.

3. Water suppression variability: A further problem with MRSI is that water suppression can vary across the larger volume investigated with this modality due to field inhomogeneities, and potentially impact upon metabolite quantitations.

4. Voxel bleed: Another major disadvantage of MRSI is voxel bleed. Specifically, the spectrum of adjacent voxels can contaminate that of the VOI, and can have positive or negative effects due to the point spread function. Special filters used prior to Fourier transformation (a post-

processing step, discussed below) can limit this, but requires larger voxel sizes and hence reduced MRSI image resolution.

Conversely MRSI offers some unique advantages.

1. Spatial spectroscopy: The modality permits better spatial resolution and allows imaging with detailed coverage over larger lesion areas.

2. Multiple voxels: and hence considerably more data, can be collected in a single assessment.

Generally therefore, where high sensitivity, accurate metabolite estimation is required from a single anatomical locus, SVS is preferred, while MRSI provides the ability to acquire data from multiple voxels. However the longer TE for MRSI means that the sensitivity is usually limited to estimations for the larger peaks such as NAA and Cr (Drost et al. 2002, van der Graaf 2010, Bertholdo et al. www.ajnr.org/site/fellows/file/MRS-chapter-Castillo.pdf).

Figure 2-3 Sample Spectra. Single Voxel MRS (A) and CSI (B)

A

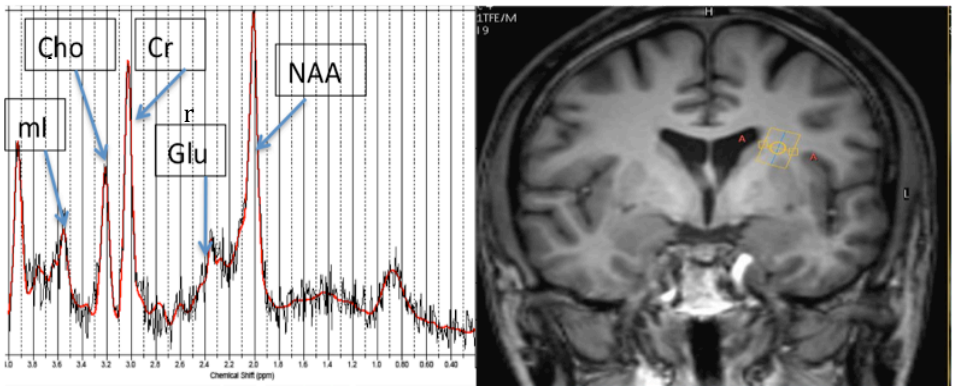

B

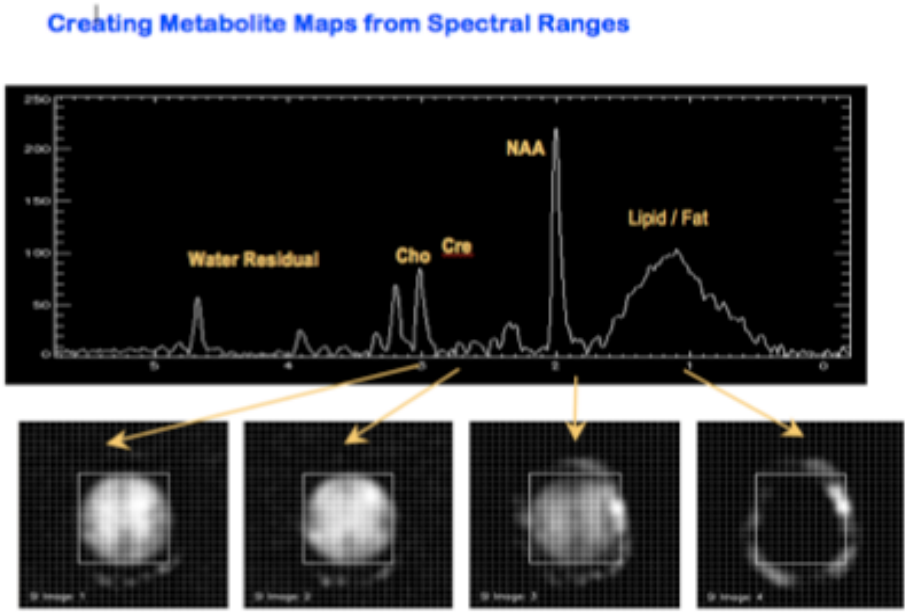

2.3.6 Short and long echo times (TE)

The use of MRS can be selected for both short (20-40ms) and long echo times (135-288ms). Short echo times have the advantage of being able to identify metabolite peaks more sensitively, with higher SNR and less signal loss due to T2 and T1 weighting and therefore identifying signals that will not be detected at higher TE. As a result the spectra are generally more complex, with a greater number of peaks, and overlap which must be interpreted and quantified with care. Metabolites such as myo-inositol (mI) are among those metabolites quantifiable at short TE only. Conversely, the spectra obtained with longer TE are less complex, more easily interpreted at the expense of lower SNR and suppression of some metabolites' signals (Bertholdo et al. www.ajnr.org/site/fellows/file/MRS-chapter-Castillo.pdf).

2.3.7 Potential sources of artifact & other considerations

Signal to Noise Ratio (SNR)

The SNR is the signal from a metabolite and is given by the area under its peak. It represents the ratio of the amplitude of the signal to the background noise amplitude. The MR signal represents the voltage induced in the receiver coil by the precession of the Nuclear Magnetisation Vector in the transverse plane, and occurs at time intervals (echo time, TE). The noise is the unrequired signal that is generated by the system itself, patient and environment (Westbrook 2009) and is dependent on several factors including; main field strength (B_0), use of small local coils and adequate position of the receiver coil. Short TR (Repetition Time)

between pulses diminishes SNR by reducing the time for longitudinal recovery and therefore for subsequent transverse magnetization and hence detectable signal at subsequent RF pulses. Similarly, increasing echo time (TE) the time between the radiofrequency pulse and the time at which the transverse magnetization signal is received is also important – if too much of the transverse magnetization signal dephases or decays, then the signal amplitude will also diminish. As a consequence S/N will depend on the duration of the STEAM or PRESS echo, and SNR can be improved with a longer signal duration which can be obtained with good quality shimming (Drost et al 2002, Wesbrook 2009, van der Graaf 2010). SNR can also be maximized by maximizing the number of signals (n) added. The NSA (number of signal averages) or the number of times a signal is sampled provides a greater amplitude of signal intensity, although this is at the cost of sampling time (Drost et al 2002, van der Graaf 2010). Spectral noise can be evaluated by measuring the standard deviation in a signal-free region. Of note noise is VOI size independent, while signal is linearly related to size of voxel; leading to a preference for larger voxels. Although this must be considered against the disadvantages of increasing voxel size which may include the undesired incorporation of brain structures and/or CSF (Drost et al 2002, Bertholdo et al. www.ajnr.org/site/fellows/files/MRS-chapter-Castillo.pdf,)

Shimming

The shimming process increases magnetic field homogeneity improving SNR and reducing peak widths to improve sensitivity. The efficacy of shimming algorithms -

which are usually automated - can be assessed using an MRS phantom, which also can indicate Bo field homogeneity (See Drost et al. 2002 for details). Most systems now incorporate first order shims, and unsuppressed water signal is used to perform this.

Eddy current

Magnetic field gradient pulses (that can be used in slice selection, see Fig 2.2) generate eddy current artifacts or heterogeneities in the magnetic field, through the creation of their own magnetic fields. They can distort peaks, affecting peak fitting to modelled line shapes. The currents can be subcategorized as zero and first order eddy currents. Zero order eddy currents are time-varying magnetic B_0 field offsets, and do not affect spin dephasing within the voxel and hence no reduction in SNR. First order eddy currents, conversely, represent time-varying first order or higher field gradient, and will dephase spins leading to SNR reduction. Eddy current peak distorting effects can be limited in a number of ways, but one of the most widely used methods is using an eddy current correction (ECC) which is the first post-processing step, and involves point by point phase correction of the time domain signal, using unsuppressed water as the reference. ECC enables line-shape corrections in addition to removal of offsets from zero order phasing and is automated through software packages such as LCModel (Drost et al. 2002).

Water issues

The very high concentration of water (around 36 M) in the brain necessitates suppression to prevent the obscuration of metabolite signals which exhibit signal in the order of 1-10 mM. Water suppression is achieved through, nulling the longitudinal magnetization of water and a dephasing of the decaying transverse signal, at the first RF pulse in the localization sequence – that is, prevention of signal generation in either T1 relaxation or T2 decay. It is performed using repeated sequences of radio-frequency pulsing, but is affected by T1 relaxation, and RF-pulse flip angles. Two methods which are used to achieve this are WET (Water suppression through Enhanced T1 effects, Ogg et al. 1994) and CHemical Shift Selective water suppression or CHESS (Haase et al. 1985). The CHESS technique utilses a specific sequence of narrow band RF pulses, followed by a dephasing or crusher gradient, which destroys any residual water signal prior to the initiation of the PRESS or STEAM sequence. The suppression sequences can also be usefully removed to permit quantification of the water signal which can be subsequently used for water-related corrections such as eddy current correction (ECC) and as a reference for absolute metabolite concentrations (Drost et al. 2002, van der Graaf 2010, Bertholdo et al. www.ajnr.org/site/fellows/files/MRS-chapter-Castillo.pdf).

Chemical shift displacement (CSD)

Slice selection normally is achieved through the application of a foot-head magnetic field gradient in the z-axis of the patient. This gradient generates a

differential Larmor frequency across the length of the patient/field. By matching the frequency of the RF pulse to that of the Larmor frequency within the region of interest, slice selection occurs, and an MRI signal is produced only from that region. Furthermore, a short TE allows for precise volume selection. The CSD artifact arises from the fact that signals with different chemical shifts within a given volume of tissue will experience different (frequency determined) slice selections. This will mean that signals will not all originate from identical tissue volume, and will be exacerbated by the longer TE, hence less accurate volume selection, used with certain sequences. This is therefore more of an issue with PRESS than STEAM due to the more protracted TE, a consequence of the longer performance of the two 180 ° RF pulses (van der Graaf 2010) (See Figures 2-2 & 2-4).

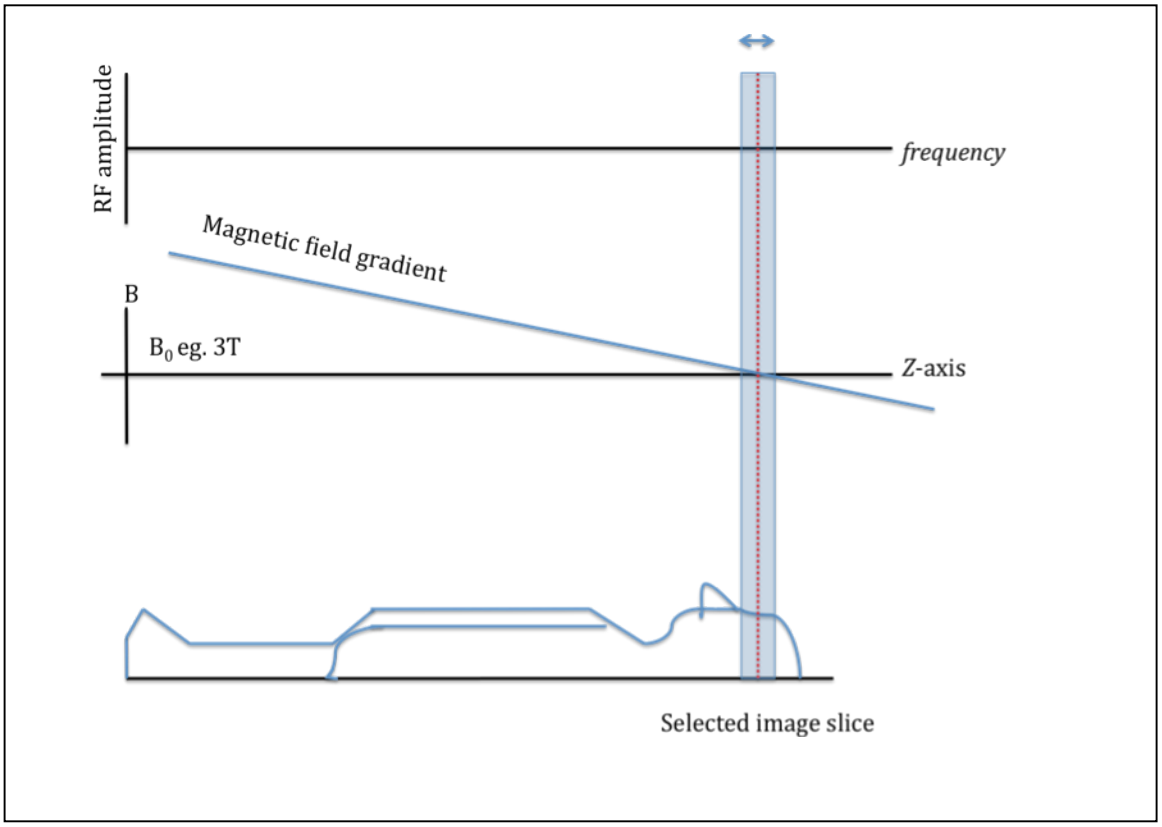

Figure 2-4 Slice selection. The double arrowhead highlights the transmitted RF bandwidth. The region selected for imaging is the one in which Larmor frequency is matched by the transmitted RF pulse.

Field strength

Higher field strength increases spatial resolution, hence greater distance between metabolite peaks facilitating their differentiation (although linewidth increases with greater field strength, necessitating shorter TE). Higher field strength also has the advantage of improving SNR and reducing acquisition times (Bertholdo et al. www.ajnr.org/site/fellows/files/MRS-chapter-Castillo.pdf,).

Other limitations

Due to the high field strengths employed during MRS, or indeed any MR imaging, imaging of patients with ferromagnetic implants (such as aneurysm clips), dental work or other medical devices (eg. pacemakers) can be dangerous and may preclude use of this modality. Precautions such as contacting the device manufacturer, may be necessary in some cases. Similarly, individuals at risk of intr-orbital metal splinters (eg. welders), may need orbital x-ray first to exclude any intraocular splinters. A subject's or patient's claustrophobia may also ultimately prevent imaging, although often in such instances a sedative, or if absolutely necessary a General Anaesthetic, may be of some assistance. Patient movement is also a source of artifact for standard MR imaging, causing a degradation of structural images and in MRS may attenuate the signal-to-noise ratio (SNR) (Taylor-Robinson et al 1996, Thiel et al. 2002).

2.3.8 Post-processing overview

The post-processing steps involved in MRS include; i) zero filling, ii) multiplication with a filter, iii) ECC, iv) water suppression filter, v) Fourier Transformation, vi) phasing, and vii) baseline correction. Since periodic functions can be expressed as a summation of sinusoids of different amplitudes and frequencies, Fourier Transformation (FT) refers to a method by which these sinusoids can therefore be assessed. ECC has already been discussed and is often the first step in post-processing (Drost et al. 2002, Bertholdo et al. www.ajnr.org/site/fellows/files/MRS-chapter-Castillo.pdf, van der Graaf 2010).

The quantification of metabolite peaks is achieved through integrals of resonances. One of the most widely used models is LCModel (Linear Combination of Mode Spectra, Provencher 1993) and is discussed below. One of its advantages is that the program can be used for analysis of short TE spectra which are more dense in terms of their spectral patterns. This is possible because the program utilizes the full spectrum for each metabolite in its modeling, taking full advantage of a metabolite's signature when assessing 'busy' spectra. For less sensitive spectra, or ^{31}P-MRS the program jMRUI is often used. Both programs provide information on the quality of fit with the Cramer-Rao Lower Bound as an error estimation (Schirmer & Auer 2000, Provencher 2001, Bertholdo et al. www.ajnr.org/site/fellows/files/MRS-chapter-Castillo.pdf, van der Graaf 2010).

Since metabolite quantification of signal intensity is in arbitrary units, ratios are often used to quantify metabolite concentrations - thus, many papers report

metabolites normalized to creatine, although this carries the concern that in many diseases, brain creatine may also be altered. Hence where possible in the research scenario and where results are required for comparative purposes with other subject groups, the reporting of absolute concentrations, with water as the internal reference is preferable. Ideally a standardization in the reporting of such research findings would be important to avoid inherent confusion that normalizing to creatine may cause. Such a seemingly simple step can have significant implications, for example in the questioning of a utility for MRS as a biomarker for certain disease states; and has been an issue for HD itself, as will become apparent later. It also allows, in theory, direct comparisons of results in literature and aids longitudinal imaging studies of the same subjects. However, even where identical assessment paradigms are repeated at the same institution, it is important that quality assessment and control scans (on healthy volunteers) are performed and compared with departmental reference, at initiation and intermittently during research to ensure that slight variations in acquisition, post-processing and quantification are adjusted for prior to starting a study proper (van der Graaf 2010).

2.3.9 The LCModel

The Linear Combination model or LCModel is a software package, developed by Provencher (Provencher 1993), as an automated tool for MRS post-processing and metabolite quantitation. It is discussed in detail in Chapter 5.

2.3.10 The major MRS metabolites

The following are among the most widely reported metabolite peaks:

(Total) N-acetyl aspartate or tNAA, sometimes just NAA (peak at 2.02 ppm) but actually represents the summed NAA and NAAG (N-acetyl aspartyl glutamate) peaks. This metabolite is identifiable in both white and grey matter and was initially believed to be a measure of neuronal density/integrity, yet an increasing amount of data now indicates this measure to be also a marker of neuronal health, as evidenced by a partial recovery over time of tNAA levels in multiple sclerosis lesions and in MELAS (Davie et al. 1994, De Stefano et al. 2000). Reductions of tNAA are seen where there is neuronal destruction or displacement, as is seen with brain tumours (Imamura 2003). tNAA is not found in mature oligodendroglial cells (Urenjak et al. 1993), and it displays significant regional variation in brain and there is some evidence to suggest generally higher levels in grey matter, attributable to a higher neuronal density (Imamura 2003).

(Total) Creatine or tCr, (peak at 3.00 ppm) sometimes reported as just Cr but represents the summed Cr and PCr (phosphocreatine). PCr is a high-energy reservoir that is found in high levels in tissues dependent on aerobic glycolysis such as brain. Cr occurs in much higher levels in astrocytes and oligodendrocytes than in neurons (Urenjak et al. 1993), and the reduction in tCr levels indicates energy deficits in glial cells, and hence impairment in neuronal energy supply (Imamura 2003). Disease states and tissues subjected to severe physiological compromise are often associated with a reduction in tCr (Imamura 2003). tCr also appears to be a potentially useful marker of gliosis (Suhy et al. 2000).

(Total) Choline, tCho or just Cho, (peak at 3.20 ppm) comprises glycerophosphocholine (GPC) and Phosphocholine (PC), which cannot be separated using proton MRS. Cho is widely accepted to be a marker of cell membrane turnover, specifically it is a measure of the formation of new, and breakdown of old cell membranes. The GPC may predominantly represent catabolic processes, while the PC is believed to represent synthetic and catabolic processes (Imamura 2003). As a consequence an increased tCho is seen at MRS in CNS neoplasms, including meningioma (Kugel et al. 1992) with increasing tumour grade associated with an increase in Cho (Herminghaus et al. 2002). Higher Cho can also reflect high cellularity within a given tissue, such as that seen in inflammation (Venkatesh et al. 2001). tCho is found in higher concentrations in glial cells (Urenjak et al. 1993).

Lactate or Lac (doublet peak at 1.35 ppm) within the normal brain is at the lower limits of MRS detection and hence raised levels generally point to a disease state. Anaerobic glycolysis is a major contributor to Lac production, and hence, it may be supposed that disease states affecting mitochondrial function, where normal aerobic glycolysis takes place, might be associated with Lac increments. As such Lac can become elevated in a range of different pathologies. After stroke, Lac rises acutely and reflects the severity of the ischaemia (Houkin et al. 1993). In brain neoplasms also, Lac increments are associated, most likely as a result of ischaemia in the diseased tissues (Ott et al. 1993, Imamura 2003). In inflammatory processes also, Lac appears to reflect anaerobic glycolysis by inflammatory cells such as macrophages (Imamura 2003). By the same token mitochondrial encephalopathies are associated with increased cerebral Lac due to an interruption of normal aerobic metabolism (Leach et al. 1992, Imamura 2003).

Glutamate (Glu), **glutamine** (Gln) (peaks at 2.2-2.4 ppm and 3.6-3.8 ppm) commonly referred to as the combined Glx (Glu + Gln); Glx can be used to differentiate brain tumour histology, such as oligodendroglioma and astrocytoma (van der Graaf 2010). Glu is an important excitatory neurotransmitter, that is important in the redox cycle, and there is some evidence that it may provide an in-vivo indication of excitotoxicity in neurodegenerative processes (Glodzik et al.

2008). Gln elevations are found in varied encephalopathies (Fayed et al. 2006, van der Graaf 2010).

Myo-inositol (or mI) (peak at 3.56 ppm) occurs at high levels in astrocytes, and is often thought to reflect the degree of astrocytosis or glial cell proliferation within a tissue (Kantarci 2007). Elevations in this metabolite have been described in Alzheimer's disease and appear to follow the pathological progression (Kantarci et al. 2008). mI elevations can occur in other situations where there is a proliferation of glial cells, for example in inflammation, and may also be an indicator of myelin breakdown (van der Graaf 2010).

2.4 *In vivo* brain MRS as a research biomarker

A practical and effective *in vivo* biomarker of brain metabolism should fulfill some basic criteria.

Quality	Comment
Accessible	The modality should be readily available for either clinical+/-research work.
Automated	The modality should ideally limit operator-dependent error, hence an automated process of data acquisition and quantification.
Reproducible	The modality must avoid, so far as is possible, measurement errors.
Robust to image quality	The modality should provide utilizable data despite potential degradation by movement or other artifact.
Sensitive to biochemical change	The modality should identify sub-cellular pathological change, although clearly difficult to verify *in vivo*.
Time & Cost efficient	The modality should allow timely data acquisition, and be practicable within the limits of research funding & clinical access.

Table 2-1 Basic criteria of an ideal biomarker

LCModel, one of the most widely used SVS software anaysis packages, has a reproducibility with less than 5% Coeffcient of Variation at scan, rescan on the major metabolites in one study (Provencher 2001). Reproducibility and avoidance of erroneous longitudinal data collection will also depend on accurate placement of voxels in identical (or close to), anatomical location slices at follow up imaging.

The accessibility, time and cost efficiency factors are major advantages of MRS as a biomarker, since the only pre-requisite for the modality is the scanner, and software package. It is therefore both widely accessible, and relatively inexpensive. Furthermore, the imaging is rapidly achieved within standard MRI brain scan time.

2.5 Observational MRS studies in HD

2.5.1 Cross-sectional

Historically, the evidence regarding certain metabolite alterations in HD has been conflicting. A number of cross-sectional studies evaluating the biomarker potential of MRS in HD, preceding this work, had shown variable metabolite changes.

Reynolds et al. identified a heterogeneous pattern of metabolite alteration in HD, proposing that individual metabolites did not provide sufficient biomarker potential and raising the possibility instead that metabolite panels may provide greater sensitivity to disease state (Reynolds et al. 2005). The overall pattern they observed in symptomatic individuals was some combination of reduced NAA, increased Glx, elevated Lac and Cr deficits that was variable between individuals. The authors raise the possibility of predominance of differential pathophysiological processes as the disease progresses (Reynolds et al. 2005) – a supposition that has some support from animal models (Graham et al. 2009).

Other groups have reported similar patterns. Thus striatal NAA reductions have been suggested in manifest HD in small studies, interpreted as a loss of neurons or neuronal viability (Jenkins et al. 1993, Davie et al. 1994, Hoang et al. 1998, Sanchez-Pernaute et al. 1999, Ruocco et al. 2007). NAA/Cr reductions in the thalamus of manifest individuals, a brain region not associated with early atrophy in HD, is suggestive of a more diffuse disease process occurring even in relatively spared brain structures (Ruocco et al. 2007). Raised basal ganglia and occipital

cortex Cho (Cho/NAA) levels have also been reported in manifest HD possibly indicating gliosis (Jenkins et al. 1993, Jenkins et al. 1998, Hoang et al. 1999). Meanwhile striatal glutamate and lactate elevations, and creatine reductions have also been identified, including among cases of manifest juvenile HD – whom typically display a more aggressive disease course (Hoang et al. 1998, Sanchez-Pernaute et al. 1999, Reynolds et al. 2005, Reynolds et al. 2008).

The authenticity of purported elevations in brain lactate, a possible indicator for dysregulation of energy metabolism in HD, remains unclear. Martin et al. demonstrated elevations of parieto-occipital and cerebellar Lac/Cr and Lac/NAA and also predicted a trend to higher CSF Lac/NAA in HD affected individuals. These findings were interpreted as regionally non-specific lactate increments (Martin et al. 2007). Furthermore these findings reinforced earlier suggestions of lactate elevations, measured as Lac/NAA, in occipital cortex of manifest (Jenkins et al. 1993, Jenkins et al. 1998) but not pre-manifest individuals (Jenkins et al. 1998). Further evidence for a diffuse failure of normal energy metabolism in HD comes from reported Lac/NAA elevations in the basal ganglia in manifest HD (Jenkins et al. 1993). Similarly, frontal Lac/Cho elevations were noted in mildly symptomatic manifest and pre-manifest individuals in another study. Interestingly, these same individuals were those least likely to exhibit NAA/Cho alterations supporting the notion of differential metabolite alterations with disease stage, or as the authors suggest, reflecting achievement of a steady state of Lac, through a plateau in rates of neuronal loss (Harms et al. 1997). The supposition that Lac is increased among

these individuals is strongly contested by the work of others, whose findings indicate that these ratios signify alterations in the other metabolite NAA or Cr (Taylor-Robinson et al. 1996, Sánchez-Pernaute et al. 1999).

The role of MRS as a means of measuring disordered energy metabolism within the HD brain may also gain support from the finding of Cr reductions (Hoang et al. 1998, Reynolds et al. 2005, Reynolds et al. 2008) and increased Glx/Cr levels in manifest HD brain. The earlier finding that inhibitors of mitochondrial function are able to replicate patterns of striatal damage seen in HD and which can be abrogated through the use of NMDA antagonists hints as to the potential importance of the identification of raised Glx/Cr in HD, specifically the potential loss of glutamate/glutamine regulation through longstanding energy failure and subsequent enhancement of excitotoxic pathways (Di Figlia, 1990, Davie et al. 1990, Taylor-Robinson et al. 1994, Taylor-Robinson et al. 1996). It is notable however that these reports did not identify consistently, significant Lac changes in their subjects (Davie et al. 1990, Taylor-Robinson et al. 1996).

Unfortunately, for many of the, especially earlier MRS studies to date, the findings must be read guardedly given the caveat of combined metabolite reporting. Specifically, that the reporting of a metabolite relative to Cr, NAA or Cho is liable to be fraught with uncertainty as to absolute metabolite change, since there is evidence that each of these comparator metabolites may be altered in HD, as can be seen in Table 2-2 below.

2.5.2 MRS in pre-manifest HD

The work of several groups implicate a metabolic derangement preceding disease onset, specifically striatal NAA and Cr reductions together with higher Lac and Glu levels than controls (Jenkins et al. 1998, Sanchez-Pernaute et al. 1999, Reynolds et al. 2005, Reynolds et al. 2008). In one study of 14 pre-manifest HD gene carriers, Cho reductions were observed in the frontal lobe, while basal ganglia spectral patterns remained normal (Gomez-Anson et al. 2007). The authors suggest this alteration reflects possible constitutional brain development abnormalities in HD, and particularly the possible existence of co-existent dysfunctional oligodendrocyte activity (Gomez-Anson et al. 2007). While this supports the presence of metabolite changes in pre-manifest HD, it suggests a lack of metabolite change in a brain region affected early in the disease process, a finding that may have been influenced by study size and/or heterogeneity in time to predicted disease onset (not reported in the study). This finding was also contrary to the earlier description of Cho (Cho/Cr) elevations in the pre-manifest HD basal ganglia (Jenkins et al. 1998), a region of early and selective neurodegeneration in HD. It is important to note that other studies have been unable to identify any metabolite change in pre-manifest disease (Taylor-Robinson et al. 1996, Van Oostrom et al. 2007).

2.5.3 Challenging the biomarker role of MRS in HD

A number of other studies question the utility of MRS as a biomarker. In their study of pre-manifest individuals, Van Oostrom and colleagues did not identify significant differences in putaminal NAA or putamen/thalamic NAA compared to controls, nor did the authors report any disturbance for other commonly reported metabolites (Van Oostrom et al. 2007). Interestingly, despite the lack of clear metabolite changes, this group identified significant changes among pre-manifest individuals on PET and volumetric imaging measures, leading the authors to question the sensitivity of MRS as an HD biomarker modality in pre-manifest HD. Similarly, Martin and colleagues identified no difference in HD levels of NAA/Cr or Cho/Cr (Martin et al. 2007). In a small study of five early symptomatic HD patients, and a single pre-manifest HD gene carrier, there was no difference in striatal NAA/Cr or Cho/Cr compared to controls (Taylor-Robinson et al. 1996). Another study has contested spectroscopic evidence for altered energy metabolism in the HD brain, the group identifying no alteration in Lac or other measures taken to be markers of cellular energetic processes (Hoang et al. 1998). The authors of this particular study, go further suggesting that reports of lactate elevations are actually a function of CSF contamination in at least one of the earlier studies (Jenkins et al. 1993).

To summarise therefore, the nature of neurochemical disturbance in pre-manifest, as for manifest, HD remains unclear and less decipherable for the multitude of small, studies with heterogeneous methodologies and patient selection. The situation is further compounded by inter-study differences in measurements of

either combined or absolute metabolite measures and, undoubtedly also by the complexity of HD, with its diverse clinical phenotypes.

2.5.4 Phenotypic correlates

In both pre-manifest and manifest HD individuals altered metabolites, specifically striatal NAA and Lac/NAA (taken by the authors to be indicative of Lac) has been associated with a linear measure for disease progression or a measure of exposure to mutant huntingtin protein, the Disease Burden Score (DBS, calculated as age*CAG-35.5) (Jenkins et al. 1993, Jenkins et al. 1998, Van Oostrom et al. 2007). The authors further identified stronger chemical correlations with disease progression amongst those with CAG repeat expansions >45, and weaker correlations below this threshold, leading to the suggestion that the rate of neurochemical change may vary.

Other groups were not able to replicate NAA metabolite associations with CAG repeat size possibly because of the use of metabolite ratios rather than absolute levels (Harms et al. 1997, Ruocco et al. 2007). Absolute Cr reductions correlated with CAG repeat length in individuals of a given age, suggesting again the influence of disease burden on regional brain metabolite alterations (Sánchez-Pernaute et al. 1999), while another group showed a trend to reduction in NAA/Cr with disease duration (Ruocco et al. 2007). Other work did not identify any relationship between NAA/Cho and disease duration or patient age (Harms et al. 1997). Overall,

identification of metabolite correlates with measures of disease progress underlines the importance of examining absolute metabolite estimations.

The Ruocco group was unable to correlate motor dysfunction, as measured by UHDRS score, with NAA/Cr ratio (Ruocco et al. 2007), however, another group identified strong correlations between declining performance on both a tapping task and the UHDRS-TMS with basal ganglia NAA reductions (r=-0.73 and-0.85, respectively). Lower levels of NAA also correlated with lower scores on a verbal fluency task (Sánchez-Pernaute et al. 1999). Interestingly, this study, which assessed both pre-manifest and manifest individuals, also identified a correlation between Cr reductions and performance on a number of cognitive and motor tasks (Sánchez-Pernaute et al. 1999). Cho reductions, in pre-manifest HD, with impaired performance on cognitive tasks (Gomez-Anson et al. 2007). Hence subclinical frontal lobe dysfunction may be linked with an anatomically appropriate metabolite abnormality.

2.5.5 Longitudinal & interventional MRS studies in HD

Relatively few longitudinal observational MRS studies have been performed for HD, and of those, most were actually clinical drug trials. Over two years, creatine supplements, administered as a potential neuroprotective to mitigate against defects in energy metabolism in HD, raised brain creatine levels (at one and two years) inferred by reduced NAA/Cr (Tabrizi et al. 2003, Tabrizi et al. 2005). In another, shorter experiment of only 8-10 weeks, also studying the effects of

creatine supplementation in symptomatic HD, no cortical Cr alterations were identified, although Glx was reduced – a finding interpreted by the authors as indicative of a potentially therapeutic, anti-excitotoxic response. Specifically, creatine mediated uptake of Glu (Bender et al. 2005).

Another MRS study examined the anti-excitotoxic, anti-glutamatergic, riluzole, in manifest HD. In this small study riluzole tended to reduce Lac/NAA and Lac/Cr ratios in the basal ganglia, that was interpreted by the authors as a reduction in Lac, a finding suggestive of a possible neuroprotective effect. These changes did not correlate with improvement in motor phenotype (Rosas et al. 1999).

A third therapeutic trial investigated CoQ10 supplementation as a means to augment aberrant energy metabolism in HD. At baseline both occipital Lac/NAA and CSF lactate-pyruvate ratios were elevated – consistent with altered oxidative metabolism – measurements that were reversed through the effects of CoQ10 over just two months of treatment. Furthermore, after discontinuing supplementation, cortical Lac/NAA returned to baseline. Given that CoQ10 is an anti-oxidant cofactor in oxidative metabolism pathways the authors interpret these findings as evidence of a potential neuroprotective role in HD, supportive of earlier findings of CoQ10 mediated abrogation of excitotoxicity in animal models of glutamate neurotoxicity (Beal et al. 1994, Koroshetz et al. 1997).

Collectively, these studies have therefore provided evidence that MRS may be a sensitive measure for subtle longitudinal neurochemical change in response to therapeutic interventions over even very short periods of follow up.

Overall, these studies are important. They not only suggest methods of potential neuroprotection, but also indicate that MRS may be sensitive to subtle, restorative neurochemical alterations over even very short periods of follow up and which may be vital for informing future drug development.

2.5.6 7T MRS in HD:

At the time of undertaking this experimental work, few 7T studies had been undertaken. The results of more recent work at this field strength will be discussed in Chapter 7.

This thesis was undertaken with the specific aim to more fully elucidate the role of MRS as a biomarker for HD, both in terms of the cross-sectional metabolite patterns at different disease stages, but also in longitudinal patterns of change. Beyond this, the aim was to identify whether biochemical alterations paralleled a clinical, motor decline in HD, and hence be considered an objective surrogate for clinical deterioration. Lastly, my objective was to identify whether there may be an indirect biomarker role for MRS in HD in identifying new plasma or "wet" biomarker metabolite candidates suitable for interrogation and potential exploitation. To this end, this thesis will examine three modalities within the major biomarker classes: imaging, clinical and biosamples.

Metabolite alteration in HD	Brain region	Disease stage*	N= (P, M, C =pre, manifest, Controls)	Ref.
Cross-sectional				
Some variation of: ↓ NAA, ↓ Cr, ↑ Glx, ↑ Lac	Putamen	Pre-manifest (9.4+/- 6.8yrs to pred. onset) Manifest (MDD; 0-3yrs)	17 P/ 10 M/ 10 C	Reynolds et al. 2005
↓ Cr, ↑ Glx, ↑ Lac, ↑ mI	Putamen, Thalamus	Juvenile HD	1 P/ 6 M	Reynolds et al. 2008
NS metabolite alterations	Putamen	Pre-manifest	19 P/ 9 C	Van Oostrom et al. 2007
↓ NAA/Cr	Thalamus	Manifest (MDD: 9.3 yrs (SD 4.4))	22 M/ 25 C	Ruocco et al. 2007
↓ Lac/NAA NS - NAA/Cr, Cho/Cr	Parieto-occipital Cerebellum	Manifest	23 M/ 28 C	Martin et al. 2007
Frontal: ↓Cho Basal ganglia: NS – all metabolites.	Frontal Basal ganglia	Pre-manifest	14 P/ 17 C	Gomez-Anson et al. 2007

↓ NAA, Cr	Basal ganglia	Pre-manifest (asymptomatic) Manifest (MDD: 5yrs (SD 0.9))	4 P/ 6 M/ 5 C	Sánchez-Pernaute et al. 1999
WM: ↑ mI/Cr GM & WM: ↓ NAA/Cr Basal Ganglia: ↓NAA (NS) & Cr, ↑mI & Cho	GM, WM, Basal ganglia	Manifest	15 M/ 20 C	Hoang et al. 1998
All HD (Basal ganglia) : ↓ NAA/Cr Pre-manifest HD (Basal ganglia): ↑ Lac/Cr, ↑ Cho/Cr Manifest HD (Occipital cortex): ↑ Lac/NAA, ↑ Cho/NAA	Basal ganglia Occipital cortex	Pre-manifest Manifest (DDR; 0-15 yrs)	8 P/ 31 M/ 17 C	Jenkins et al. 1998
↓ NAA/Cho** ↑ Lac/Cho***	Frontal	Pre-manifest (asymptomatic) Manifest: -mild-severe (UHDRS 15-85)	4 P/ 17 M/ 19 C	Harms et al. 1997
Manifest HD (Striatum): ↑ Glx/Cr Manifest HD Cortex & Pre-manifest (all regions): No metabolite alteration	Striatum Occipital cortex Temporal cortex	Pre-manifest (asymptomatic) Manifest (early HD; DDR; 1-3 yrs)	1 P/ 5 M/ 14 C	Taylor-Robinson et al. 1996
Manifest HD (Striatum): ↑ Glx/Cr	Striatum Thalamus	Pre-manifest (asymptomatic) Manifest	1 P/ 3 M/ 14 C	Taylor-Robinson et al. 1994

Manifest HD: ↑ Glx/Cr In some cases: ↓ NAA/Cr ↑ Lac/Cr	Putamen & Globus pallidus	Manifest (MDD; 3 yrs)	9 M/ 9 C	Davie et al. 1994
Manifest HD (Occipital cortex): ↑ Lac/NAA, ↑ Cho/NAA Manifest HD (Basal ganglia): ↑ Lac/NAA,↑ Cho/NAA, ↑ Cr/NAA	Occipital cortex Basal ganglia	Pre-manifest (asymptomatic) Manifest (mild to moderate disability. MDD; 5.7+/-2.9 yrs)	2 P/ 16 M/ 12 C	Jenkins et al. 1993
Longitudinal & clinical therapeutic studies				
Riluzole: Basal ganglia: ↓ Lac/NAA, Lac/Cr (Trend) Occipital cortex: NS	Occipital cortex Basal ganglia	Manifest (mdd: 6.1yrs (SD 4.1))	8 M 15 C	Rosas et al. 1999
Cr supplement ↓ Glx, Glu & Gln NS - Cr	Parieto-occipital cortex	Manifest (mdd: 4.0yrs (SD 2.1))	17 M	Bender et al. 2005
Cr supplement ↑ Cr	Occipital lobe	Manifest	8 M/1 C	Tabrizi et al. 2003 Tabrizi et al. 2005
CoQ10 supplement ↓ Lac/NAA	Occipital cortex	Manifest	18 M	Koroshetz et al. 1997

Table 2-2 Magnetic Resonance Spectroscopy studies in HD. This table includes only studies preceding the work presented in this thesis. Metabolite abnormalities identified in all brain regions, unless region specified. Subsequent studies are discussed in Chapter 7. BG-basal ganglia, DDR-

disease duration range, GM-(cerebral) Grey Matter, MDD-mean disease duration, NS-not significant, OC-Occipital cortex, WM-(Cerebral) White Matter, *and age to predicted onset/disease duration where available.** In moderate and severely impaired manifest individuals, *** In both manifest and pre-manifest individuals.

3 Methods overview

3.1 Subjects

All of the subjects recruited in this study, were participants in either the "TRACK-HD" or "UBC Biomarker" biomarkers studies, taking place at the University of British Columbia (UBC), Vancouver, Canada. The aim of these studies was to identify and validate, both novel and existing putative biomarkers for HD. The modalities assessed included clinical, CSF and plasma biosamples, and imaging modalities. Full, written informed consent was obtained from all subjects where individuals had capacity. Where disease severity precluded this, subject agreement and assent of the next of kin was attained. The studies were approved by the Clinical Research Ethics Board at UBC. All HD subjects, both pre-manifest and manifest participants had, prior to these studies, been given their genetic diagnosis. Manifest individuals had also been previously and separately counseled regarding their clinical disease status.

3.1.1 TRACK-HD

TRACK-HD is an ongoing, multi-national longitudinal observational study of HD. Taking place over four sites; Leiden, London, Paris and Vancouver, this study is currently collecting data for its sixth year. The study evaluates clinical, biosample and imaging biomarker modalities. Participants at all sites comprise, pre-manifest gene carriers (Pre-HD) with a disease burden score >/=250 (age x (CAG-35.5)) (Penney et al. 1997). The DBS, an index of mutant huntingtin protein exposure, was used to select Pre-manifest HD individuals closer to predicted disease onset to

maximize comparisons with Controls. At the Vancouver site, of 25 Pre-manifest HD individuals involved in the main MRS baseline study, 22 had DBS of >250, however scores between 220-240 in the remaining three. Early HD individuals had been diagnosed by an HD specialist as having clinical onset of disease, with a diagnostic confidence level, based on the UHDRS-TMS, of 4/4 (equivalent to a >/=99% confidence that the individual had manifest HD). Assessments were performed at baseline, and then at approximately 12-monthly intervals. Data from the first 24 months of follow-up are presented here.

3.1.2 UBC Biomarker study

The UBC Biomarker study is a completed cross-sectional biosamples study in which paired blood and CSF samples were taken from controls and HD gene carriers. The HD gene carriers comprised individuals at each stage of the disease-pre-manifest, early, mid and late-stage manifest disease. Pre-HD individuals were defined by absence of sufficient motor findings on the Unified Huntington Disease Rating Scale-Total Motor Score (UHDRS-TMS) to meet clinical diagnosis of HD. The manifest HD group comprised clinically diagnosed individuals with reduced Unified Huntington Disease Rating Scale-Total Functional Capacity (UHDRS-TFC) consistent with Early, Middle and Late Stages HD, (as defined by UHDRS-TFC Score; 13/13 representing full independent function, 0/13 representing complete dependence). Informed consent was obtained from subjects except demented subjects, from whom assent was obtained (together with that of the next of kin).

3.1.3 Control subjects

The control subjects participating in either of the two studies were healthy individuals with no history of neurological or other major medical disorder. Controls were at-risk individuals who had received a negative HD genetic test result or unaffected spouses or friends with no family history of HD. As for the HD groups, all control subjects were recruited at the Centre for Huntington Disease, UBC Hospital.

3.2 Clinical assessments

The clinical assessment for the UBC Biomarker Study involved a full history, neurological examination, the standard Unified Huntington Disease Rating Scale-Total Motor Score (UHDRS-TMS) and Unified Huntington Disease Rating Scale-Total Functional Capacity (UHDRS-TFC) assessment (see Appendices 1 & 2). Where information for the UHDRS-TFC was difficult to obtain from a significantly cognitively affected individual, collateral history was obtained from a care-giver or spouse. For the TRACK-HD study these same assessments and a more comprehensive motor assessment was undertaken at baseline and annual visits.

3.2.1 TRACK-HD Qualitative Motor Assessment Battery

The TRACK-HD Qualitative Motor (QMotor) Battery utilized a pre-calibrated force transducer (Mini-40, ATI Industrial Automation, NC, USA) for all force transducer-based evaluations (Figure 1.1). The force transducer had a circular contact surface of 40 mm diameter. Its modular design enabled easy configuration/reconfiguration

for both glossomotographic (tongue pressure tasks) and digitomotographic (finger tapping) assessments. The individual assessments are detailed in Chapter 4. All data was sampled at 400 Hz, stored and analyzed on a flexible laboratory computer system (WINSC/WINZOOM, University of Umeå, Sweden). Data collection was performed by the author. Data processing and generation was performed blinded in the motor laboratory at the University of Munster using automated software.

3.3 Magnetic Resonance Spectroscopy

Subjects underwent MRI examination at 3T (Philips Achieva MR scanner). MR spectra were obtained using single-voxel PRESS localization sequence in the left putamen. Scan parameters included 3.5cm x 1cm x 1.5cm (5.25 cm^3) voxel size. A voxel of this size inevitably incorporated WM adjacent to putamen, however no other GM or CSF was included. Repetition time (TR) was 2000ms, Echo time (TE)=35ms, 1024 samples performed per spectrum. There were 128 signal averages. Spectral bandwidth was 2000Hz. Second order shimming was performed. Water concentration was 43,300mM. The default LCModel basis set for Philips at 3.0T, TE=35 ms was used for analysis. T1-weighted images were collected for volumetric analyses (for TRACK-HD) using 3DT1 Fast Field Echo (TR=7.7ms, TE=3.5ms, voxel size=1.1x1.1x1.1mm^3, 164 slices). Time constraints prevented repeat scanning where spectra were inadequate, or affected by movement. If TRACK-HD study images were also poor, subjects were recalled for re-examination and repeat spectra used. Screenshots were taken for individual voxel placements. This enabled correct 3D voxel positioning at follow-up visits,

through the manual placing of the voxel-of-interest (VOI) in the corresponding MRI slice on consecutive scans.

3.4 Plasma & CSF biosamples

3.4.1 Gas Chromatography/Mass Spectrometric (GC-MS) assay of myo-inositol

GC-MS analysis was performed using a Saturn 2100T model GC-MS (Varian, Inc., Walnut Creek, CA). The ion trap MS was equipped to deliver methane vapor into the source for chemical ionization and to perform selected ion monitoring. GC separation was carried out using Rtx-50 low bleed MS column (30 m × 0.250 mm, 0.25 μm film-thickness, Restek Corp. Bellefonte, PA). Stock solutions of myo-inositol (Sigma-Aldrich , St. Louis, MO) were prepared in water containing 10% methanol and stored at 4°C.

The samples preparation has been reported previously (Shetty, H.U. 1995a, b; Ma, K. 2006), the samples containing myo-inositol and the added internal standard ($^2H_6$ *myo-inositol*, CDN Isotope, Canada) were converted to acetate derivatives using acetic anhydride and pyridine (Alltech, Deerfield, IL) by heating for 2 hours at 80 ^{0} C. The reaction products were dissolved in a mixture of ethyl acetate and hexane and washed with $NaHCO_3$ solution (Sigma-Aldrich, St. Louis, MO). The organic layer was evaporated to dryness and the residue was reconstituted in ethyl acetate. The derivatized sample was injected (splitless) into the GC-MS at a column temperature of 150°C. The column temperature was increased first to 190°C at a rate of 10°C/min and then to 230°C at 2°C/min. When the target molecules were

eluted out, the column was heated (10°C /min) to 290°C and held at this temperature for 9 min and then returned to the initial condition. The MS was operated in the chemical ionization mode using methane as the reagent gas. The fragment ions *m/z* 373 for myo-inositol and *m/z* 379 for $^{2}H_{6}$ my-inositol were selectively monitored. The ratio of peak area to the internal standard for myo-inositol was used from the standard curves generated. mI was obtained from Sigma Chemical Co.(St. Louis, MO). Pyridine and acetic anhydride were obtained from Alltech Associates, Incorporated (Deerfield, IL), and solvents were from Burdick & Jackson (Muskegon, MI). The deuterium-labelled internal standard from Merck Sharp & Dohme/Isotopes (Canada). The gas chromatograph/mass spectrometer was a Finnigan MAT ITS40 (San Jose, CA). The capillary column was from Restek Corp. (Bellafonte, PA). This study was conceived of and designed by the author, whom also initiated a collaboration with Prof Rapoport's group. The procedure was undertaken by Professor Rapoport's group (including Dr's Ken Ma and Uemesha Shetty) based at Maryland, USA.

3.4.2 S100B assay

Immunoassay methods were used to measure S100B. The S-100 Beta ELISA kit from Alpco Diagnostics (48-S1BHU-E01, 26G Keewaydin Drive, Salem, NH 03079) was used for the quantitative determination of S100B in plasma samples. The assay is based on the sandwich model enzyme linked immunosorbent assay. Duplicate 30ul aliquots of plasma sample were assayed. During the first immune reaction, S100B in standards/samples were bound to rabbit anti-bovine S100B

antibody coating the surface of the microplate. After incubation and plate washing, labelled antibody (biotinylated rabbit anti-bovine S100B antibody) was added to bind to the antigen-antibody complex. Then, HRP labeled streptavidin (SA-HRP) was added to form the biotinylated rabbit anti-bovine S100-antigen-antibody complex. Finally HRP enzyme activity was determined by o-phenylenediamine dihydrochloride (OPD) and the concentration of human S100B in samples calculated. The lower limit for detection in the assay was 98pg/ml.

3.4.3 LPO-586 assay

A commercially available lipid peroxidation kit (LPO-586, Bioxytech) was used to measure the malondialdehyde (MDA) and 4-hydroxyalkenal (HAE) concentrations in patient plasma. Lipid peroxidation products malondialdehyde (MDA) and 4-hydroxyalkenals (HAE) were quantified in 200ul plasma aliquots. The assay is based on the reaction of a chromogenic reagent, N-methyl-2-phenylindole (R1), with MDA and 4-hydroxyalkenals at 45°C to yield a stable chromophore with maximal absorbance at 586 nm. All samples were tested in duplicate. The chromogenic reagent, (0.650 ml) was poured into a polypropylene microcentrifuge tube. EDTA plasma (0.2 mL) was added and the mixture vortex-mixed. The reaction was started by adding 0.15 mL of 10.4 mol/L methanesulfonic acid, mixing, and incubating at 45°C for 60min. The reaction mixture was cooled to room temperature and 0.2ml clarified samples were transferred to microtitre plate and absorbance determined at 586nm.

3.5 Statistical analysis of results

The statistical packages StatPlus:mac LE:2009 © 2001-2009 (AnalystSoft Inc., Vancouver) and GraphPad Prism version 4.0 for Windows, (GraphPad Software, San Diego California, USA, www.graphpad.com) were used in this work for linear regression, and One-Way ANOVA/Student's t-tests, respectively.

4 Clinical motor biomarkers

4.1 Chapter Introduction

The confirmation of the presence of cognitive, motor and neuropsychiatric abnormalities in pre-manifest individuals (Paulsen et al. 2006, Duff et al. 2007, Paulsen et al. 2008, Tabrizi et al. 2009) reinforce the concept of a prodromal period, in which individuals maintain functional capacity despite the onset of neuronal dysfunction; a time that represents the optimal window of opportunity in which to initiate disease-modifying therapy. Furthermore as phenotypic rather than neuroimaging or biochemical measures the progression, or arrest, of clinical motor endpoints in therapeutic trials have obvious functional implications for the individual. There is a strong rationale therefore for developing clinical HD biomarkers.

A unique aspect of the TRACK-HD study has been the adaptation of tasks comprising the motor section of the standard UHDRS assessment (such as tongue control and finger tapping) into an objective quantitative motor battery that uses novel, modular, laboratory equipment (Figure 4-3). In this chapter motor data, both standard and novel Quantitative Motor measures, collected by the author from the Vancouver TRACK-HD cohort will be presented. The purpose will be primarily to correlate the HD motor phenotype, and hence an aspect of clinical disease progression, with putaminal metabolite changes assessed by MRS (see Chapter 5). Of the multitude of QMotor tasks, only those with evidenced and robust, sensitivity will be considered, specifically tasks from among the

digitomotographic (finger tapping) and glossomotographic (tongue pressure) modalities.

4.2 Investigation of the role of standard motor measures as biomarkers for HD

4.2.1 Introduction

The Unified Huntington Disease Rating Scale (UHDRS) and each of its four domains; behavioural, cognitive, functional and motor were developed by the Huntington Study Group (HSG) as a means of assessing response to therapeutic interventions in symptomatic HD (HSG, 1996). This paper, in describing the UHDRS-Total Motor Score (UHDRS-TMS) demonstrated a high level of inter-rater reliability among 24 manifest HD individuals ranging from early to mid-stage disease, with an intraclass correlation coefficient of 0.94 (HSG, 1996). Furthermore the UHDRS-TMS, along with the functional checklist, exhibited a high level of internal consistency. However, over 6 months of evaluation the utility of the UHDRS-TMS and UHDRS-Total Functional Capacity (UHDRS-TFC) as a measure of disease progression in 180 manifest individuals was unclear (HSG, 1996). Despite this, the UHDRS-TFC and TMS have, since then, been used widely at Huntington Study Group (HSG) clinical sites in North America, Europe, and Australia. Together with modified motor scores derived from the UHDRS-TMS, this scale has been used extensively as an outcome measure in HD therapeutic trials (Tabrizi et al., 2005, HSG: TETRA-HD, 2006, Hersch et al., 2006; Landwehrmeyer et al. 2007, HSG TREND investigators, 2008, Kieburtz et al. 2010, de Yebenes et al. 2011) but also more widely as a quantifiable clinical assessment of HD patients.

It should be noted however, that by their very nature as observer-rated clinical measures, both UHDRS-TMS and UHDRS-TFC are effectively performed un-blinded for early HD individuals, at least. Consequently these scales are inherently open to observer bias and subjectivity. Furthermore, since the UHDRS-TFC is a patient/witness reported measure this may also be subject to inaccuracies for a wide range of reasons, including denial of loss of independence. The UHDRS-TMS was designed for evaluations in manifest HD (HSG, 1996), with uncertain sensitivity in pre-manifest HD, and is susceptible to inter-rater variability, possibly especially so in these individuals (deBoo et al. 1998). These limitations in the UHDRS-TMS have led to demand for the development of a battery of quantifiable motor tests such as the QMotor battery used in TRACK-HD. This battery was designed with the aim of identifying motor dysfunction and its progression in pre-manifest individuals, the ideal group in which to initiate neuroprotective strategies.

The aim of this experiment was to evaluate the efficacy of clinical biomarker measures, specifically the widely used UHDRS-TMS and TFC in HD, with a view to subsequent comparison to novel motor measures-the Quantitative Motor or QMotor tasks in section 4.3. The evaluation of both standard and novel motor measures is critical to the evaluation of MRS as a biomarker for HD.

4.2.2 Methods

Subjects

All subjects were recruited and evaluated at UBC, Vancouver, as part of TRACK-HD (Tabrizi et al. 2009). Participants were enrolled between January and August 2008. Subjects were evaluated using UHDRS-TMS and UHDRS-TFC at three visits; baseline, 12 and 24 months between January 2008 and September 2010. Enrolled participants were Early HD (n=30), Pre-manifest or PreHD (n=30) or Controls (n=30, partners or unaffected relatives of PreHD/Early HD subjects). Early HD individuals had all received the genetic diagnosis and been diagnosed with clinical onset but maintained a level of independent function compatible with Early Stage disease based on UHDRS-TFC (UHDRS-TFC; Early Stage 1 TFC ≥ 11 to ≤ 13 or Early Stage 2 TFC ≥ 7 to ≤ 10) (see Appendix 2, Shoulson & Fahn, 1979). PreHD participants were selected based on; i) CAG repeat expansion within the *HTT* gene (40 CAG repeats or greater), ii) UHDRS motor component score of five or less, indicating absence of marked motor deficits and iii) DBS of 220 or greater at baseline. The DBS, an index of mutant huntingtin protein exposure was calculated as outlined. Of 30 Pre-HD individuals at baseline, 27 had DBS of >250 with scores between 220-240 in the remaining three.

Because major drug changes, specifically alterations in neurotropic medications, such as antipsychotics, anxiolytics and antidepressants can have an impact on clinical features; specifically on suppression of chorea, all subjects undertaking major medication changes between visits were excluded from a second analysis of this data.

Procedures

All subjects underwent the standard assessment using the UHDRS-TMS and UHDRS-TFC as per standardised procedure, performed by the author of this work (see Appendices 1 & 2). In order to meet TRACK-HD Quality Control standards, the assessor was required to perform an annual revalidating evaluation. This required the correct UHDRS-TMS assessment, on each occasion, of three videotaped HD-affected individuals rated by Ralf Reilmann of the EHDN (http://www.euro-hd.net/html/disease).

4.2.3 Results

Subject Distribution

	Controls (n without major drug changes, same all visits)	Pre-HD (n without major drug changes, same all visits)	Early HD (n without major drug changes, same all visits)
Baseline	33 (25)	30 (19)	33 (17)
12 Months	30	30	31
24 Months	29	29	29

Table 4-1 Subject numbers at sequential visits. Loss of subjects in any group was due to drop out to further follow up.

UHDRS-TMS

At baseline, UHDRS-TMS among Pre-HD individuals was not significantly different from Controls-a likely reflection of the upper tolerated UHDRS-TMS of 5 for Pre-HD during recruitment. Interestingly, at 12 and 24 months an increasing

separation between motor scores was seen between Pre-HD and Controls, with the difference reaching significance at the 12 month cross-sectional analysis. Predictably the Early HD group was distinguishable from Controls and Pre-HD individuals at baseline and subsequent time points (Figure 4-1). Over 24 months the trend therefore was of increase in TMS in HD gene positive individuals (see Figures 4-1 and 4-2). As might be expected, given the development of the UHDRS-TMS primarily for the measurement of motor deficits in manifest disease, the evaluation detected greater change over 24 months in Early HD than in Pre-HD individuals. On longitudinal evaluations of the same individuals (including therefore only individuals attending all 3 visits) the same pattern was evident although it is notable that the maximal change in motor scores, for both HD groups, was at the 12 month timepoint.

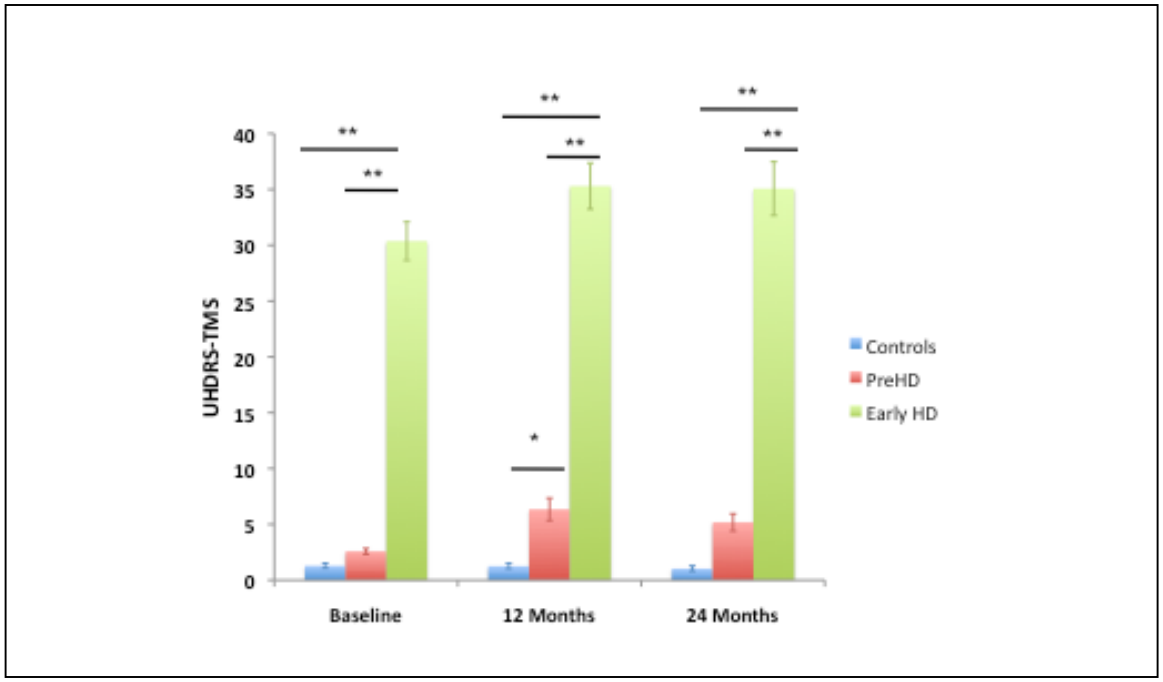

Figure 4-1 Cross-sectional analyses of UHDRS-TMS in Control, Pre-HD and Early HD. All comparisons made using One-Way ANOVA with post-hoc Newman-Keuls Multiple Comparison Test. *p<0.05, **p<0.01, ***p<0.001.

Because the UHDRS-TMS reflects an individual's chorea, medications widely used to suppress chorea-specifically neuroleptics and the VMAT2 inhibitor, tetrabenazine, can have a marked affect on the individual's overall score. Similarly, concomitant acute mood disturbances and anxiety can amplify motor deficits, generating simple errors on, for example, rapid alternating hand movement and the Luria three-step test of psychomotor processing. Based on the crude presumption that individuals on stable neuroleptic/antidepressant medication over the 24 months, will not have a significant change in the degree to which medication may have affected their motor phenotype, UHDRS-TMS was evaluated both in cross-section and longitudinally excluding individuals exposed to marked

changes in drug regimens. Such changes were defined, specifically for neuroleptics, tetrabenazine, antidepressants and benzodiazepines as 1) discontinuation of the drug, (not substituted by another drug of the same class) or 2) initiation of a regular medication. After removal of these individuals, the same patterns of subgroup changes as those demonstrated in Figures 4-2 persisted.

UHDRS-TFC:

The UHDRS-TFC, a signifier of loss of functional independence, was unsurprisingly largely unaffected in Pre-HD individuals compared to Controls. Thus, it was only in Early HD that TFC was significantly reduced compared to Controls or Pre-HD individuals. There was some evidence of progressive TFC reduction in Early HD, at 12 months, and a smaller, non-significant, further decline in function at 24 months. An observation supported by the lack of change on longitudinal analysis of this subgroup (Figure 4-2).

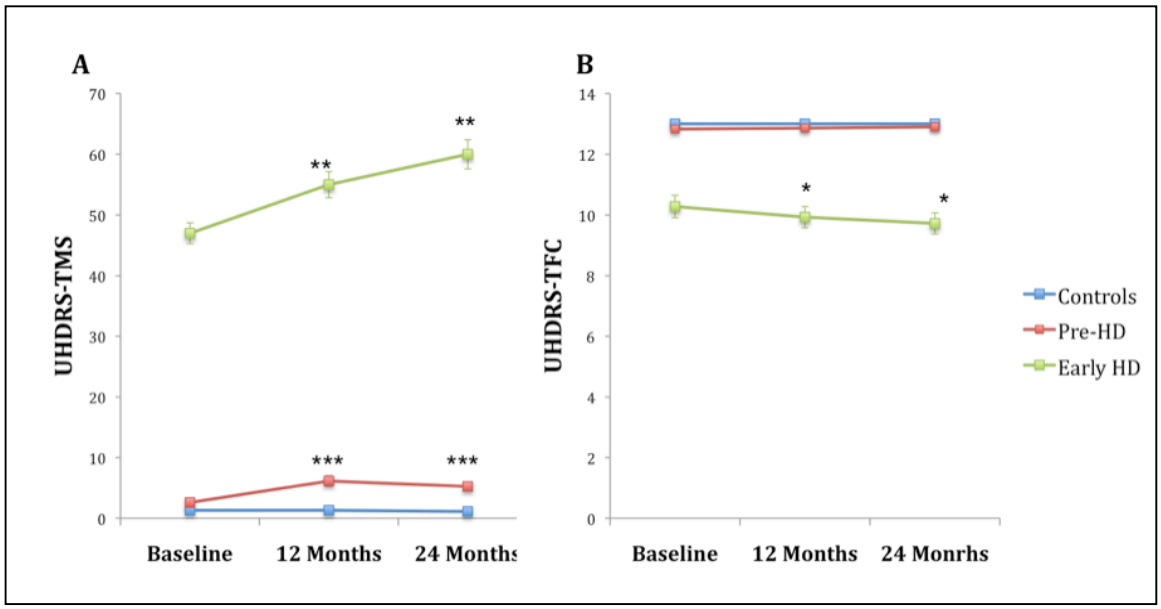

Figure 4-2A and B Shows longitudinal progression in UHDRS-TMS and TFC over 24 months. Asterisks over time points correspond to significance vs. baseline measure, while asterisks over connecting lines (none present), would suggest significance between two time points (eg. progression between 12 to 24 months). * p,0.05, ** p<0.01, *** p<0.001. Error bars denote SEM. Measures at all time points were paired, and paired t-tests used for comparisons.

4.2.4 Discussion

Despite the smaller size of our cohort compared to the main TRACK-HD study, the UHDRS-TMS and less so, the TFC demonstrated longitudinal sensitivity to disease progression in Early HD. The motor score also identified motor decline in pre-manifest disease also. The findings presented here follow the pattern, over 24 months, of UHDRS change in the entire TRACK-HD study, albeit with predictably less sensitivity to dynamic changes over shorter, 12 month, intervals (Tabrizi et al. 2012). In that study both the TMS and TFC correlated with brain tissue atrophy, specifically loss of white matter, grey matter and whole brain volume. Interestingly, loss of caudate volume but not putamen was associated with changes in TFC, and vice versa for TMS (Tabrizi et al. 2012). Further work needs to be done to elucidate the causal nature of these associations, likely utilizing fMRI.

As discussed, both the UHDRS-TMS and TFC have been widely used in therapeutic studies in symptomatic HD and this may be merited given their ability to outperform a number of tasks from a novel, custom-designed Qmotor battery developed specifically to measure subtle progression of motor deficits in pre-manifest and symptomatic individuals (Tabrizi et al. 2012). The UHDRS-TMS is therefore a useful measure by which to correlate the motor phenotype of HD with *in vivo* metabolic markers of neuronal dysfunction and against which to compare the efficacy of other biomarker modalities. The UHDRS-TFC has clear, obvious limitations in pre-manifest disease where deficits in independent functioning due to HD are, by definition, improbable. This lack of sensitivity of the UHDRS-TFC over

the disease's full course will limit its utility as a marker for therapeutic trials, particularly given the interest in disease modification in pre-symptomatic individuals.

One particular concern is how a scale designed to measure features in symptomatic HD, will perform as a measure of disease progression in presymptomatic or pre-manifest HD individuals. The UHDRS-TMS, has to some extent been validated now in pre-manifest HD (Paulsen et al. 2008, Biglan et al. 2009, Tabrizi et al. 2012), although is likely relatively insensitive to subtle motor changes in these individuals. In the entire TRACK-HD cohort, over just 12 months of longitudinal follow-up UHDRS-TMS was able to demonstrate a significant deterioration for all HD groups compared to controls. It also identified differential rates of motor disease progression among all HD subgroups, including pre-manifest individuals furthest from predicted disease onset (>10.8 years), and distinguishable from controls. This distinction was made with an efficacy comparable with some of the strongest longitudinal biomarkers volumetric imaging measures of putamen, caudate and whole brain volume (Tabrizi et al. 2011).

The mean annualised rates of UHDRS-TMS decline in this restricted cohort (Controls, mean+/-SD; -0.129+/-0.598, Pre-HD; 1.28+/-1.67, Early HD; 2.35+/-3.77) were actually slightly greater than those measured in the overall TRACK-HD study-12 month longitudinal study (Tabrizi et al. 2011). The mean annual

deterioration in UHDRS-TMS over 24 months was also greater in all Pre-HD and Early HD subgroups than Controls. In early HD subgroups UHDRS-TFC exhibited significant decline from baseline to 12 months and 12 to 24 months of follow-up (Tabrizi et al. 2011, Tabrizi et al. 2012). Over 24 months decline in UHDRS-TMS, modelled as an outcome measure using derived effect sizes, outperformed all other clinical measures (cognitive, QMotor and psychiatric) in Pre-HD, the majority of cognitive and QMotor measures and all psychiatric measures in Early HD (Tabrizi et al. 2012).

The performance of the conventional HD motor assessment (TMS) against the novel Qmotor battery is now being more intensively scrutinized within the TRACK-HD study (Tabrizi et al. 2012). The next section will now focus upon the Qmotor battery and its ability to track progression within the smaller UBC cohort.

4.3 Investigation of the role of quantitative motor measures as HD biomarkers

4.3.1 Introduction

Quantitative Motor (QMotor) tasks were developed as objective equivalents of the standard, UHDRS-Total Motor Score (UHDRS-TMS) evaluation. The UHDRS-TMS has well recognized limitations including the potential for inter-rater variability and examiner subjectivity or bias. Furthermore, given the development of the UHDRS-TMS as a tool for assessing manifest HD subjects, it may exhibit relative insensitivity to motor deficits within pre-manifest HD individuals. A growing body of work suggests that force-transducer based assessments are able to detect early motor deficits in pre-HD individuals (Paulsen et al. 2008, Tabrizi et al. 2009, Bechtel et al. 2010, Tabrizi et al. 2012), and decline in performance on tapping based tasks has also been associated with time to predicted disease onset (Paulsen et al. 2008).

Of the Qmotor battery, in cross-sectional analyses across all TRACK-HD sites, glossomotographic (tongue pressure) and digitomotographic (finger tapping) tasks outperformed other Qmotor tasks, cognitive and neuropsychiatric measures suggesting that of clinical biomarkers these measures may be among the most sensitive by which to differentiate group performance. Specifically, these tasks were sensitive enough to differentiate PreHD-A individuals (>10.8 years from onset) from Controls, PreHD-A from PreHD-B (<10.8 years from onset), PreHD-B from Early HD 1 (stage I disease) and Early HD stages 1 from 2-among the most

challenging cross-sectional differentiations (Tabrizi et al. 2009). In longitudinal analyses digitomotographic and, less so glossomotographic, QMotor measures in early HD exhibited statistically significant change compared to controls. One measure in particular, the mean intertap interval (non-dominant hand) even demonstrated progression over 12 and 24 months in both pre-manifest HD-A and B groups (Tabrizi et al. 2012). It is important to note, however, that for any given clinical marker, including Qmotor, UHDRS-TMC and cognitive assessment, measurement of disease progression over 24 months was inferior compared to one or more of the study's volumetric neuroimaging biomarkers (Tabrizi et al. 2012).

A large cross-sectional analysis of digitomotography (tapping-based tasks using a force transducer) utilizing the international, entire TRACK-HD cohort identified correlations with UHDRS-TMS among HD, PreHD and all gene positive individuals. This correlation with an established scale for clinical and research orientated measurement of motor dysfunction, suggests digitomotography may usefully track global phenotypic progression (Bechtel et al. 2010). Importantly, this work confirmed that tasks within two digitomotographic modalities-speeded tapping and metronome tapping were able to distinguish Controls, PreHD and Early HD groups from one another and confirming earlier suggestions of the presence of subtle, sub-diagnostic motor deficits in pre-manifest HD (Penney et al. 1990, Kirkwood et al. 1999) up to even a decade or greater prior to predicted disease onset (Paulsen et al. 2008, Bechtel et al. 2010). Indicating even greater sensitivity, the subgroups PreHD-A (>10.8 years from predicted disease onset), PreHD-B

(<10.8 years from predicted disease onset), Early HD Stage 1 and Early HD Stage 2 (early manifest disease categorized by UHDRS-TFC) were all distinguishable from each other and Controls using digitomotographic and less so, glossomotographic measures (Tabrizi et al. 2009, Bechtel et al. 2010). Of the tasks, speeded tapping appeared more sensitive to the earliest changes in HD, while metronome tapping appeared better able to distinguish early manifest individuals with Stages 1 and 2 disease. Performance on these tasks was correlated with predicted onset of disease within five years among PreHD individuals and also with volumetric imaging measures of striatal, cortical and white matter atrophy and cortical thickness. The latter implies possible aetiological association of these phenotypic measures with the underlying neuropathology (Bechtel et al. 2010). Thus, in gene positive individuals (early HD and pre-manifest HD) variability in speeded tapping tap duration and variability in speeded tapping inter-tap onset interval correlated with atrophy of the putamen, caudate, internal capsule, external capsule, regional WM, and also parietal, occipital and primary motor cortex as measured by VBM and cortical thickness measurements, respectively (Bechtel et al. 2010).

In early HD, decline in speeded-tapping intertap interval over 24 months was significantly associated with worsening global motor dysfunction as measured by UHDRS-TMS decline (partial correlation=0.219, p=0.024) and was one of relatively few clinical markers that correlated with TMS (Tabrizi et al. 2012). Interestingly, deteriorating performance on quantitative motor tasks did not significantly correlate with decline in independent function as measured by the UHDRS-TFC

over the same duration. Importantly, effect sizes calculated on the basis of decline over 24 months suggested that "variability of speeded-tapping tap duration", one of the most sensitive quantitative motor measures was larger than UHDRS-TFC and TMS, both of which have been widely used as outcome measures in therapeutic trials (Tabrizi et al. 2012).

These findings collectively support earlier evidence of the reproducibility and reliability of digitomotographic deficiencies in manifest HD, and their progression over time (Michell et al. 2008, Paulsen et al. 2008, Tabrizi et al. 2009, Bechtel et al. 2010).

In this Chapter, digitomotographic and glossomotographic tasks will be evaluated as markers of disease progression in HD, with a view to ultimately comparing the biomarker utility of these measures to Magnetic Resonance Spectroscopy in subsequent Chapters.

4.3.2 Methods

Subjects:

Subjects were selected as outlined in Section 4.2.2.

Procedures:

Digitomotography (Tapping Measures):

In digitomotographic assessments (Figure 4-3), the subject placed the palm of the non-dominant hand upon a support platform directly in front of the force transducer. The set-up allowed the subject to easily tap the force transducer with the index finger. The start of a tap was defined as a force rise of 0.05 N above maximal baseline level. The tap ended when it dropped to 0.05 N before reaching the baseline level again. Non-dominant hand performance measures were the primary outcome variables of interest in these assessments, due to their higher sensitivity to group differentiation and disease progression (Tabrizi et al. 2009, Tabrizi et al. 2012) although dominant hand performance was also examined for the purpose of comparison with metabolite measures within the left putamen, and are considered in Chapter 5.

<u>A. Speeded tapping tasks:</u>

During speeded tapping the subject was required to tap at their maximal rate between two cues (a start and a stop tone), 10 seconds apart. Automated software generated the following three primary outcome measures for speeded tapping;

i) 'Tap Duration Variability',

ii) Inter-Onset-Interval variability in inter-onset intervals or 'Repetition Time Variability',

iii) mean interpeak intervals or 'Mean Inter-tap Time'

B. Metronome tapping tasks:

During digitomotography, precision of timing for self-paced tapping was also recorded. Subjects matched auditory cues (1.8Hz rate) and continued tapping with the same frequency for 10 seconds after cues had stopped. Five trials were performed. Automated software generated the following two primary outcome measures for metronome tapping; Variability of deviations of:

i) Inter Onset Interval – 'Deviation Of Tap Initiation From Paced Rhythm'

ii) Mid Tap Interval – 'Deviation from Paced Rhythm (middle of taps)'

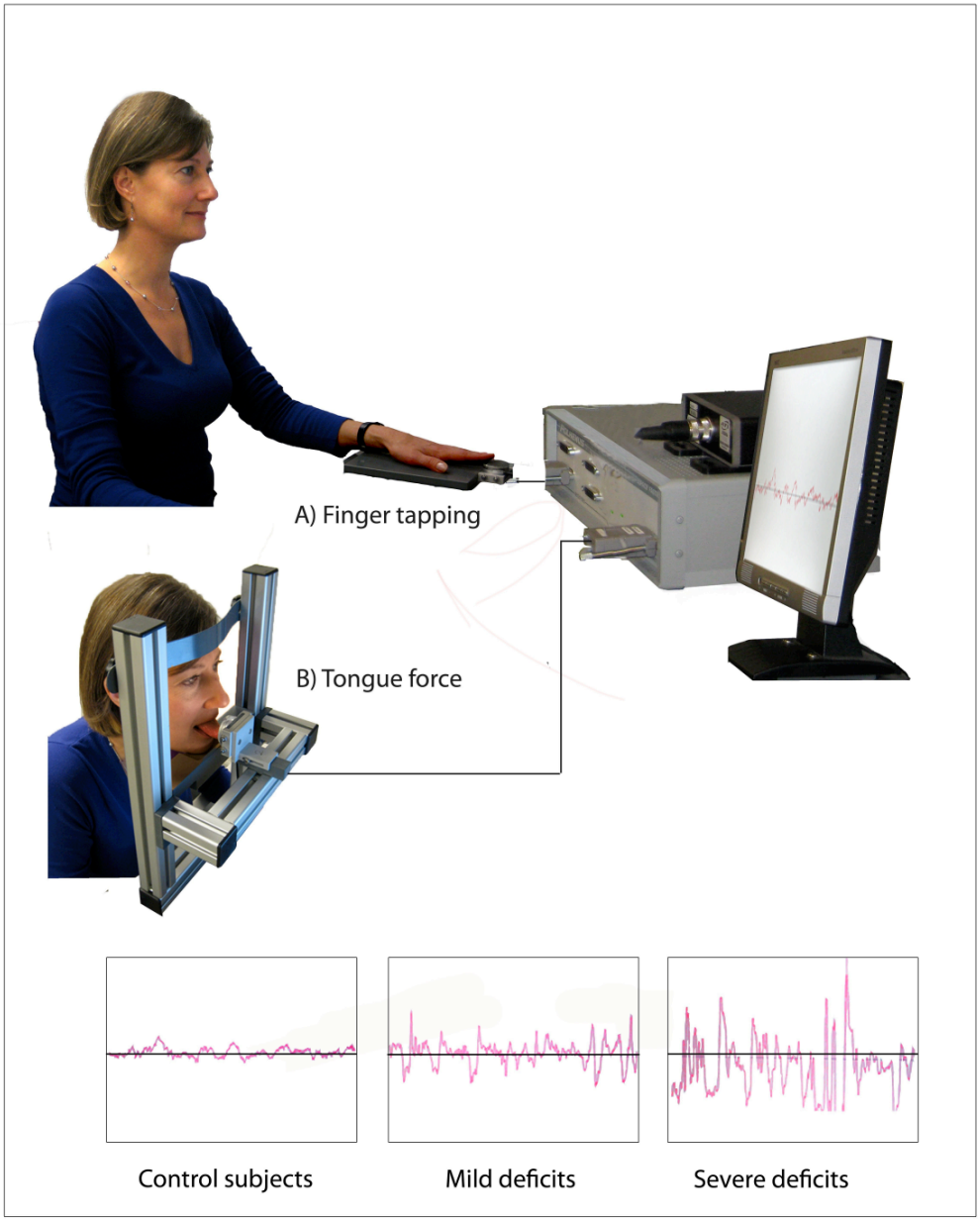

Figure 4-3 The QMotor apparatus. A Digitomotography, B. Glossomotography.

Glossomotography (Tongue Force Measurements):

Glossomotography (Figure 4-3) involves assessment of isometric forces during sustained tongue protrusion using a force transducer. Subjects seated on a chair facing a table, rested their chin upon a height-adjustable base, with the force transducer mounted 2cm from the lips. The surface of the transducer covered by a disposable cover, the subject was asked, upon a cueing tone, to open their mouth widely and protrude their tongue against the transducer. Using the tongue they were asked to generate sufficient isometric force to match a target force (0.5N) presented, as a straight line, on a monitor for 20 seconds, until a second cueing tone was heard. This was repeated until the subject had performed a total of four trials at two pressures: 0.25N and 0.5N. Tongue pressure variability (coefficient of variation) and contact time (percentage of time tongue was contacting transducer) were calculated for a 15s period prior to the second (final) queing tone for each trial. Tongue pressure tasks involved midline protrusion of the tongue. No lateral tongue movement was required.

4.3.3 Results

Subject distribution

	Controls	PreHD	Early HD
Baseline	31	25	32
12 Months	28	25	27
24 Months	27	25	26

Table 4-2 Subject numbers at sequential visits. Loss of subjects in any group was due to drop out to further follow up.

Cross-sectional analyses of QMotor performance in HD

In cross-sectional analyses both of the glossomotographic tasks; the logarithmised Static Coefficient of Variation and the Tongue Contact Time were able to distinguish Controls and PreHD individuals from Early HD individuals. However only the Static Coefficient of Variation enabled the more subtle differentiation of Controls from PreHD individuals (Fig. 4-4A & B). Similarly, all digitomotographic tasks (both speeded tapping and metronome tapping tasks), were able to distinguish Early HD and PreHD individuals from Controls, but only two of the three speeded tapping tasks (Tap Duration and Repetition Time variability) and one of the two metronome tasks (Deviation from Paced Rhythm, middle of the taps) were able to distinguish PreHD individuals from Controls (Fig. 4-5A-D). Of all the digitomotographic tasks, Speeded Tapping; Repetition Time Variability

enabled the most consistent and strongest discrimination of PreHD from Control individuals in cross-sectional analyses.

Figure 4-4 Cross-sectional Glossomotographic analyses. Tongue contact time (A) and Static tongue force (coefficient of variation) (B). Error bars denote SEMs. Statistical significance *One-way ANOVA*, *p<0.05, **p<0.01, ***p<0.001.

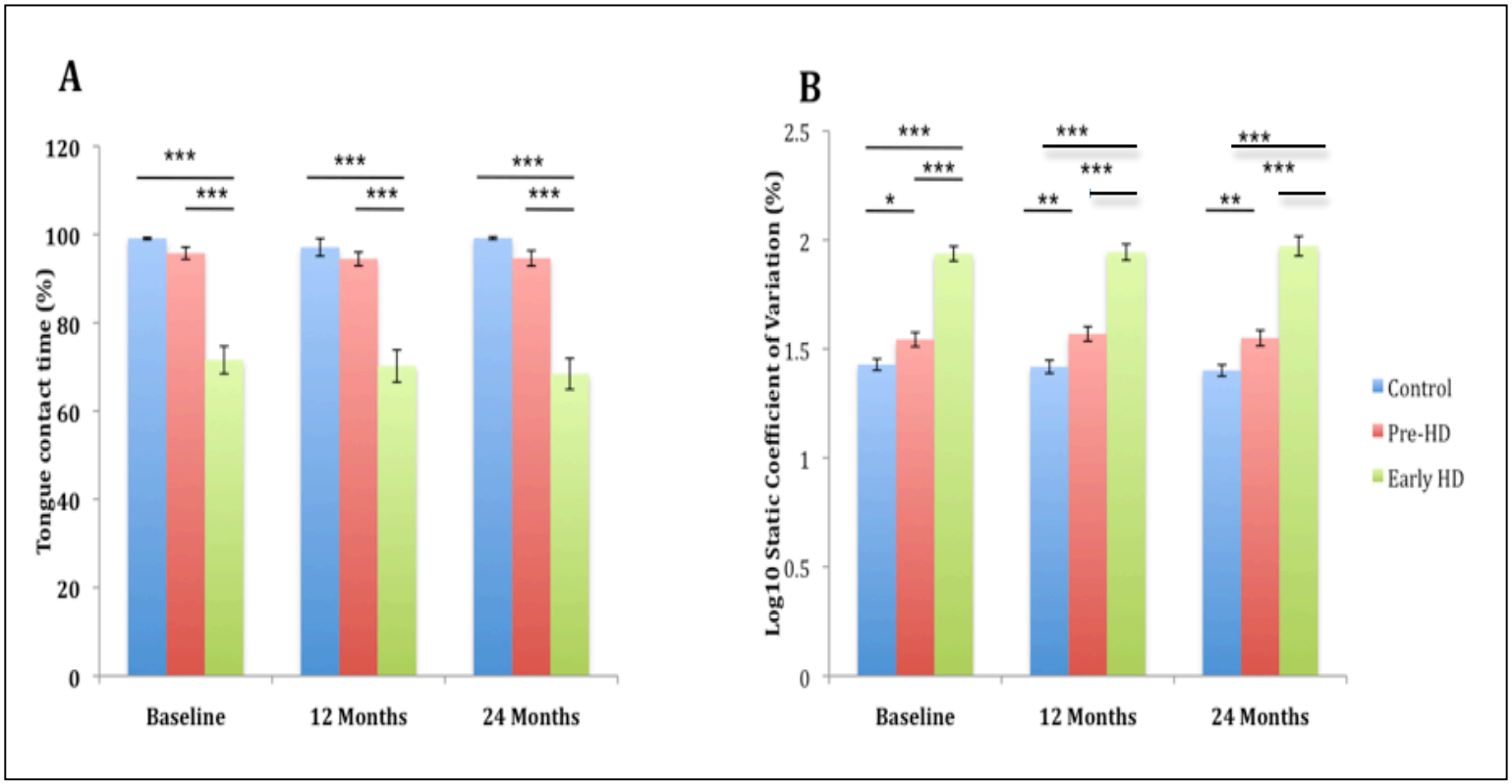

Figure 4-5 Cross-sectional Digitomotographic Analyses. A, B, C represent speeded tapping tasks, D & E represent metronome tasks. All logarithms displayed as positive to facilitate display. A reresents deviation in tap duration, B. the mean inter-tap time, C the repetition time deviation. D is a measure of tap initiation variability at the start of the metronome tapping task (1/SD), while E shows tap precision (deviation from paced rhythm) in the middle of the tapping task. Error bars denote SEMs. *p<0.05, **p<0.01.

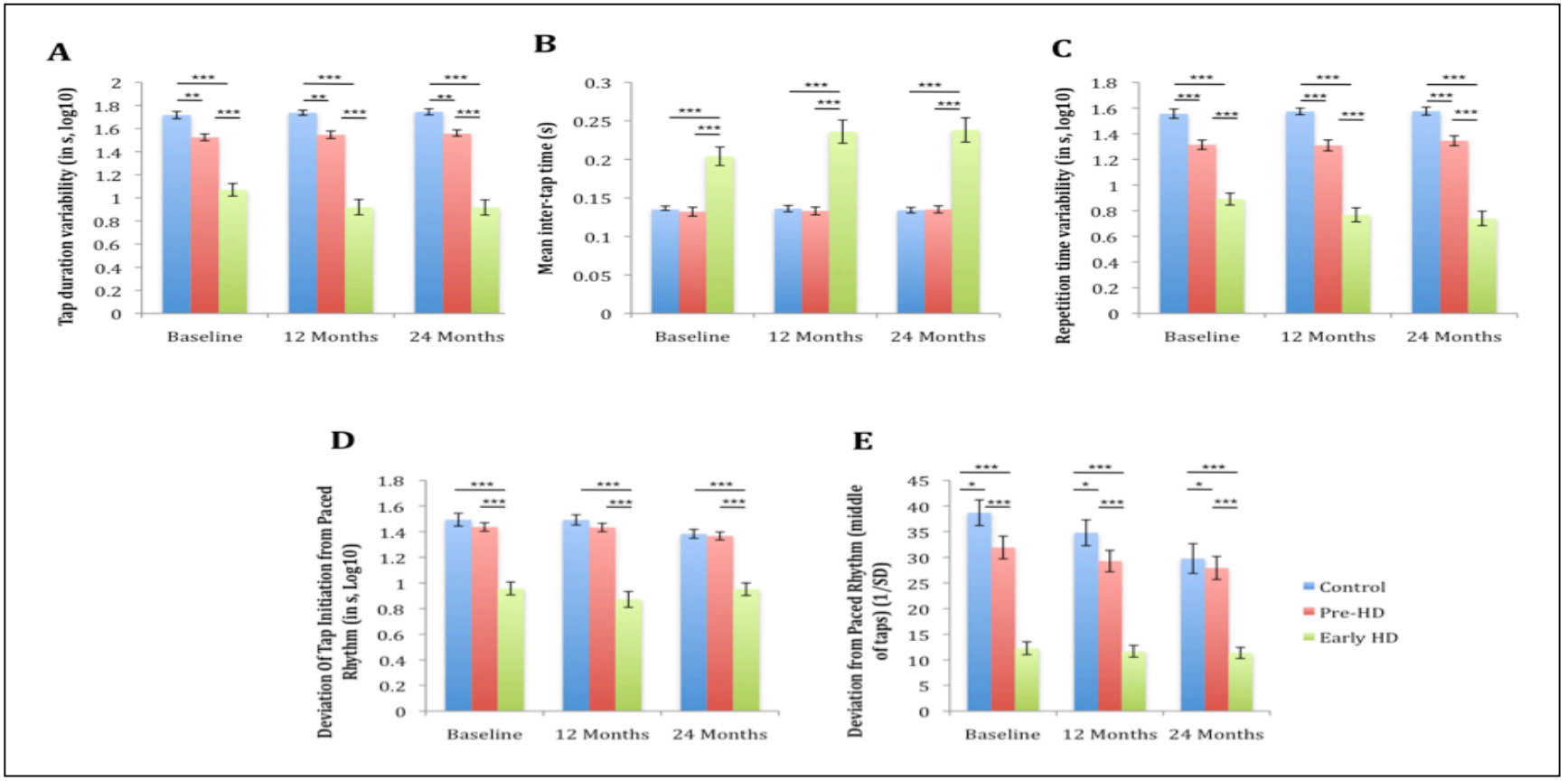

Longitudinal analyses of glossomotography & digitomotography:

On the glossomotographic tasks, none of the three subject groups showed any longitudinal change in their performance on the measures of tongue motor impersistence (Static Coefficient of Variation) or ability to keep tongue in contact with the pressure transducer (Tongue Contact Time) (data not shown). On longitudinal analyses of digitomotographic measures all of the Speeded Tapping tasks permitted some longitudinal measurement of disease progression, but only in the Early HD group (Fig 4-6). The Metronome Tapping tasks were unable to quantify any disease progression. The strongest measures of disease progression at 12 and 24 months compared to baseline were for Tap Duration variability and Repetition Time variability, with less significant longitudinal change seen for Mean Inter-Tap time measurement. No measure showed a significant longitudinal change from 12 Month to 24 Months. Correlations of quantitative motor performance with putaminal MRS findings are discussed in the next chapter.

Figure 4-6 Longitudinal analyses of Digitomotographic Tasks. A, B, C represent speeded tapping tasks, D & E; metronome tasks. All logarithms displayed as positivey. A represents deviation in tap duration, B; mean inter-tap time, C; repetition time deviation. D; measure of tap initiation variability at start of metronome tapping (1/SD), while E; tap precision (deviation from paced rhythm) in middle of tapping task (middle of taps). Error bars denote SEMs. Probabilities (asterisks) displayed over inter-connecting lines show comparisons between corresponding visits. Asterisks over a time point, correspond to probability of that time point vs. baseline. *p<0.05, **p<0.01, ***p<0.001.

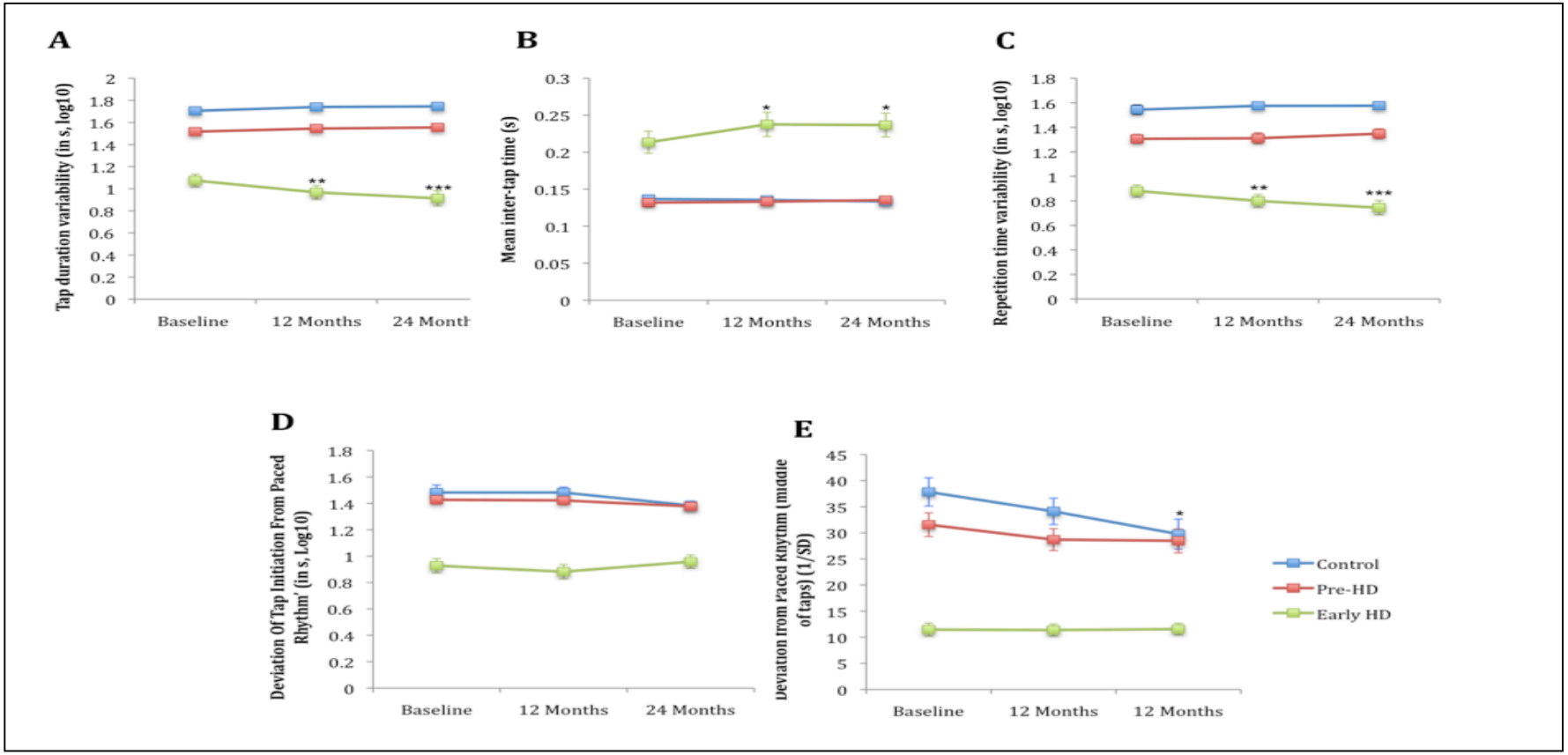

4.3.4 Discussion

Within this limited cohort, the Quantitative Motor tasks, both glossomotographic and digitomotographic, showed sensitivity to distinguish HD individuals; both PreHD and Early HD from Controls on cross-sectional analyses. These findings support the earlier description of impaired performance on objectively quantifiable motor performance in pre-manifest and symptomatic HD. The measurement of tongue force impersistence (tongue pressure variability), and control of movement (contact time) identified significant motor deficits in a similarly sized pre-manifest and manifest HD cohort (20 Controls, 15 PreHD, 20 Symptomatic HD) (Reilmann et al. 2010). Digitomotographic impairments have also been reported in pre-manifest individuals (n=61), compared to controls (Kirkwood et al. 2000). Furthermore in the main TRACK-HD study, a number of QMotor tasks including Speeded Tapping (Tap Duration Variability), Metronome Tapping (Deviation from a Paced Rhythm), Tongue Pressure Variability (Static Force Coefficient of Variation) were all able to distinguished all three groups (Controls, PreHD and Early HD) at baseline, 12 and 24 months (Tabrizi et al. 2009, Tabrizi et al. 2011, Tabrizi et al. 2012). As expected for a much larger study with over 360 participants, these inter-group differentiations reported for the main TRACK-HD study reached a much greater statistical significance than those reported here for the Vancouver cohort only. Overall this work echoes earlier studies' findings confirming, among this cohort, objectively quantifiable motor deficits among HD individuals a mean of 11.9 years before the individual reaches the predicted clinical, diagnostic threshold.

It is the demonstration of longitudinal change, and hence genuine disease progression within a cohort, that is the greater challenge. This assessment is more discriminating than cross-sectional evaluations that effectually, in the comparison of pre-manifest and early HD individuals, will often involve comparing individuals often decades apart in terms of their progression along the disease timeline (Tabrizi et al. 2012). Cross-sectional comparisons of biomarker modalities in this context have limited applicability in the measurement of disease progression in an individual or in testing the efficacy of a novel therapy in a clinical trial. Predictably, both digitomotographic and glossomotographic tasks performed less favourably on longitudinal analyses, but evolution of disease was demonstrable in some cases. While glossomotographic and metronome tapping tasks were unable to display motor deterioration in the HD groups over 24 months, the speeded tapping tasks were more sensitive identifying progression of motor dysfunction in Early HD. This demonstration of longitudinal change albeit only among Early HD subjects is impressive given the comparatively small cohort, but was, disappointingly, not replicated for PreHD subjects. This likely, in part, reflects the need for testing greater numbers of pre-manifest subjects to identify deteriorating subclinical motor function, since a digitomotographic task was able to identify motor progression in the main TRACK-HD study (Tabrizi et al. 2012). It is noteworthy that in all cases, based on the comparative levels of significance at consecutive visits, the first 12 months accounted for either all or most of the deterioration in motor performance; a finding that may suggest the presence of some practice

effect at the 24 month visit. Nevertheless, for two of the tasks consecutive deteriorations were demonstrable at 12 and 24 months, suggesting a real, sensitive measure of deterioration. The finding demonstrated here is important since this represents one of the first reports of consistent, objectively measurable motor decline over just 12 months within a small cohort (Andrich et al. 2007, Michell et al. 2008) and notably, in the absence of more detailed analysis of digitomotographic tasks, progression was only identifiable over a considerably longer duration (3 years) (Andrich et al. 2007).

4.4 Chapter Conclusions

Interestingly, while metronome tapping tasks were not generally associated with longitudinal change for any of the groups-there was the exception of the Deviation from a Paced Rhythm assessment in which between 12 and 24 months, a significant difference was noted between Controls but neither of the HD groups. The reason for this is unclear, but may conceivably be related to altered motivation during tasks among healthy volunteers. By comparison, within the UBC cohort, longitudinal UHDRS-TMS assessment at 12 and 24 months, was for both Early and PreHD groups, sensitive to disease progression. This sensitivity to progression in pre-manifest individuals was not evident with the QMotor analyses, but there was no evidence of significant change in UHDTS-TMS between 12 and 24 months indicative of a possible operator bias at the 12 month visit, as already discussed, and a clear potential weakness of the standardized, but subjective clinical score. This pattern was also present for the entire TRACK-HD cohort, with evidence of

marked difference in the first 12 months of follow-up that subsequently failed to decline at the same rate at later follow-up (Tabrizi et al. 2012). The UHDRS-TFC, again showed a significant difference at 12 and 24 months versus baseline, but there was no significant progression in the second year of follow-up, also suggestive of possible observer bias. The UHDRS-TMS was a less useful cross-sectional discriminator, showing no robust sensitivity to distinguish PreHD and Control individuals. Taking these results together, the Quantitative Motor tasks performed reasonably well, but were ultimately outperformed by the UHDRS-TMS in this cohort. However, the ability to show evolving, significant deterioration beyond 12 months of follow up (compared to baseline) suggests that these measures; specifically the non-dominant hand speeded tapping tasks, may be more reliable and consistent measures than the UHDRS-TMS. Clearly, to evaluate this properly, additional follow up assessment would be required. Also, as previously mentioned, the potential for subjectivity should be noted here; in that a single examiner reviewing the same subjects at intervals may subconsciously bias scoring on follow up evaluations.

UHDRS-TMS performed well as a measure of motor progression over the initial 12 months, but as an unblinded, essentially subjective measure, it is open to bias. This perhaps explains its initial ability to outperform the longitudinal quantitative motor assessments in the cohort studied here and in the larger TRACK-HD cohort. Despite this, while one would not expect there to be cross-sectional discrimination at baseline for pre-manifest HD and control individuals, the fact that at 12 and 24

months these individuals remained indistinguishable is a clear limitation of this measure, especially considering that at all time-points putaminal metabolites were able to make such distinctions, and that the ultimate goal of HD therapies will be to ameliorate disease in pre-manifest individuals. By comparison, a number of digitomotographic tasks and one glossomotographic task were, like NAA measurements, sufficiently sensitive to consistently distinguish pre-manifest and control individuals. Overall, with regard to motor measures, based on these findings, quantitative motor measures may be useful in longitudinal therapeutic studies in Early HD, but such studies will likely need considerably larger numbers to appreciate abrogation of the disease process, especially so if examining pre-manifest individuals and may require a tailored QMotor battery incorporating specific task measurements. Another factor to consider is that, as for structural imaging measures, the expected outcome of a successful therapeutic will likely be an amelioration of either atrophy or motor decline rather than a reversal of change. The difficulty here is that, such amelioration will likely be subtle, requiring considerable cohorts, and possibly execution over a protracted period, given that atrophy itself is subtle and that the disease is slowly progressive (Tabrizi et al. 2011). This contrasts with the significant theoretical advantage of meaurement of brain metabolites, which may well exhibit reversibility in tandem with improving neuronal health (Shemesh et al. 2010).

The UHDRS-TMS has demonstrable utility as a sensitive biomarker. It has been shown to be reproducible and reliable across clinical sites-important attributes for

any clinical trial outcome measure (Tabrizi et al. 2012), and is clinically meaningful.

Interestingly, in the main TRACK-HD study the UHDRS-TMS was able to identify longitudinal change in both PreHD A and B, as well as Early HD 1 and Early HD 2 subgroups, a feat only matched by one other of the clinical evaluations; the speeded tapping inter-tap interval analysis, and with a level of significance greater than any other clinical measure. Furthermore, the effect size of UHDRS-TMS across all HD individuals over 24 months approached that measured for several volumetric imaging parameters. These findings provide some justification for the widespread use of the UHDRS-TMS in numerous clinical trials for HD. The UHDRS-TMS also provides a more global measure of motor dysfunction than the isolated and task-specific quantitative motor tasks and is therefore likely to have greater functional significance.

The 24-month TRACK-HD paper reports both the UHDRS-TMS and the Quantitative Motor longitudinal findings (Tabrizi et al. 2012). In the overall cohort, of all the quantitative motor measures including both glossomotographic and digitomotographic tasks, only the speeded tapping non-dominant mean inter-tap measurement was able to show a significant progression over 24 months in not only Early HD subjects but also PreHD A and B subjects also. This was a finding only replicated by the UHDRS-TMS and certain volumetric imaging measures (Tabrizi et al. 2012), and clearly a disappointing performance for a number of

other quantitative motor measures evaluated in the study; with which it was hoped that clear patterns of 24 month progression in pre-manifest disease would be demonstrable. The findings presented here reflect those of the main TRACK-HD study, showing the inability of a significant proportion of existing QMotor battery tasks to identify disease progression in pre-manifest HD. This has clear implications for the investigation of disease modifying therapies among this clinical group. Conversely, motor progression was readily demonstrable in Early symptomatic patients. Since the majority of therapeutic trials focus on disease modification or symptomatic treatment in manifest HD individuals (DOMINO, TREND-HD, TETRA-HD, CARE-HD, Riluzole in HD, DIMOND, HORIZON, HART, CREST-E, 2-CARE (Huntington Study Group 2001, Huntington Study Group 2006, Landwehrmeyer et al. 2007, Stack & Ferrante, 2007, Huntington Study Group TREND-HD Investigators 2008, HSG Research Resources Page accessed 2010, Kieburtz et al. 2010) the QMotor tasks still have utility. The comparative efficacy of Magnetic Resonance Spectroscopy, a putative HD biomarker and measure of physiological change at the cellular level, will now be considered, together with the relationship between brain metabolites and motor phenotype.

5. Magnetic Resonance Spectroscopy biomarkers of HD

5.1 Chapter Introduction

As discussed in Chapter 2, MRS has previously been evaluated as a biomarker modality in pre-manifest and early HD. However, the literature is conflicted with regard to the utility of MRS elucidated metabolites as potential biomarkers in HD. In an attempt to address these discrepant findings, arising in part from small subject numbers, poorly comparable outcome measures and heterogeneity within patient cohorts, the primary purpose of this thesis and the experiments detailed in this Chapter was to determine the potential of MRS as an HD biomarker using large numbers of subjects in defined, homogeneous clinical cohorts. Furthermore the MRS evaluations performed here, unlike many other published reports, specifically and deliberately focused on MRS outcome measures normalized to unsuppressed water rather than to other metabolites such as tCr which are affected in HD.

To make a full assessment of MRS as an HD biomarker, the experiments described herein include cross-sectional and longitudinal assessments of this modality, the correlation of metabolite measures with markers of motor dysfunction (as discussed in Chapter 4), together with an assessment of possible partial volume WM effects, and finally suggestions for the development of this modality as an outcome measure for therapeutic trials in HD.

5.2 Investigation of MRS as a cross-sectional HD biomarker

5.2.1 Introduction

To evaluate a possible biomarker role for MRS in HD, baseline MRS was performed in a TRACK-HD cohort comprising Control, Pre-HD and Early HD individuals. While earlier studies have attempted to address this question, their cumulative outcome has been far from clear. This cohort was larger and used a higher, 3 Tesla, field strength than most earlier studies providing a higher SNR than standard 1.5 Tesla MRS to enable better discrimination of metabolites and maximize utilizable data.

The discrepancies concerning MRS in HD have arisen, largely as a consequence of studying this modality within heterogeneous HD subject cohorts. Therefore, as per TRACK-HD protocols, heterogeneity within all groups was minimized. The manifest, "Early" HD cohort was defined as individuals with mild impairment in functional independence as determined by UHDRS TFC. The Pre-HD cohort was homogenized by specifically including only individuals relatively close to predicted disease onset, as ascertained by a DBS above a pre-specified threshold, but that were still effectively asymptomatic, as ensured by absent or only minimal motor features measurable on the UHDRS TMS. These methods of group homogenization are detailed in 4.2.2. The hypothesis for the cross-sectional and longitudinal (Chapter 5.3) experiments were that putaminal metabolites, specifically NAA and tNAA, were different in both pre-manifest and early HD compared to controls, and that these alterations would progress over time (24 months).

5.2.2 Methods

Subjects

All subjects were recruited and evaluated at UBC, Vancouver, as part of TRACK-HD (Tabrizi et al. 2009). Of Ninety-six participants enrolled between January and September 2008, eighty-five underwent MRS imaging. These comprised Early HD (n=30), Pre-HD (n=25) and Control (n=30) individuals.

Procedures

Subjects underwent MRS examination at 3T as outlined in Section 3.3. MRS spectra were fit using LCModel (Provencher, 1993). LCModel analyses a spectrum as a linear combination of models of *in vitro* spectra based upon the individual metabolite solutions (Provencher 2001). The analysis takes advantage of a virtually model-free constrained regularization method, a statistical technique that tries to match the smoothest lineshape and baseline that is consistent with the data, but avoids the problems associated with using over or under-restrictive parameters when fitting the models to the sampled peaks. This is achieved through 'regularisation' which ensures that only complexity required by the data itself, is assimilated into the baseline or shape of the peaks. This responsiveness to the data avoids a fixed parameterized model, and permits fitting with only the most appropriate model based on the sampling from thousands of human brain spectra (Provencher 2001). A further advantage of the model, is the use of *a priori* knowledge of all spectral information, allowing more accurate fitting for all peaks (Schirmer & Auer 2000, Provencher 2001). This assists with interpretation of

metabolite contributions to baseline and enables automatic estimation of the true baseline - an advantage of the method given that baseline variability significantly impacts metabolite quantification (Schirmer & Auer 2000). LCModel also provides useful Cramér-Rao Lower Bounds (CRLB) information that represents an estimate of reliability and permits exclusion of unreliable data based on the imposition of a pre-ordained acceptable standard deviation for the data eg. an SD<20%.

The direct validation of any analytical software for MRS *in vivo* is impossible. The issue being that to sample metabolites directly in the brain in a live individual is not possible, and in any case, even a sample taken for biopsy is at risk of metabolic degradation by the time analysis has taken place. However, some validation of the model has been successfully undertaken with both analyses of phantoms and Monte Carlo method simulations (Provencher 2001). The model has exhibited, on the whole, good levels of reproducibility on test, re-test analyses. One group demonstrated intraclass correlation coefficients of between 0.84-0.9 for the ratio NAA/Cr among subjects with varied brain pathologies, in four different brain regions at 1.5T, a performance comparable with manufacturer's software packages. Scans were performed sequentially in this study, and it is noteworthy that coefficients varied according to metabolite, such that the correlation for absolute NAA varied between 0.58 to 0.89 depending on brain region, with the manufacturer's software only marginally outperforming LCModel (Fayed et al. 2009). In another study intra-individual spectra recorded at repeat scanning sessions (six over fourteen days) demonstrated coefficients of variation (CV)

ranging in normal brain from 3.8% for absolute NAA to 11.9% for absolute Glx - better than those derived from metabolite ratios. Unsurprisingly, inter-individual comparisons' CVs were higher for both absolute (CV 7.6% NAA to 23.1% Glx) and relative metabolite measurements (CV 8.5% NAA/Cr to 23.5% Glx/Cr) than in the intra-individual assessments which the authors attribute to a (probably) *normal* metabolite distribution among a cohort, to regional variations attributable by varying voxel components (eg. inclusion of CSF) and to age differences among their cohort (Schirmer & Auer 2000). Furthermore these results were comparable with earlier work (Marshall et al 1996). In terms of longitudinal reproducibility of measurements using LCModel in the same study of healthy control individuals underwent two sequential MRS evaluations either at the same session or at two weeks apart, and neither interval significantly affected serial metabolite measurements (either absolute or relative (to Cr)). The intra-individual CV was <7% for NAA, Cho and Cr and <9% for mI and were not operator dependent, suggesting robust metabolite estimations over longitudinal evaluations (Schirmer & Auer 2000). This robustness of MRS measures is also supported by sequential evaluations among a cohort of healthy volunteers, which showed no significant change in metabolite estimations over two months (Hoshino et al. 1999). Overall, a number of benefits are associated with the LCModel software, foremost of which include the accuracy of the metabolite measurements but also the reproducibility of the measure.

Metabolites were normalized to unsuppressed water spectrum. LCModel estimates "concentration" measurement reliability, returning standard deviations (%SD) for each metabolite. Standard deviations below 20% are considered reliable (Provencher, 2005), higher %SD were excluded. Five metabolites of principal interest were examined: tNAA (summed NAA and NAAG, neuronal integrity marker), tCr (summed Cr and PCr, brain energy metabolism and potential gliosis marker), tCho (predominantly GPC and PC, marker of neuronal membrane turnover), Glu (CNS excitatory neurotransmitter) and MI (astrocyte marker). NAA measurements, in addition to tNAA, were also performed.

To estimate contribution of WM (non-putaminal) volumes to metabolite concentrations, blinded, manual voxel segmentation was performed using a basic method. Percentage putaminal tissue in three (3mm) slices per voxel (top, middle, bottom) was measured using Photoshop (Adobe Systems, Inc.) and averaged giving "percentage putamen volume per voxel" (see Table 5-2). Figure 5-1 shows putaminal voxel placement and sample spectra.

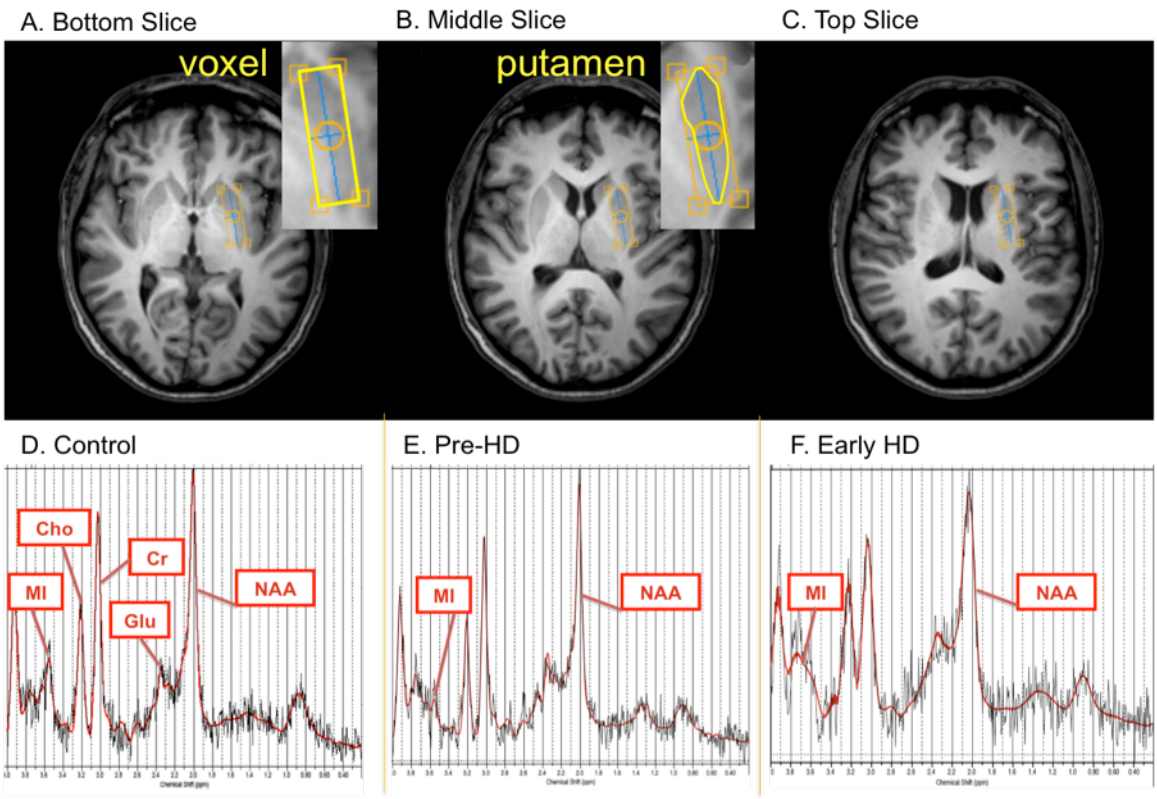

Figure 5-1 Samples of manual putamen segmentation and MR Spectra by subject group.

Statistics

The participant groups recruited into TRACK-HD were gender and age matched across all, international, sites rather than separately at individual sites. All group comparisons were made using one-way ANOVA with *post-hoc* Newman-Keuls Multiple Comparison Tests.

5.2.3. Results

Baseline Demographics

Of 85 individuals that underwent MRS at baseline, spectra were obtained from 84 individuals (30 Controls, 25 Pre-HD, 29 Early HD). Table 5-1 shows group demographics. Adequate LCModel data fits were obtained for; tNAA, tCr and tCho for all 84 individuals, MI for 74 (28 Controls, 21 Pre-HD, 25 Early HD), Glu for 74 individuals (29 Controls, 23 Pre-HD, 22 Early HD), NAA for 73 individuals (30 Controls, 24 Pre-HD, 19 Early HD). MR spectra were not included if poor fit quality (%SD > 20) precluded accurate measurement. Exclusion was blind to participant group.

	Controls	Pre-HD	Early HD
Mean Age (years, SD)	46.60 (11.93)	39.90 (10.76)*	48.16 (10.93)
Women (%)	63% (n=19/30)	56% (n=14/25)	28% (n=8/29)
Antidepressant Use	17% (n=5/30)	32% (n=8/25)	72% (n=21/29)
Neuroleptic Use	-	-	34% (n=10/29)

Table 5-1 Baseline demographics. *Only in Pre-HD was the mean age different from both Early HD and Controls ($p<0.05$, one-way ANOVA with post-hoc Newman-Keuls Multiple Comparison Test).

Putaminal segmentations

To enable comment upon the possible impact of non-putaminal (white matter) tissue partial volume effects, basic segmentations were performed. Relative tissue measurements made using this basic method are demonstrated in Table 5-2. A progressively lower mean percentage putamen per voxel, across groups from

Control through Pre-HD to Early-HD, was identified. Furthermore, the upper and lower limits of percentage putamen per voxel among Early HD individuals was markedly lower than for either Control or Pre-HD groups.

Importantly the identification of marked WM tissue contributions to total intravoxel tissue volume based on putaminal segmentations suggests that inevitably, white matter will have contributed to the observed metabolite concentrations. As discussed later in this Chapter, these partial WM volume effects would have likely markedly confounded observed results for tCr, Glu and tCho. Therefore, the work presented here focused on NAA, tNAA and/or mI.

	Control	**Pre-HD**	**Early HD**
Mean (% putamen/voxel)	59.1	55.2	40.2
Standard Deviation	5.1	7.9	5.8
Minimum	44.8	39.3	27.2
Maximum	68.3	70.7	51.2

Table 5-2 Putaminal segmentations Control vs. Pre-HD ($p>0.05$), Control vs. Early HD ($p<0.0001$), Pre-HD vs. Early HD ($p<0.0001$).

Metabolite differences across groups

Figure 5-2 shows metabolite differences between groups. For all metabolites significant differences were evident between Control and Early HD groups, however only NAA exhibited any difference in Pre-HD compared to controls. In Early HD, tNAA and tCr were 15% and 18% lower than in Controls ($p<0.001$). In contrast, MI was 50% higher in Early HD compared to Pre-HD ($p<0.01$). These findings suggest sensitivity for these metabolites as markers of altered neurochemistry in Early HD, and NAA in Pre-HD.

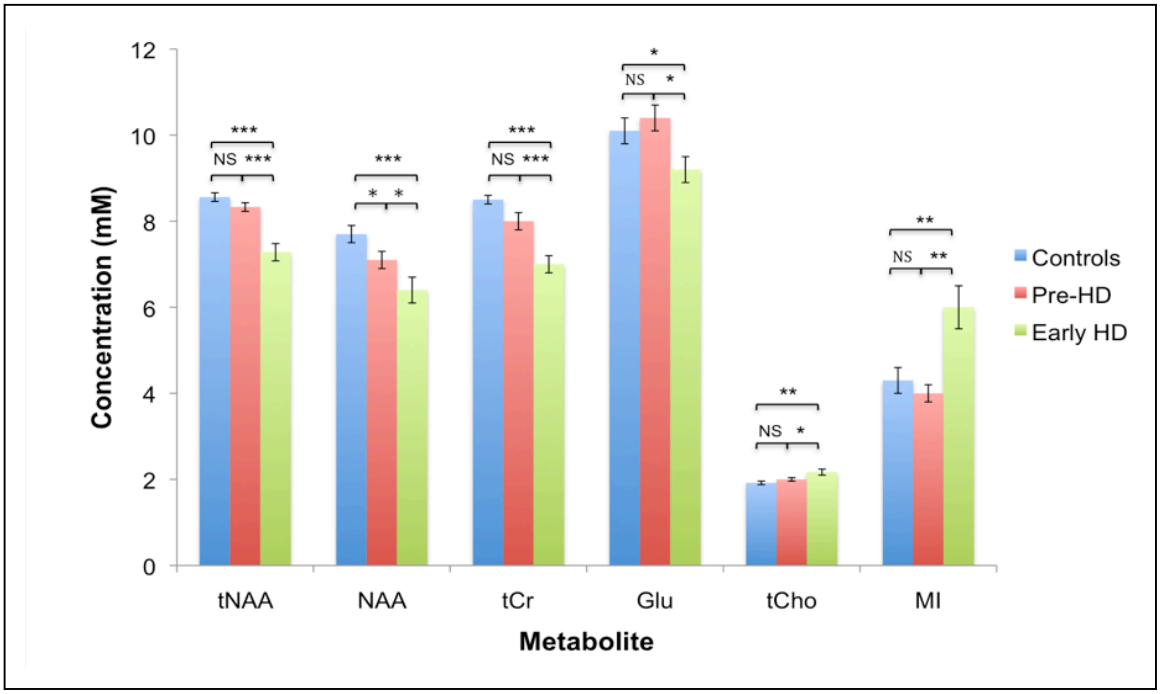

Figure 5-2 MRS in Controls, Pre-manifest and Early HD at baseline. Error bars denote standard error of the mean for each group. Levels of significance; * $p<0.05$, ** $p<0.01$, *** $p<0.001$. Group comparisons were made using one-way ANOVA with *post-hoc* Newman-Keuls Multiple Comparison Tests.

5.2.4 Discussion

An objective of this study was to clarify conflicting reports regarding the utility of MRS as an HD biomarker modality. The focus was MI, tNAA and their differences between Control, Pre-HD and Early HD individuals. One of the strengths of this study is the normalisation of metabolites to unsuppressed water signal, an accepted technique previously performed only in relatively few published HD spectroscopy studies (Hoang et al. 1998, Sanchez-Pernaute et al. 1999, Reynolds et al. 2005). By avoiding normalisation to other metabolites (e.g. tCr), which are also disturbed in the HD brain (Reynolds et al. 2005), these measurements more likely reflect true biochemical change and permit direct comparison between studies. Furthermore, unlike most HD MRS studies, which utilised 1.5T magnets (Davie et al. 1994, Taylor-Robinson et al. 1996, Sanchez-Pernaute et al. 1999, Bender et al. 2005, Gómez-Ansón et al. 2007, van Oostrom et al. 2007) the 3T field strength used here provides improved SNR, minimising the number of unreliable and therefore rejected metabolite estimations, enhancing the proportion of utilisable data. This study also had larger, more homogeneous subject groups than earlier studies.

The role of NAA in neuronal function is poorly understood. Synthesized within mature neurons tNAA concentration within GM reflects neuronal number and viability, while in WM it is a marker of axonal density (Tallan, 1956, Pouwels et al. 1997, Gujar et al. 2005). It has also been suggested that NAA is a marker of mitochondrial dysfunction, and hence energy metabolism, rather than neuronal cell loss. Inhibition of complexes I, III, IV, V in the mitochondrial respiratory chain,

within isolated rat brain mitochondria, has been associated with a reduction in NAA (Bates et al. 1996).

Total NAA was 15% lower in Early HD than Controls. These findings are consistent with reportedly lower tNAA in akinetic HD (-66%) compared to controls (Sanchez-Pernaute et al. 1999). Interpretation of findings from other studies, however, is limited by reporting tNAA values normalised to other metabolites, obscuring individual metabolite changes. Lower striatal and thalamic tNAA/tCr has been reported in early HD (Jenkins et al. 1998, Ruocco et al. 2005). Mean tNAA/tCr was comparable in the groups (mean (SD), Controls; 1.01 (0.10) vs. Pre-HD; 1.04 (0.09) vs. Early HD; 1.05 (0.17), $p>0.05$), suggesting that early HD absolute tNAA levels, in previous reports, may have been lower than these observations. NAA reductions have been reported on MR spectra of transgenic HD mice (van Dellen et al. 2000), and in putamen of HD affected individuals (Dunlop et al. 1992).

Lack of a consistent striatal NAA and tNAA alteration in pre-manifest and early HD has been reported (Reynolds et al. 2005, van Oostrom et al. 2007), although pre-manifest cohort heterogeneity, in terms of time to predicted disease onset (range: -7 to +29 years *vs.* +7 to +18 years in this study), may have obscured metabolite variation in one study (Reynolds et al. 2005). Heterogeneity in pre-manifest HD group was minimized by ensuring adherence to a maximum UHDRS motor score, a practice not specifically reported in other studies (Reynolds et al. 2005, van Oostrom et al. 2007).

Myo-inositol is an osmolyte and astrocyte marker that is elevated in AD (Moats et al. 1994, Griffith et al. 2008). Manifest HD in adults and juveniles has been associated with high striatal mI (Hoang et al. 1998, Reynolds et al. 2005). We demonstrate mI differences in Early HD. Similar metabolite changes occur in asymptomatic individuals carrying gene defects associated with familial AD. Interestingly, in "pre-manifest AD" tNAA was reduced, and tNAA/MI discriminated pre-symptomatic spectra from controls (Godbolt et al. 2006).

Putaminal metabolite changes are pertinent since this is a site of early atrophy, identifiable years prior to clinical diagnosis (Aylward et al. 1996). Furthermore, putaminal atrophy correlates with psychomotor and motor deficits in pre-manifest HD and early HD (Harris et al. 1996, Jurgens et al. 2008). The observations suggest a potential role for MRS in evaluating the ability of an intervention to slow disease progression, even in pre-manifest disease. It should be borne in mind, however, that these cross-sectional assessments performed at a single time-point, complement but do not replace longitudinal comparisons.

NAA was less robustly measured than tNAA (11 measurement exclusions vs. no exclusions) and is difficult to differentiate from NAAG, the other tNAA constituent. The lower NAA in Pre-HD compared to Controls, was not accompanied by significantly lower tNAA than in controls. However, NAA analyses should be treated cautiously, even though potential causes of NAAG artifact: spectral

linewidth broadening (mean (SD), Pre-HD; 8.00 (2.37) Hz vs. Controls; 7.55 (1.66) Hz, $p>0.05$) and low SNRs (Pre-HD; 9.36 (2.12) vs. Controls; 10.17 (2.18), $p>0.05$) were comparable in Pre-HD and Controls. NAA was 8% lower in Pre-HD than Controls.

In all groups tCr values were comparable to tNAA, while normally tNAA is about 30-40% higher (depending on brain region) (Baker et al. 2008). The findings are supported by very similar, low tNAA/tCr ratios identified within basal ganglia structures of controls, pre-manifest and manifest HD individuals at 1.5T and 7T MRS (Hoang et al. 1998, van den Bogaard et al. 2009). This possibly reflects increased basal energy metabolism within these structures (Hoang et al. 1998). Since all spectra were analyzed using the same protocol with consistent scaling applied across metabolites, scaling difficulties would not have affected a single metabolite in isolation or comparisons of estimated tNAA and tCr.

Spectral quality was worst in Early HD, with lower SNRs (mean (SD), Early HD; 6.83 (1.91), Controls; 10.17 (2.18), $p<0.001$) and broader spectral linewidths (Early HD; 10.51 (2.67) Hz, Controls; 7.55 (1.66) Hz, $p<0.001$) than Controls. Since many individuals with early HD are choreic, it is likely that movement artifact could have contributed to the attenuated SNR in this group (Taylor-Robinson et al. 1996). Could these SNR reductions have been responsible for the altered NAA and MI estimations in this group? Based on findings from a 4T MRS study, we would expect the SNR reductions and linewidth increases seen in the Early HD group to

generate up to 4-6% variation in tNAA and MI estimations (Bartha, 2007). Small SNR or linewidth effects alone would therefore not account for the larger MI and tNAA differences in Early HD. Furthermore, at the lower field strength of 1.5T, marked SNR reduction and linewidth broadening either did not affect estimated tNAA or generated only 4% increases in tNAA and MI estimations (Kanowski et al. 2004, Macri et al. 2004).

While the earliest HD neuropathological changes occur in caudate and putamen (Vonsattel et al. 1985), the putamen was selected to avoid averaging CSF into the brain parenchymal compartment. CSF partial volume effects may generate spurious metabolite measurements (Hoang et al. 1998) and is a risk with caudate voxel placement. Due to scanning time restrictions and the finding of early metabolic changes within the left striatum in pre-manifest HD (Sanchez-Pernaute et al. 1999), the left putamen was chosen as the structure of interest.

The use of larger voxels to improve SNR generates partial volume white matter effects through inclusion of non-putaminal tissue within the voxel. A 3T MRS study of brain metabolites reported lower MI in WM than GM (Baker et al. 2008). This suggests that partial volume WM effects caused by loss of putaminal volume in transition from pre-manifest to early HD would diminish the MI difference observed. Hence the concentrations presented may underestimate true MI differences. Studies indicate a cortical GM/WM tNAA ratio of between 0.8-1.2 in adulthood (Pouwels, 1998, Lundbom et al. 1999). We cannot guarantee that WM

components are not, partly, responsible for group tNAA differences, but the findings are consistent with smaller voxel studies that minimized partial volume effects (Jenkins et al. 1998, Sanchez-Pernaute et al. 1999). Higher tCho and lower Glu, tCr are found in WM (Baker et al. 2008) making it impossible to know whether these observations reflect authentic pathophysiological change and hence further analyses of these metabolites, in this work, is limited. Estimations of "Percentage putamen volumes per voxel" were performed solely to ascertain the importance of partial volume effects in interpreting results.

Subjects participating in TRACK-HD were demographically matched across international sites rather than at individual sites, explaining demographic discrepancies between groups in this study. Fewer Early HD women may have impacted metabolite concentrations for this group but an earlier study of regional brain MRS did not identify relevant gender differences in tNAA or MI (Pouwels, 1998). Mean age in Pre-HD was lower than Early HD and Control groups (which were comparable). Consequently age differences would not explain metabolite differences in Early HD.

Use of neurotropic medications was highest in Early HD (Table 1). Antidepressant use in a total of over 30 depressed individuals was associated with either unchanged or increased cortical tNAA/tCr ratios at 1.5T and 3T (Gonul et al. 2006, Kaymak et al. 2009). All neuroleptic medicated Early HD patients were taking atypical agents. Atypical antipsychotic medication usage in over 50 schizophrenia

patients did not impact water-normalized thalamic or caudate tNAA levels (1.5T) (Szulc et al. 2007, Bustillo et al. 2008). In a further study at 1.5T an atypical neuroleptic caused 27% elevation in thalamic MI/H_2O levels (Szulc et al. 2005). While one-third of Early HD individuals could have experienced medication induced MI elevations, this would not explain the 50% higher mean MI concentration. Although not all studies were water-normalized, the evidence suggests that neurotropic usage would not explain the findings reported here.

To improve this study in future work, we would aim to also ensure intra-subject and inter-subject Co-efficients of Variation (CV) are estimated to ensure reproducibility of measures for both scanner, and the specific scan protocol. For intra-subject calculations, ideally a test subject would be used.

MRS has advantages over other putative imaging biomarker modalities such as PET. MRS data collection is less expensive and time-consuming, and does not require intravenous tracer isotope injection (Antonini et al. 1996, Andrews et al. 1999, Reynolds et al. 2005). Additionally, MRS may be less prone to inter-operator variability than some volumetric biomarker applications (Henley et al. 2010). These collective advantages support ongoing assessment of MRS as an HD biomarker modality. Furthermore, the ability of MRS to track pathological change at the biochemical level makes it potentially responsive to acute therapeutic interventions. In a creatine supplementation study in early HD, MRS identified cortical glutamate reductions within 10 weeks (Bender et al. 2005). Other

pathological and MRS studies have identified normalisation of metabolites following acute neurological lesions (Demougeot et al. 2003, Shemesh et al. 2010). Thus MRS can potentially identify early reversal of pathological processes, a finding that would be unlikely with structural imaging. The next experiment details the longitudinal measurement of these metabolite alterations.

5.3 Investigation of MRS as a longitudinal HD biomarker.

5.3.1 Introduction

"A biomarker measure should correlate reliably with disease progression…[it] should have low variability in the control population" (Weir, Sturrock & Leavitt, 2011).

By definition therefore the validation of any putative biomarker, and determination of its potential as a clinical trial outcome measure, necessitates its longitudinal evaluation. In this cohort, as with other observational studies comparing pre-manifest and early HD individuals, a cross-sectional comparison of these two groups is not sufficient to infer longitudinal change. Cross-sectional analyses provide a static overview of different disease stages at a specific timepoint thus comparison of group means for early and pre-manifest HD is, potentially, a comparison between very different individuals in terms of accrual of pathology. These groups differ by many years, even decades, in terms of their exposure to underlying pathophysiological processes. Consequently, cross-sectional effects are considerably larger than longitudinal effects. Having established baseline cross-sectional inter-group metabolite differences in Section 5.2, longitudinal evaluation within the same cohort was performed at 12-monthly intervals over the subsequent 24 months (ie. at two further time points).

5.3.2 Method

Participants

At 12 months and at 24 months, 77 and 76 respectively, of the individuals originally enrolled at baseline underwent follow up MRS (12 months; 28 Control, 25 Pre-HD, 24 Early HD. 24 months; 27 control, 24 pre-manifest HD, 25 Early HD. These cohorts were not identical at both time points), see Table 5.3.1 for demographic details of cohorts. At 12 months one subject, and at 24 months, a second Pre-HD subject had reached a stage of "peri-phenoconversion", with an associated rise in diagnostic confidence level from 1/4 to 2/4 (equivalent to a change from "non-specific motor anomalies or <50% confidence that subject has manifest HD" to "motor abnormalities that may be signs of HD or 50-89% confidence"). Data from these individuals remained within the Pre-HD grouping. Since the expectation was that all HD individuals had progressed, the cohort was no longer required to fit the baseline inclusion criteria in the previous experiment. For analyses in this experiment, further subgrouping was performed as per the major initial TRACK-HD publication (Tabrizi et al. 2009). Thus pre-manifest HD individuals were subclassified as Pre-HD A or Pre-HD B based on time to predicted disease onset of >10.8 years or <10.8 years respectively. This duration was the Pre-HD group median to predicted disease onset across all TRACK-HD sites. Early HD subjects were subcategorized, based on their level of functional independence as measured by the UHDRS-TFC, as either Early Stage I or Stage II (Shoulson & Fahn, 1979).

Procedures & Statistics

MRS imaging procedures and statistics were performed as outlined in the previous experiment.

5.3.3 Results

Demographics

Subject demographics at baseline, 12 and 24 month visits are displayed in Table 5-3.

Baseline	**Controls**	**Pre-HD**	**Early HD**
Successful scans (n=84/85)	30/30	25/25	29/30
Women %	63	56	28
Age (Yrs, SD)	46.60 (11.9)	39.90 (10.8)*	48.16 (10.9)
Subgroups (N=)	-	Pre-HD A=15 Pre-HD B=10	Early HD 1=13 Early HD 2=16
12 Months			
Successful scans (n=76/77)	28/28	25/25	23/24
Women %	64	60	35
Age (Yrs) (Mean/ SD)	47.98 (11.2)	41.1 (10.2)*	49.4 (10.7)
V1-V2 interscan interval (Yrs) (Mean/SD)	0.97 (0.06)	0.92 (0.06)	0.99 (0.07)
Subgroups (N=)	-	Pre-HD A=16 Pre-HD B=9	Early HD 1=10 Early HD 2=13
24 Months			
Successful scans (n=74/76)	27/27	22/24	24/25
Women %	59	59	33
Age (Yrs) (Mean/ SD)	49.17 (11.27)	40.59 (10.76)**	51.60 (10.72)
Mean V2-V3 interscan interval	1.10 (0.24)	1.06 (0.09)	1.08 (0.08)
Subgroups (N=)	-	Pre-HD A=15 Pre-HD B=7	Early HD 1=12 Early HD 2=12

Table 5-3 Demographics of successfully scanned subjects. Note that all subjects were evaluated as per their original subgroups (Pre-HD A/B or Early HD 1/2) regardless of their progression to the

alternative subgroup over the duration of the study. This was to optimize recognition of longitudinal effects. Asterisks refer to age Pre-HD age differences vs. Control and Early HD groups; *p<0.05, **p<0.01. Ages were calculated to the nearest month.

Cross-sectional analyses of NAA, tNAA & MI at all timepoints

At all time points NAA, tNAA and MI demonstrated reproducible and consistent group differences. Of the metabolites tNAA demonstrated the most consistent differences between Pre-HD and Control subjects. The difference ranged from 3% lower in Pre-HD vs. Controls at baseline (non-significant) to 5% lower at 12 months and 7% lower at 24 months. All metabolites were consistently altered in Early HD compared to Controls and Pre-HD subjects (Figure 5-3).

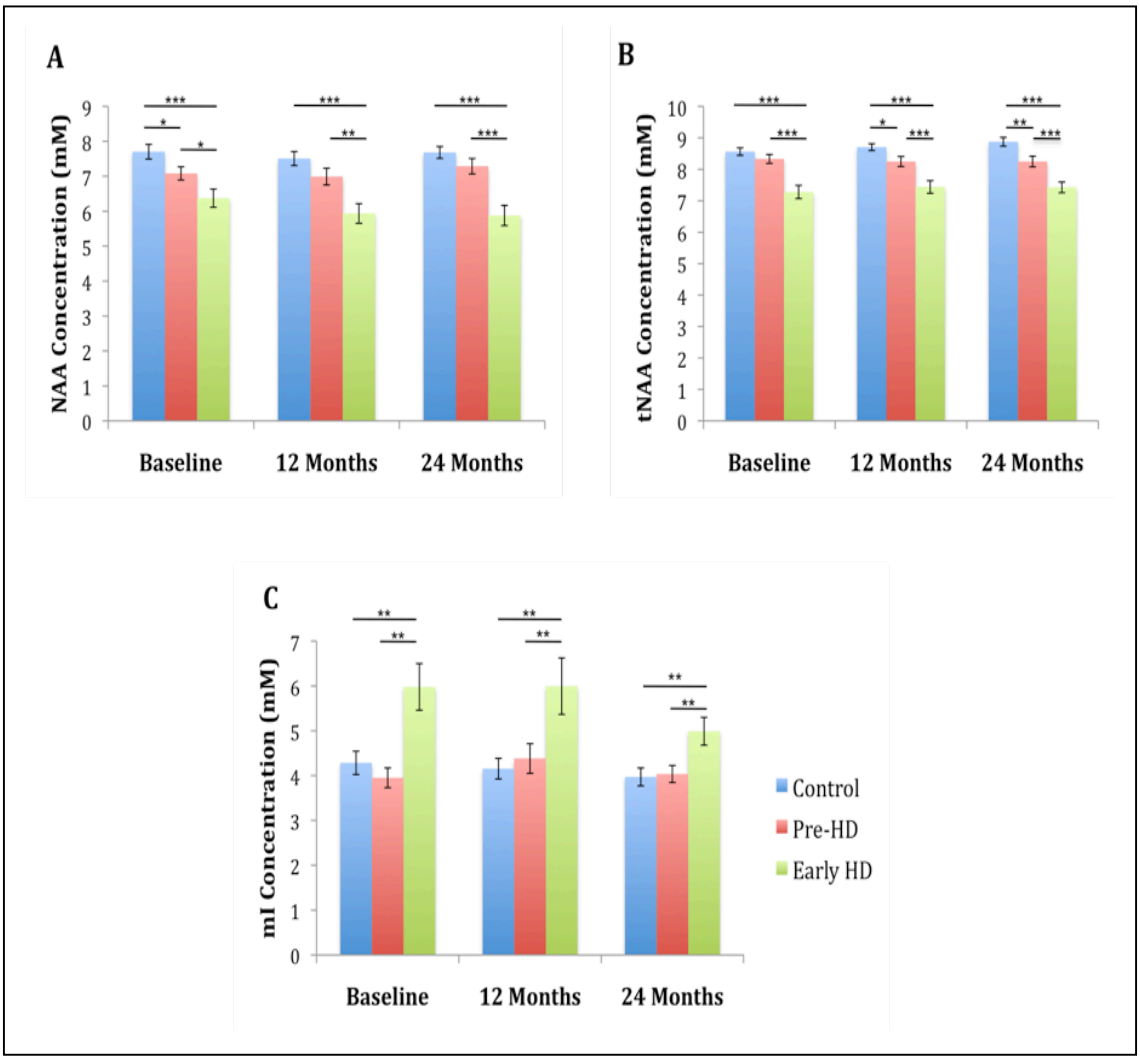

Figure 5-3 A-D. Cross-sectional MRS in Control, Pre-HD and Early HD subjects at baseline, 12 & 24 months. Data arranged by metabolite; A. NAA, B. tNAA, C. MI. Error bars denote standard error of the mean for each group. Asterisks indicate level of significance; * $p<0.05$, ** $p<0.01$, *** $p<0.001$. Group comparisons were made using one-way ANOVA with post-hoc Newman-Keuls Multiple Comparison Tests.

Subgroup cross-sectional analyses at baseline, 12 and 24 months

Categorising into Pre-HD A, Pre-HD B, Early HD I and Early HD II subgroups at all time points, consistent differences in tNAA and NAA were seen in Early HD, most markedly in Early HD Stage 2. Interestingly across serial visits this subgroup demonstrated a progressive increase in the statistical significance level of these metabolite differences compared to other subgroups. At most time points a trend to lower levels of these metabolites were observed in Pre-HD A and Pre-HD B compared to Controls but these generally did not reach significance. Consistently higher MI was identified in Early HD Stage 2 individuals than in all other subgroups (Figure 5-4).

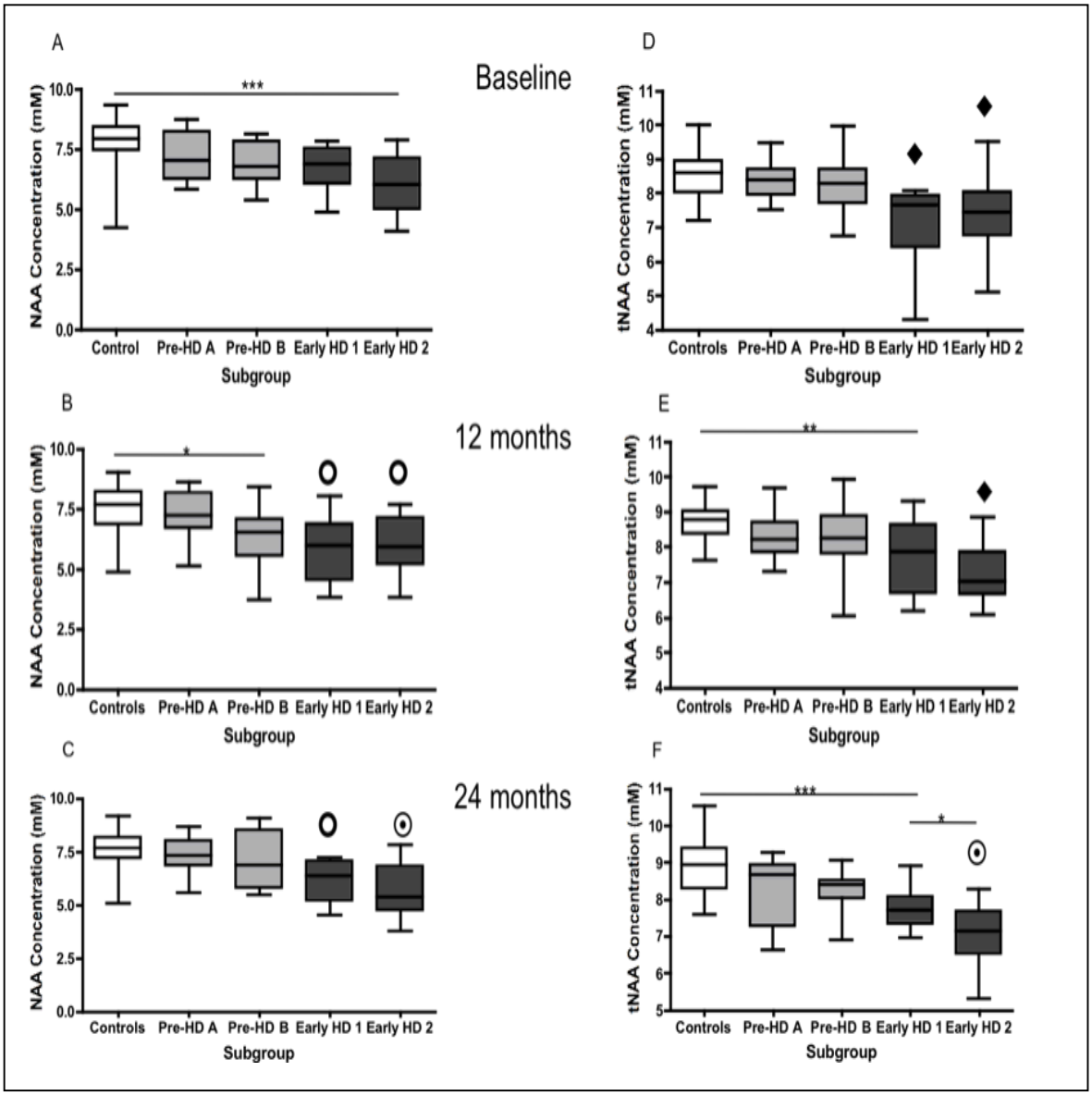
A
Baseline
D
***
NAA Concentration (mM)
tNAA Concentration (mM)
Control
Controls
Pre-HD A
Pre-HD B
Early HD 1
Early HD 2
Subgroup
B
12 months
E
*
**
C
24 months
F
***
*

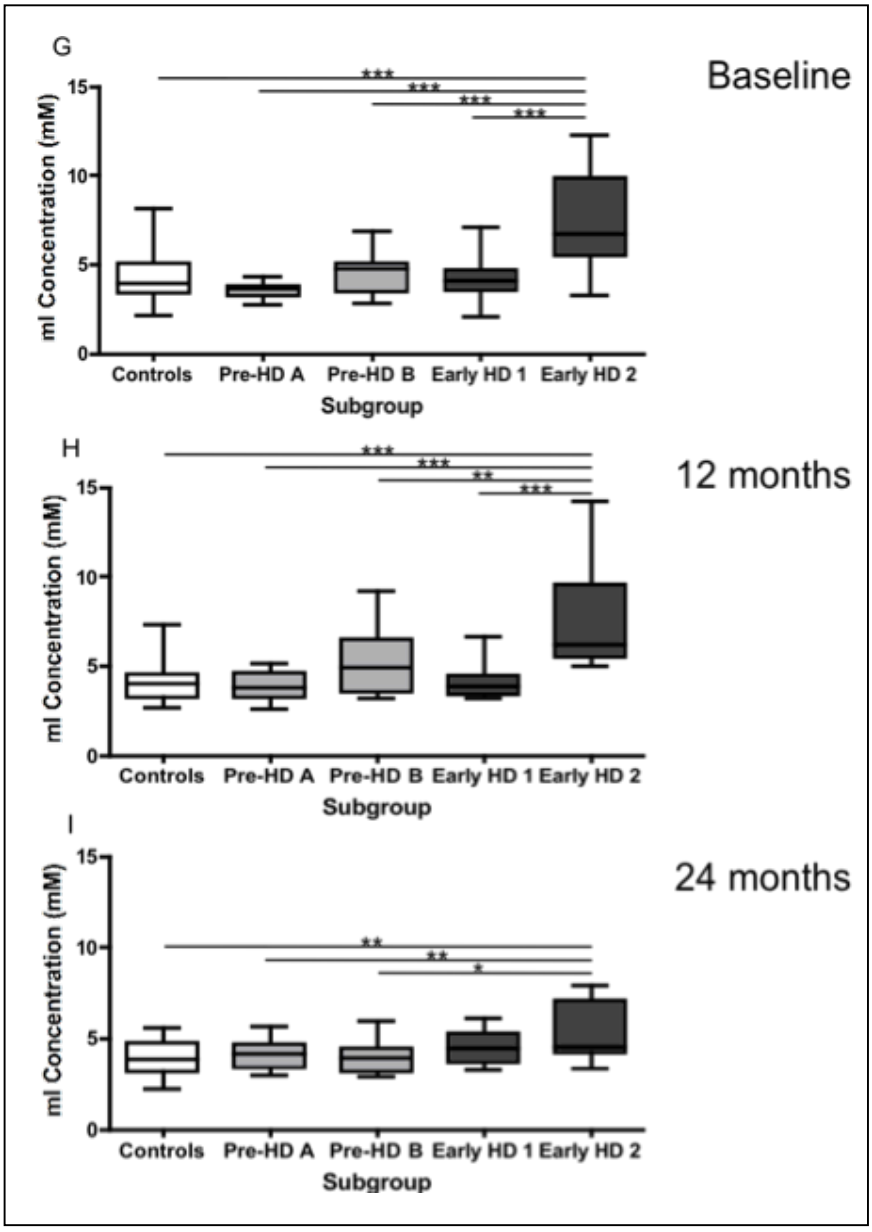

Figure 5-4 A-I (Presented in two boxes). Subgroup cross-sectional analyses at baseline, 12 months & 24 months. Figures 5-4 A-I reflect cross-sectional subgroup analyses by metabolite. A, B, C demonstrate NAA by subgroup at baseline, 12 and 24 months respectively. D, E, F indicate tNAA and G, H, I; MI by subgroup at three time points. Individual significance levels denoted above corresponding line *p<0.05, **p<0.01, ***p<0.001. Where five or more inter-group comparisons reached significance, the following symbols denote significance for specific comparisons; ○ p<0.01

vs. Controls, p<0.05 vs Pre-HD A. ♦p<0.001 vs. controls, p<0.01 vs. Pre-HD A, p<0.05 vs. Pre-HD B. ⦿p<0.001 vs. controls & Pre-HD A, p<0.05 vs. Pre-HD B.

Longitudinal analysis across 24 months

Longitudinal analyses by group are shown in Figure 5-5. No metabolite nor the ratios MI/NAA or MI/tNAA demonstrated any significant longitudinal change. Longitudinal analysis by subgroup were also performed for NAA (13 Pre-HD A, 4 Pre-HD B, 7 Early HD1, 4 Early HD2 subjects), tNAA (13 Pre-HD A, 5 Pre-HD B, 9 Early HD1, 10 Early HD2 subjects), MI (9 Pre-HD A, 3 Pre-HD B, 6 Early HD1, 8 Early HD2 subjects), MI/tNAA (9 Pre-HD A, 3 Pre-HD B, 6 Early HD1, 8 Early HD2 subjects) and MI/NAA (9 Pre-HD A, 2 Pre-HD B, 5 Early HD1, 3 Early HD2 subjects) but only for subjects with paired longitudinal data across all visits. No significant longitudinal change was identified for NAA, tNAA, mI, mI/tNAA subgroups (data not shown). In Early HD Stage I mI/NAA trended to a 32% increase (p=0.057) over 24 months (data not shown).

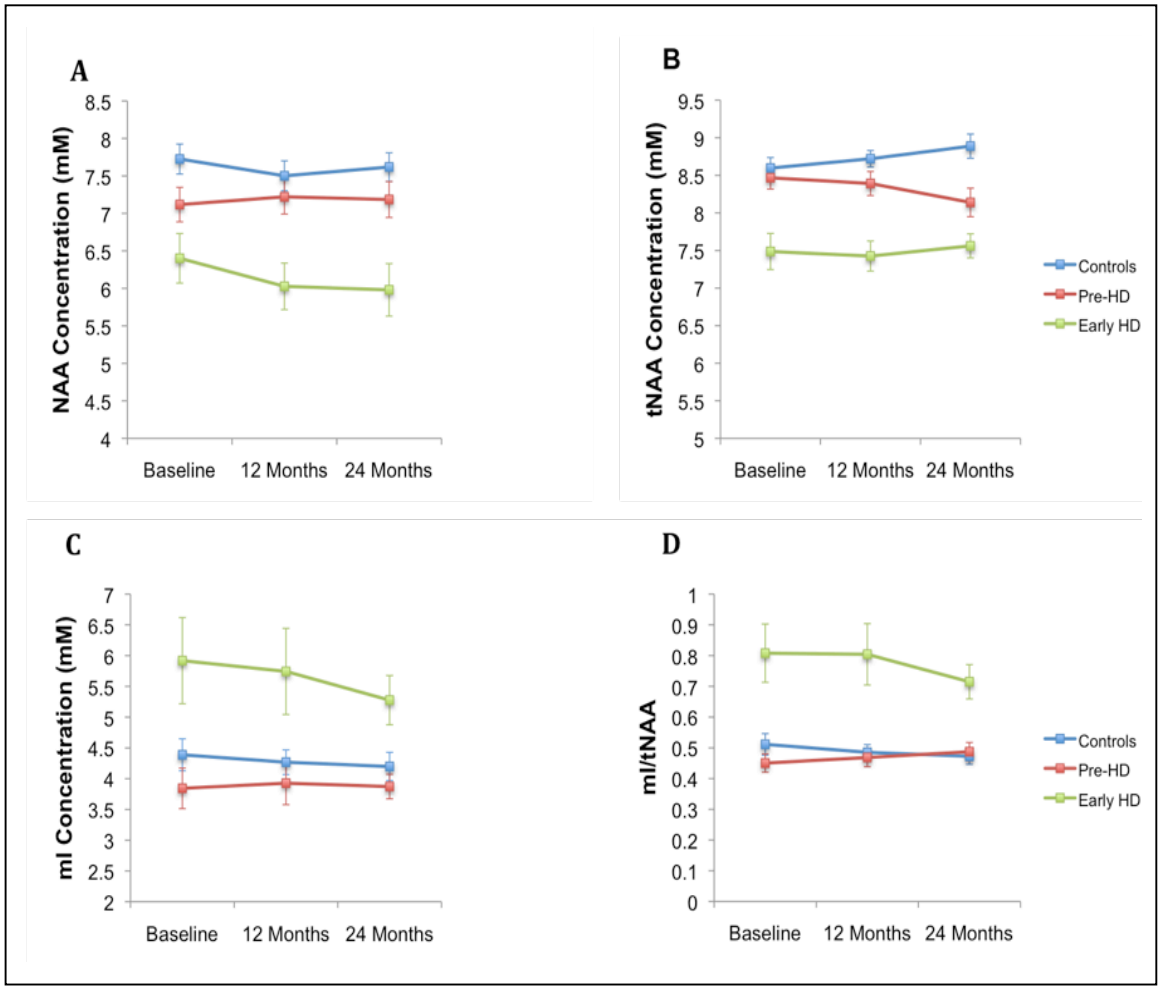

Figure 5-5 A-D. Longitudinal metabolite analyses by subject group. Longitudinal analyses for Controls, Pre-HD and Early HD at Baseline, 12 months and 24 months are given by metabolite (A. NAA, B. tNAA, C. MI, D. MI/tNAA). No longitudinal difference was identified for any metabolite at any of the three time points, nor in mI/NAA (not shown). Error bars indicate standard errors.

Medication effects (Tables 5-4 & 5-5)

Antidepressant (the single largest psychoactive monotherapy) usage by Early HD individuals at all three visits was associated with a non-significant trend to lower tNAA and NAA, and higher MI levels (Tables 5-4 & 5-5). At no time-point did these trends reach a significant difference. In Pre-HD the opposite trend was identified; tNAA and NAA trended to higher levels among antidepressant using individuals, although fewer Pre-HD than Early HD individuals used antidepressants. Among Controls antidepressant usage was not associated with consistent alterations in tNAA and NAA. Importantly MI, in nearly all antidepressant medicated and "any medication" groups over the three time-points, trended to higher levels than the comparable un-medicated groups, regardless of subject grouping.

To evaluate further, group analysis was performed after excluding all individuals taking any psychoactive medication (Table 5-5). Despite the exclusion of data and the relatively low subject numbers in the Early HD groups tNAA was consistently, significantly lower than Controls in one or both gene positive groups (Pre-HD/Early HD) at all time points. In all cases there was, at least, a trend to lower tNAA and NAA in Pre-HD and Early HD individuals.

Group/ Visit/ Metabolite	No drugs Mean (SD, N)	Antidepressant (AD) Only Mean (SD, N)	Antipsychotics (AP) Only Mean (SD, N)	AD + 1 or more other drug[a] Mean (SD, N)	Other drug only[b] or combined with AP Mean (SD, N)	Any medication Mean (SD, N)
Controls						
Baseline;						
tNAA	8.6 (0.6, 25)	8.5 (0.9, 4)	-	-	8.1 (SV)	8.4 (0.4, 5)
NAA	7.8 (0.9, 25)	6.9 (2.2, 4)	-	-	8.1 (SV)	7.1 (0.9, 5)
mI	4.1 (1.2, 23)	5.4 (2.3, 4)	-	-	3.8 (SV)	5.1 (0.9, 5)
12 Months;						
tNAA	8.7 (0.6, 24)	8.7 (0.2, 4)	-	-	-	8.7 (0.2, 4)
NAA	7.5 (0.9, 24)	7.8 (1.6, 4)	-	-	-	7.8 (1.6, 4)
mI	4.3 (1.1, 20)	3.3 (0.7, 4)	-	-	-	3.3 (0.7, 4)
24 Months;						
tNAA	8.9 (0.8, 25)	8.6 (0.5, 3)	-	-	-	8.6 (0.5, 3)
NAA	7.6 (0.9, 25)	8.0 (0.3, 3)	-	-	-	8.0 (0.3, 3)
mI	3.9 (0.9, 24)	5.6 (SV)	-	-	-	5.6 (SV)
Pre-HD						
Baseline;						
tNAA	8.2 (0.5, 18)	8.5 (1.1, 5)	-	8.7 (1.2, 2)	-	8.6 (0.4, 7)
NAA	6.9 (0.9, 17)	7.6 (0.6, 5)	-	6.5 (0.9, 2)	-	7.3 (0.3, 7)
mI	3.7 (0.8, 15)	4.7 (1.4, 5)	-	3.6 (SV)	-	4.5 (0.5, 6)
12 Months;						
tNAA	8.1 (0.8, 18)	8.6 (0.7, 7)	-	-	-	8.6 (0.7, 7)
NAA	6.9 (1.2, 18)	7.1 (1.2, 5)	-	-	-	7.1 (1.2, 5)
mI	3.9 (0.8, 17)	6.1**(2.3,5)	-	-	-	6.1**(2.3,5)
24 Months;						
tNAA	8.2 (0.9, 17)	8.3 (0.3, 5)	-	-	-	8.3 (0.3, 5)
NAA	7.2 (1.0, 17)	7.7 (1.0, 4)	-	-	-	7.7 (1.0, 4)
mI	3.9 (0.8, 16)	4.3 (1.1, 5)	-	-	-	4.3 (1.1, 5)
Early HD						
Baseline;						
tNAA	7.5 (0.9, 6)	7.0 (1.2, 13)	6.9 (1.2, 2)	7.8 (1.4, 7)	-	7.3 (0.3, 22)
NAA	6.5 (1.1, 5)	5.9 (1.3, 7)	6.8 (1.2, 2)	6.7 (0.9, 5)	-	6.3 (0.3, 14)
mI	3.8 (1.2, 4)	5.9 (2.3, 11)	4.1 (0.3, 2)	7.4 (3.1, 7)	-	6.3 (0.6, 20)
12 Months;						
tNAA	7.6 (0.6, 4)	7.1 (0.6, 9)	7.5 (1.9, 2)	7.6 (1.2, 7)	8.9 (SV)	7.4 (0.2, 19)
NAA	6.1 (1.1, 4)	5.7 (1.2, 6)	5.9 (2.9, 2)	6.0 (1.2, 6)	6.3 (SV)	5.9 (0.3, 15)
mI	3.9 (0.9, 2)	6.5 (3.3, 8)	3.4 (0.1, 2)	6.9 (2.4, 6)	5.5 (SV)	6.3 (0.7, 17)
24 Months;						
tNAA	8.0 (0.5, 6)	7.4 (0.8, 7)	-	7.1 (0.9, 10)	6.9 (SV)	7.2*(0.8,18)
NAA	6.8 (1.1, 4)	5.8 (0.8, 5)	-	5.6 (1.2, 6)	4.5 (SV)	5.6 (0.3, 12)
mI	4.4 (1.4, 4)	4.8 (0.7, 5)	-	5.4 (1.6, 10)	3.3 (SV)	5.1 (0.4, 16)

Table 5-4 Table demonstrating effect of different medications on metabolite profiles within different groups at the three time points. Asterisks in the above table refer to cross-sectional comparisons between medication use vs. non-medication using subjects in a particular group at a particular time point. *p<0.05, **p<0.01, ***p<0.001. SV; Single value. SVs could not be included in analyses. [a]Either AP, Benzodiazepine, Sodium valproate, Memantine or Dopamine agonist. [b]Either

Benzodiazepine, Sodium valproate, Memantine or Dopamine agonist. Multiple correlations were performed with one-way ANOVA with post hoc Newman-Keuls Multiple Comparison Test, while two group comparisons were made using unpaired Student's t-test.

	Controls Mean (SD, N)	**Pre-HD Mean (SD, N)**	**Early HD Mean (SD, N)**
Baseline;			
tNAA	8.60 (0.64, 25)	8.24 (0.48, 18)	7.46 (0.89, 6)***•
NAA	7.82 (0.93, 25)	6.98 (0.99, 17)**	6.53 (1.12, 5)*
mI	4.11 (1.20, 23)	3.73 (0.80, 15)	3.81 (1.19, 4)
12 Months;			
tNAA	8.70 (0.61, 24)	8.10 (0.79, 18)**	7.62 (0.56, 4)*
NAA	7.47 (0.99, 24)	6.95 (1.18, 18)	6.07 (1.06, 4)
mI	4.33 (1.10, 20)	3.90 (0.82, 17)	3.90 (0.99, 2)
24 Months;			
tNAA	8.91 (0.79, 25)	8.23 (0.88, 17)**	8.00 (0.50, 6)*
NAA	7.64 (0.97, 25)	7.20 (1.00, 17)	6.84 (1.14, 4)
mI	3.97 (0.98, 24)	3.97 (0.80, 16)	4.40 (1.36, 4)

Table 5-5 Cross-sectional evaluations of metabolites in Control, Pre-HD and Early HD groups after excluding individuals taking medications (data re-presented from Table 5-4. above for accessibility). SV=Single Value. Asterisks refer to comparisons against Control values. While circles refer to comparisons against Pre-HD individuals at a given time-point, *p<0.05, **p<0.01, ***p<0.001. •p<0.05.

5.3.4 Discussion

This investigation represents the first reported longitudinal, purely observational study of MRS in HD. Existing longitudinal MRS data in HD derives from therapeutic trials and generally did not include a non-treatment or placebo arm (Koroshetz et al. 1997, Rosas et al. 1999, Tabrizi et al. 2003, 2005, Bender et al. 2005).

Most strikingly, these observations over 24 months consistently replicate the cross-sectional baseline findings of alterations in NAA, tNAA in Pre-HD and Early HD and mI in Early HD. There was, however, a notable lack of longitudinal change in all of these metabolites suggesting that metabolite measures may be relatively non-dynamic, robust biomarkers of the disease state. These findings challenge the concept of putaminal metabolite change as a dynamic longitudinal marker for HD. Nevertheless, subtle indicators for longitudinal progression are suggested in the cross-sectional data, with increasingly significant tNAA differences in Pre-HD compared to Controls across sequential study visits. Similarly, on subgroup analyses, most notably the Early HD Stage II group showed increasingly significant differences in tNAA and NAA compared to other subgroups over the 24 months. These cross-sectional findings failed to translate in the paired longitudinal analyses. This likely reflects the significant proportion of subjects excluded from longitudinal analyses due to either a failure of successful scan at one of the timepoints or the unreliable measurement of a given metabolite at one timepoint ie. successful imaging was required at all three timepoints for these analyses. While these longitudinal data failed to achieve appreciable longitudinal change it

should be remembered that this cohort is relatively small compared to those reported in many observational imaging studies (Paulsen et al. 2008). However, in an even smaller cohort using a caudate boundary shift integral technique, up to 3% caudate volume change was previously seen in early HD over the same duration (Hobbs et al. 2009) further supporting a relative lack of longitudinal sensitivity for this modality. Conversely, the robustness of MRS measures in this cohort over time may indicate tNAA as a relatively static marker of the HD disease state, and one that, used in therapeutic studies, could confer advantages over dynamic markers. This re-envisioning of a biomarker role for MRS is expanded more fully below.

How is a lack of longitudinal metabolite change over this duration possible? Firstly, as measures of neuronal health/viability and of gliosis respectively, tNAA and MI can be taken to be sensitive but non-specific markers of the disease process. That is, while multiple pathogenic processes have been associated with HD, these metabolites will likely reflect the net outcome of these processes, regardless of the contribution of each pathogenic and endogenous neuroprotective mechanism at a given time. Ultimately these processes may reach a steady state whereby tNAA for example, reaches a plateau in Early HD at which further tNAA loss only occurs over much longer periods. Secondly, if we make an assumption, that GM alone is contributing to the putaminal tNAA reductions reported, then it is possible that as disease progresses tissue volume loss and change in absolute metabolite mass reaches equilibrium such that further changes in concentration are not seen until the individual reaches a more advanced stage.

Considering that; 1) diverse pathogenic mechanisms have been implicated in HD, 2) for at least some of these mechanisms their relative importance may vary according to stage in the disease process (Graham et al. 2009) and 3) that the metabolites themselves could reflect different aspects of the same disease process, it is perhaps not surprising that longitudinal progression in metabolite measures may vary in different HD subgroups within this study. Consequently, over short durations of follow-up, patterns of evolving, longitudinal metabolite change unquantifiable in larger, more heterogeneous, groups (eg. Early HD or Pre-HD) may only be identifiable within the subgroups. Of all the longitudinal analyses, only on the longitudinal comparisons of Early HD Stage I individuals, was any longitudinal change approaching significance measurable (MI/NAA) over the three timepoints. Further maximizing homogeneity using even narrower subcategorisations eg. Pre-HD divided into three groups; near, mid and far-to-predicted diagnosis, as has been used in Predict-HD (Aylward et al. 2011), may prove more informative still. However, in the absence of a study weighted to specifically evaluate larger subgroups, such sub-categorisations become untenable. The requirement for only individuals with matched metabolites at serial visits eg. for each manifest HD individual to have measurable NAA at each time point, in order for them to be included in paired Student's t-test analyses depletes the utilizable longitudinal cohort. This is especially so since, due to movement artifact, this group is more likely to have rejected metabolite estimations at a given

timepoint. Similarly without larger cohorts apparent differences in subgroup metabolite patterns fail to reach statistical significance.

In terms of statistical analyses Longitudinal Linear Mixed Effects (LME) models can be a powerful tool for assessing longitudinal imaging changes in clinical studies. They offer a more powerful and flexible method of analyzing longitudinal data than many other methods, and are able to handle unbalanced data including missing time point data, imperfect timing of follow up analyses, and the effects of subject dropout. LME models can avoid potential sources of bias inherent in assuming that repeated measures within pairs over time, are independent, as can be an issue with paired *t*-tests. LME also incorporates fixed and random effects or cofactors of interest, that enable the interpretation of the effect of co-variances of interest to be estimated at follow up. The model has been shown to provide greater sensitivity, in realistic settings than other methods of longitudinal analysis such as repeated measures ANOVA and so is highly appropriate as a model for real-world observational studies of imaging measures including MRS as a biomarker. Although longitudinal LME models were not used in this work, our further work will seek to incorporate this paradigm into longitudinal MRS analyses.

Importantly, the possibility of using other MRI technologies including volumetric MRI, has been proposed as an alternative or an enhancement to mathematical methods of subject stratification such as the DBS and time to predicted disease onset proposed by Langbehn (Langbehn et al. 2004). MRS could be similarly used,

stratifying for example Pre-HD individuals by a specified tNAA range, to optimise homogeneity within subject groups and ensuring that only individuals at a truly pathologically similar stage of disease are compared.

Chard and colleagues have shown that MRSI could be combined with Statistical Parametric Mapping techniques to provide tissue specific information about metabolites within a given voxel, in their case cortical GM and 'Normal-Appearing White Matter' in Multiple Sclerosis. In doing so differential metabolite changes within tissues comprising the voxel were estimable (Chard et al. 2002). Using motion controlled PRESS sequences, investigators have also estimated, through linear regression of tissue volume *vs* metabolite concentration, metabolite concentrations for a given tissue type within a single voxel through the application of FAST segmentation (FAST, FMRIB's Automated Segmentation Tool), part of the Functional MRI of the Brain (FMRIB) set of algorithms (www.fmrib.ox.ac.uk/, Zhang et al. 2001). As part of further work, it would be valuable to attempt to apply, not only the concept of motion controlled MRI to obtain PRESS images of difficult-to-estimate metabolites, but also to accurately segment and estimate metabolite signatures for different tissue components, using the methods described to maximize utilizable information from MRS for any given study, and to avoid partial volume effects. In addition, over time, using these methods, linear regression may be useful in demonstrating the longitudinal metabolite change, while avoiding the confounding effects of altered putaminal volume within the voxel.

At baseline there was demonstrably poorer scan quality in Early HD individuals than in Control or Pre-HD groups, with significantly lower SNRs (mean (SD), Early HD; 6.83 (1.91), Pre-HD; 9.36 (2.12) & Controls; 10.17 (2.18), $p<0.001$). Similar patterns of reduced SNR in early HD compared to controls was demonstrable at subsequent 12 month (Early HD; 6.70 (2.06), Pre-HD; 7.92 (2.20), Early HD; 9.68 (2.18). E vs. P ($p>0.05$), E vs. C ($p<0.001$), P vs. C ($p<0.01$)) and 24 month visits (Early HD; 6.54 (1.82) vs. Pre-HD; 9.32 (2.61) & Controls; 9.82 (1.96), $p<0.001$). Importantly, lower SNR reduces sensitivity to less reliably measured metabolites hence a reduced determination of metabolites MI and NAA compared to tNAA.

Interestingly, a measure of tissue homogeneity-the spectral linewidth or FWHM was increased consistently in Early HD across timepoints- at baseline (Early HD; 10.51 (2.67) Hz vs. Pre-HD; 8.00 (2.36)Hz & Controls; 7.55 (1.66) Hz, $p<0.001$) at 12 months (Early HD; 9.95 (2.56)Hz vs. Pre-HD; 7.76 (2.02)Hz & Control; 7.77 (1.6)Hz, P vs. E ($p<0.01$), E vs. C ($p<0.001$), C vs. P ($p>0.05$)) and at 24 months (Early HD; 9.61 (2.03)Hz vs. Pre-HD; 7.28 (2.08)Hz & Controls; 7.54 (1.8)Hz, $p<0.001$). Such increments commonly altered tissue composition and usually reflect either increased tissue water or iron infiltration and may therefore support earlier work suggesting altered striatal iron in HD (Bartzokis et al. 2007). This finding itself warrants future study, perhaps through the use of an iron imaging technique such as Susceptibility Weighted Imaging or SWI.

Analysing the effects of medications on brain metabolites revealed trends to reduced tNAA/NAA levels when all medicated Early HD individuals were compared against all un-medicated individuals. This was with the exception of tNAA among medication-using HD individuals at 24 months where significantly lower levels were identified. It is an interesting observation that AD should have this effect, given the general consideration that NAA/tNAA are markers of neuronal health, and in itself would be worthy of re-evaluation in future cohorts. This could simply be selection bias in that more affected manifest individuals are more likely to be using AD. Summarising medication-related observations, across all groups no consistent, significant alteration in tNAA or NAA appeared to be generated by medication usage, while an almost consistent trend to mI elevations was identified among individuals using AD alone or in combination with other drugs. The exclusion of medicated individuals tellingly revealed a persistence of many tNAA group differences, despite its restriction of the cohort size. This further evinces the robustness of this metabolite as an outcome measure. By contrast, mI showed less consistent patterns of difference suggesting that group effects may, at least in part, be engendered by medication effects. To assess whether medication effects could have attenuated longitudinal change in these metabolites we performed paired analysis in un-medicated individuals only. No significant longitudinal change in any metabolite was observed for any of the groups across the 24 months (data not shown).

For tNAA, in Pre-HD depending on time point, up to 7/25 (28%) individuals were taking anti-depressants +/- additional psychotropic medication, while among Controls also depending on time-point, up to 4/30 (13%) were taking anti-depressants medication. Of note, this compares reasonably well with antidepressant usage in around 21.9% pre-manifest HD and 13% of unaffected controls reported among around 1000 PREDICT-HD subjects. Furthermore the authors report that their data may actually be an under-estimation, because they excluded individuals whom were suffering from unstable illness (Rowe et al. 2012). The high rates of depression, may well reflect the overlapping brain regions implicated in depression and HD (Rowe et al. 2012).

The data from the three study visits identifies tNAA as the most promising of the three metabolite measures based on its sensitivity in Pre-HD and its robustness (at all three visits it was the most consistently measurable metabolite). As such it may be thought of as a metabolite marker of the disease state (see Figure 5-6). If we were to test a therapeutic with estimated efficacy to partially normalise tNAA to 50% of the difference between Control vs. Early HD, based on longitudinal data from these groups, we would obtain a relative effect size (RES) of 0.80, while 80% and 20% normalization would give RES of 1.29 and 0.32. In order to detect such differences with 80% power at the 5% significance level total numbers of subjects required (that would be split equally between two treatment arms) for such a study would need to be around 350, 52 and fewer than 30 depending on whether

20%, 50% or 80% normalization of tNAA levels are expected. These numbers are feasible based on recruited numbers for earlier therapeutic studies.

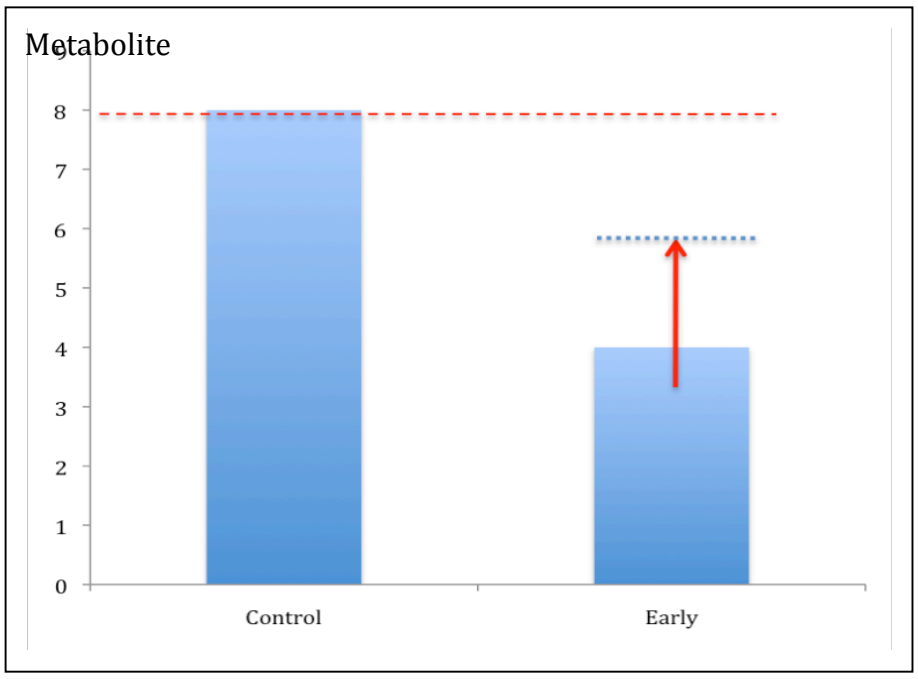

Figure 5-6 Partial, therapeutic, normalisation of a metabolite eg. tNAA from a disease state level.

The further development of MRS metabolite measures as biological markers of disease progression and neurodegenerative process requires their correlation with meaningful phenotypic, including motor, measures and change and will be considered in the next investigation.

5.4 Investigation of MRS as a marker of motor phenotypic progression

5.4.1 Introduction

One of the major goals of biomarker development is the measurement of disease progression among the pre-manifest population who lack overt motor dysfunction. This is especially important as the ultimate aim of disease modification will be preventing onset of neuropathological processes in this group. One measure that has been used to this end is the Disease Burden Score or DBS.

The attempt to associate putaminal pathology (as assessed by MRS) with motor dysfunction is logical. Together with the caudate, this nucleus is affected early in the disease course, with evidence of striatal atrophy at 15-20 years prior to clinical onset (Paulsen et al. 2008, Weir et al. 2011). Within the striatum, selective medium-sized spiny neurons (MSN) loss occurs with relative sparing of striatal interneurons (Vonsattel et al. 1998). In animal HD models, striatal interneurons exhibit differential vulnerability to damage and cell loss such that cholinergic interneurons are relatively spared while parvalbumin-containing GABA-ergic interneurons demonstrate reduced survival (Meade et al. 2000). The dysfunction and loss of striatal parvalbuminergic interneurons, which receive significant cortical input (Lapper et al. 1992), likely play a role in HD related corticostriatal dysfunction. The MSN project to the internal segment of the globus pallidus (GPi) by either the direct or indirect pathway. The latter pathway is so named due to its projection through the globus pallidus external segment (GPe), and subthalamic

nucleus prior to reaching the GPi. The GPi exerts control over cortical motor planning and execution via thalamic connections (Graybiel et al. 1994). Broadly speaking, the direct pathway appears to act to facilitate cortical motor programs whilst the indirect pathway inhibits these programs (Albin et al. 1989). The indirect pathway MSNs appear to be affected first, resulting in impaired enkephalin expression, with subsequent involvement of the direct pathway MSNs (which express Substance P). Differential involvement of these direct pathways may explain the biphasic movement disorder associated with HD, in which early hyperkinesia evolves into bradykinesia and eventual akinesia (Reiner et al. 1988, Albin et al. 1990, Richfield et al. 1995, Sapp et al. 1995, Sun et a. 2002).

A number of studies have examined the relationship between neuropathological measures such as putamen volume and aspects of clinical phenotype commonly, motor dysfunction. Across both pre-manifest and early manifest individuals impaired digitomotographic performance was associated with atrophy of the striatum, including putamen (Bechtel et al. 2010), and in TRACK-HD, volumetric MRI measurement of putamen volume, using BRAINS (Brain Research: Analysis of Images, Networks, and Systems, Iowa City, Iowa, USA) (Magnotta et al. 2002), identified an association of atrophy with UHDRS-TMS in Early HD across 24 months (partial Pearson correlation -0.258, p=0.012) (Tabrizi et al. 2012). Among a subgroup of pre-manifest individuals with phenotypic characteristics suggestive of progression approaching onset of overt disease (‘progressors’), putaminal atrophy trended to greater reductions than in non-progressors (p=0.067).

Measurement of putaminal atrophy was one of the strongest TRACK-HD biological markers, consistently exhibiting one of the highest effect sizes for change over 24 months. It was also one of few measures able to differentiate the earliest Pre-HD A subgroup from controls (Tabrizi et al. 2012). The clinical effects of putaminal atrophy are not limited to motor dysfunction. Indeed among pre-manifest individuals, total striatal volume loss correlated with deteriorating performance on a number of cognitive tasks including Stroop and Verbal Fluency tasks (Paulsen et al. 2010). On a small scale, MRS estimations of tNAA and tCr (Sanchez-Pernaute et al. 1999) have previously been correlated with cognitive and motor performance. Associations such as these may, to some extent, identify the meaningful clinical impact of proximal pathogenic processes. They may also have some role in discriminating whether a putative marker is measuring an aspect of the true neurodegenerative process or simply epiphenomena.

The aim of this experiment was to assess whether brain metabolite alterations correlated with motor phenotypic measures and DBS – the hypothesis being that both tNAA decrements and mI increments would correlate with increasing disease burden and worsening motor phenotype.

5.4.2 Methods

Participants

This experiment involved all those subjects outlined in Table 5.3.1 ie. only those individuals who were not successfully scanned at a given time-point were excluded from metabolite-motor correlations performed at that time-point.

Procedures

MRS imaging procedures were as per Investigation 5.2. For this investigation, all subjects had a DBS calculated and underwent clinical evaluation using UHDRS-TMS and the Qmotor battery as detailed in the previous chapter. All tapping tasks reported here were performed with the right hand, hence only data from right-handed individuals were included here to minimise bias. The right hand digitomotographic tasks only were selected for correlation, since imaging was of the contralateral, left, putamen. No metronome tapping tasks with the dominant hand were performed at 24 months for TRACK-HD cohort-a decision made by the Central Co-ordination for the entire TRACK-HD study.

Statistics

Scatter plots and linear regression were used to compare metabolites against DBS and motor outcomes. Linear correlations were investigated using the method of least squares.

5.4.3 Results

Correlation with DBS & motor performance (Figure 5-7 & Table 5-6)

A significant trend for tNAA reductions with increasing DBS was identified across Pre-HD and Early HD. This association held across all three visits. For all early HD metabolites, with the exception of UHDRS-TMS correlations, weaker, or absent, correlations were observed at 12 and 24 months compared with baseline (Table 5.4.1). Generally metabolites correlated across a larger number of quantitative motor tasks when evaluated for the combined Pre-HD and Early HD groups, likely because of the larger combined sample size. Correlations broadly appeared most robust with the speeded tapping measures. Of the metabolites NAA most closely and consistently correlated with motor phenotypic measures of disease.

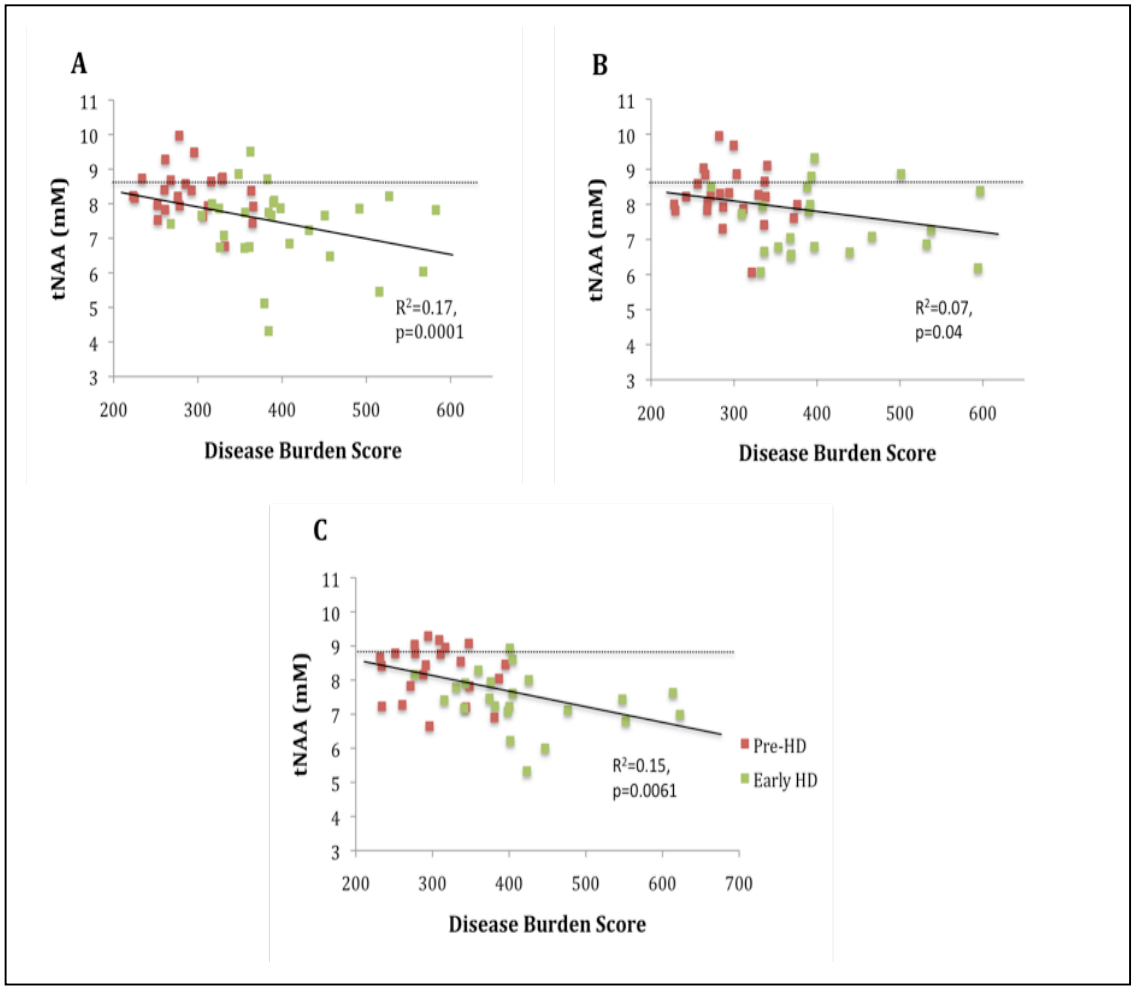

Figure 5-7 tNAA correlation with DBS. Correlations between Disease Burden Score (DBS) and tNAA. Figures A, B & C represent baseline, 12 month and 24 month evaluations. The dashed line represents the Control mean tNAA concentration.

	Early HD			*Pre-HD & Early HD*		
Baseline	tNAA	NAA	mI	tNAA	NAA	mI
UHDRS-TMS	NS	NS	0.23 (<0.05)	-	-	-
Metronome Tapping: Self-paced tap precision	NS	0.71 (<0.0001)	NS	NS	NS	NS
Metronome Tapping: Deviation of tap initiation	NS	0.47 (<0.01)	NS	NS	0.37 (0.0001)	NS
Tongue contact time*	NS	0.21 (0.05)	NS	-	-	-
Tongue pressure variability	NS	0.24 (<0.05)	NS	0.30 (<0.0001)	0.24 (<0.001)	NS
Speeded tapping: Tap duration	NS	NS	NS	0.14 (0.006)	0.14 (0.017)	0.23 (0.001)
Speeded tapping: Repetition time	NS	0.27 (0.023)	NS	Not linear	0.23 (0.002)	Not linear
12 Months						
UHDRS-TMS	NS	NS	NS	-	-	-
Metronome Tapping: Self-paced tap precision	Not linear	NS	NS	Not linear	Not linear	NS
Metronome Tapping: Deviation of tap initiation	NS	NS	NS	0.16 (0.011)	0.15 (0.011)	NS
Tongue contact time*	NS	NS	NS	-	-	-
Tongue pressure variability	NS	NS	NS	Not linear	0.21 (0.0016)	Not linear
Speeded tapping: Tap duration	NS	NS	NS	0.14 (0.017)	0.22 (0.0026)	NS
Speeded tapping: Repetition time	NS	NS	NS	Not linear	Not linear	NS
24 Months						
UHDRS-TMS	0.25 (0.012)	0.35 (0.012)	0.14 (0.1)	-	-	-
Metronome Tapping: Self-paced tap precision	-	-	-	-	-	-
Metronome Tapping: Deviation of tap initiation	-	-	-	-	-	-
Tongue contact time	NS	NS	NS	-	-	-
Tongue pressure variability	NS	NS	NS	Not linear	Not linear	0.18 (0.0068)
Speeded tapping: Tap duration	NS	NS	NS	Not linear	0.37 (0.0002)	0.21 (0.005)
Speeded tapping: Repetition time	Not linear	0.22 (0.05)	NS	Not linear	0.45 ($2x10^{-5}$)	Not linear

Table 5-6 Correlations between metabolite concentration and motor performance in HD.

Note that for UHDRS-TMS and tongue contact time at all time points, marked ceiling effects among

Pre-HD individuals precluded unbiased correlations. Hence no correlations across Pre-HD and Early HD are reported for these tasks.

5.4.4 Discussion

Over serial visits the changing correlations with motor performance likely reflects variability in individual motor and MRS measures and differential sensitivity of the two biomarker modalities to phenotypic and disease progression. The strength of correlations between tNAA and Disease Burden Score also showed some fluctuation between visits. At all visits, the same subjects with a DBS of between 500-550 or greater consistently exhibited a lower tNAA than control mean. Based on this robustness over 24 months, and the already outlined potential for reversibility in NAA/tNAA reductions, this metabolite could be a useful outcome measure for therapeutic trials. In this context, the lack of sensitivity to longitudinal change over time could be viewed as a benefit of this biomarker modality. In this model, it could be possible to identify partial reversal (given the low variability in tNAA measurements) of group tNAA decrements towards control levels among individuals of a given DBS as illustrated in Figure 5-7. The development of such a model would depend initially on the evaluation of tNAA in larger HD cohorts, ideally at different disease stages.

5.5 Investigation of White Matter Effects on tNAA estimates

5.5.1 Introduction

As can be seen from Chapter 5.2, voxel contamination with tissues extraneous to the region of interest (for example, WM) is a concern with MRS. These partial volume effects can bias results, rendering interpretation of specific metabolite alterations unreliable and limiting the modality's usefulness.

Several methods have been employed to attempt to address the impact of partial volume contributions upon metabolite estimations. One group has used the application of pulse suppression bands to the tissue adjacent to the ROI-in this case the amygdala-a small brain region particularly susceptible to partial volume effects. Through reducing these effects, intra-individual scan-rescan reliability was improved. However the technique involved adjusting voxel volume on a subject-by-subject basis (Nacewicz et al. 2012). Using MRSI, an MRS technique which allows metabolite acquisition from multiple spatially diverse voxels, voxel segmentation into different tissue types has also been used to extrapolate pure GM and WM metabolite estimations (McLean et al. 2000, Guevara et al. 2012). Furthermore, one group has also recently developed a technique utilizing 2D selective radio-frequency excitations to excite pre-selected, irregularly shaped voxels only, thereby minimising partial volume effects (Busch & Finterbusch, 2011).

Two methods were used here to assess the potential impact of partial volume WM effects upon the data presented here. Firstly, in a few subjects returning for a 36 month scan a second voxel was placed immediately superior to the putaminal voxel within pure peri-putaminal WM and the tNAA measure assessed. Secondly, the patterns of longitudinal change in total (ie. bilateral) putaminal volume over the 24 months of follow up was compared against longitudinal change in putaminal metabolites to assess whether a change in putaminal volume (and hence presumably an increase in intravoxel WM) was correlated with longitudinal change in tNAA levels.

The ability to accurately estimate putaminal metabolite concentrations and absolute amounts/masses, without concerns about WM contributions, would permit utilization of a larger proportion of the total metabolite spectrum. For example, from Section 5.2 onward, tCho, tCr and tGlu were not analysed further because of concerns that tCr and tGlu were potentially artificially lowered in the Early HD group, and tCho was potentially increased, due to increasing amounts of WM in the putaminal voxel. The measurement of absolute metabolite mass within putamen could enable appreciation of total metabolite changes against well-characterized measures of structural pathology such as striatal atrophy and therefore of change over the disease course. Lastly since total metabolite mass will be a function of both putaminal volume and of metabolite change it may represent a powerful biomarker in its own right. Therefore a simple mathematical formula for such estimations will be proposed.

5.5.2 Methods

Subjects & MRS

All subjects were enrolled as per TRACK-HD requirements. Volumetric MRI measures of putaminal volume were performed as part of the main study and the technique outlined below, the MRS protocol has already been outlined. For the purposes of this investigation only subjects where putaminal and tNAA data was available for all three visits were included in these analyses. As part of an *ad-hoc* analysis to qualitatively assess the contribution of WM contamination to the metabolite levels within the putaminal voxel, in a small subset of quasi-randomised patients (N=6; 2 Controls, 3 Pre-HD and 1 Early HD) returning for a 36-month follow-up evaluation, a second adjacent MRS voxel of the same volume was placed within the WM directly superior to the original putaminal voxel (Figure 5-8). The rationale was to assess tNAA and mI within a presumably comparable region of WM for comparison.

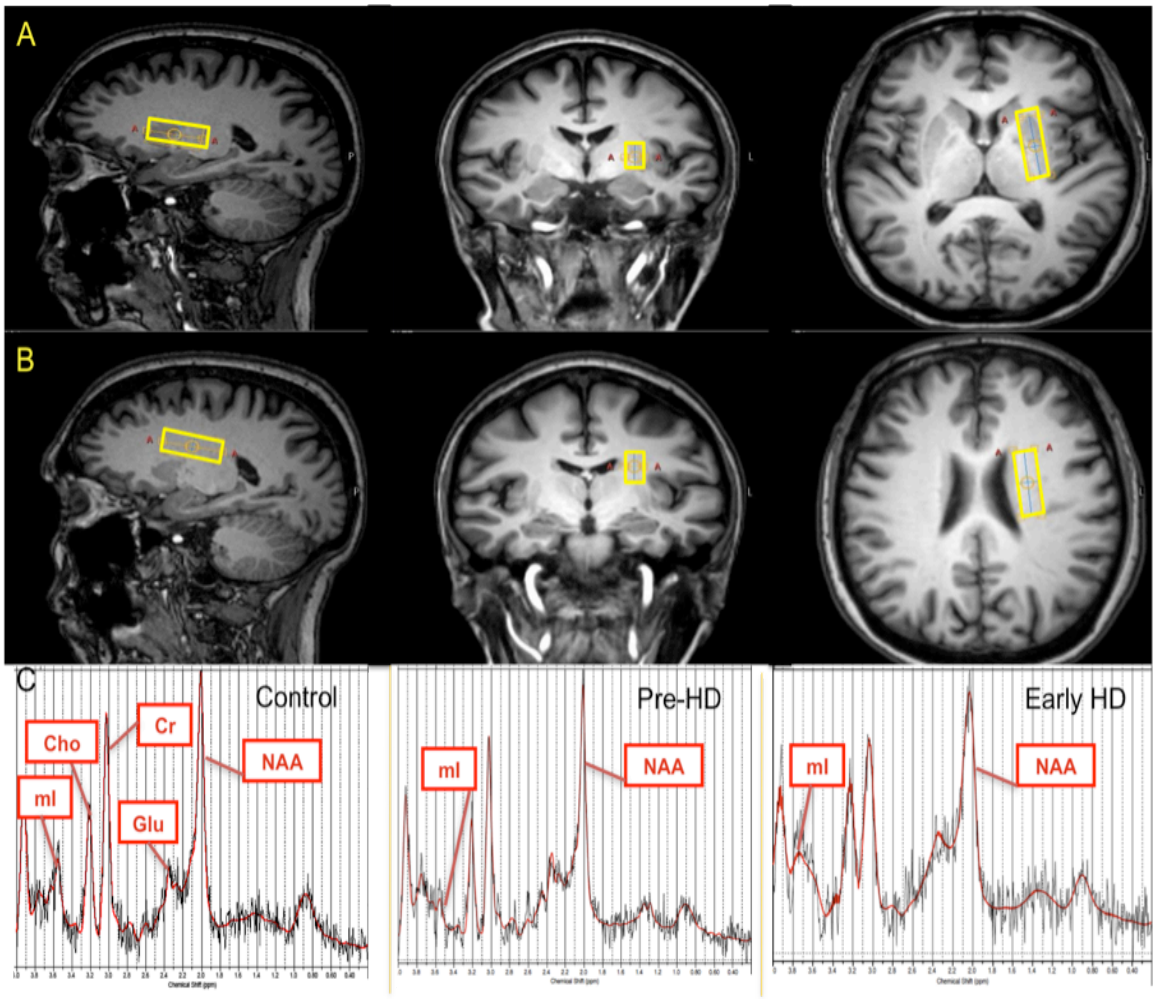

Figure 5-8 A-C. Voxel placement and MRS spectra Samples of A. Putaminal Voxel Placement, B. WM Voxel Placement, C. MR Spectra by subject group.

Imaging (Volumetric MRI)

To further establish; 1) any effect of WM contamination on putaminal metabolite measurements and 2) comparisons of relative biomarker sensitivities of putaminal MRS against putaminal volume measurement comparisons were performed against 3T MRI data acquired with standardised acquisition protocols. These included T1-weighted volumetric and T2-weighted sequences (Tabrizi et al. 2009).

IXICO (London, UK) performed rigorous quality control to ensure stability of scan acquisition over time. Putaminal volume was derived with fully automated segmentation and subtraction with Brain Research: Analysis of Images, Networks, and Systems software (version 2) (Brain Research: Analysis of Images, Networks, and Systems, Iowa City, Iowa, USA) (Magnotta et al. 2002). Segmentations and registrations were visually inspected by trained image analysts with the diagnosis masked to ensure accuracy of tissue delineation and matching of scans. The segmentations were performed by Hans Johnson, University of Iowa. WM MRS was performed exactly as per the protocol for putamen outlined in 5.2, with the exception of the voxel's placement.

Statistical Analyses

Pairwise longitudinal comparisons of putamen volume (expressed as a percentage of total intracranial volume) and putaminal tNAA were made using Student's t-tests with Bonferroni corrections for multiple comparisons. Putaminal and WM tNAA comparisons were qualitative only, because of the low subject numbers.

5.5.3 Results

Comparison with longitudinal putaminal volume

Figure 5-9 demonstrates that despite significant longitudinal reductions in left putaminal volume, no significant changes in tNAA were identifiable over the three time points. Furthermore, in this Pre-HD cohort (restricted only to those with both tNAA and putaminal volume data at all timepoints) putaminal tNAA was not different in cross-section between Pre-HD and Controls at baseline or 12 months (Mean(SD), Baseline: Control vs. Pre-HD; 8.50 (0.64) vs. 8.63(0.71) p=0.56, 12 Months: Control vs. Pre-HD; 8.75 (0.58) vs. 8.42 (0.69), p=0.099) while putaminal volume was significantly different (Mean (SD), Baseline: Control vs. Pre-HD: 0.34 (0.008) vs. 0.30 (0.011) p=0.02, 12 Months; 0.33 (0.008) vs. 0.30 (0.011), p=0.01 Student's t-test) between these restricted groups. Together these observations support the notion that cross-sectional group differences in tNAA are not simply the result of white matter contributions.

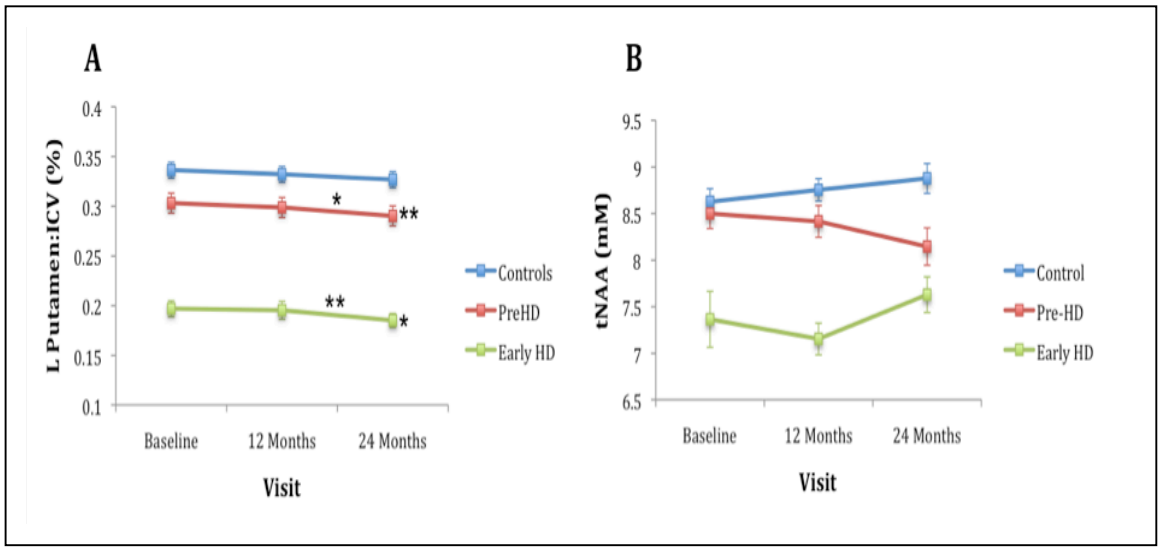

Figure 5-9 Comparing Longitudinal Progression over 24 months in Putaminal Volume and tNAA. Figure A illustrates progression in putaminal atrophy measured as a ratio to intracranial volume (ICV). Figure B illustrates a lack of significant change in tNAA over this duration. Note that only subjects with measurements (for both tNAA and putaminal volume) paired across all three visits were included in this analysis. Asterisks are placed according to the relationship they represent, if next to the 24 month visit they represent comparisons against baseline visit, * $p<0.05$, ** $p<0.01$. Comparisons made with paired Student's t-tests with Bonferroni correction.

Evaluation of white matter effects

To better understand potential white matter effects upon metabolite concentrations, metabolite measurements were considered in a second, predominantly white matter, voxel immediately superior and almost adjacent to the original putaminal voxel. This evaluation was performed *ad-hoc* in 6 individuals returning for their 36-month analysis. Both NAA and tNAA tended to be lower in WM than in the putaminal voxel in Pre-HD and Controls. While the mean NAA difference was considerable (-14.4% Controls, -12.2% Pre-HD), it was less for tNAA (-4.0% Controls, -1.7% Pre-HD) and would be unlikely to explain the cross-sectional group differences observed. Furthermore, regardless of tissue type, all NAA and tNAA measurements were lower in Pre-HD than their comparator in Controls. For mI, the tendency was for a lower WM value arguing against a WM effect in these cross-sectional observations. Of note mI was not quantifiable (SD% above threshold) in one Pre-HD putaminal voxel. Only a single Early HD subject was included in this analysis (NAA(WM)/(Put): 5.55/5.39; tNAA(WM)/(Put): 6.50/5.39; mI(WM)/(Put): 3.70/3.91).

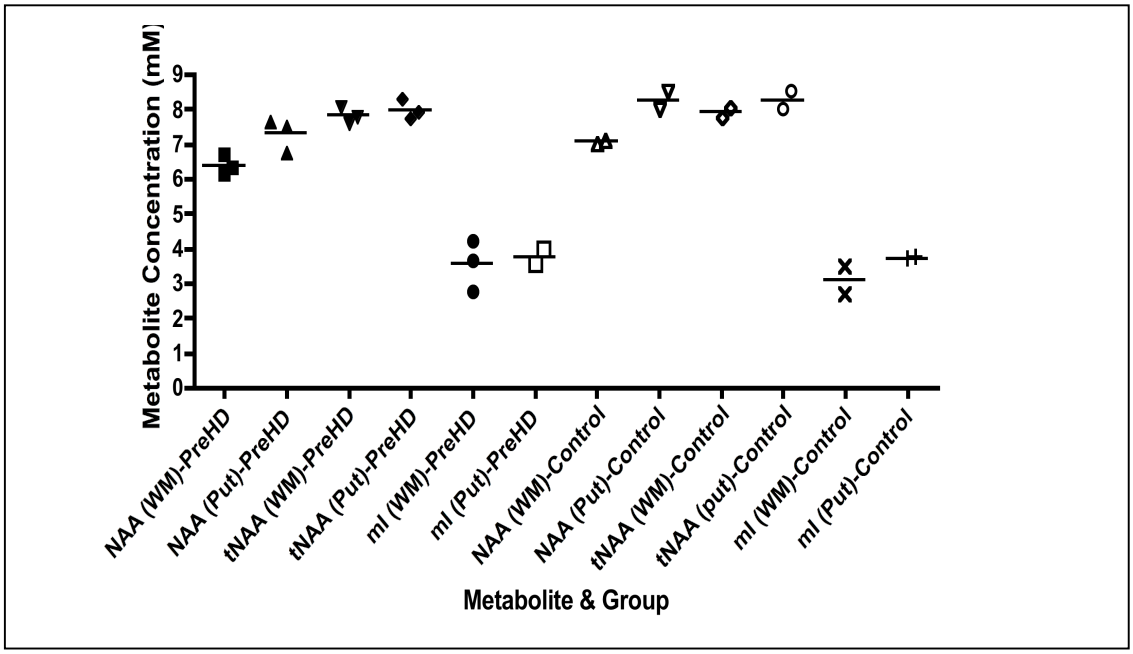

Figure 5.10 Comparison of White Matter and Putaminal Metabolites. In a restricted number of our cohort evaluation of metabolites within a second, adjacent WM voxel was performed. Only PreHD (N=3) and Controls (N=2) are displayed. This evaluation was performed in only a single Early HD subject (see text).

5.5.4 Discussion

In a subset of the cohort (N=56; 24 Controls, 17 Pre-HD, 15 Early HD) that had both tNAA and volumetric MRI measures at all visits, there was a small but significant, progressive reduction in left putamen:ICV ratios in HD groups while mean tNAA concentrations remained unchanged across 24 months. One possibility here for the lack of direct correspondence between the reduction in tNAA and putaminal volumes, (Figure 5-9) may be the fact that tNAA may actually be reflecting neuronal mitochondrial function, and hence cellular energy deficits rather than just neuronal loss.

While this illustrates the sensitivity of volumetric imaging measures as markers of longitudinal disease progression, even over just 12 months, it also demonstrates a comparable lack of longitudinal sensitivity of tNAA. The lack of tNAA alteration, despite increasing WM contamination of the putaminal voxel (a consequence of decreasing putaminal volume), also supports the theory that the cross-sectional group differences represent genuine differences in tissue concentration of metabolites rather than purely partial-volume effects.

To assess further the impact of white matter partial-volume effects we analysed metabolites within a second, WM voxel adjacent to the putaminal voxel. Observations of a lower mean NAA and very marginally lower mean tNAA in WM might have had some impact on the lower measurements of these metabolites, cross-sectionally, among Pre-HD and Early HD individuals. However, two

observations argue against WM effects being strongly confounding. Firstly, the WM represented a much larger proportion of the second voxel than the putaminal voxel thus, even for NAA where the mean WM concentration was most different from the putaminal value, we would expect that voxel contamination with WM could only generate a small fraction of the lower mean NAA seen in the almost pure WM voxel. It would not be expected to account for the more marked and consistent putaminal tNAA differences seen at consecutive cross-sectional analyses. Secondly, from restricted comparisons both WM and putaminal NAA was lower in Pre-HD than in Controls (by gross observation, numbers too low to perform meaningful statistical analysis), suggesting that these metabolite differences among Pre-HD individuals vs. Controls are genuine changes, and that parallel metabolite changes within both tissue types may be occurring concomitantly.

One way of answering these concerns regarding the WM partial volume effects would be to mathematically calculate putaminal tNAA based on the volumetric measurements of putaminal volume, and the WM tNAA measurements. Here, and only here in this manuscript will tNAA concentration be identified instead as [tNAA] for clarity.

Referring to the absolute amounts of tNAA:

$tNAA_{TV} = tNAA_{Put} + tNAA_{WM}$

Where TV is Total Voxel, Put is putamen and WM is White Matter

Then since;

$tNAA_{TV} = Volume_{TV}.[tNAA]_{TV}$

$tNAA_{Put} = tNAA_{TV} - tNAA_{WM}$

Or,

$$[tNAA]_{Put} = \frac{tNAA_{TV} - tNAA_{WM}}{Volume_{Put}}$$

Unfortunately such a calculation was not possible in this cohort, since voxels frequently did not incorporate the entire putamen. Nevertheless such an estimation would provide a useful measure of total NAA which could be correlated against independent measures of pathology such as putamen volume. Furthermore, since absolute tNAA would also be dependent on volume, the measure may provide a compound (ie. combination of two biomarker modalities putamen volume and tNAA), sensitive marker of disease state.

5.6 Chapter Conclusions

In conclusion, MRS, and specifically the brain metabolites tNAA, NAA and mI have demonstrable potential as biomarker measures in HD, although their usefulness as longitudinal measures over shorter, 12-24 month durations may be limited compared to other biomarker measures (Tabrizi et al. 2012). Nevertheless, the

cohort considered here was considerably smaller than those of many observational, biomarker studies. Furthermore the robustness of these measures, especially tNAA may be of real benefit as an outcome measure for therapeutic trials. Furthermore, the analyses of WM effects support the validity of tNAA estimations, suggesting that these metabolite changes were not predominantly generated by partial volume WM effects. While the lack of metabolites' consistent correlation with motor measures is apparent, the correlation of tNAA with DBS, together with the trend for significantly lower tNAA in Early HD is important, and may assist in developing tNAA and other metabolites as outcome measures for therapeutic trials.

The next chapter will focus on the extrapolation of the role of MRS in defining potential new peripheral HD biomarkers.

6 Biosample or "Wet" HD biomarkers

6.1. Chapter Introduction

The advantages of measuring peripheral, "wet" markers of disease progression in HD have already been discussed in Chapter 1. Having identified putaminal elevations of the gliosis marker mI using MRS in early HD, the objective of the following studies was to identify whether peripheral gliosis measures were also altered in HD plasma and CSF.

6.2 Investigation of *myo-inositol* (mI) as a peripheral HD biomarker

6.2.1. Introduction

The *in vivo* putaminal metabolite changes identified using MRS and discussed in Chapter 5 parallel similar findings in the Alzheimer's disease (AD) brain. In AD, 10-50% increases in regional grey matter *myo*-inositol (mI) concentrations have been reported (Miller et al. 1993, Moats et al. 1994, Parnetti et al. 1997). Furthermore, in a study of 65 AD patients, the mI/NAA (NAA, *N*-acetyl aspartate) ratio derived from MRS successfully differentiated AD from normal controls with 83% sensitivity and 98% specificity (Shonk et al. 1995). Similarly in familial AD, at 2T MRS, a further 13 affected patients were compared against controls. NAA/mI was significantly reduced due to a 16% increase in mI vs. Controls. Furthermore, NAA/mI and mI/Cr correlated with MMSE score. Metabolites also correlate with extent of atrophy (CSF/GM voxel composition) (Rose et al. 1999). The elevation of mI in neurodegenerative disorders using MRS, appears to be a non-disease specific and reproducible finding, observed in AD, dementia associated with Down

Syndrome (Shetty et al. 1995) and now in HD (Sturrock et al. 2010). Furthermore mI alterations also occur in transgenic AD mouse models. Frontal cortical and hippocampal mI was measured and significant mI/Cr elevations were identified compared to control mice. At 8 months a chosen mI/Cr threshold was also able to correctly differentiate 95% of mice (Chen et al. 2009). Furthermore, ante-mortem NAA/mI ratio at MRS correlated well with neurofibrillary pathological stage (Braak stage) at post-mortem in AD affected individuals (Kantarci et al. 2008).

If plasma or CSF mI exhibited patterns of change consistent with the MRS findings, this metabolite would provide a cheaper, more accessible alternative to the imaging biomarker modality. Among controls and individuals with AD (N=10, each group) mI was quantified in CSF & plasma using a gas chromatographic-mass spectrometric (GC-MS) technique. Mean CSF concentration and plasma concentration of mI in AD, showed a trend to elevation, that did not quite reach significance, when compared with controls (C vs AD, 24.9+/-4.4 vs. 28.6 +/-4.9 mg/L (CSF); 4.3+/-1.3 vs. 4.48+/-1.15 (Plasma)). This study however, clearly evaluated only small groups (Shetty et al. 1996). A simple blood, or even CSF metabolic biomarker for HD would have several advantages over imaging biomarkers in terms of ease of administration, availability and reduced time and cost burden. Furthermore metabolic biomarkers may have the potential to identify the reversal of pathophysiological processes (Bender et al. 2005) following even acute experimental HD therapies. Such a reversal would unlikely to be identifiable on structural brain imaging.

The objective for this experiment was therefore to identify whether parallel alterations in peripheral mI concentrations occurred in HD, the hypotheses being that plasma and CSF mI levels were elevated in pre-manifest HD and that plasma and CSF mI levels would increase with advancing HD disease stage on cross-sectional evaluation.

6.2.2 Methods

Subjects

Blood samples from thirty-five subjects participating in the University of British Columbia (UBC) Biomarker Study cohort were evaluated; 10 in each of Pre-HD and Late HD groups, 7 Controls and 8 Early/Mid-HD individuals. Subjects were age and, where feasible, gender-matched. Controls were individuals who had received a negative HD genetic test result. HD individuals had full-penetrance HD gene expansion (CAG$\geq$40), with the exception of one Pre-HD, one Early HD and one Mid-stage HD individual (CAG repeats=36, 39, 37, respectively).

Procedures

Gas chromatographic/mass spectrometric (GC/MS) assay of myo-inositol. mI in CSF and plasma were quantified using a method developed by Prof. SI Rapoport's team (Shetty et al. 1995, Shetty et al. 1995). In brief, CSF (25 ul) or plasma (100ul) was mixed with an internal standard ([$^2H_6$]myo-inositol), deproteinized and

evaporated under vacuum. The residue was heated with acetic anhydride/pyridine/4-dimethylaminopyridine, dissolved in hexane/ethyl acetate and washed with sodium bicarbonate. The organic layer was evaporated to dryness, and the residue reconstituted in ethyl acetate. An aliquot of this solution was injected into the GC/MS. Polyols were resolved on a capillary column (50% phenyl-50% methyl polysiloxane), and individual species detected and quantitated using chemical ionization in an ion trap mass spectrometer (12). mI yielded a highly abundant fragment ion corresponding to the loss of one CH3COOH residue from the protonated molecule. The ion m/z 373 for myo-inositol. The constituent ion m/z 379 of the internal standard was also acquired simultaneously. The concentration of mI in CSF or plasma was read from the standard curve generated.

mI was obtained from Sigma Chemical Co.(St. Louis, MO). Pyridine and acetic anhydride were obtained from Alltech Associates, Incorporated (Deerfield, IL), and solvents were from Burdick & Jackson (Muskegon, MI). The deuterium-labelled internal standard from Merck Sharp & Dohme/Isotopes (Canada). The gas chromatograph/mass spectrometer was a Finnigan MAT ITS40 (San Jose, CA). The capillary column was from Restek Corp. (Bellafonte, PA).

Statistical Analysis

Cross-sectional group analysis was performed using One-Way ANOVA with *post-hoc* Newman Keuls Multiple Comparison Test. Linear regressions with DBS and UHDRS-TMS were performed using the method of least squares.

6.2.3 Results

Subject demographics

Details of subjects participating in the project are outlined below in Table 6-1. Of all subjects participating plasma mI was measured for all subjects except one Pre-HD subject, for whom estimation was below limit of detection. CSF mI was estimated for all participants.

	Controls (n=7)	Pre-HD (n=10)	Early (2)/Mid-HD (6) (n=8)	Late HD (n=10)
Age (Mean, SD)	49.9 (17.0)	39.4 (13.7)	49.1 (7.8)	54.4 (12.3)
Women: Men	4:3	5:5	3:5	5:5
UHDRS-TFC (Mean, SD)	13 (0)	12.5 (0.7)	7.9 (2.7)	1.2 (1.4)

Table 6-1 Subject demographics. No significant difference was identified between mean group ages.

Plasma & CSF mI in HD gene carriers:

In both plasma and CSF, mI trended to elevation among HD gene carriers irrespective of disease stage, though the higher levels did not reach significance when compared to Controls. Interestingly, Control levels of the metabolite were higher in plasma than CSF. See Figure 6-1.

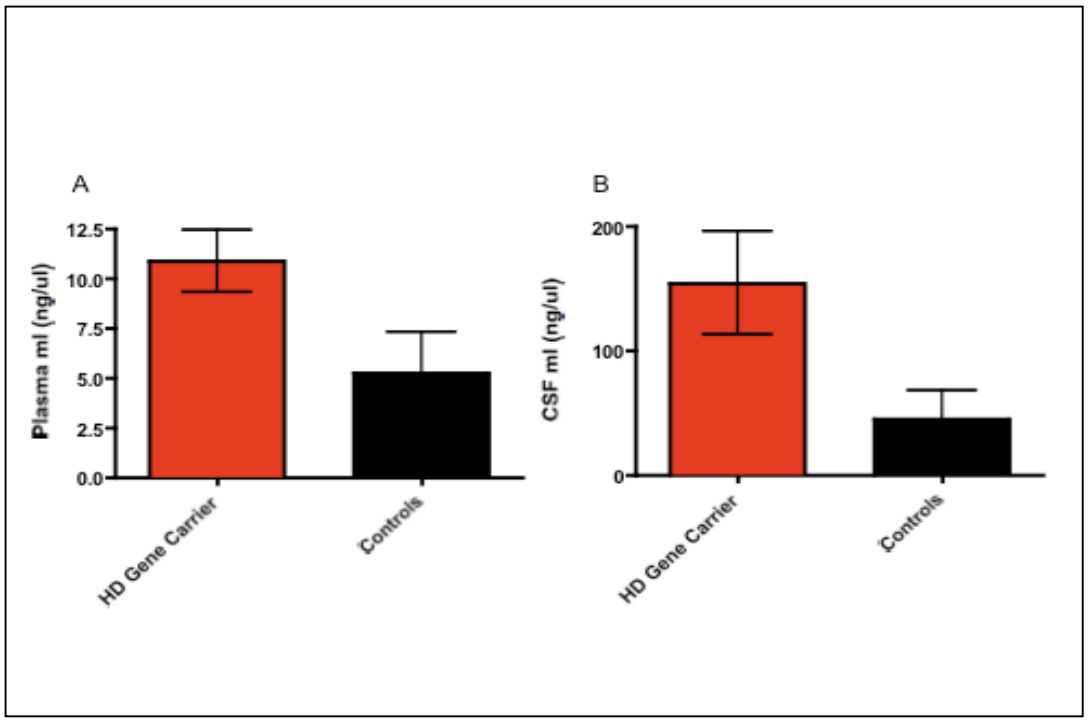

Figure 6-1 Plasma and CSF mI levels in HD gene carriers and controls. A and **B** show plasma and CSF concentrations respectively. Columns represent group means, with error bars denoting SEM.

Plasma & CSF mI by HD disease group:

In CSF, mI levels in Pre-HD and Manifest HD groups displayed a wide spread, with many estimations clustering around concentrations seen in Controls, and a few extreme results elevating the mI means within the HD groups. Despite a trend to higher CSF mI in Pre-HD and manifest HD groups, no HD groups were significantly different compared to Controls (Figure 6-2). In plasma, mI differences between groups were more marked, with a general trend for higher [mI] at more advanced disease stages, though no group difference reached statistical significance.

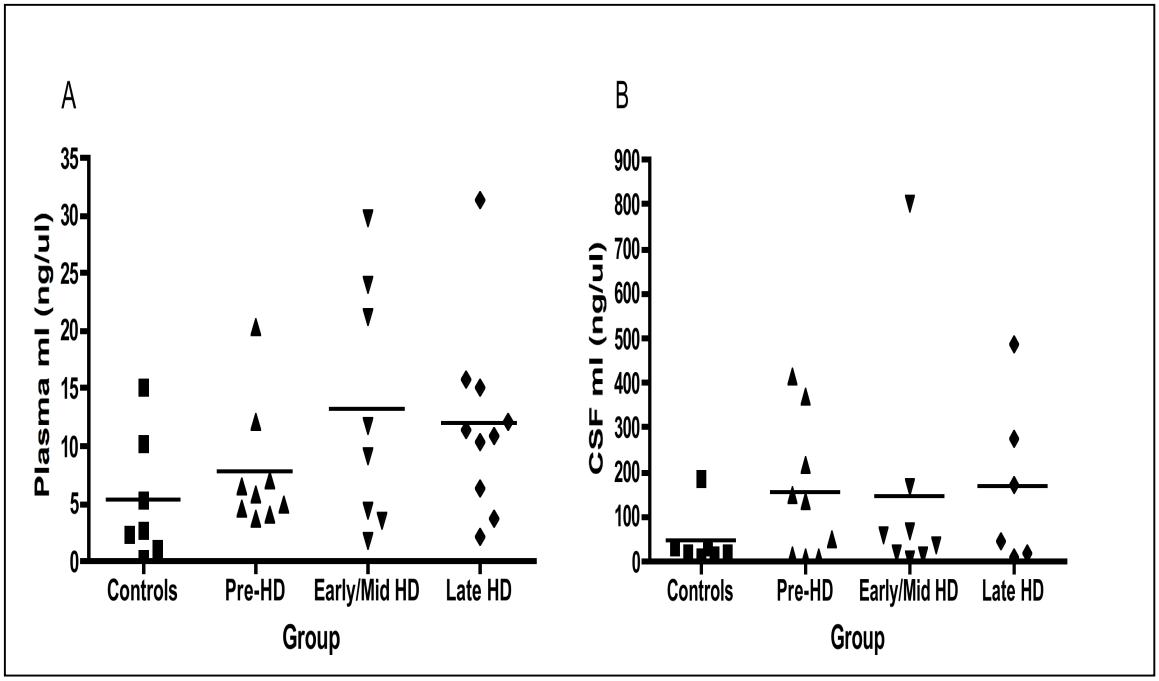

Figure 6-2 Plasma (A) and CSF (B) mI levels in HD and controls. Group lines represent mean values.

Correlating plasma and CSF mI with DBS:

Attempted correlation of plasma and CSF mI with DBS did not reveal a clear linear or non-linear relationship (R^2=0.043, p=0.31, and R^2=0.033, p=0.43, respectively. Data not shown).

Correlating plasma and CSF mI:

As can be seen from Figure 6-3, no clear linear or non-linear relationship was identifiable between plasma and CSF mI levels. This was, at least partly, caused by an apparent "floor effect" which was particularly evident among CSF mI measures, (as also displayed in Figure 6-2).

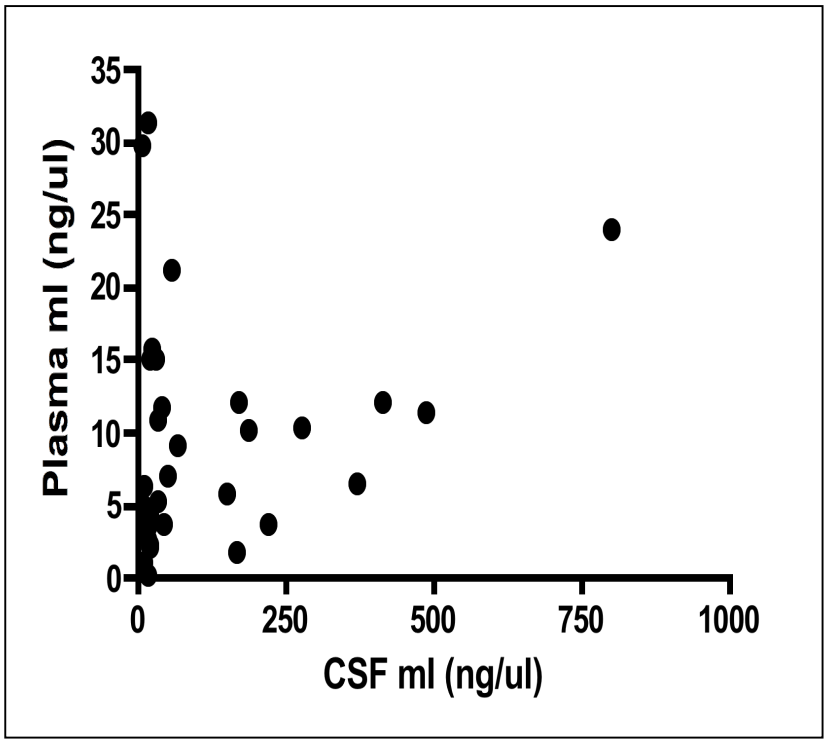

Figure 6-3. Correlation of Plasma and CSF mI levels. Across all subjects, a correlation between plasma and CSF mI levels was sought.

6.2.4 Discussion

The CSF and plasma mI concentrations identified in this study trended to elevation in HD individuals compared to controls, but group differences did not reach significance. CSF estimations showed marked floor effects for all subject groups and group differences appear to have been largely generated by a minority of more extreme measures. Plasma mI measures were more interesting, and exhibited cross-sectional increments for most subjects with more advanced disease stages. Nevertheless, HD groups displayed a wide spread of data with marked overlap

with Controls. Consequently, pooling all HD gene-carrying individuals did not identify a clear group difference in CSF or plasma mI compared to Controls.

The metabolite myo-inositol (mI), often referred to as inositol, is synthesized *de novo* from glucose in brain, kidney, liver and testes (Hauser & Finelli, 1963) and is a physiologically important osmolyte within the CNS. Its role appears to be the maintenance of neuronal cell volume through compensating for chronic alterations in cellular tonicity (Strange et al. 1992, Lay et al. 1998). Furthermore, its derivatives appear to play important roles in cell homeostasis, including receptor regulation (Sasakawa et al. 1995), signal transduction, vesicle trafficking (Gaidarov et al. 1996), neurotransmitter release (Llinas et al. 1994, Ohara-Imaizumi et al. 1997) and may also play a role in determining cellular death and survival (Fisher, 2002).

The CNS is atypical in terms of its high concentrations of mI (Sigal et al. 1993), yet the extent to which the metabolite is differentially concentrated in neuronal or glial cells is unclear (see Fisher, 2002 for a review). It has been suggested that the metabolite is principally localized to glia (Glanville et al. 1989, Brand et al. 1993), a finding reinforced by data from MRS studies (Ross et al. 1998, Broom et al. 2007). Hence the most likely cause of elevated mI levels measured by MRS in HD would appear to be astrocytosis, a process that is implicated in some of the earliest stages of the disease process. Pathologically progressive astrocytosis occurs within the

striatum in a directional pattern that parallels neurodegeneration (Vonsattel, 1998).

In this cohort mean plasma mI concentration for Controls was slightly lower than, but overlapped with, a previously published normal range for plasma mI while for manifest HD individuals the mean approximated or just exceeded this same range (0.8-1.2mg/100ml, Hammerman et al. 1980). However, the CSF levels we identified in this study were markedly higher than those in comparable studies. Thus, mean (SD) CSF mI in Controls was 44.8 (62.9), and among all HD individuals 134.8 (189.4) ng/uL compared to control values of 24.9 (4.4) ng/uL (reported as mg/L, Shetty et al. 1996). Thus, despite a comparable control cohort size, use of the same analytical technique and a standardized controlled sampling procedure, estimations reported here also displayed greater variability suggesting a limited robustness and reproducibility for this particular mI assay. Unfortunately, to date, no other direct assay for mI in plasma or CSF has been widely reported.

The R_{CSF} a ratio of CSF:plasma mI concentration can provide a measurement of the degree to which plasma measures were derived from brain mI, with values>2 indicating the source to be principally the CNS (Shetty et al. 1996). R_{CSF} in this cohort was greater than 2 for all groups (mean (SD); Controls:16.2 (21.1), Pre-HD:24.0 (24.5), Early/Mid-HD:18.4(31.4), Late HD: 17.6 (14.7)), confirming previous identification of predominant CSF source for plasma mI in control and AD patient plasma (Shetty et al. 1996). The R_{CSF} presented here are however much

greater than previously reported at ≈6-7 in control, AD and DS patients (Shetty et al. 1995, Shetty et al. 1996), and exhibit large SDs, indicating potentially some inaccuracy in assay method and/or inter-sample variation as a result of differences in processing. The inability to correlate plasma and CSF mI levels has been previously reported in AD patients, but in that same study the correlation was strong in controls (Shetty et al. 1996). Plasma and CSF mI values for the Control group in the present experiment, did not have a definite linear relationship in the relatively small sample group. The plasma mI elevation at different stages was, surprisingly, more apparent than in CSF-which was relatively stable across HD groups. It is possible therefore that an additional disease associated factor, such as increasing Blood Brain Barrier (BBB) permeability, may be affecting mI passage into the plasma, and that group differences reflect this differential permeability rather than elevations in absolute brain mI. Although research has not largely focused on damage to the BBB in HD, there is evidence from animal chemical models to suggest markedly increased disruption of, and extravasation across, the barrier within the excitotoxic milieu of the HD striatum (Duran-Vilaregut et al. 2009, Franciosi et al. 2012).

Given the lack of biomarker utility of peripherally sampled mI, the next experiment examined alternative peripheral markers of gliosis in HD plasma.

6.3 Investigation of the astrocyte marker, S100B and lipid peroxidation products as peripheral HD biomarkers.

6.3.1 Introduction

To better assess a potential biomarker role for peripheral measures of gliosis in HD, an alternate measure of astrocytosis, the measurement of astrocytic protein S100B was undertaken. Within cerebrospinal fluid (CSF), S100B is a predominantly astrocytic protein with cytokine-like functions. It exerts autocrine and paracrine effects on glia, neurons and microglia (Rothermundt et al. 2003). At micromolar levels, S100B exhibits cytotoxic properties, whilst at nanomolar levels it is neurotrophic (Petzold et al. 2003). S100B in CSF of individuals with AD and FTLD (n=31, 36, respectively) was significantly higher (c. + 60%) than that of controls, and furthermore showed moderately strong negative correlation with brain atrophy in AD (Petzold et al. 2003). While elevations of this marker have not been identified in serum with primary progressive multiple sclerosis (treated with IFN beta-1a) (Lim et al. 2004), elevations in CSF S100B have been identified in 20 relapsing-remitting MS subjects compared to controls (Rejdak et al. 2007). These findings may not be surprising given evidence that the inflammatory process in the primary progressive form of the disease appears to be occuring behind a sealed Blood-Brain Barrier. In stroke, S100B has shown some sensitivity to neural damage over days (Dassan et al. 2009).

One study has reported baseline measurements of S100B in serum of individuals with advanced HD (n=15, and controls n=11). While group means were different,

this difference did not reach significance (controls; 0.09+/-0.01, HD patients; 0.13+/-0.02ug/ml) (Stoy et al. 2005). However, the small cohort size likely impacted this finding. The ready measurement of S100B using basic ELISA kits would make this a relatively cheap and readily accessible biomarker for HD.

Lipid Peroxidation Products

To complement the investigation of S100B, a second complimentary component of the inflammatory process was also examined; that of oxidative stress. S100B may play a role in inducing oxidative stress and consequent apoptosis (Hu & Van Eldik, 1996), thereby stimulating the production of lipid peroxidation products such as 4-hydroxynonenal. To investigate whether LPO exhibited superior biomarker properties to S100B and mI, the quantification of combined hydroxynonenal and malondialdehyde (LPO) was undertaken.

More than one animal model of HD has demonstrated a degree of lipid peroxidation in a way that correlates with neurological dysfunction supporting a role for oxidative damage in HD pathogenesis (see Stoy et al. 2005). Of note, even in a small cohort of pre-manifest gene-carrying individuals (n=11), these individuals had significantly elevated measurments of plasma malondialdehyde (as part of lipid peroxidation product combination), as did a similarly sized cohort of symptomatic individuals (with disease of moderate severity) compared to controls (Klepec et al. 2007). These findings suggest that lipid peroxidation products may offer an advantage over a number of other putative markers, namely that these

metabolites may be measurably changed in the presymptomatic HD population. Another study produced supportive findings, identifying significant, eight-fold elevations in the combined 4-hydroxynonenal and malondialdehyde among an advanced (but small, n=11) HD cohort (Stoy et al. 2005). Furthermore lipid peroxidation may correlate well with with cognitive decline and chorea scores in symptomatic HD (Klepec et al. 2007). The combined lipid peroxidation products 4-hydroxynonenal and malondialdehyde (denoted as LPO) are readily measurable using a colorimetric method utilised for this project (Stoy et al. 2005).

On the basis of previous demonstration of these metabolites' potential biomarker roles in neurodegeneration, their relative accessibility and complementary roles in inflammatory processes the objective of this project was to evaluate the usefulness of plasma S100B and LPO in distinguishing disease stage within a larger HD cohort.

6.3.2 Methods

Subjects:

Samples from forty subjects enrolled in the UBC Biomarker Study cohort were analysed; 10 in each of Control, Pre-HD, Early/Mid-Stage HD and Late HD groups. The subject groups and ethical approval for the study were as outlined in the previous Experiment. One Pre-HD individual and one Early HD individual involved in this experiment possessed reduced-penetrance CAG expansion of 36 and 39, respectively.

Procedures

Subjects were evaluated using UHDRS-TMS and UHDRS-TFC evaluations. Disease burden score (DBS) (measure of exposure to mutant protein) was calculated as (CAG-35.5)*Age.

Sample collection

Whole blood samples were collected into 10ml EDTA anticoagulated vacutainers and immediately centrifuged 1500rpm for 15 mnutes and the resulting plasma was frozen at -20°C.

S100B assay

Immunoassay methods were used to measure S100B. The S-100 Beta ELISA kit from Alpco Diagnostics (48-S1BHU-E01, 26G Keewaydin Drive, Salem, NH 03079) was used for the quantitative determination of S100B in plasma samples. The assay is based on the sandwich model enzyme linked immunosorbent assay. Duplicate 30ul aliquots of plasma sample were assayed. During the first immune reaction, S100B in standards/samples were bound to rabbit anti-bovine S100B antibody coating the surface of the microplate. After incubation and plate washing, labelled antibody (biotinylated rabbit anti-bovine S100B antibody) was added to bind to the antigen-antibody complex. Then, HRP labeled streptavidin (SA-HRP) was added to form the biotinylated rabbit anti-bovine S100-antigen-antibody complex. Finally HRP enzyme activity was determined by o-phenylenediamine

dihydrochloride (OPD) and the concentration of human S100B in samples calculated. The lower limit for detection in the assay was 98pg/ml.

LPO-586 assay

A commercially available lipid peroxidation kit (LPO-586, Bioxytech) was used to measure the malondialdehyde (MDA) and 4-hydroxyalkenal (HAE) concentrations in patient plasma. Lipid peroxidation products malondialdehyde (MDA) and 4-hydroxyalkenals (HAE) were quantified in 200ul plasma aliquots. The assay is based on the reaction of a chromogenic reagent, N-methyl-2-phenylindole (R1), with MDA and 4-hydroxyalkenals at 45°C to yield a stable chromophore with maximal absorbance at 586 nm. All samples were tested in duplicate. The chromogenic reagent, (0.650 ml) was poured into a polypropylene microcentrifuge tube. EDTA plasma (0.2 mL) was added and the mixture vortex-mixed. The reaction was started by adding 0.15 mL of 10.4 mol/L methanesulfonic acid, mixing, and incubating at 45°C for 60min. The reaction mixture was cooled to room temperature and 0.2ml clarified samples were transferred to microtitre plate and absorbance determined at 586nm.

Statistical Analysis

Cross-sectional group analysis was performed using One-Way ANOVA with *post-hoc* Newman Keuls Multiple Comparison Test. Linear regressions with DBS and UHDRS-TMS were performed using the method of least squares.

6.3.3 Results

Demographics

Demographics of enrolled participants are displayed in Table 6-2 below.

	Controls (n=10)	Pre-HD (n=10)	Early (5)/Mid (5) (n=10)	Late HD (n=10)
Age (Mean, SD)	47.2 (16.3)	39.4 (13.7)	49.3 (6.1)	54.4 (12.3)
Women: Men	6:4	5:5	4:6	5:5
UHDRS-TFC (Mean, SD)	13(0)	12.5(0.7)	9.8(2.2)	1.2(1.4)

Table 6-2 Subject demographics. No significant age difference was identifiable between groups.

S100B and LPO in Gene Positive subjects and Controls

As can be seen from Figure 6-4, LPO for combined HD gene positive individuals was significantly higher than for controls (p=0.026), while there was no significant difference in S100B between groups, despite a subtle trend.

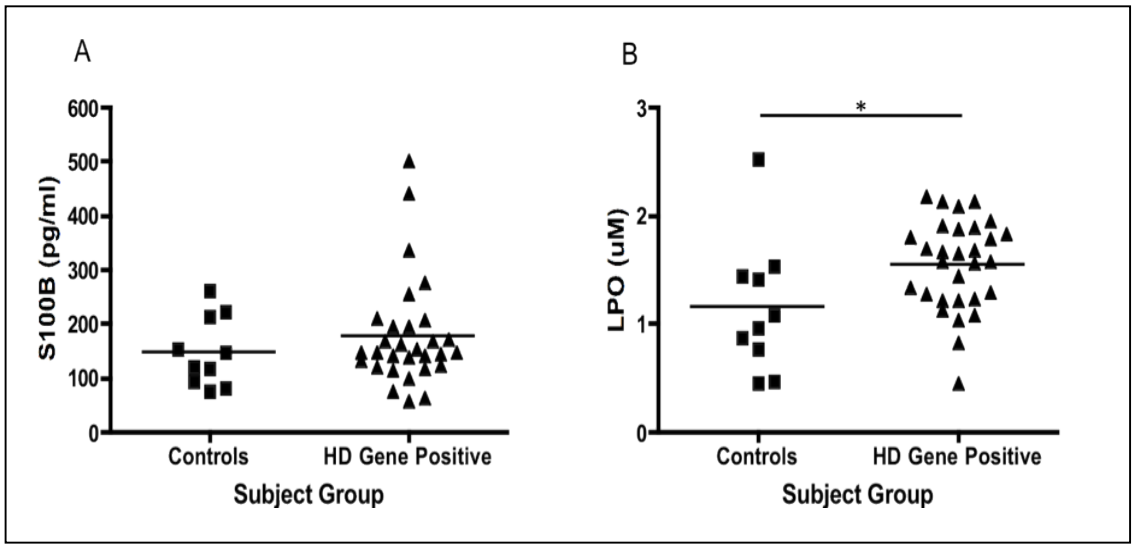

Figure 6-4 Effect of HD gene status on S100B and LPO plasma levels. While the HD gene positive group, comprising the combined subgroups (Pre-HD, Early/Mid-Stage HD and Late HD) only trended to higher S100B levels, this group demonstrated significant elevations in LPO compared to Controls.

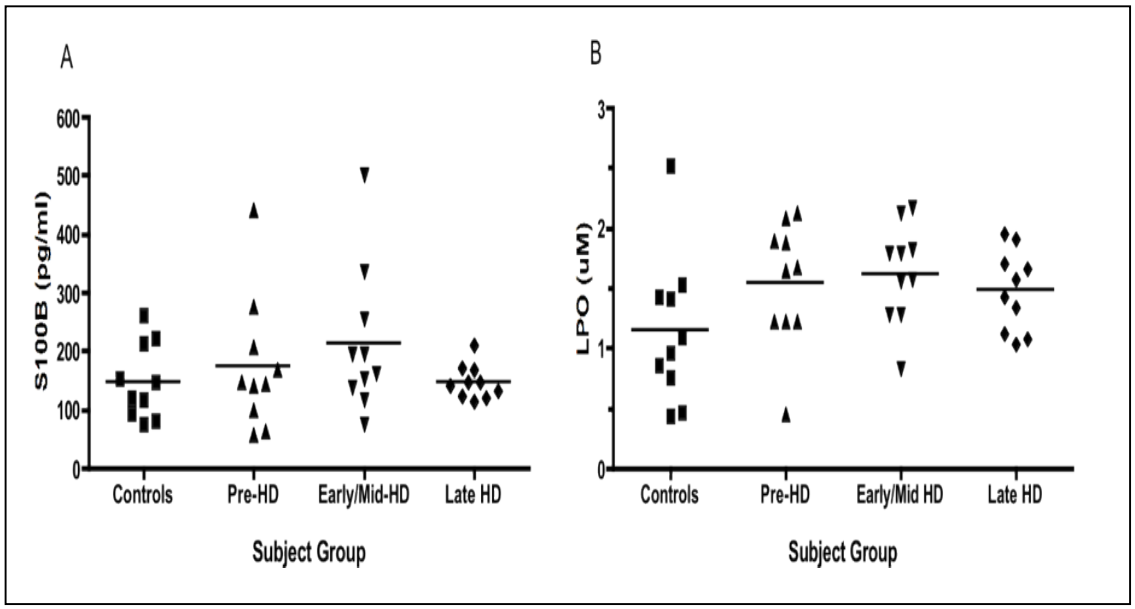

Figure 6-5 Effects of HD subgroup on S100B and LPO plasma levels. While for both metabolites a general trend to elevation was seen in virtually all HD subgroups, no significant subgroup difference was identified.

After separating subjects into respective groupings; control, Pre-HD, Early/Mid-stage HD and Late-stage HD, no significant difference was identifiable between any group, although the data suggest a trend to increased LPO in HD gene carriers in all HD groups, while only for Pre-HD and Early/Mid-HD groups was there suggestion of S100B elevation vs. Controls.

Correlation of disease burden score with plasma LPO and S100B

To assess whether a linear relationship between DBS and these metabolites existed, a linear regression using the Method of Least Squares was performed. No clear linear or non-linear correlation was apparent on examination of data distribution (Figure 6-6).

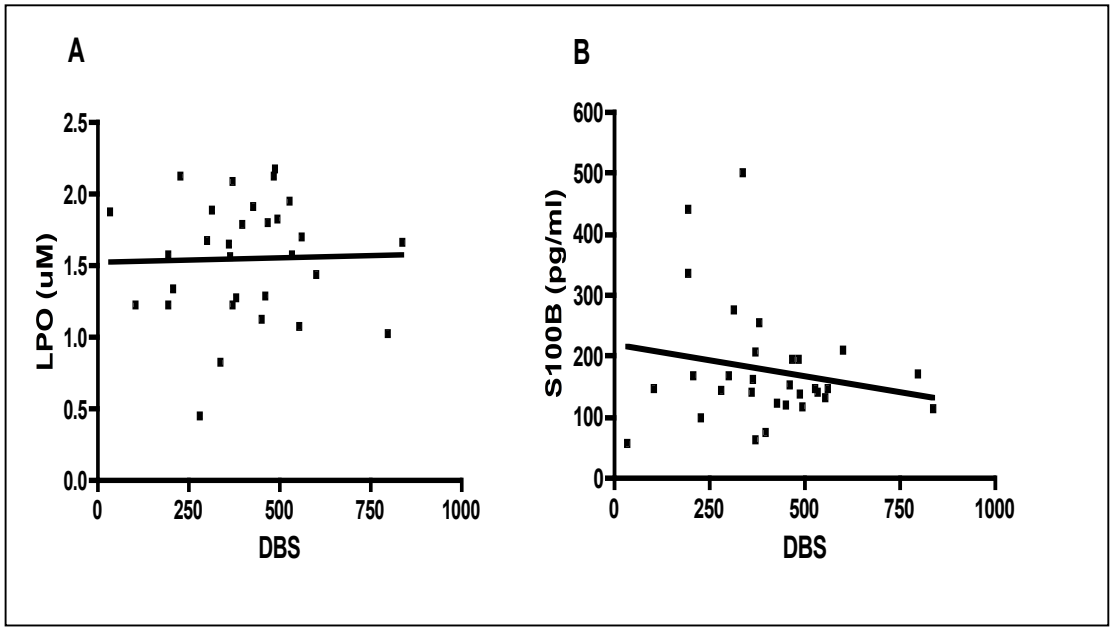

Figure 6-6 Correlation of DBS with plasma (A) LPO and (B) S100B. Attempted correlation revealed no clear relationship between either of these metabolites and disease burden (LPO; R^2=-0.036, p=0.90; S100B; R^2=-0.0009, p=0.33).

Correlation of plasma S100B and mI

As two markers of glial activation, the relationship between these two metabolites was examined for those subjects for whom both were evaluated within our cohort (n=30, 7 Controls, 9 Pre-HD, 4 Early/Mid-Stage HD and 10 Late HD). No linear

correlation was identifiable by inspection of the data nor linear regression analysis.

Correlation of plasma S100B and LPO

To assess for a possible correlation between two aspects of the inflammatory process, we sought evidence for a linear relationship between the oxidation product LPO, and S100B (Figure 6-7).

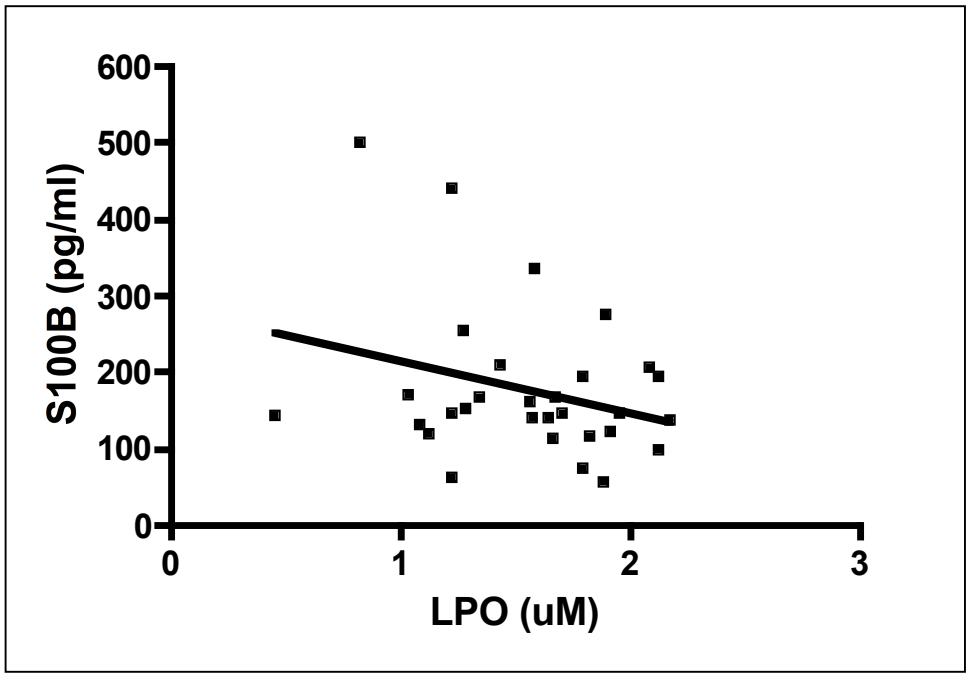

Figure 6-7 Correlation of plasma LPO and S100B levels. No clear linear or non-linear correlation between these two metabolites was identifiable. ($R^2=5*10^{-5}$, p=0.97).

6.3.4 Discussion

The trend demonstrated here, to higher plasma S100B in gene positive individuals compared to Controls, was subtle and did not reach significance. Could the early S100B rise then fall suggest a neuroprotective response? Certainly the literature suggests that low levels of S100B are neurotrophic, with *in vitro* evidence that they promote neurite outgrowths and neuronal survival during development in embryonic chicks (Van Eldik et al. 1991).

Beyond noting a general trend for a subtle S100B increase in Pre-HD and Early/Mid-Stage HD individuals, more detailed inferences about the evolution of S100B change as HD progresses, based on cross-sectional group differences in the cohort, was difficult. The limitation of small cohort sizes, and also some extreme values in Pre-HD and Early/Mid-HD groups may have influenced reported observations. While a larger cohort could be informative, it is nevertheless telling that even when considering all HD positive individuals together, still only a trend to increased S100B levels was identified. Furthermore, these results replicate the data of the only other reported observational evaluation of S100B in HD subjects (Stoy et al. 2005). This, smaller study (controls 15, advanced HD patients 11) also identified a small S100B elevation in HD, that did not achieve significance. As the authors suggest, their findings and the data presented here supports the suggestion that S100B may rise in the earliest stages of neuronal damage, declining shortly afterwards (Stoy et al. 2005).

Despite the absence of a clear blood biomarker role for S100B in HD, there is still a significant rationale for evaluating its potential utility as a CSF biomarker. There is evidence of regionally selective astrogliosis occuring at early HD pathological grades (Grade 1 at post-mortem) (Vonsattel, 2008) and S100B is a widely accepted marker of astrocytosis. Furthermore in a number of neurological conditions including stroke and some neurodegenerative disorders elevations in S100B have been identified. Thus, in stroke CSF S100B increments have been associated with cerebral infarct size and clinical severity (Aurell et al. 1991). In the Alzheimer disease (AD) brain at post-mortem there is evidence of over-expression of S100B (Griffin et al. 1989) and increased CSF levels in AD and FTD patients compared to controls (Green et al. 1997). However, serum levels of S100B in AD do not appear to be elevated (Mecocci et al. 1995). As for any putative blood biomarker, there is a strong rationale for the CSF counterpart to be a more sensitive neurodegeneration marker; the CSF measure will not have been filtered through the BBB to reach the blood. Furthermore, the CSF measure will not have been contaminated by non-CSF sources of S100B.

The lack of correlation between plasma mI and S100B may appear surprising; both are used as surrogate measures of astrocyte activation. At MRS, mI is widely utilized as a measure of gliosis and mI levels correlate with gliosis in inflammatory demyelination (Bitsch et al. 1999, Kantarci et al. 2008). However, it should be remembered that while earlier MRS studies identified mI elevations in HD, most of these studies examined specific regions, selectively vulnerable to HD pathology

such as striatum (Hoang et al. 1998, Sturrock et al. 2010). Hence, the literature contains insufficient data to comment whether mI elevations in HD are regionally selective, and therefore whether absolute mI alterations will be detectable in plasma (after it has also passed through the filter presented by the BBB). In addition, while both may be elevated in the HD brain it is unknown to what differing degrees these metabolites may be altered on crossing the BBB.

One concern with regard to the use of S100B as a plasma biomarker is its elevation in non-brain trauma and burn victims (Anderson et al. 2001, Anderson et al. 2001). While these would unlikely be significant causes for concern in the context of the protein as an HD biomarker, it does raise the issue that S100B may be a relatively non-specific marker of astrocyte activation.

LPO levels were significantly higher in the grouped HD gene positive group and on subgroup cross-sectional analysis, in all groups including Pre-HD, trended to higher concentrations than Controls. It is interesting to note that if the single outlier Control value (>2 SD from the group mean) is excluded, all HD groups show significant difference from Controls.

6.4 Chapter Conclusions

The findings reported here collectively suggest limited biomarker utility for both central and peripheral measurements of mI and indicate that this metabolite should not be a priority target for future biomarker studies in HD, at least not

using the assay methods used in this experiment. This work does not suggest that plasma S100B is any more sensitive a biomarker than plasma or CSF mI. Perhaps the evaluation of S100B within CSF would yield more valuable results in delineating a novel biomarker for HD. Furthermore, while these findings did not quite replicate the eightfold elevation previously identified in advanced HD (Stoy et al. 2005), they suggest biomarker potential for LPO, although the metabolite appeared more an indicator of disease trait rather than state given the lack of change across the various HD groups. Despite this apparent inability to delineate disease progression, such a marker of the disease trait remains theoretically valuable, since it is potentially amenable to therapeutic reversal irrespective of disease severity.

7 Thesis Conclusions

This thesis has examined the role of Magnetic Resonance Spectroscopy as a biological marker for disease progression and as potential outcome measure for therapeutic studies in HD. To date, numerous potential biomarker modalities have been postulated in HD, with varying sensitivity. Volumetric imaging measures of regional and global brain atrophy remain among the most sensitive measures of disease progression, yet imaging markers of altered neurophysiology, such as brain metabolites, may theoretically prove the most sensitive to onset of disease since they precede tissue loss (Jenkins et al. 2000). In contrast to structural imaging, the biomarker role of MRS has remained uncertain despite its evaluation in a number of studies over the past twenty years. Nonetheless this modality carries great potential as a biomarker. In addition, the modeling of MRS as an outcome measure for therapeutic trials, and the calculation of sample sizes for such a trial have not previously been reported.

The main focus of this thesis was therefore to elucidate, in the largest cohort of HD patients evaluated using MRS, this biomarker role, to identify key metabolites of interest for further study, and to investigate correlations between brain metabolites and phenotypic measures. Further to this, calculations of sample sizes were performed based on a model, which may be adapted for therapeutic studies. Lastly this thesis evaluated 'wet' biomarker targets, identified directly as a consequence of the spectroscopy investigations.

7. 1 MRS as a biomarker for HD

By comparison with the QMotor measures, brain metabolite measurement, specifically tNAA, also exhibited cross-sectional differences between Pre-HD and Controls. Importantly, cross-sectional metabolite differences were able to differentiate a pre-manifest HD cohort from control subjects despite an absence of any detectable group difference on standard motor phenotype measures. Unlike QMotor measures and the UHDRS-TMS, however, the metabolites assessed here failed to exhibit any longitudinal change. The lack of sensitivity of metabolite measures to disease progression over 24 months may be partially a consequence of sample size, but nevertheless may provide a significant advantage in terms of the development of reliable outcome measures in clinical trials, as discussed below. It is also notable that in this work, as well as that produced by others (Tabrizi et al. 2011), that putaminal volumes identified longitudinal change at 24 months, and even at 12 month intervals among pre-manifest and Early HD individuals, further emphasizing the sensitivity of these volumetric measures to atrophy.

MRS proved to be a better discriminator of disease state than either plasma or CSF measures examined in this study, though undoubtedly influenced by the considerably smaller biosamples cohort. The identification of peripherally sampled, biomarkers for HD has clear advantages over all other biomarker modalities in terms of potential efficiency and availability. While promising

candidates are continually being identified, to date this modality has not demonstrated the sensitivity of imaging modalities.

7.2 MRS as a surrogate marker for clinical motor phenotype progression

Disappointingly tNAA and mI correlated poorly with motor measures of disease progression. However, this likely relates to several factors. Firstly, reviewing a snapshot of disease among just pre-manifest and early disease may well limit such correlations, that is, in a larger cohort evaluating both pre-manifest and late or end-stage disease, may well identify an association. The lack of longitudinal change in all metabolites, compared to the clear evolution of motor measures over time suggests non-comparable rates of change between these modalities. Thus, tNAA changes appear to occur very slowly. The increment in mI is interesting, as it is unclear when precisely this occurs, apparently at some point in early symptomatic rather than pre-manifest disease, and clearly this work shows possible confounding secondary to psychotropic medication usage-a finding which gains support from earlier work (Szulc et al. 2005). NAA much more closely followed trends in QMotor performance, especially in Early HD, although the reason for this is unclear. Other studies have been at odds in their correlation of MRS metabolite measures, specifically NAA/Cr and NAA with motor performance (Sanchez-Pernaute et al. 1999, Ruocco et al. 2007) although the discrepancy likely relates to both region selection and use of composite measures. It is interesting that frontal lobe metabolite measures correlate with cognitive task performance (Gomez-Anson et al. 2007) and it would be worthwhile, given the increasing appreciation of

the importance of WM atrophy in HD (Paulsen at al. 2010, Dumas et al. 2011), to examine correlations between motor and cognitive performance with metabolite profiles within this tissue. Disease Burden Score was, albeit weakly, inversely correlated with putaminal tNAA at all time points in this cohort. A finding that gains some support from earlier work (Jenkins et al. 1993, Jenkins et al. 1998, Van Oostrom et al. 2007), and may be useful in developing this modality as a biomarker for future clinical trials, as outlined previously.

While the prospect of a spectroscopic biomarker that correlates closely with the disease phenotype is appealing, presumably it will not preclude the biomarker use of this modality in identifying abrogation of pathophysiological change which may actually precede the halting of clinical progression.

7.3 Using MRS to identify novel wet biomarkers

The initial findings at baseline of alterations in the gliosis marker mI prompted scrutiny of biosample measurements of mI, another established marker of astrocytosis, S100B, and also S100B-induced lipid peroxidation products (LPO). S100B levels were not significantly elevated in HD affected individuals. Plasma LPO in contrast was significantly elevated among HD individuals. mI also trended to increase in HD plasma and CSF, suggesting at least limited biomarker potential for both of these measures. The lack of significant findings in these secondary analyses should not disparage the future MRS informed search for biosample markers. The cohort here was small, and examination of these same metabolites,

specifically LPO metabolites, in CSF may prove considerably more sensitive. MRS has stimulated the work of other groups, identifying reductions in peripherally measured creatine kinase brain iso-enzymes (Kim et al. 2010). Furthermore, the cross-sectional work reported here in Chapter 5 and published (Sturrock et al. 2010), has stimulated the search for a peripheral NAA measure (Ruggieri et al. 2012). The results, within a small cohort, are promising and appear to correlate with a number of motor phenotype measures. One can anticipate that, as higher field strength scanners are used, permitting the reliable detection of more obscure metabolite markers, the potential for identifying future peripheral targets can only increase.

7.4 The future of MRS as an HD biomarker

It is likely that higher, 3T and even 7T, field strengths will play an increasingly important role in the development of MRS as a biomarker for HD. Increasing spectral resolution in this way permits the measurement of lower concentration metabolites and can potentially permit metabolite quantifications from very small voxels of interest thus avoiding partial volume effects. This appears to be a particular strength of 7T imaging. This work, reported after the cross-sectional data reported in Chapter 5 was published, has supported the findings of NAA, Glu and also Cr reductions in early HD striatum (van den Bogaard et al. 2011, Unschuld et al. 2012). In these studies correlations with a number of cognitive and motor measures have been identified, suggesting that this field strength may potentially allow tracking of phenotypic progression. Furthermore, metabolite

alterations were identifiable in relatively non-atrophied brain, supporting the concept of detection of physiological changes prior to tissue loss.

The evaluation of mouse models of HD using MRS has already yielded useful insights into HD pathophysiology. Studies in transgenic mice have confirmed NAA reductions preceding neuronal loss, identifying the role of this measure as a marker of neuronal health but also supporting theories of impaired glutamatase activity leading to a pro-glutamatergic state in HD (Jenkins et al. 2000, Tsang et al. 2006, Tkac et al. 2007, Heikkinen et al. 2012). Such models have also provided some evidence of reversibility of phenotypic and metabolic (NAA and Cr) impairments (Ferrante et al. 2000, Andreassen et al. 2001). More recent work at very high field strengths (9.4T), has displayed a greater discriminant ability for cortical metabolites than atrophy measures at very early disease stage (Zacharoff et al. 2012)-an exciting finding given the dominance of volumetric imaging measures among putative HD biomarkers.

The appreciation of MRS as an HD biomarker for therapeutic trials will also continue to benefit from future trials in these animal models. Both transgenic and chemical models are associated with an accelerated disease course therefore one may suppose that they can define the natural evolution of metabolite change in the diseased brain to enable the identification of disease stage-specific metabolite markers (Jenkins et al. 2005). The measurement of metabolite alterations in 'disease abrogated' animals (Graham et al. 2006) could provide a unique insight

into the expected metabolite signature in effectively disease-modified patients. This may identify early the halting of disease progression and potentially years before any evidence is available from other biomarker measures - reducing the duration of therapeutic trials and reducing the proportion of 'false-negative' trials.

Given the increasing emphasis on WM tissue loss and structural change as a biomarker for HD (Paulsen et al. 2010, Dumas et al. 2011, Aylward et al. 2011, Aylward et al. 2012), it seems probable that deep WM will become a focus for future MRS studies in HD. Indeed, volumetric evidence suggests that WM atrophy may be almost as good as (Tabrizi et al. 2013), or even a better (Aylward et al. 2011) longitudinal marker of progression than striatal atrophy in pre-manifest disease, suggesting that MRS within these tissues may be particularly sensitive to the earliest changes in HD. One further advantage of such quantifications would be the certainty of voxel placement within a homogeneous tissue type thus preventing partial volume effects, maximising accurate metabolite estimations.

Future work specifically may seek to identify correlations between WM and striatal metabolite alterations including tNAA, with cognitive outcome measures also, particularly given the widely demonstrated correlations between atrophy in these regions and a variety of such measures. In addition, I would aim in future work to look for possible MRS markers for clinical phenotype, for example the specific interrogation of particular metabolites, at baseline, for their relationship

with the subsequent development of predominant cognitive, psychiatric and motor phenotypes.

In determining imaging biomarkers for HD, one concern is that a single biomarker is unlikely sufficient to capture the complexity of the disease process. Bohanna and colleagues have suggested that a more realistic approach to observational and therapeutic studies may be the development of a multi-modal imaging approach. They suggest that a functional or physiological marker could be used in the short to middle term (possibly early pre-manifest to early symptomatic stages) with structural or atrophy measures being used to measure progression in the middle to long term (possibly early/middle symptomatic to advanced disease stage). The very earliest changes, at the neurophysiological or microstructural level, precede significant tissue loss thus at this stage the authors propose modalities such as DTI or fMRI, saving volumetric imaging measures for later in the disease course where structural changes are more easily measured (Bohanna et al. 2008). Clearly, with further work at high field strengths, MRS could fit into this paradigm alongside DTI and fMRI to potentially measure some of the earliest changes in the HD brain.

7.5 MRS as an outcome measure for therapeutic trials in HD

The concept of MRS as a cross-sectional, disease state measure for HD is contrary to the traditional view of metabolites and other biomarkers of disease in HD – specifically that a biomarker should track, or change as the disease progresses. Nevertheless, even the concept outlined in Chapter 5 regarding the reversal of

brain metabolite alterations in individuals of a given DBS, could readily be applied to pre-manifest individuals in a sufficiently large cohort, a useful strategy perhaps for future therapeutic trials in pre-manifest disease.

Using realistic, hypothetical effect sizes the amelioration of tNAA deficits among early symptomatic HD individuals may be achievable with feasible sample sizes. A 20% normalisation of putaminal tNAA in early HD individuals of a given DBS could be demonstrable with just 175 subjects per treatment arm. If higher rates of normalisation were anticipated, then this number could fall significantly. The specific advantage here is the reproducibility of the measure, reducing variability and hence maximising the relative effect size. This in turn will reduce study cost. Furthermore, the lack of group variability across three time points over 24 months of follow up would make group resolution in serially measured tNAA-in response to a specific therapeutic significantly more convincing. tNAA is especially attractive in this regard. Firstly, because unlike the other metabolites examined in detail, NAA and mI, it is consistently more estimable (fewer subjects with >20% SD) and secondly because it was the metabolite most reliably altered in pre-manifest disease. Thus, it is possible to consider that, after stratifying by for example years to predicted onset or DBS in a sufficiently large cohort, group tNAA resolution may be an achievable aim among asymptomatic carriers of the gene defect.

In conclusion, this work shows, for the first time, robustness for tNAA and NAA alterations in Pre-HD and Early HD over 2 years of longitudinal study and suggests

a model by which this metabolite could be exploited as an outcome measure for future observational and therapeutic studies.

7.6 Summary

The *in vivo* estimation of brain metabolites using MRS offers a promising and sensitive modality for measuring disease stage in HD. Furthermore they are robust, tenable and realistic outcome measures for therapeutic trials. Future work developing these measures will be an important step in fully realising the HD biomarker potential of MRS. This thesis has investigated a hitherto uncertain biomarker, clarified its biomarker potential and outlined new, unique roles for this modality in future HD clinical trials.

Appendices

Appendix 1: UHDRS-TMS Scoring

OCULAR PURSUIT (horizontal and vertical)

0 = complete (normal)

1 = jerky movement

2 = interrupted pursuits/full range

3 = incomplete range

4 = cannot pursue

SACCADE INITIATION (horizontal and vertical)

0 = normal

1 = increased latency only

2 = suppressable blinks or head movements to

3 = unsuppressable head movements

4 = cannot initiate saccades

SACCADE VELOCITY (horizontal and vertical)

0 = normal

1 = mild slowing

2 = moderate slowing

3 = severely slow, full range

4 = incomplete range

DYSARTHRIA

0 = normal

1 = unclear, no need to repeat

2 = must repeat to be understood

3 = mostly incomprehensible

4 = mute

TONGUE PROTRUSION

0 = can hold tongue fully protruded for 10 seconds

1 = cannot keep fully protruded for 10 seconds

2 = cannot keep fully protruded for 5 seconds

3 = cannot fully protrude tongue

4 = cannot protrude tongue beyond lips

MAXIMAL DYSTONIA (trunk and extremities)

0 = absent

1 = slight/intermittent

2 = mild/common or moderate/intermittent

3 = moderate/common

4 = marked/prolonged

MAXIMAL CHOREA (face, mouth, trunk and extremities)

0 = absent

1 = slight/intermittent

2 = mild/common or moderate/intermittent

3 = moderate/common

4 = marked/prolonged

RETROPULSION PULL TEST

0 = normal

1 = recovers spontaneously

2 = would fall if not caught

3 = tends to fall spontaneously

4 = cannot stand

FINGER TAPS (right and left)

0 = normal (>/=15/5 sec.)

1 = mild slowing and or reduction in amplitude (11-14/5 sec.)

2 = Moderately impaired. Definite and early fatiguing. May have occasional arrests in movement (7-10/5 sec.).

3 = Severely impaired. Frequent hesitation in initiating movements or arrests in ongoing movements (3-6/5 sec.)

4 = Can barely perform the task (0-2/5 sec.)

PRONATE/SUPINATE-HANDS (right and left)

0 = normal

1 = mild slowing and/or irregular

2 = moderate slowing and irregular

3 = severe slowing and irregular

4 = cannot perform

LURIA (fist-hand-palm test)

0 = >/= 4 in 10 seconds, no cue

1 = <4 in 10 seconds, no cue

2 = >/= 4 in 10 seconds, with cues

3 = <4 in 10 seconds with cues

4 = cannot perform

PRONATE/SUPINATE HANDS (right and left)

0 = absent

1 = slight or present only with activation

2 = mild to moderate

3 = severe, full range of motion

4 = severe with limited range

BRADYKINESIA-BODY

0 = normal

1 = minimally slow (? normal)

2 = mildly but clearly slow

3 = moderately slow, some hesitation

4 = markedly slow, long delays in initiation

GAIT

0 = normal gait, narrow base

I = wide base and/or slow

2 = wide base and walks with difficulty

3 = walks only with assistance

4 = cannot attempt

TANDEM WALKING

0 = normal for 10 steps

1 = 1 to 3 deviations from straight line

2 = >3 deviations

3 = cannot complete

4 = cannot attempt

Appendix 2: UHDRS-TFC Scoring

FUNCTIONAL CAPACITY

OCCUPATION

0 = unable

1 = marginal work only

2 = reduced capacity for usual job

3 = normal

FINANCES

0 = unable

1 = major assistance

2 = slight assistance

3 = normal

DOMESTIC CHORES

0 = unable

1 = impaired

2 = normal

ADL

0 = total care

1 = gross tasks only

2 = minimal impairment

3 = normal

CARE LEVEL

0 = full time skilled nursing

1 = home or chronic care

2 = home

Glossary

AD = Alzheimer's disease

CAG = the Cytosine-Adenine-Guanine trinucleotide

Cr = creatine

DBS=Disease Burden Score

FWHM = Full-Width Half Maximum

Glu = glutamate

GPC = glycerophosphocholine

GM = Grey Matter

HD = Huntington disease

MI = myo-inositol

MRS = 1H-Magnetic Resonance Spectroscopy

NAA = *N*-acetyl aspartate

NAAG = *N*-acetyl aspartylglutamate

PC = phosphocholine

PCr = phosphocreatine

Pre-HD = Pre-manifest HD

SNR = Signal-to-Noise-Ratio

tCho = total choline

tCr = total creatine

TFC = Total Functional Capacity

TMS = Total Motor Score

tNAA = total *N*-acetyl aspartate

UHDRS = Unified Huntington's Disease Rating Scale

VBM = Voxel-Based Morphometry

WM = White Matter.

Publications

Sturrock A, Laule C, Decolongon J, Dar Santos R, Coleman AJ, Creighton S, Bechtel N, Reilmann R, Hayden MR, Tabrizi SJ, Mackay AL, Leavitt BR. Magnetic resonance spectroscopy biomarkers in pre-manifest and early Huntington disease. Neurology. 2010;75(19):1702-1710.

Sturrock A, Leavitt BR. Murine models of Huntington disease. Future Neurology 2009;4(5):617-638.

Sturrock A, Leavitt BR. The clinical and genetic features of Huntington disease. J Geriatr Psychiatry Neurol. 2010;23(4):243-259.

Tabrizi SJ, Langbehn DR, Leavitt BR, Roos RA, Durr A, Craufurd D, Kennard C, Hicks SL, Fox NC, Scahill RI, Borowsky B, Tobin AJ, Rosas HD, Johnson H, Reilmann R, Landwehrmeyer B, Stout JC; TRACK-HD investigators. Biological and clinical manifestations of Huntington's disease in the longitudinal TRACK-HD study: cross-sectional analysis of baseline data. Lancet Neurol. 2009;8(9):791-801.

Tabrizi SJ, Reilmann R, Roos RA, Durr A, Leavitt B, Owen G, Jones R, Johnson H, Craufurd D, Hicks SL, Kennard C, Landwehrmeyer B, Stout JC, Borowsky B, Scahill RI, Frost C, Langbehn DR; TRACK-HD investigators. Potential endpoints for clinical trials in pre-manifest and early Huntington's disease in the TRACK-HD study: analysis of 24 month observational data. Lancet Neurol. 2012;11(1):42-53.

Tabrizi SJ, Scahill RI, Durr A, Roos RA, Leavitt BR, Jones R, Landwehrmeyer GB, Fox NC, Johnson H, Hicks SL, Kennard C, Craufurd D, Frost C, Langbehn DR, Reilmann R, Stout JC; TRACK-HD Investigators. Biological and clinical changes in pre-manifest and early stage Huntington's disease in the TRACK-HD study: the 12-month longitudinal analysis. Lancet Neurol. 2011;10(1):31-42.

Tabrizi SJ, Scahill RI, Owen G, Durr A, Leavitt BR, Roos RA, Borowsky B, Landwehrmeyer B, Frost C, Johnson H, Craufurd D, Reilmann R, Stout JC, Langbehn DR; TRACK-HD Investigators. Predictors of phenotypic progression and disease onset in pre-manifest and early-stage Huntington's disease in the TRACK-HD study: analysis of 36-month observational data. Lancet Neurol. 2013;12(7):637-649.

Weir DW, Sturrock A, Leavitt BR. Development of biomarkers for Huntington's disease. Lancet Neurol. 2011;10(6):573-590.

Acknowledgements

Many people made this work possible, and I am grateful to every one. Firstly, I thank all of the patients and healthy volunteers at the Centre for Huntington disease, from who I have learnt so much over the years, about not only the disease but about the much wider effects of HD on families. I thank them for the time, effort, and even at times comfort that they were prepared to sacrifice in order to participate in this study.

I owe a huge debt of gratitude to my supervisor, Dr Blair R. Leavitt whose expert guidance, invaluable support and friendship through every step of this project, made this MD(Res) possible. It has been an amazing and life changing education and I am hopeful that I can continue my work with individuals with this devastating disease.

Thanks also to everyone at the Centre for Huntington Disease, UBC Hospital, Vancouver. Especial thanks to Allison Coleman, Joji Decolongon, Rachelle Dar Santos, who were all not only excellent educators in the intricacies of clinical research but moreso were a part of my life for all of my time in Vancouver. Indeed without their strong friendship and support during the time of my settling in Canada, this thesis would not have been possible and I am very thankful to them. Thanks also to Susan Creighton, Dr Alex Goumeniouk, Dr Lynn Raymond, Susan Tolley and Kimberly Carter from whom I learnt so much about Huntington disease and its management in the most holistic sense.

I am extremely grateful to Sarah Tabrizi at the Institute of Neurology for giving me the great opportunity to participate in TRACK-HD at the Centre for Huntington disease, and for her tireless support. Very many thanks also to Rachael Scahill of the ION imaging team, for her discussions of numerous structural imaging issues.

I am extremely grateful to Alex MacKay, whose expert contribution to this project was critical to its direction and successful completion. Very many thanks also to Corree Laule PhD, whom taught me extensively on the use and interpretation of MRS and its associated methodologies. Also to Katy Wyper, clinical fellow at the Department, whose assistance with data analysis logistics was critical. I would also like to thank the radiographers in the UBC MRI Department for their efforts and patience in acquiring the scans used for this work.

I am extremely grateful to Ruth Milner, at the CFRI, Vancouver for her sound statistical advice and support throughout the execution of this study. Ruth advised on the most appropriate testing paradigms at various stages during these studies.

I would also like to thank all of the Leavitt Lab, particularly Angela Gurney, Austin Hill, Jasmin Yang and David Weir for their many hours of effort in obtaining, processing and assaying CSF and plasma samples. I am also grateful to Prof Stanley Rapoport, Ken Ma, Uemesha Shetty at NIH, Maryland, for their work and significant effort in performing the mI assay.

I would like to thank CHDI a non-profit organisation dedicated to finding treatments for HD, Gail Owen, Beth Borowsky Sherry Lifer, Saiqah Munir, Daniel van Kammen, Ethan Signer, Katja Vitkin, Felix Mudoh Tita, Irina Vainer, Theresia Kelm, Tanka Acharya, the Laboratory of Neuro Imaging UCLA (LONI) and IXICO for their assistance in all areas of this study. I would also like to thank Ralf Reilmann, Natalie Bechtel and Stefan Bohlen for their work on developing the QMotor battery and their work that essentially formed part of this thesis.

Lastly, I'd like to thank my parents Anita and Chris, and brother, Damon for their unwavering support both in the decision to move to Canada and in my completion of this research.

References

Albin RL, Greenamyre JT. Alternative excitotoxic hypotheses. Neurology. 1992;42(4):733-738.

Albin RL, Young AB, Penney JB. The functional anatomy of basal ganglia disorders. Trends Neurosci. 1989;12(10):366-375.

Albin RL, Young AB, Penney JB, et al. Abnormalities of striatal projection neurons and N-methyl-D-aspartate receptors in presymptomatic Huntington's disease. N Engl J Med. 1990; 322(18):1293-1298

Anderson RE, Hansson LO, Nilsson O, Liska J, Settergren G, Vaage J. Increase in serum S100a1-B and S100BB during cardiac surgery arises from extracerebral sources. Ann Thorac Surg 2001;71:1512-1517.

Anderson RE, Hansson LO, Nilsson O, Dijlai-Merzoug R, Settergren G. High Serum S100B levels for trauma patients without head injuries. Neurosurgery 2001;48:1255-1260.

Andreassen OA, Dedeoglu A, Ferrante RJ, Jenkins BG, Ferrante KL, Thomas M, Friedlich A, Browne SE, Schilling G, Borchelt DR, Hersch SM, Ross CA, Beal MF. Creatine increase survival and delays motor symptoms in a transgenic animal model of Huntington's disease. Neurobiol Dis. 2001;8(3):479-491.

Andrews TC, Weeks RA, Turjanski N, Gunn RN, Watkins LH, Sahakian B, Hodges JR, Rosser AE, Wood NW, Brooks DJ. Huntington's disease progression. PET and clinical observations. Brain 1999; 122 (12): 2353-2363.

Andrich J, Saft C, Ostholt N, Müller T. Assessment of simple movements and progression of Huntington's disease. J Neurol Neurosurg Psychiatry. 2007;78(4):405-407.

Andrich JE, Wobben M, Klotz P, Goetze O, Saft C. Upper gastrointestinal findings in Huntington's disease: patients suffer but do not complain. J Neural Transm 2009;116(12):1607-1611.

Antonini A, Leenders KL, Spiegel R, Meier D, Vontobel P, Weigell-Weber M, Sanchez-Pernaute R, de Yébenez JG, Boesiger P, Weindl A, Maguire RP. Striatal glucose metabolism and dopamine D2 receptor binding in asymptomatic gene carriers and patients with Huntington's disease. Brain 1996; 119 (6): 2085-2095.

Aronin N, Kim M, Laforet G, DiFiglia M. Are there multiple pathways in the pathogenesis of Huntington's disease? Philos Trans R Soc Lond B Biol Sci. 1999;354(1386):995-1003.

Arrasate M, Mitra S, Schweitzer ES, Segal MR, Finkbeiner S. Inclusion body

formation reduces levels of mutant huntingtin and the risk of neuronal death. Nature. 2004;431(7010):805-810.

Auinger P, Kieburtz K, McDermott MP. The relationship between uric acid levels and Huntington's disease progression. Movement Disorders 2010;25(2):224-228.

Aurell A, Rosengren LE, Karlsson B, Olsson JE, Zbornikova V, Haglid KG. Determination of S-100 and glial fibrillary acidic protein concentrations in cerebrospinal fluid after brain infarction. Stroke 1991;22:1254-1258

Aylward EH, Codori AM, Barta PE, Pearlson GD, Harris GJ, Brandt J. Basal ganglia volume and proximity to onset in presymptomatic Huntington disease. Arch Neurol 1996; 53(12): 1293-1296.

Aylward EH, Codori AM, Rosenblatt A, Sherr M, Brandt J, Stine OC, Barta PE, Pearlson GD, Ross CA. Rate of caudate atrophy in presymptomatic and symptomatic stages of Huntington's disease. Mov Disord 2000 May;15(3):552-560.

Aylward EH, Li Q, Stine OC, Ranen N, Sherr M, Barta PE, Bylsma FW, Pearlson GD, Ross CA. Longitudinal change in basal ganglia volume in patients with Huntington's disease. Neurology 1997;48(2):394-399.

Aylward EH, Liu D, Nopoulos PC, Ross CA, Pierson RK, Mills JA, Long JD, Paulsen JS;

PREDICT-HD Investigators and Coordinators of the Huntington Study Group. Striatal volume contributes to the prediction of onset of Huntington disease in incident cases. Biol Psychiatry. 2012;71(9):822-828.

Aylward EH, Nopoulos PC, Ross CA, Langbehn DR, Pierson RK, Mills JA, Johnson HJ, Magnotta VA, Juhl AR, Paulsen JS; PREDICT-HD Investigators and Coordinators of Huntington Study Group. J Neurol Neurosurg Psychiatry. 2011;82(4):405-410.

Aylward EH, Sparks BF, Field KM, Yallapragada V, Shpritz BD, Rosenblatt A, Brandt J, Gourley LM, Liang K, Zhou H, Margolis RL, Ross CA. Onset and rate of striatal atrophy in preclinical Huntington disease. Neurology 2004;63(1):66-72.

Aziz NA, Pijl H, Frölich M, Elst JPSd, van der Bent C, Roelfsema F. Growth hormone and ghrelin secretion are associated with clinical severity in Huntington's disease. European Journal of Neurology 2010;17(2):280-288.

Aziz NA, Pijl H, Frölich M, Maurits van der Graaf AW, Roelfsema F, Roos RA. Leptin secretion rate increases with higher CAG repeat number in Huntington's disease patients. Clin Endocrinol (Oxf) 2009a.

Aziz NA, van der Burg JM, Roos RA, Maison P, Saleh N, Bachoud-Levi AC. High insulinlike growth factor I is associated with cognitive decline in Huntington disease. Neurology 2011;76(7):675-676.

Backman L, Robins-Wahlin TB, Lundin A, Ginovart N, Farde L. Cognitive deficits in Huntington's disease are predicted by dopaminergic PET markers and brain volumes. Brain 1997;120 (Pt 12)(Pt 12):2207-2217.

Baker EH, Basso G, Barker PB, Smith MA, Bonekamp D, Horská A. Regional Apparent Metabolite Concentrations in Young Adult Brain Measured by 1H MR Spectroscopy at 3 Tesla. J Mag Res Imaging 2008; 27: 489 – 499.

Bartha R. Effect of signal-to-noise ratio and spectral linewidth on metabolite quantification at 4 T. NMR Biomed. 2007; 20(5): 512-521.

Bartzokis G, Cummings J, Perlman S, Hance DB, Mintz J. Increased basal ganglia iron levels in Huntington disease. Arch Neurol 1999;56(5):569-574.

Bartzokis G, Lu PH, Tishler TA, Fong SM, Oluwadara B, Finn JP, Huang D, Bordelon Y, Mintz J, Perlman S. Myelin breakdown and iron changes in Huntington's disease: pathogenesis and treatment implications. Neurochem Res 2007;32(10):1655-1664.

Bates G, Harper P, Jones L. Huntington's Disease. New York, NY: Oxford University Press; 2002.

Bates TE, Strangward M, Keelan J, Davey GP, Munro PM, Clark JB. Inhibition of N-acetylaspartate production: implications for 1H MRS studies in vivo. Neuroreport. 1996;7(8):1397-1400.

Battaglia G, Cannella M, Riozzi B, Orobello S, Maat-Schieman ML, Aronica E, Busceti CL, Ciarmiello A, Alberti S, Amico E, Sassone J, Sipione S, Bruno V, Frati L, Nicoletti F, Squitieri F. Early defect of transforming growth factor beta-1 formation in Huntington's disease. J Cell Mol Med 2010 15(3):555-571.

Battista N, Bari M, Tarditi A, Mariotti C, Bachoud-Levi AC, Zuccato C, Finazzi-Agrò A, Genitrini S, Peschanski M, Di Donato S, Cattaneo E, Maccarrone M. Severe deficiency of the fatty acid amide hydrolase (FAAH) activity segregates with the

Huntington's disease mutation in peripheral lymphocytes. Neurobiol Dis 2007;27(1):108-116.

Beal MF. Aging, energy, and oxidative stress in neurodegenerative diseases. Ann Neurol. 1995;38(3):357-366.

Beal MF. Mitochondria take center stage in aging and neurodegeneration. Ann Neurol. 2005;58(4):495-505.

Beal MF, Hyman BT, Koroshetz W. Do defects in mitochondrial energy metabolism underlie the pathology of neurodegenerative diseases? Trends Neurosci. 1993;16(4):125-131.

Beal MF, Kowall NW, Ellison DW, Mazurek MF, Swartz KJ, Martin JB. Replication of the neurochemical characteristics of Huntington's disease by quinolinic acid. Nature. 1986; 321(6066):168-171.

Bechtel N, Scahill RI, Rosas HD, Acharya T, van den Bogaard SJ, Jauffret C, Say MJ, Sturrock A, Johnson H, Onorato CE, Salat DH, Durr A, Leavitt BR, Roos RA, Landwehrmeyer GB, Langbehn DR, Stout JC, Tabrizi SJ, Reilmann R. Tapping linked to function and structure in pre-manifest and symptomatic Huntington disease. Neurology. 2010;75(24):2150-2160.

Bender A, Auer DP, Merl T, Reilmann R, Saemann P, Yassouridis A, Bender J, Weindl A, Dose M, Gasser T, Klopstock T. Creatine supplementation lowers brain glutamate levels in Huntington's disease. J Neurol 2005;252(1):36-41.

Berent S, Giordani B, Lehtinen S, Markel D, Penney JB, Buchtel HA, Starosta-Rubinstein S, Hichwa R, Young AB. Positron emission tomographic scan investigations of Huntington's disease: cerebral metabolic correlates of cognitive function. Ann Neurol 1988;23(6):541-546.

Bertholdo D, Watcharakorn A, Castillo M. Brain Magnetic Resonance Spectroscopy. www.ajnr.org/site/fellows/files/MRS-chapter-Castillo.pdf.

Bhattacharyya PK, Phillips MD, Stone LA, Lowe MJ. In-vivo MRS measurement of gray-matter and white-matter GABA concentration in sensorimotor cortex using a motion- controlled MEGA-PRESS Sequence. Magn Reson Imaging. 2011; 29(3): 374–379.

Bitsch A, Bruhn H, Vougioukas V, Stringaris A, Lassmann H, Frahm J, Brück W. Inflammatory CNS demyelination: histopathologic correlation with in vivo quantitative proton MR spectroscopy. AJNR Am J Neuroradiol. 1999;20(9):1619-1627.

Bjorkqvist M, Leavitt BR, Nielsen JE, Landwehrmeyer B, Ecker D, Mulder H, Brundin P, Petersén A. Cocaine- and amphetamine-regulated transcript is increased in Huntington disease. Mov Disord 2007;22(13):1952-1954.

Bjorkqvist M, Petersen A, Bacos K, Isaacs J, Norlen P, Gil J, Popovic N, Sundler F, Bates GP, Tabrizi SJ, Brundin P, Mulder H. Progressive alterations in the hypothalamic-pituitary-adrenal axis in the R6/2 transgenic mouse model of Huntington's disease. Hum Mol Genet 2006;15(10):1713-1721.

Bjorkqvist M, Petersen A, Nielsen J, Ecker D, Mulder H, Hayden MR, Landwehrmeyer B, Brundin P, Leavitt BR. Cerebrospinal fluid levels of orexin-A are not a clinically useful biomarker for Huntington disease. Clin Genet 2006;70(1):78-79.

Bjorkqvist M, Wild EJ, Thiele J, Silvestroni A, Andre R, Lahiri N, Raibon E, Lee RV, Benn CL, Soulet D, Magnusson A, Woodman B, Landles C, Pouladi MA, Hayden MR, Khalili-Shirazi A, Lowdell MW, Brundin P, Bates GP, Leavitt BR, Möller T, Tabrizi SJ. A novel pathogenic pathway of immune activation detectable before clinical onset in Huntington's disease. J Exp Med 2008;205(8):1869-1877.

Bohanna I, Georgiou-Karistianis N, Hannan AJ, Egan GF. Magnetic resonance imaging as an approach towards identifying neuropathological biomarkers for Huntington's disease. Brain Res Rev. 2008;58(1):209-225.

Bonilla E, Estévez J, Suárez H, Morales LM, Chacin de Bonilla L, Villalobos R, Dávila JO. Serum ferritin deficiency in Huntington's disease patients. Neurosci Lett 1991;129(1):22-24.

Borovecki F, Lovrecic L, Zhou J, Jeong H, Then F, Rosas HD, Hersch SM, Hogarth P, Bouzou B, Jensen RV, Krainc D. Genome-wide expression profiling of human blood reveals biomarkers for Huntington's disease. Proceedings of the National Academy of Sciences of the United States of America 2005;102(31):11023-11028.

Brand A, Richter-Landsberg C, Leibfritz D. Multinuclear NMR studies on the energy metabolism of glial and neuronal cells. Dev. Neurosci. 1993;15:289–298.

Broom KA, Anthony DC, Lowe JP, Griffin JL, Scott H, Blamire AM, Styles P, Perry VH, Sibson NR. MRI and MRS alterations in the preclinical phase of murine prion disease: association with neuropathological and behavioural changes. Neurobiol Dis. 2007;26(3):707-717.

Browne SE, Beal MF. Oxidative damage in Huntington's disease pathogenesis. Antioxid Redox Signal 2006;8(11-12):2061-2073.

Browne SE, Ferrante RJ, Beal MF. Oxidative stress in Huntington's disease. Brain Pathol 1999 Jan;9(1):147-163.

Busch MG, Finsterbusch J. Spatially 2D-selective RF excitations using the PROPELLER trajectory: basic principles and application to MR spectroscopy of irregularly shaped single voxel. Magn Reson Med. 2011;66(5):1218-1225.

Bustillo JR, Rowland LM, Jung R, Brooks WM, Qualls C, Hammond R, Hart B, Lauriello J. Proton magnetic resonance spectroscopy during initial treatment with antipsychotic medication in schizophrenia. Neuropsychopharmacology. 2008; 33(10): 2456-2466.

Butters N, Wolfe J, Martone M, Granholm E, Cermak LS. Memory disorders associated with Huntington's disease: verbal recall, verbal recognition and procedural memory. Neuropsychologia. 1985;23(6):729-743.

Cepeda C, Ariano MA, Calvert CR, Flores-Hernández J, Chandler SH, Leavitt BR, Hayden MR, Levine MS. NMDA receptor function in mouse models of Huntington disease. J Neurosci Res. 2001;66(4):525-539.

Cha JH. Transcriptional dysregulation in Huntington's disease. Trends Neurosci. 2000;23(9):387-392.

Cha JH, Frey AS, Alsdorf SA, Kerner JA, Kosinski CM, Mangiarini L, Penney JB Jr, Davies SW, Bates GP, Young AB. Altered neurotransmitter receptor expression in transgenic mouse models of Huntington's disease. Philos Trans R Soc Lond B Biol Sci. 1999;354(1386): 981-989.

Chard DT, Griffin CM, McLean MA, Kapeller P, Kapoor R, Thompson AJ, Miller DH. Brain metabolite changes in cortical grey and normal-appearing white matter in clinically early relapsing-remitting multiple sclerosis. Brain. 2002;125(Pt 10):2342-2352.

CHDI Foundation Inc. Available at: http://www.huntington-assoc.com/enrollhd.pdf, Accessed March 12th 2011.

Chen CM, Wu YR, Cheng ML, Liu JL, Lee YM, Lee PW, Soong BW, Chiu DT. Increased oxidative damage and mitochondrial abnormalities in the peripheral blood of Huntington's disease patients. Biochem Biophys Res Commun 2007 7/27;359(2):335-340.

Chen SQ, Wang PJ, Ten GJ, Zhan W, Li MH, Zang FC. Role of myo-inositol by magnetic resonance spectroscopy in early diagnosis of Alzheimer's disease in APP/PS1 transgenic mice. Dement Geriatr Cogn Disord. 2009;28(6):558-566.

Chikhale EG, Balbo A, Galdzicki Z, Rapoport SI, Shetty HU. Measurement of myo-inositol turnover in phosphatidylinositol: description of a model and mass spectrometric method for cultured cortical neurons. Biochemistry, 2001, 40: 11114-11120.

Choo YS, Johnson GV, MacDonald M, Detloff PJ, Lesort M. Mutant huntingtin directly increases susceptibility of mitochondria to the calcium-induced permeability transition and cytochrome c release. Hum Mol Genet. 2004;13(14):1407-1420.

Ciammola A, Sassone J, Cannella M, Calza S, Poletti B, Frati L, Squitieri F, Silani V. Low brain-derived neurotrophic factor (BDNF) levels in serum of Huntington's disease patients. Am J Med Genet B Neuropsychiatr Genet 2007;144B(4):574-577.

Ciarmiello A, Cannella M, Lastoria S, Simonelli M, Frati L, Rubinsztein DC, Squitieri F. Brain white-matter volume loss and glucose hypometabolism precede the clinical symptoms of Huntington's disease. J Nucl Med 2006;47(2):215-222.

Constantinescu R, Romer M, Oakes D, Rosengren L, Kieburtz K. Levels of the light subunit of neurofilament triplet protein in cerebrospinal fluid in Huntington's disease. Parkinsonism Relat Disord 2009 3;15(3):245-248.

Coyle JT, Schwarcz R. Lesion of striatal neurones with kainic acid provides a model for Huntington's chorea. Nature. 1976; 263(5574):244-246.

Craufurd D, Thompson JC, Snowden JS. Behavioral changes in Huntington Disease. Neuropsychiatry Neuropsychol Behav Neurol. 2001;14(4):219-226.

Cunha L, Oliveira CR, Diniz M, Amaral R, Concalves AF, Pio-Abreu J. Homovanilic acid in Huntington's disease and Sydenham's chorea. J Neurol Neurosurg Psychiatry 1981;44(3):258-261.

Dalrymple A, Wild EJ, Joubert R, Sathasivam K, Björkqvist M, Petersén A, Jackson GS, Isaacs JD, Kristiansen M, Bates GP, Leavitt BR, Keir G, Ward M, Tabrizi SJ. Proteomic profiling of plasma in Huntington's disease reveals neuroinflammatory activation and biomarker candidates. J Proteome Res 2007;6(7):2833-2840.

Dassan P, Keir G, Brown MM. Criteria for a clinically informative serum biomarker

in acute ischaemic stroke: a review of S100B. Cerebrovasc Dis. 2009;27(3):295-302.

Davie CA, Barker GJ, Quinn N, Tofts PS, Miller DH. Proton MRS in Huntington's disease. Lancet. 1994;343(8912):1580.

Davies SW, Turmaine M, Cozens BA, DiFiglia M, Sharp AH, Ross CA, Scherzinger E, Wanker EE, Mangiarini L, Bates GP. Formation of neuronal intranuclear inclusions underlies the neurological dysfunction in mice transgenic for the HD mutation. Cell. 1997;90(3):537-548.

Dawbarn D, De Quidt ME, Emson PC. Survival of basal ganglia neuropeptide Y-somatostatin neurones in Huntington's disease. Brain Res. 1985;340(2):251-260.

Demougeot C, Bertrand N, Prigent-Tessier A, Garnier P, Mossiat C, Giroud M, Marie C, Beley A. Reversible loss of N-acetyl-aspartate in rats subjected to long-term focal cerebral ischemia. J Cereb Blood Flow Metab. 2003;23(4):482-489.

Dennhardt J, LeDoux MS. Huntington disease in a nonagenarian mistakenly diagnosed as normal pressure hydrocephalus. J Clin Neurosci. 2010;17(8):1066-1067.

De Stefano N, Narayanan S, Matthews PM, Mortilla M, Dotti MT, Federico A, Arnold DL. Proton MR spectroscopy to assess axonal damage in multiple sclerosis and other white matter disorders. J Neurovirol. 2000; Suppl 2:S121-S129.

de Yebenes JG, Landwehrmeyer B, Squitieri F, Reilmann R, Rosser A, Barker RA, Saft C, Magnet MK, Sword A, Rembratt A, Tedroff J; MermaiHD study investigators. Pridopidine for the treatment of motor function in patients with Huntington's disease (MermaiHD): a phase 3, randomised, double-blind, placebo-controlled trial.Lancet Neurol. 2011;10(12):1049-1057.

Dexter DT, Carayon A, Javoy-Agid F, Agid Y, Wells FR, Daniel SE, Lees AJ, Jenner P, Marsden CD. Alterations in the levels of iron, ferritin and other trace metals in Parkinson's disease and other neurodegenerative diseases affecting the basal ganglia. Brain 1991;114 (Pt 4)(Pt 4):1953-1975.

Di Figlia M. Excitotoxic injury of the neostriatum: a model for Huntington’s disease. Trends Neurosci 1990;13:28.

Drost DJ, Riddle WR, Clarke GD; AAPM MR Task Group #9. Proton magnetic resonance spectroscopy in the brain: report of AAPM MR Task Group #9. Med Phys. 2002; 29(9):2177-2197.

Dubinsky RM. No going home for hospitalized Huntington's disease patients. Mov Disord 2005;20(10):1316-1322.

Duff K, Paulsen JS, Beglinger LJ, Langbehn DR, Stout JC; Predict-HD Investigators of the Huntington Study Group. Psychiatric symptoms in Huntington's disease before diagnosis: the predict-HD study. Biol Psychiatry. 2007;62(12):1341-1346.

Dumas EM, van den Bogaard SJ, Ruber ME, Reilman RR, Stout JC, Craufurd D, Hicks SL, Kennard C, Tabrizi SJ, van Buchem MA, van der Grond J, Roos RA. Early changes in white matter pathways of the sensorimotor cortex in pre-manifest Huntington's disease. Hum Brain Mapp 2012. 33(1):203-212.

Dunlop DS, Mc Hale DM, Lajtha A. Decreased brain N-acetylaspartate in Huntington's disease. Brain Res 1992; 580(1-2): 44-48.

Duran R, Barrero FJ, Morales B, Luna JD, Ramirez M, Vives F. Oxidative stress and plasma aminopeptidase activity in Huntington's disease. J Neural Transm 2010;117(3):325-332.

Duran-Vilaregut J, del Valle J, Camins A, Pallàs M, Pelegrí C, Vilaplana J. Blood-brain barrier disruption in the striatum of rats treated with 3-nitropropionic acid. Neurotoxicology. 2009;30(1):136-143.

Estorch M, Carrio I. Future challenges of multimodality imaging. Recent Results Cancer Res. 2013;187:403-415.

European Huntington's Disease Network. Available at: http://www.euro-hd.net/html/registry, Accessed March 12th 2011.

Fang Q, Strand A, Law W, Faca VM, Fitzgibbon MP, Hamel N, Houle B, Liu X, May DH, Poschmann G, Roy L, Stühler K, Ying W, Zhang J, Zheng Z, Bergeron JJ, Hanash S, He F, Leavitt BR, Meyer HE, Qian X, McIntosh MW. Brain-specific proteins decline in the cerebrospinal fluid of humans with Huntington disease. Mol Cell Proteomics 2009 Mar;8(3):451-466.

Fayed N, Modrego PJ, Medrano J. Comparative test-retest reliability of metabolite values assessed with magnetic resonance spectroscopy of the brain. The LCModel versus the manufacturer software. Neurol Res. 2009; 31(5):472-477.

Fayed N, Olmos S, Morales H, Modrego PJ. Physical basis of magnetic resonance spectroscopy and its application to central nervous system diseases. Am J Applied Sci. 2006; 3:1836-1845.

Feigin A, Tang C, Ma Y, Mattis P, Zgaljardic D, Guttman M, Paulsen JS, Dhawan V, Eidelberg D. Thalamic metabolism and symptom onset in preclinical Huntington's disease. Brain 2007;130(Pt 11):2858-2867.

Fernandes HB, Baimbridge KG, Church J, Hayden MR, Raymond LA. Mitochondrial sensitivity and altered calcium handling underlie enhanced NMDA-induced apoptosis in YAC128 model of Huntington's disease. J Neurosci. 2007; 27(50):13614-13623.

Ferrante RJ, Andreassen OA, Jenkins BG, Dedeoglu A, Kuemmerle S, Kubilus JK, Kaddurah-Daouk R, Hersch SM, Beal MF. Neuroprotective effects of creatine in a transgenic mouse model of Huntington's disease. J Neurosci. 2000 Jun 15;20(12):4389-4397.

Ferrante RJ, Kowall NW, Beal MF, Martin JB, Bird ED, Richardson EP Jr. Morphologic and histochemical characteristics of a spared subset of striatal neurons in Huntington's disease. J Neuropathol Exp Neurol. 1987;46(1):12-27.

Ferrante RJ, Kowall NW, Beal MF, Richardson EP Jr, Bird ED, Martin JB. Selective

sparing of a class of striatal neurons in Huntington's disease. Science. 1985;230(4725):561-563.

Ferrante RJ, Kowall NW, Cipolloni PB, Storey E, Beal MF. Excitotoxin lesions in primates as a model for Huntington's disease: histopathologic and neurochemical characterization. Exp Neurol. 1993;119(1):46-71.

Fisher ER, Hayden MR. Multisource ascertainment of Huntington disease in Canada: Prevalence and population at risk. Mov Disord. 2013 [Epub ahead of print].

Fisher SK, Novak JE, Agranoff BW. Inositol and higher inositol phosphates in neural tissues: homeostasis, metabolism and functional significance. J Neurochem. 2002;82(4):736-754.

Folstein SE, Chase GA, Wahl WE, McDonnell AM, Folstein MF. Huntington disease in Maryland: clinical aspects of racial variation. Am J Hum Genet. 1987;41(2):168-179.

Forrest CM, Mackay GM, Stoy N, Spiden SL, Taylor R, Stone TW, Darlington LG. Blood levels of kynurenines, interleukin-23 and soluble human leucocyte antigen-G at different stages of Huntington's disease. J Neurochem 2010 Jan;112(1):112-122.

Franciosi S, Ryu JK, Shim Y, Hill A, Connolly C, Hayden MR, McLarnon JG, Leavitt BR. Age-derendent neurovascular abnormalities and altered microglial morphology in the YAV128 mouse model of Huntington disease. Neurobiol dis. 2012;45(1):438-449.

Gaidarov I, Chen Q, Falck JR, Reddy KK, Keen JH. A functional phosphatidylinositol 3,4,5-trisphosphate/phosphoinositide binding domain in the clathrin adaptor AP-2 a subunit. Implications for the endocytic pathway. J. Biol. Chem 1996; 271:20922–20929.

Garcia Ruiz PJ, Mena MA, Sanchez Bernardos V, Diaz Neira W, Gimenez Roldan S, Benitez J, García de Yebenes J. Cerebrospinal fluid homovanillic acid is reduced in untreated Huntington's disease. Clin Neuropharmacol 1995;18(1):58-63.

Gaus SE, Lin L, Mignot E. CSF hypocretin levels are normal in Huntington's disease patients. Sleep 2005;28(12):1607-1608.

Georgiou-Karistianis N. A peek inside the Huntington's brain: will functional imaging take us one step closer in solving the puzzle? Exp Neurol 2009;220(1):5-8.

Glanville NT, Byers DM, Cook HW, Spence MW, Palmer FB. Differences in the metabolism of inositol and phosphoinositides by cultured cells of neuronal and glial origin. Biochim. Biophys. Acta 1989;1004:169–179.

Glodzik L, King KG, Gonen O, Liu S, De Santi S, de Leon MJ. Memantine decreases hippocampal glutamate levels: a magnetic resonance spectroscopy study. Prog Neuropsychopharmacol Biol Psychiatry. 2008; 32(4): 1005–1012.

Godbolt AK, Waldman AD, MacManus DG, Schott JM, Frost C, Cipolotti L, Fox NC, Rossor MN. MRS shows abnormalities before symptoms in familial Alzheimer disease. Neurology 2006; 66(5): 718-722.

Goldberg YP, Nicholson DW, Rasper DM, Kalchman MA, Koide HB, Graham RK, Bromm M, Kazemi-Esfarjani P, Thornberry NA, Vaillancourt JP, Hayden MR. Cleavage of huntingtin by apopain, a proapoptotic cysteine protease, is modulated by the polyglutamine tract. Nat Genet. 1996;13(4): 442-449.

Gómez-Ansón B, Alegret M, Muñoz E, Sainz A, Monte GC, Tolosa E. Decreased frontal choline and neuropsychological performance in preclinical Huntington disease. Neurology 2007; 68(12): 906-910.

Gonul AS, Kitis O, Ozan E, Akdeniz F, Eker C, Eker OD, Vahip S. The effect of antidepressant treatment on N-acetyl aspartate levels of medial frontal cortex in drug-free depressed patients. Prog Neuropsychopharmacol Biol Psychiatry. 2006; 30(1): 120-125.

Graham RK, Pouladi MA, Joshi P, Lu G, Deng Y, Wu NP, Figueroa BE, Metzler M, André VM, Slow EJ, Raymond L, Friedlander R, Levine MS, Leavitt BR, Hayden MR. Differential susceptibility to excitotoxic stress in YAC128 mouse models of Huntington disease between initiation and progression of disease. J Neurosci. 2009;29(7):2193-2204.

Graybiel AM, Aosaki T, Flaherty AW, Kimura M. The basal ganglia and adaptive motor control. Science. 1994 23;265(5180):1826-1831.

Green AJE, Harvey RJ, Thompson EJ, Rossor MN. Increased S100 in the cerebrospinal fluid of patients with frontotemporal dementia. Neurosci Lett 1997;235:5-8.

Greene JG, Porter RH, Eller RV, Greenamyre JT. Inhibition of succinate dehydrogenase by malonic acid produces an ‘‘excitotoxic’’ lesion in rat striatum. J Neurochem. 1993;61(3): 1151-1154.

Griffin WS, Stanley LC, Ling C, White L, MacLeod V, Perrot LJ, White CL 3rd, Araoz C. Brain interleukin 1 and S-100 immunoreactivity are elevated in Down syndrome and Alzheimer disease. Proc Natl Acad Sci U S A. 1989;86(19):7611-7615.

Guevara P, Duclap D, Poupon C, Marrakchi-Kacem L, Fillard P, Le Bihan D, Leboyer M, Houenou J, Mangin JF. Automatic fiber bundle segmentation in massive

tractography datasets using a multi-subject bundle atlas. Neuroimage. 2012;61(4):1083-1099.

Gujar, SK, Maheshwari S, Bjorkman-Burtscher I, Sundgren, PC. Magnetic Resonance Spectroscopy. J Neuro-Ophthalmol 2005; 25(3): 217-226.

Gusella JF, Wexler NS, Conneally PM, Naylor SL, Anderson MA, Tanzi RE et al. A polymorphic DNA marker genetically linked to Huntington's disease. Nature. 1983;306: 234–238.

Haase A, Frahm J, Hanicke W, Matthaei D. 1H NMR chemical shift selective (CHESS) imaging. Phys Med Biol. 1985; 30:341–344

Hajek M, Dezortova M. Introduction to clinical in vivo MR spectroscopy. Eur J Radiol. 2008; 67(2):185-193.

Hammerman MR, Sacktor B, Daughaday WH. myo-Inositol transport in renal brush border vesicles and it inhibition by D-glucose. Am J Physiol. 1980;239(2):F113-120.

Hansotia P, Wall R, Berendes J. Sleep disturbances and severity of Huntington's disease. Neurology. 1985;35(11): 1672-1674.

Hantraye P, Riche D, Maziere M, Isacson O. A primate model of Huntington's disease: behavioral and anatomical studies of unilateral excitotoxic lesions of the caudate-putamen in the baboon. Exp Neurol. 1990;108(2):91-104.

Harms L, Meierkord H, Timm G, Pfeiffer L, Ludolph AC. Decreased N-acetyl-aspartate/choline ratio and increased lactate in the frontal lobe of patients with Huntington's disease: a proton magnetic resonance spectroscopy study. J Neurol Neurosurg Psychiatry. 1997;62(1):27-30.

Harris GJ, Aylward EH, Peyser CE, Pearlson GD, Brandt J, Roberts-Twillie JV, Barta PE, Folstein SE. Single photon emission computed tomographic blood flow and magnetic resonance volume imaging of basal ganglia in Huntington's disease. Arch Neurol 1996; 53(4): 316-324.

Harris GJ, Codori AM, Lewis RF, Schmidt E, Bedi A, Brandt J. Reduced basal ganglia blood flow and volume in pre-symptomatic, gene-tested persons at-risk for Huntington's disease. Brain 1999;122 (Pt 9)(Pt 9):1667-1678.

Harris GJ, Pearlson GD, Peyser CE, Aylward EH, Roberts J, Barta PE, Chase GA, Folstein SE. Putamen volume reduction on magnetic resonance imaging exceeds caudate changes in mild Huntington's disease. Ann Neurol 1992;31(1):69-75.

Hauser G, Finelli VN. The biosynthesis of free and phosphatide myo-inositol from

glucose in mammalian tissues. J. Biol. Chem. 1963;238:3224–3228.

Hayden MR. Huntington's Chorea. Berlin, Germany: Springer-Verlag; 1981.

Heikkinen T, Lehtimäki K, Vartiainen N, Puoliväli J, Hendricks SJ, Glaser JR, Bradaia A, Wadel K, Touller C, Kontkanen O, Yrjänheikki JM, Buisson B, Howland D, Beaumont V, Munoz-Sanjuan I, Park LC. Characterization of neurophysiological and behavioral changes, MRI brain volumetry and 1H MRS in zQ175 knock-in mouse model of Huntington's disease. PLoS One. 2012;7(12):e50717.

Henley S, Bates GP, Tabrizi SJ. Biomarkers for neurodegenerative diseases. Curr Opin Neurol 2005 December;18(6):698-705.

Henley SM, Wild EJ, Hobbs NZ, Scahill RI, Ridgway GR, Macmanus DG, Barker RA, Fox NC, Tabrizi SJ. Relationship between CAG repeat length and brain volume in pre-manifest and early Huntington's disease. J Neurol. 2009;256(2):203-212.

Herminghaus S, Pilatus U, Möller-Hartmann W, Raab P, Lanfermann H, Schlote W, Zanella FE. Increased choline levels coincide with enhanced proliferative activity of human neuroepithelial brain tumors. NMR Biomed. 2002;15(6):385-392.

Hersch SM, Gevorkian S, Marder K, Moskowitz C, Feigin A, Cox M, Como P, Zimmerman C, Lin M, Zhang L, Ulug AM, Beal MF, Matson W, Bogdanov M, Ebbel E, Zaleta A, Kaneko Y, Jenkins B, Hevelone N, Zhang H, Yu H, Schoenfeld D, Ferrante R, Rosas HD. Creatine in Huntington disease is safe, tolerable, bioavailable in brain and reduces serum 8OH2'dG. Neurology 2006;66(2):250-252.

Heuser IJ, Chase TN, Mouradian MM. The limbic-hypothalamic-pituitary-adrenal axis in Huntington's disease. Biol Psychiatry 1991;30(9):943-952.

Hoang TQ, Bluml S, Dubowitz DJ, et al. Quantitative proton-decoupled 31P MRS and 1H MRS in the evaluation of Huntington's and Parkinson's diseases. Neurology 1998; 50(4): 1033-1040.

Hobbs NZ, Henley SM, Ridgway GR, Wild EJ, Barker RA, Scahill RI, Barnes J, Fox NC, Tabrizi SJ. The progression of regional atrophy in pre-manifest and early Huntington's disease: a longitudinal voxel-based morphometry study. J Neurol Neurosurg Psychiatry 2010;81(7):756-763.

Hobbs NZ, Henley SM, Wild EJ, Leung KK, Frost C, Barker RA, Scahill RI, Barnes J, Tabrizi SJ, Fox NC. Automated quantification of caudate atrophy by local registration of serial MRI: evaluation and application in Huntington's disease. Neuroimage 2009;47(4):1659-1665.

Hodgson JG, Agopyan N, Gutekunst CA, Leavitt BR, LePiane F, Singaraja R, Smith DJ, Bissada N, McCutcheon K, Nasir J, Jamot L, Li XJ, Stevens ME, Rosemond E, Roder JC, Phillips AG, Rubin EM, Hersch SM, Hayden MR. A YAC mouse model for Huntington's disease with full-length mutant huntingtin, cytoplasmic toxicity, and selective striatal neurodegeneration. Neuron. 1999;23(1):181-192.

Hoshino Y, Yoshikawa K, Inoue Y, Asai S, Nakamura T, Ogino T, Umeda M, Iwamoto A. Reproducibility of short echo time proton magnetic resonance spectroscopy using point-resolved spatially localized spectroscopy sequence in normal human brains. Radiat Med. 1999; 17(2):115-120.

Houkin K, Kamada K, Kamiyama H, Iwasaki Y, Abe H, Kashiwaba T. Longitudinal changes in proton magnetic resonance spectroscopy in cerebral infarction. Stroke. 1993;24(9):1316-1321.

Howe FA, Barton SJ, Cudlip SA, Stubbs M, Saunders DE, Murphy M, Wilkins P, Opstad KS, Doyle VL, McLean MA, Bell BA, Griffiths JR. Metabolic profiles of human brain tumors using quantitative in vivo 1H magnetic resonance spectroscopy.

Magn Reson Med. 2003; 49:223–232.

Hu J, Van Eldik LJ. S100 beta induces apoptotic cell death in cultured astrocytes via a nitric oxide-dependent pathway. Biochim Biophys Acta. 1996;1313(3):239-245.

Huntington's Disease Collaborative Research Group. A novel gene containing a trinucleotide repeat that is expanded and unstable on Huntington's disease chromosomes. Cell. 1993; 72(6):971-983.

Huntington G. ''On Chorea.'' Med Surg Report Phila. 1872;26(15):317-321.

HSG research resources page. HSG Web site. http://www. huntington-study-group.org/. Accessed 17th September, 2012.

Huntington Study Group. A randomized, placebo-controlled trial of coenzyme Q10 and remacemide in Huntington's disease. Neurology. 2001;57(3):397-404.

Huntington Study Group. Tetrabenazine as antichorea therapy in Huntington disease: a randomized controlled trial. Neurology. 2006;66(3):366-372.

Huntington Study Group TREND-HD Investigators. Randomized controlled trial of ethyl-eicosapentaenoic acid in Huntington disease: the TREND-HD study. Arch Neurol. 2008;65(12): 1582-1589.

Huntington Study Group. Unified Huntington's Disease Rating Scale-99. Huntington Study Group (1999).

Huntington Study Group. 2011; Available at: http://www.huntington-study-group.org/ClinicalResearch/ClinicalTrialsObservationalStudiesinProgress/COHORT/tabid/83/Default.aspx, Accessed March 12th 2011.

Imamura K. Proton MR spectroscopy of the brain with a focus on chemical issues. Magn Reson Med Sci. 2003;2(3):117-132.

Jenkins BG, Andreassen OA, Dedeoglu A, Leavitt B, Hayden M, Borchelt D, Ross CA, Ferrante RJ, Beal MF. Effects of CAG repeat length, HTT protein length and protein context on cerebral metabolism measured using magnetic resonance spectroscopy in transgenic mouse models of Huntington's disease. J Neurochem. 2005;95(2):553-562.

Jenkins BG, Klivenyi P, Kustermann E, Andreassen OA, Ferrante RJ, Rosen BR, Beal MF. Nonlinear decrease over time in N-acetyl aspartate levels in the absence of neuronal loss and increases in glutamine and glucose in transgenic Huntington's disease mice. J Neurochem. 2000 May;74(5):2108-2119.

Jenkins BG, Koroshetz WJ, Beal MF, Rosen BR. Evidence for impairment of energy

metabolism in vivo in Huntington's disease using localized 1H NMR spectroscopy. Neurology. 1993;43(12):2689-2695.

Jenkins BG, Rosas HD, Chen YC, Makabe T, Myers R, MacDonald M, Rosen BR, Beal MF, Koroshetz WJ. 1H NMR spectroscopy studies of Huntington's disease: correlations with CAG repeat numbers. Neurology. 1998;50(5):1357-1365.

Jurgens CK, Jasinschi R, Ekin A, Witjes-Ane MN, Middelkoop H, van der Grond J, Roos RA. MRI T2 Hypointensities in basal ganglia of pre-manifest Huntington's disease. PLoS Curr 2010;2:RRN1173.

Jurgens CK, van de Wiel L, van Es AC, Grimbergen YM, Witjes-Ané MN, van der Grond J, Middelkoop HA, Roos RA. Basal ganglia volume and clinical correlates in 'preclinical' Huntington's disease. J Neurol 2008; 255(11): 1785-1791.

Kanowski M, Kaufmann J, Braun J, Bernarding J, Tempelmann C. Quantitation of simulated short echo time 1H human brain spectra by LCModel and AMARES. Magn Reson Med. 2004; 51(5): 904-912.

Kantarci K. 1H magnetic resonance spectroscopy in dementia. Br J Radiol 2007; 80 (Spec No. 2): S146–152.

Kantarci K, Knopman DS, Dickson DW, Parisi JE, Whitwell JL, Weigand SD. Alzheimer disease: postmortem neuropathologic correlates of antemortem 1H MR spectroscopy metabolite measurements. Radiology 2008; 248: 210–220.

Kantarci K, Petersen RC, Przybelski SA, Weigand SD, Shiung MM, Whitwell JL, Negash S, Ivnik RJ, Boeve BF, Knopman DS, Smith GE, Jack CR Jr. Hippocampal volumes, proton magnetic resonance spectroscopy metabolites, and cerebrovascular disease in mild cognitive impairment subtypes. Arch Neurol. 2008; 65(12): 1621-1628.

Katsuno M, Adachi H, Sobue G. Getting a handle on Huntington's disease: the case for cholesterol. Nat Med 2009;15(3):253-254.

Kaymak SU, Demir B, Oğuz KK, Sentürk S, Uluğ B. Antidepressant effect detected on proton magnetic resonance spectroscopy in drug-naïve female patients with first-episode major depression. Psychiatry Clin Neurosci 2009; 63(3): 350-356.

Kieburtz K, McDermott MP, Voss TS, Corey-Bloom J, Deuel LM, Dorsey ER, Factor S, Geschwind MD, Hodgeman K, Kayson E, Noonberg S, Pourfar M, Rabinowitz K, Ravina B, Sanchez-Ramos J, Seely L, Walker F, Feigin A; Huntington Disease Study

Group DIMOND Investigators. A randomized, placebo-controlled trial of latrepirdine in Huntington disease. Arch Neurol. 2010;67(2):154-160.

Kim J, Amante DJ, Moody JP, Edgerly CK, Bordiuk OL, Smith K, Matson SA, Matson WR, Scherzer CR, Rosas HD, Hersch SM, Ferrante RJ. Reduced creatine kinase as a central and peripheral biomarker in Huntington's disease. Biochim Biophys Acta. 2010;1802(7-8):673-681.

Kim JS, Kornhuber HH, Holzmuller B, Schmid-Burgk W, Mergner T, Krzepinski G. Reduction of cerebrospinal fluid glutamic acid in Huntington's chorea and in schizophrenic patients. Arch Psychiatr Nervenkr 1980;228(1):7-10.

Kipps CM, Duggins AJ, Mahant N, Gomes L, Ashburner J, McCusker EA. Progression of structural neuropathology in preclinical Huntington's disease: a tensor based morphometry study. J Neurol Neurosurg Psychiatry 2005;76(5):650-655.

Kirkwood SC, Siemers E, Bond C, Conneally PM, Christian JC, Foroud T. Confirmation of subtle motor changes among presymptomatic carriers of the Huntington disease gene. Arch Neurol. 2000; 57(7): 1040-4.

Kirkwood SC, Siemers E, Stout JC, Hodes ME, Conneally PM, Christian JC, Foroud T. Longitudinal cognitive and motor changes among presymptomatic Huntington disease gene carriers. Arch Neurol 1999;56: 563–568.

Klepac N, Relja M, Klepac R, Hećimović S, Babić T, Trkulja V. Oxidative stress parameters in plasma of Huntington's disease patients, asymptomatic Huntington's disease gene carriers and healthy subjects: a cross-sectional study. J Neurol. 2007;254(12):1676-1683.

Kloppel S, Henley SM, Hobbs NZ, Wolf RC, Kassubek J, Tabrizi SJ, Frackowiak RS. Magnetic resonance imaging of Huntington's disease: preparing for clinical trials. Neuroscience 2009;164(1):205-219.

Koroshetz WJ, Jenkins BG, Rosen BR, Beal MF. Energy metabolism defects in Huntington's disease and effects of coenzyme Q10. Ann Neurol. 1997;41(2):160-165.

Kowall NW, Ferrante RJ, Beal MF, et al. Neuropeptide Y, somatostatin, and reduced nicotinamide adenine dinucleotide phosphate diaphorase in the human striatum: a combined immunocytochemical and enzyme histochemical study. Neuroscience. 1987;20(3):817-828.

Krause A, Temlett J, Van der Meyden K, Ross CA, Callahan C, Margolis RL. CAG/CTG repeat expansions at the HDL2 locus are a common cause of Huntington disease in black South Africans. Am J Hum Genet. 2002;71:528S.

Kugel H, Heindel W, Ernestus RI, Bunke J, du Mesnil R, Friedmann G. Human brain tumors: spectral patterns detected with localized H-1 MR spectroscopy. Radiology. 1992;183(3):701-709.

Kurlan R, Goldblatt D, Zaczek R, Jeffries K, Irvine C, Coyle J, Shoulson I. Cerebrospinal fluid homovanillic acid and parkinsonism in Huntington's disease. Ann Neurol 1988;24(2):282-284.

Kuwert T, Lange HW, Langen KJ, Herzog H, Aulich A, Feinendegen LE. Cortical and subcortical glucose consumption measured by PET in patients with Huntington's disease. Brain 1990;113 (Pt 5)(Pt 5):1405-1423.

Landwehrmeyer GB, Dubois B, de Ye´benes JG, et al. Riluzole in Huntington's disease: a 3-year, randomized controlled study. Ann Neurol. 2007;62(3):262-272.

Langbehn DR, Brinkman RR, Falush D, Paulsen JS, Hayden MR, International Huntington's Disease Collaborative Group. A new model for prediction of the age of onset and penetrance for Huntington's disease based on CAG length. Clin Genet 2004;65(4):267-277.

Langbehn DR, Hayden MR, Paulsen JS, PREDICT-HD Investigators of the Huntington Study Group. CAG-repeat length and the age of onset in Huntington disease (HD): a review and validation study of statistical approaches. Am J Med Genet B Neuropsychiatr Genet 2010;153B(2):397-408.

Lapper SR, Smith Y, Sadikot AF, Parent A, Bolam JP. Cortical input to parvalbumin-immunoreactive neurones in the putamen of the squirrel monkey. Brain Res. 1992 May 15;580(1-2):215-24.

Leach M, Le Moyec L, Podo F. MRS of tumors:basic principles. In: de Certaines JD, Bovee WMMJ, Podo Eds. Magnetic resonance spectroscopy in biology and medicine. Oxford: Pergamon Press, 1992: 297-299.

Leavitt BR, Guttman JA, Hodgson JG, Kimel GH, Singaraja R, Vogl AW, Hayden MR. Wild-type huntingtin reduces the cellular toxicity of mutant huntingtin in vivo. Am J Hum Genet. 2001;68(2):313-324.

Leblhuber F, Peichl M, Neubauer C, Reisecker F, Steinparz FX, Windhager E, Windhager E, Maschek W. Serum dehydroepiandrosterone and cortisol measurements in Huntington's chorea. J Neurol Sci 1995 Sep;132(1):76-79.

Leoni V, Mariotti C, Tabrizi SJ, Valenza M, Wild EJ, Henley SMD, Hobbs NZ, Mandelli ML, Grisoli M, Björkhem I, Cattaneo E, Di Donato S. Plasma 24S-hydroxycholesterol and caudate MRI in pre-manifest and early Huntington's disease. Brain 2008;131(11):2851-2859.

Llinas R, Sugimori M, Lang EJ, Morita M, Fukuda M, Niinobe M, Mikoshiba K. The inositol high-polyphosphate series blocks synaptic transmission by preventing vesicular fusion: a squid giant synapse study. Proc. Natl Acad. Sci. USA 1994;91:12990–12993.

Lovrecic L, Kastrin A, Kobal J, Pirtosek Z, Krainc D, Peterlin B. Gene expression changes in blood as a putative biomarker for Huntington's disease. Movement Disorders 2009;24(15):2277-2281.

Lundbom N, Barnett A, Bonavita S, Patronas N, Rajapakse J, Tedeschi, Di Chiro G. MR Image Segmentation and Tissue Metabolite Contrast in 1H Spectroscopic Imaging of Normal and Aging Brain. Magn Reson Med 1999; 41: 841–845.

Luthi-Carter R, Strand A, Peters NL, Solano SM, Hollingsworth ZR, Menon AS, Frey AS, Spektor BS, Penney EB, Schilling G, Ross CA, Borchelt DR, Tapscott SJ, Young AB, Cha JH, Olson JM. Decreased expression of striatal signaling genes in a mouse model of Huntington's disease. Hum Mol Genet. 2000;9(9):1259-1271.

Ma K, Deutch J, Villacrese NE, Rosenberger TA, Rapoport SI, Shetty HU. Measuring brain uptake and incorporation into brain phosphatidylinositol of plasma Plasma myo-[$^{2}H_{6}$]Inositol in Unanesthetized Rats: An Approach to Estimate In Vivo Brain Phosphatidylinositol Turnover . Neurochem Res. 2006, 31 (6), 759-765.

McLean MA, Woermann FG, Barker GJ, Duncan JS. Quantitative analysis of short echo time (1)H-MRSI of cerebral gray and white matter. Magn Reson Med. 2000;44(3):401-411.

Macrì MA, Garreffa G, Giove F, *et al*. In vivo quantitative 1H MRS of cerebellum and evaluation of quantitation reproducibility by simulation of different levels of noise and spectral resolution. Magn Reson Imaging. 2004; 22(10): 1385-1393.

Magazi DS, Krause A, Bonev V, Moagi M, Iqbal Z, Dludla M, van der Meyden CH. Huntington's disease: genetic heterogeneity in black African patients. S Afr Med J. 2008;98(3):200-203.

Maglione V, Cannella M, Martino T, De Blasi A, Frati L, Squitieri F. The platelet maximum number of A2A-receptor binding sites (Bmax) linearly correlates with age at onset and CAG repeat expansion in Huntington's disease patients with predominant chorea. Neurosci Lett 2006;393(1):27-30.

Maglione V, Giallonardo P, Cannella M, Martino T, Frati L, Squitieri F. Adenosine A2A receptor dysfunction correlates with age at onset anticipation in blood platelets of subjects with Huntington's disease. Am J Med Genet B Neuropsychiatr Genet 2005;139B(1):101-105.

Magnotta VA, Harris G, Andreasen NC, O'Leary DS, Yuh WT, Heckel D. Structural MR image processing using the BRAINS2 toolbox. Comput Med Imaging Graph. 2002 Jul-Aug;26(4):251-264.

Mangiarini L, Sathasivam K, Seller M, Cozens B, Harper A, Hetherington C, Lawton M, Trottier Y, Lehrach H, Davies SW, Bates GP. Exon 1 of the HD gene with an expanded CAG repeat is sufficient to cause a progressive neurological phenotype in transgenic mice. Cell. 1996;87(3):493-506.

Mann DM, Oliver R, Snowden JS. The topographic distribution of brain atrophy in Huntington's disease and progressive supranuclear palsy. Acta Neuropathol. 1993;85(5):553-559.

Markianos M, Panas M, Kalfakis N, Vassilopoulos D. Plasma testosterone in male patients with Huntington's disease: relations to severity of illness and dementia. Ann Neurol 2005;57(4):520-525.

Markianos M, Panas M, Kalfakis N, Vassilopoulos D. Plasma testosterone, dehydroepiandrosterone sulfate, and cortisol in female patients with Huntington's disease. Neuro Endocrinol Lett 2007;28(2):199-203.

Markianos M, Panas M, Kalfakis N, Vassilopoulos D. Plasma homovanillic acid and prolactin in Huntington's disease. Neurochem Res 2009;34(5):917-922.

Marshall I, Wardlaw J, Cannon J, Slattery J, Sellar RJ. Reproducibility of metabolite peak areas in 1H MRS of brain. Magn Reson Imaging 1996; 14: 281–292.

Martin WR, Wieler M, Hanstock CC. Is brain lactate increased in Huntington's disease? J Neurol Sci. 2007;263(1-2):70-74.

Mastromauro CA, Meissen GJ, Cupples LA, Kiely DK, Berkman B, Myers RH. Estimation of fertility and fitness in Huntington disease in New England. Am J Med Genet. 1989;33(2): 248-254.

McGeer EG, McGeer PL. Duplication of biochemical changes of Huntington’s chorea by intrastriatal injections of glutamic and kainic acids. Nature.

1976;263(5577):517-519.

Meade CA, Figueredo-Cardenas G, Fusco F, Nowak TS Jr, Pulsinelli WA, Reiner A. Transient global ischemia in rats yields striatal projection neuron and interneuron loss resembling that in Huntington's disease. Exp Neurol. 2000 Dec;166(2):307-323.

Mecocci P, Parnetti L, Romano G, Scarelli A, Chionne F, Cecchetti R, Polidori MC, Palumbo B, Cherubini A, Senin U. Serum anti-GFAP and anti-S100 autoantibodies in brain aging, Alzheimer's disease and vascular dementia. J Neuroimmunol 1995;57:165-170.

Meier A, Mollenhauer B, Cohrs S, Rodenbeck A, Jordan W, Meller J, Otto M. Normal hypocretin-1 (orexin-A) levels in the cerebrospinal fluid of patients with Huntington's disease. Brain Res 2005;1063(2):201-203.

Michell AW, Goodman AO, Silva AH, Lazic SE, Morton AJ, Barker RA. Hand tapping: a simple, reproducible, objective marker of motor dysfunction in Huntington's disease. J Neurol. 2008;255(8):1145-52.

Miller BL, Moats RA, Shonk T, Ernst T, Woolley S, Ross BD. Alzheimer disease: depiction of increased cerebral myo-inositol with proton MR spectroscopy. Radiology. 1993;187(2):433-437.

Moats RA, Ernst T, Shonk TK, Ross BD. Abnormal cerebral metabolite concentrations in patients with probable Alzheimer disease. Magn Reson Med. 1994;32(1): 110-115.

Mochel F, Benaich S, Rabier D, Durr A. Validation of plasma branched chain amino acids as biomarkers in huntington disease. Arch Neurol 2011;68(2):265-267.

Mochel F, Charles P, Seguin F, Barritault J, Coussieu C, Perin L, Le Bouc Y, Gervais C, Carcelain G, Vassault A, Feingold J, Rabier D, Durr A. Early energy deficit in Huntington disease: identification of a plasma biomarker traceable during disease progression. PLoS One 2007 Jul 25;2(7):e647.

Morales LM, Este´vez J, Sua´rez H, Villalobos R, Chacı´n de Bonilla L, Bonilla E. Nutritional evaluation of Huntington disease patients. Am J Clin Nutr. 1989;50(1):145-150.

Morton AJ, Wood NI, Hastings MH, Hurelbrink C, Barker RA, Maywood ES. Disintegration of the sleep-wake cycle and circadian timing in Huntington's disease. J Neurosci. 2005;25(1):157-163.

Murri L, Iudice A, Muratorio A, Polleri A, Barreca T, Murialdo G. Spontaneous nocturnal plasma prolactin and growth hormone secretion in patients with

Parkinson's disease and Huntington's chorea. Eur Neurol 1980;19(3):198-206.

Nacewicz BM, Angelos L, Dalton KM, Fischer R, Anderle MJ, Alexander AL, Davidson RJ. Reliable non-invasive measurement of human neurochemistry using proton spectroscopy with an anatomically defined amygdala-specific voxel. Neuroimage. 2012;59(3):2548-2559.

Nance MA. Huntington disease: clinical, genetic, and social aspects. J Geriatr Psychiatry Neurol. 1998;11(2):61-70.

Nance MA, Sanders G. Characteristics of individuals with Huntington disease in long-term care. Mov Disord. 1996;11(5):542-548.

National Huntington Disease Research Roster. Statistics, May 1998. Indianapolis, IN: Indiana University; 1998.

Nelson SJ, Graves E, Pirzkall A, Li X, Antiniw Chan A, Vigneron DB, McKnight TR. In vivo molecular imaging for planning radiation therapy of gliomas: an application of 1H MRSI. J Magn Reson Imaging 2002; 16:464–476.

Nicoli F, Vion-Dury J, Maloteaux JM, Delwaide C, Confort-Gouny S, Sciaky M, Cozzone PJ. CSF and serum metabolic profile of patients with Huntington's chorea: a study by high resolution proton NMR spectroscopy and HPLC. Neurosci Lett

1993;154(1-2):47-51.

Nopoulos PC, Aylward EH, Ross CA, Mills JA, Langbehn DR, Johnson HJ, Magnotta VA, Pierson RK, Beglinger LJ, Nance MA, Barker RA, Paulsen JS; PREDICT-HD Investigators and Coordinators of the Huntington Study Group. Smaller intracranial volume in prodromal Huntington's disease: evidence for abnormal neurodevelopment. Brain 2011;134(Pt 1):137-142.

Nopoulos P, Magnotta VA, Mikos A, Paulson H, Andreasen NC, Paulsen JS. Morphology of the cerebral cortex in preclinical Huntington's disease. Am J Psychiatry 2007;164(9):1428-1434.

Ogg RJ, Kingsley PB, Taylor JS. WET, a T1- and B1-insensitive water suppression method for in vivo localized 1H NMR spectroscopy. J Magn Reson. 1994;B 104:1–10.

Ohara-Imaizumi M, Fukuda M, Niinobe M, Misonou H, Ikeda K, Murakami T, Kawasaki M, Mikoshiba K, Kumakura K. Distinct roles of C2A and C2B domains of synaptotagmin in the regulation of exocytosis in adrenal chromaffin cells. Proc. Natl Acad. Sci. USA 1997;94:287–291.

Ott D, Hennig J, Ernst T. Human brain tumors: assessment with in vivo proton MR spectroscopy. Radiology. 1993;186(3):745-752.

Panov AV, Gutekunst CA, Leavitt BR, Hayden MR, Burke JR, Strittmatter WJ, Greenamyre JT. Early mitochondrial calcium defects in Huntington's disease are a direct effect of polyglutamines. Nat Neurosci. 2002;5(8):731-736.

Parnetti L, Tarducci R, Presciutti O, Lowenthal DT, Pippi M, Palumbo B, Gobbi G, Pelliccioli GP, Senin U. Proton magnetic resonance spectroscopy can differentiate Alzheimer's disease from normal aging. Mech Ageing Dev. 1997;97(1):9-14.

Paulsen JS, Hayden M, Stout JC, Langbehn DR, Aylward E, Ross CA, Ross CA, Guttman M, Nance M, Kieburtz K, Oakes D, Shoulson I, Kayson E, Johnson S, Penziner E; Predict-HD Investigators of the Huntington Study Group. Preparing for Preventive Clinical Trials: The Predict-HD Study. Arch Neurol 2006;63(6):883-890.

Paulsen JS, Langbehn DR, Stout JC, Aylward E, Ross CA, Nance M, Guttman M, Johnson S, MacDonald M, Beglinger LJ, Duff K, Kayson E, Biglan K, Shoulson I, Oakes D, Hayden M; Predict-HD Investigators and Coordinators of the Huntington Study Group. Detection of Huntington's disease decades before diagnosis: the Predict-HD study. J Neurol Neurosurg Psychiatry. 2008;79(8):874-880.

Paulsen JS, Nopoulos PC, Aylward E, Ross CA, Johnson H, Magnotta VA, Juhl A, Pierson RK, Mills J, Langbehn D, Nance M; PREDICT-HD Investigators and Coordinators of the Huntington's Study Group (HSG). Striatal and white matter predictors of estimated diagnosis for Huntington disease. Brain Res Bull 2010;82(3-4):201-207.

Paulsen JS, Ready RE, Hamilton JM, Mega MS, Cummings JL. Neuropsychiatric aspects of Huntington's disease. J Neurol Neurosurg Psychiatry. 2001;71(3):310-314.

Paulsen JS, Zimbelman JL, Hinton SC, Langbehn DR, Leveroni CL, Benjamin ML, Reynolds NC, Rao SM. fMRI biomarker of early neuronal dysfunction in presymptomatic Huntington's Disease. AJNR Am J Neuroradiol 2004;25(10):1715-1721.

Pavese N, Andrews TC, Brooks DJ, Ho AK, Rosser AE, Barker RA, Robbins TW, Sahakian BJ, Dunnett SB, Piccini P. Progressive striatal and cortical dopamine receptor dysfunction in Huntington's disease: a PET study. Brain 2003 May;126(Pt 5):1127-1135.

Pearson JS, Petersen MC, Lazarte JA, Blodgett HE, Kley IB. An educational approach to the social problem of Huntington's chorea. Proc Staff Meet Mayo Clin. 1955;30(16):349-357.

Penney JB Jr, Vonsattel JP, MacDonald ME, Gusella JF, Myers RH. CAG repeat number governs the development rate of pathology in Huntington's disease. Ann Neurol 1997;41(5):689-692.

Penney JB Jr, Young AB, Shoulson I, Starosta-Rubenstein S, Snodgrass SR, Sanchez-Ramos J, Ramos-Arroyo M, Gomez F, Penchaszadeh G, Alvir J. Huntington's disease in Venezuela: 7 years of follow-up on symptomatic and asymptomatic individuals. Mov Disord. 1990;5(2):93-99.

Peschanski M, Bachoud-Le´vi AC, Hantraye P. Integrating fetal neural transplants into a therapeutic strategy: the example of Huntington's disease. Brain. 2004;127(pt 6):1219-1228.

Petersen A, Gil J, Maat-Schieman ML, Björkqvist M, Tanila H, Araújo IM, Smith R, Popovic N, Wierup N, Norlén P, Li JY, Roos RA, Sundler F, Mulder H, Brundin P. Orexin loss in Huntington's disease. Hum Mol Genet. 2005;14(1):39-47.

Petzold A, Jenkins R, Watt HC, Green AJ, Thompson EJ, Keir G, Fox NC, Rossor MN.

Cerebrospinal fluid S100B correlates with brain atrophy in Alzheimer's disease. Neurosci Lett. 2003;336(3):167-170.

Pietz J, Lutz T, Zwygart K, Hoffmann GF, Ebinger F, Boesch C, Kreis R. Phenylalanine can be detected in brain tissue of healthy subjects by 1H magnetic resonance spectroscopy. J Inherit Metab Dis. 2003; 26:683–692.

Pillon B, Dubois B, Ploska A, Agid Y. Severity and specificity of cognitive impairment in Alzheimer's, Huntington's, and Parkinson's diseases and progressive supranuclear palsy. Neurology. 1991;41(5):634-643.

Popovic V, Svetel M, Djurovic M, Petrovic S, Doknic M, Pekic S, Miljic D, Milic N, Glodic J, Dieguez C, Casanueva FF, Kostic V. Circulating and cerebrospinal fluid ghrelin and leptin: potential role in altered body weight in Huntington's disease. Eur J Endocrinol 2004;151(4):451-455.

Potenza RL, Tebano MT, Martire A, Domenici MR, Pepponi R, Armida M, Pèzzola A, Minghetti L, Popoli P. Adenosine A(2A) receptors modulate BDNF both in normal conditions and in experimental models of Huntington's disease. Purinergic Signal 2007;3(4):333-338.

Pouwels PJ, Frahm J. Differential distribution of NAA and NAAG in human brain as determined by quantitative localized proton MRS. NMR Biomed. 1997;10(2):73-78.

Pratley RE, Salbe AD, Ravussin E, Caviness JN. Higher sedentary energy expenditure in patients with Huntingtons disease. Ann Neurol. 2000;47(1):64-70.

Provencher SW. Automatic quantitation of localized in vivo 1H spectra with LCModel. NMR Biomed 2001; 14: 260–264.

Provencher SW. Estimation of metabolite concentrations from localized in vivo proton NMR spectra. Magn Reson Med 1993; 30: 672–679.

Quinn N, Schrag A. Huntington's disease and other choreas. J Neurol. 1998;245(11):709-716.

Ranen NG, Stine OC, Abbott MH, Sherr M, Codori AM, Franz ML, Chao NI, Chung AS, Pleasant N, Callahan C, et al. Anticipation and instability of IT-15 (CAG)n repeats in parent-offspring pairs with Huntington disease. Am J Hum Genet 1995;57(3):593-602.

Reed TE, Chandler JH, Hughes EM, Davidson RT. Huntington's chorea in Michigan:

I. Demography and genetics. Am J Hum Genet. 1958;10(2):201-225.

Reilmann R, Rolf LH, Lange HW. Huntington's disease: The neuroexcitotoxin aspartate is increased in platelets and decreased in plasma. J Neurol Sci 1994;127(1):48-53.

Reiner A, Albin RL, Anderson KD, D'Amato CJ, Penney JB, Young AB. Differential loss of striatal projection neurons in Huntington disease. Proc Natl Acad Sci U S A. 1988;85(15): 5733-5737.

Rejdak K, Petzold A, Kocki T, Kurzepa J, Grieb P, Turski WA, Stelmasiak Z. Astrocytic activation in relation to inflammatory markers during clinical exacerbation of relapsing-remitting multiple sclerosis. J Neural Transm. 2007;114(8):1011-1015.

Reynolds NC Jr, Prost RW, Mark LP. Heterogeneity in 1H-MRS profiles of presymptomatic and early manifest Huntington's disease. Brain Res 2005; 1031(1): 82-89.

Richfield EK, Maguire-Zeiss KA, Cox C, Gilmore J, Voorn P. Reduced expression of preproenkephalin in striatal neurons from Huntington's disease patients. Ann Neurol. 1995;37(3): 335-343.

Rijpkema M, Schuuring J, van der Meulen Y, van der Graaf M, Bernsen H, Boerman R, van der Kogel A, Heerschap A. Characterization of oligodendrogliomas using short echo time 1H MR spectroscopic imaging. NMR Biomed 2003; 16:12–18.

Rivera-Mancia S, Perez-Neri I, Rios C, Tristan-Lopez L, Rivera-Espinosa L, Montes S. The transition metals copper and iron in neurodegenerative diseases. Chem Biol Interact 2010 Jul 30;186(2):184-199.

Rosas HD, Hevelone ND, Zaleta AK, Greve DN, Salat DH, Fischl B. Regional cortical thinning in preclinical Huntington disease and its relationship to cognition. Neurology. 2005;65(5): 745-747.

Rosas HD, Koroshetz WJ, Jenkins BG, Chen YI, Hayden DL, Beal MF, Cudkowicz ME. Riluzole therapy in Huntington's disease (HD). Mov Disord. 1999;14(2):326-330.

Rosas HD, Salat DH, Lee SY, Zaleta AK, Pappu V, Fischl B, Greve D, Hevelone N, Hersch SM. Cerebral cortex and the clinical expression of Huntington's disease: complexity and heterogeneity. Brain 2008;131(Pt 4):1057-1068.

Rose SE, de Zubicaray GI, Wang D, Galloway GJ, Chalk JB, Eagle SC, Semple J, Doddrell DM. A 1H MRS study of probable Alzheimer's disease and normal aging: implications for longitudinal monitoring of dementia progression. Magn Reson Imaging 1999;17(2):291-299.

Ross BD, Bluml S, Cowan R, Danielsen E, Farrow N, Tan J. In vivo MR spectroscopy of human dementia. Neuroimaging Clin N. Am. 1998;8:809–822

Rothermundt M, Peters M, Prehn JH, Arolt V. S100B in brain damage and neurodegeneration. Microsc Res Tech 2003;60(6):614-632.

Rowe KC, Paulsen JS, Langbehn DR, Wang C, Mills J, Beglinger LJ, Smith MM, Epping EA, Fiedorowicz JG, Duff K, Ruggle A, Moser DJ; PREDICT-HD Investigators of the Huntington Study Group. Patterns of serotonergic antidepressant usage in prodromal Huntington disease. Psychiatry Res. 2012;196(2-3):309-314.

Ruggieri M, Serpino C, Ceci E, Sciruicchio V, Franco G, Pica C, Trojano M, Livrea P, de Tommaso M. Serum levels of N-acetylaspartate in Huntington's disease: preliminary results. Mov Disord. 2012;27(2):329-330.

Runne H, Kuhn A, Wild EJ, Pratyaksha W, Kristiansen M, Isaacs JD, Régulier E, Delorenzi M, Tabrizi SJ, Luthi-Carter R. Analysis of potential transcriptomic biomarkers for Huntington's disease in peripheral blood. Proceedings of the National Academy of Sciences 2007;104(36):14424-14429.

Ruocco HH, Lopes-Cendes I, Li LM, Cendes F. Evidence of thalamic dysfunction in Huntington disease by proton magnetic resonance spectroscopy. Mov Disord 2007; 22(14): 2052-2056.

Saft C, Schuttke A, Beste C, Andrich J, Heindel W, Pfleiderer B. fMRI reveals altered auditory processing in manifest and pre-manifest Huntington's disease. Neuropsychologia 2008;46(5):1279-1289.

Saleh N, Moutereau S, Durr A, Krystkowiak P, Azulay JP, Tranchant C, Broussolle E, Morin F, Bachoud-Lévi AC, Maison P. Neuroendocrine disturbances in Huntington's disease. PLoS One 2009;4(3):e4962.

Sanberg PR, Calderon SF, Giordano M, Tew JM, Norman AB. The quinolinic acid model of Huntington's disease: locomotor abnormalities. Exp Neurol. 1989;105(1):45-53.

Sánchez-Pernaute R, García-Segura JM, del Barrio Alba A, Viaño J, de Yébenes JG. Clinical correlation of striatal 1H MRS changes in Huntington's disease. Neurology 1999; 53(4): 806-812.

Sapp E, Ge P, Aizawa H, Bird E, Penney J, Young AB, Vonsattel JP, DiFiglia M. Evidence for a preferential loss of enkephalin immunoreactivity in the external globus pallidus in low grade Huntington's disease using high resolution image analysis. Neuroscience. 1995;64(2):397-404.

Sasakawa N, Sharif M, Hanley MR. Metabolism and biological activities of inositol pentakisphosphate and inositol hexakisphosphate. Biochem. Pharmacol 1995;50; 137–146.

Saudou F, Finkbeiner S, Devys D, Greenberg ME. Huntingtin acts in the nucleus to induce apoptosis but death does not correlate with the formation of intranuclear inclusions. Cell. 1998;95(1): 55-66.

Scahill RI, Hobbs NZ, Say MJ, Bechtel N, Henley SM, Hyare H, Langbehn DR, Jones R, Leavitt BR, Roos RA, Durr A, Johnson H, Lehéricy S, Craufurd D, Kennard C, Hicks SL, Stout JC, Reilmann R, Tabrizi SJ; TRACK-HD investigators. Clinical impairment in pre-manifest and early Huntington's disease is associated with regionally specific atrophy. Hum Brain Mapp. 2013;34(3):519-529.

Schwarcz R, Guidetti P, Sathyasaikumar KV, Muchowski PJ. Of mice, rats and men: Revisiting the quinolinic acid hypothesis of Huntington's disease. Prog Neurobiol 2009;In Press, Corrected Proof.

Schirmer T, Auer DP. On the reliability of quantitative clinical magnetic resonance spectroscopy of the human brain. NMR Biomed 2000; 13: 28–36.

Shemesh N, Sadan O, Melamed E, Offen D, Cohen Y. Longitudinal MRI and MRSI characterization of the quinolinic acid rat model for excitotoxicity: peculiar apparent diffusion coefficients and recovery of N-acetyl aspartate levels. NMR Biomed 2010; 23(2): 196-206.

Shetty HU, Holloway HW, Rapoport SI. Capillary gas chromatography combined with ion trap detection for quantitative profiling of polyols in cerebrospinal fluid and plasma. Anal. Biochem. 1995, 224:279-285

Shetty HU, Holloway HW, Schapiro MB. Cerebrospinal Fluid and plasma distribution of myo-inositol and other polyols in Alzheimer disease, Clinical Chemistry, 1996, 42:2 298-302.

Shetty HU, Schapiro MB, Holloway HW, Rapoport SI, Polyol Profiles in Down Syndrome. J.Clin.Invest. 1995. 95:542-546.

Shiwach R. Psychopathology in Huntington's disease patients. Acta Psychiatr Scand. 1994;90(4):241-246.

Shoulson I, Fahn S. Huntington disease: clinical care and evaluation. Neurology 1979; 29: 1–3.

Shonk TK, Moats RA, Gifford P, Michaelis T, Mandigo JC, Izumi J, Ross BD. Probable Alzheimer disease: diagnosis with proton MR spectroscopy. Radiology. 1995; 195(1):65-72.

Sigal SH, Yandrasitz JR, Berry GT. Kinetic evidence for compartmentalization of myo-inositol in hepatocytes. Metabolism 1993;42:395–401.

Slow EJ, van Raamsdonk J, Rogers D, Coleman SH, Graham RK, Deng Y, Oh R, Bissada N, Hossain SM, Yang YZ, Li XJ, Simpson EM, Gutekunst CA, Leavitt BR, Hayden MR. Selective striatal neuronal loss in a YAC128 mouse model of Huntington disease. Hum Mol Genet. 2003;12(13):1555-1567.

Squitieri F, Orobello S, Cannella M, Martino T, Romanelli P, Giovacchini G, Frati L, Mansi L, Ciarmiello A. Riluzole protects Huntington disease patients from brain glucose hypometabolism and grey matter volume loss and increases production of neurotrophins. Eur J Nucl Med Mol Imaging 2009;36(7):1113-1120.

Stack EC, Ferrante RJ. Huntington's disease: progress and potential in the field. Expert Opin Investig Drugs. 2007; 16(12):1933-1953.

Stahl SM, Thiemann S, Faull KF, Barchas JD, Berger PA. Neurochemistry of dopamine in Huntington's dementia and normal aging. Arch Gen Psychiatry 1986;43(2):161-164.

Stoy N, Mackay GM, Forrest CM, Christofides J, Egerton M, Stone TW, Darlington LG. Tryptophan metabolism and oxidative stress in patients with Huntington's disease. J Neurochem 2005;93(3):611-623.

Strange K. Regulation of solute and water balance and cell Volume in the central nervous system. J. Am. Soc. Nephrol. 1992;3:12–27.

Suhy J, Rooney WD, Goodkin DE, Capizzano AA, Soher BJ, Maudsley AA, Waubant E, Andersson PB, Weiner MW. 1H MRSI comparison of white matter and lesions in primary progressive and relapsing-remitting MS. Mult Scler. 2000; 6(3): 148–155.

Sun Z, Del Mar N, Meade C, Goldowitz D, Reiner A. Differential changes in striatal projection neurons in R6/2 transgenic mice for Huntington's disease. Neurobiol Dis. 2002;11(3):369-385.

Szulc A, Galinska B, Tarasow E, Dzienis W, Kubas B, Konarzewska B, Walecki J, Alathiaki AS, Czernikiewicz A. The effect of risperidone on metabolite measures in

the frontal lobe, temporal lobe, and thalamus in schizophrenic patients. A proton magnetic resonance spectroscopy (1H MRS). Pharmacopsychiatry. 2005; 38(5): 214-219.

Szulc A, Galińska B, Tarasów E, Kubas B, Dzienis W, Konarzewska B, Poplawska R, Tomczak AA, Czernikiewicz A, Walecki J. N-acetylaspartate (NAA) levels in selected areas of the brain in patients with chronic schizophrenia treated with typical and atypical neuroleptics: a proton magnetic resonance spectroscopy (1H MRS) study. Med Sci Monit. 2007; 13 Suppl 1: 17-22.

Tabrizi SJ, Blamire AM, Manners DN, Rajagopalan B, Styles P, Schapira AH, Warner TT.Creatine therapy for Huntington's disease: clinical and MRS findings in a 1-year pilot study. Neurology. 2003;61(1):141-142.

Tabrizi SJ, Blamire AM, Manners DN, Rajagopalan B, Styles P, Schapira AH, Warner TT. High-dose creatine therapy for Huntington disease: a 2-year clinical and MRS study. Neurology. 2005;64(9):1655-1656.

Tabrizi SJ, Langbehn DR, Leavitt BR, Roos RA, Durr A, Craufurd D, Kennard C, Hicks SL, Fox NC, Scahill RI, Borowsky B, Tobin AJ, Rosas HD, Johnson H, Reilmann R, Landwehrmeyer B, Stout JC; TRACK-HD investigators. Biological and clinical manifestations of Huntington's disease in the longitudinal TRACK-HD study: cross-sectional analysis of baseline data. Lancet Neurol. 2009;8(9):791-801.

Tabrizi SJ, Scahill RI, Durr A, Roos RA, Leavitt BR, Jones R, Landwehrmeyer GB, Fox NC, Johnson H, Hicks SL, Kennard C, Craufurd D, Frost C, Langbehn DR, Reilmann R, Stout JC; TRACK-HD Investigators. Biological and clinical changes in pre-manifest and early stage Huntington's disease in the TRACK-HD study: the 12-month longitudinal analysis. Lancet Neurol. 2011 Jan;10(1):31-42.

Tabrizi SJ, Reilmann R, Roos RA, Durr A, Leavitt B, Owen G, Jones R, Johnson H, Craufurd D, Hicks SL, Kennard C, Landwehrmeyer B, Stout JC, Borowsky B, Scahill RI, Frost C, Langbehn DR; TRACK-HD investigators. Potential endpoints for clinical trials in pre-manifest and early Huntington's disease in the TRACK-HD study: analysis of 24 month observational data. Lancet Neurol. 2012;11(1):42-53.

Tabrizi SJ, Scahill RI, Owen G, Durr A, Leavitt BR, Roos RA, Borowsky B, Landwehrmeyer B, Frost C, Johnson H, Craufurd D, Reilmann R, Stout JC, Langbehn DR; TRACK-HD Investigators. Predictors of phenotypic progression and disease onset in pre-manifest and early-stage Huntington's disease in the TRACK-HD study: analysis of 36-month observational data. Lancet Neurol. 2013;12(7):637-649.

Tallan HH. Studies on the distribution of N-acetyl-L-aspartate acid in brain. J Biol Chem 1956; 224: 41–45.

Taylor-Robinson SD, Weeks RA, Bryant DJ, Sargentoni J, Marcus CD, Harding AE, Brooks DJ. Proton magnetic resonance spectroscopy in Huntington's disease: evidence in favour of the glutamate excitotoxic theory. Mov Disord. 1996;11(2):167-173.

Taylor-Robinson SD, Weeks RA, Sargentoni J, Marcus CD, Bryant DJ, Harding AE, Brooks DJ. Evidence for glutamate excitotoxicity in Huntington's disease with proton magnetic resonance spectroscopy. Lancet. 1994;343(8906):1170.

Thieben MJ, Duggins AJ, Good CD, Gomes L, Mahant N, Richards F, McCusker E, Frackowiak RS. The distribution of structural neuropathology in pre-clinical Huntington's disease. Brain 2002;125(Pt 8):1815-1828.

Thiel T, Czisch M, Elbel GK, Hennig J. Phase coherent averaging in magnetic resonance spectroscopy using interleaved navigator scans: Compensation of motion artifacts and magnetic field instabilities. Mag Res Med 2002;47(6): 1077-1082.

Thiruvady DR, Georgiou-Karistianis N, Egan GF, Ray S, Sritharan A, Farrow M, Churchyard A, Chua P, Bradshaw JL, Brawn TL, Cunnington R. Functional

connectivity of the prefrontal cortex in Huntington's disease. J Neurol Neurosurg Psychiatry 2007;78(2):127-133.

Tkac I, Dubinsky JM, Keene CD, Gruetter R, Low WC. Neurochemical changes in Huntington R6/2 mouse striatum detected by in vivo 1H NMR spectroscopy. J Neurochem. 2007;100(5):1397-1406.

Trushina E, Dyer RB, Badger JD II, Ure D, Eide L, Tran DD, Vrieze BT, Legendre-Guillemin V, McPherson PS, Mandavilli BS, Van Houten B, Zeitlin S, McNiven M, Aebersold R, Hayden M, Parisi JE, Seeberg E, Dragatsis I, Doyle K, Bender A, Chacko C, McMurray CT. Mutant huntingtin impairs axonal trafficking in mammalian neurons *in vivo* and *in vitro*. Mol Cell Biol. 2004;24(18):8195-8209.

Tsang TM, Woodman B, McLoughlin GA, Griffin JL, Tabrizi SJ, Bates GP, Holmes E. Metabolic characterization of the R6/2 transgenic mouse model of Huntington's disease by high-resolution MAS 1H NMR spectroscopy. J Proteome Res. 2006;5(3):483-492.

Underwood BR, Broadhurst D, Dunn WB, et al. Huntington disease patients and transgenic mice have similar pro-catabolic serum metabolite profiles. Brain. 2006;129(4):877-886.

Unschuld PG, Edden RA, Carass A, Liu X, Shanahan M, Wang X, Oishi K, Brandt J,

Bassett SS, Redgrave GW, Margolis RL, van Zijl PC, Barker PB, Ross CA. Brain metabolite alterations and cognitive dysfunction in early Huntington's disease. Mov Disord. 2012;27(7):895-902.

Urenjak J, Williams SR, Gadian DG, Noble M. Proton nuclear magnetic resonance spectroscopy unambiguously identifies different neural cell types. J Neurosci. 1993;13(3):981-9.

van Dellen A, Welch J, Dixon RM, Cordery P, York D, Styles P, Blakemore C, Hannan AJ. N-Acetylaspartate and DARPP-32 levels decrease in the corpus striatum of Huntington's disease mice. Neuroreport 2000; 11(17): 3751-3757.

van den Bogaard SJA, Dumas EM, Teeuwisse WM, van Buchem MA, van der Grond J, Roos RAC. Exploratory 7T Magnetic Resonance Spectroscopy in Huntington's Disease. Clin Genet 2009; 76(S1): 55.

van der Graaf M. In vivo magnetic resonance spectroscopy: basic methodology and clinical applications. Eur Biophys J. 2010; 39(4):527-540.

van der Knaap, MS & Valk, J. Magnetic Resonance of Myelin Disorders (3rd edition), 2005, Springer, ISBN 13:9783540222866, Heidelberg, Germany.

Van Eldik LJ, Christie-Pope B, Bolin LM, Shooter EM, Whetsell WO Jr. Neurotrophic

activity of S-100 beta in cultures of dorsal root ganglia from embryonic chick and fetal rat. Brain Res. 1991;542(2):280-285.

van Oostrom JC, Maguire RP, Verschuuren-Bemelmans CC, Veenma-van der Duin L, Pruim J, Roos RA, Leenders KL. Striatal dopamine D2 receptors, metabolism, and volume in preclinical Huntington disease. Neurology 2005 Sep 27;65(6):941-943.

van Oostrom JC, Sijens PE, Roos RA, Leenders KL. 1H magnetic resonance spectroscopy in preclinical Huntington disease. Brain Res 2007; 1168: 67-71.

Van Raamsdonk JM, Murphy Z, Selva DM, Hamidizadeh R, Pearson J, Petersén A, Björkqvist M, Muir C, Mackenzie IR, Hammond GL, Vogl AW, Hayden MR, Leavitt BR. Testicular degeneration in Huntington disease. Neurobiol Dis. 2007;26(3): 512-520.

Varani K, Abbracchio MP, Cannella M, Cislaghi G, Giallonardo P, Mariotti C, Cattabriga E, Cattabeni F, Borea PA, Squitieri F, Cattaneo E. Aberrant A2A receptor function in peripheral blood cells in Huntington's disease. FASEB J 2003;17(14):2148-2150.

Varani K, Bachoud-Lévi A-, Mariotti C, Tarditi A, Abbracchio MP, Gasperi V, Borea PA, Dolbeau G, Gellera C, Solari A, Rosser A, Naji J, Handley O, Maccarrone M, Peschanski M, DiDonato S, Cattaneo E. Biological abnormalities of peripheral A2A receptors in a large representation of polyglutamine disorders and Huntington's disease stages. Neurobiol Dis 2007 7;27(1):36-43.

Venkatesh SK, Gupta RK, Pal L, Husain N, Husain M. Spectroscopic increase in choline signal is a nonspecific marker for differentiation of infective/inflammatory from neoplastic lesions of the brain. J Magn Reson Imaging. 2001;14(1):8-15.

Verbeke, G, Molenberghs G, Rizopoulos. Chapter 2; Random Effects Models for Longitudinal Data. Van Montfort et al. Longitudinal Research with Latent Variables. Springer-Verlag Berlin 2010.

Vonsattel JP. Huntington disease models and human neuropathology: similarities and differences. Acta Neuropathol. 2008;115(1):55-69.

Vonsattel JP, DiFiglia M. Huntington disease. J Neuropathol Exp Neurol. 1998;57(5):369-384.

Vonsattel JP, Myers RH, Stevens TJ, Ferrante RJ, Bird ED, Richardson EP Jr. Neuropathological classification of Huntington’s disease. J Neuropathol Exp Neurol. 1985;44(6):559-577.

Vymazal J, Klempir J, Jech R, Zidovska J, Syka M, Ruzicka E, Roth J. MR relaxometry in Huntington's disease: correlation between imaging, genetic and clinical parameters. J Neurol Sci 2007;263(1-2):20-25.

Walker FO. Huntington's disease. Semin Neurol. 2007;27(2): 143-150.

Warby SC, Montpetit A, Hayden AR, Carroll JB, Butland SL, Visscher H, Collins JA, Semaka A, Hudson TJ, Hayden MR. CAG expansion in the Huntington disease gene is associated with a specific and targetable predisposing haplogroup. Am J Hum Genet. 2009; 84(3):351-366.

Weir DW, Sturrock A, Leavitt BR. Development of biomarkers for Huntington's disease. Lancet Neurol. 2011 Jun;10(6):573-590.

Weiss A, Abramowski D, Bibel M, Bodner R, Chopra V, DiFiglia M, Fox J, Kegel K, Klein C, Grueninger S, Hersch S, Housman D, Régulier E, Rosas HD, Stefani M, Zeitlin S, Bilbe G, Paganetti P. Single-step detection of mutant huntingtin in animal and human tissues: a bioassay for Huntington's disease. Anal Biochem 2009;395(1):8-15.

Westbrook C. MRI at a Glance. Wiley-Blackwell; 2nd Edition. 2009.

Wexler NS, Lorimer J, Porter J, Gomez F, Moskowitz C, Shackell E, Marder K, Penchaszadeh G, Roberts SA, Gayán J, Brocklebank D, Cherny SS, Cardon LR, Gray J, Dlouhy SR, Wiktorski S, Hodes ME, Conneally PM, Penney JB, Gusella J, Cha JH, Irizarry M, Rosas D, Hersch S, Hollingsworth Z, MacDonald M, Young AB, Andresen JM, Housman DE, De Young MM, Bonilla E, Stillings T, Negrette A, Snodgrass SR, Martinez-Jaurrieta MD, Ramos-Arroyo MA, Bickham J, Ramos JS, Marshall F, Shoulson I, Rey GJ, Feigin A, Arnheim N, Acevedo-Cruz A, Acosta L, Alvir J, Fischbeck K, Thompson LM, Young A, Dure L, O'Brien CJ, Paulsen J, Brickman A, Krch D, Peery S, Hogarth P, Higgins DS Jr, Landwehrmeyer B; U.S.-Venezuela Collaborative Research Project. Venezuelan kindreds reveal that genetic and environmental factors modulate Huntington's disease age of onset. Proc Natl Acad Sci U S A. 2004;101(10): 3498-3503.

Wild EJ, Petzold A, Keir G, Tabrizi SJ. Plasma neurofilament heavy chain levels in Huntington's disease. Neurosci Lett 2007;417(3):231-233.

Wild E, Björkqvist M, Tabrizi SJ. Immune markers for Huntington's disease? Expert Review of Neurotherapeutics 2008;8(12):1779-1781.

Wolf RC, Sambataro F, Vasic N, Wolf ND, Thomann PA, Saft C, Landwehrmeyer GB, Orth M. Default-mode network changes in preclinical Huntington's disease. Exp Neurol. 2012;237(1):191-198.

Young AB, Penney JB, Starosta-Rubinstein S, Markel DS, Berent S, Giordani B, Ehrenkaufer R, Jewett D, Hichwa R. PET scan investigations of Huntington's disease: cerebral metabolic correlates of neurological features and functional decline. Ann Neurol 1986;20(3):296-303.

Zacharoff L, Tkac I, Song Q, Tang C, Bolan PJ, Mangia S, Henry PG, Li T, Dubinsky JM. Cortical metabolites as biomarkers in the R6/2 model of Huntington's disease. J Cereb Blood Flow Metab. 2012;32(3):502-514.

Zeron MM, Hansson O, Chen N, Wellington CL, Leavitt BR, Brundin P, Hayden MR, Raymond LA. Increased sensitivity to Nmethyl-d-aspartate receptor-mediated excitotoxicity in a mouse model of Huntington's disease. Neuron. 2002;33(6):849-860.

Zhang Y, Brady M, Smith S. Segmentation of brain MR images through a hidden Markov random field model and the expectation-maximization algorithm. IEEE Trans Med Imag,2001;20(1):45-57.

Zuccato C, Cattaneo E. Role of brain-derived neurotrophic factor in Huntington's

disease. Prog Neurobiol 2007;81(5-6):294-330.

Zucker B, Luthi-Carter R, Kama JA, Dunah AW, Stern EA, Fox JH, Standaert DG, Young AB, Augood SJ. Transcriptional dysregulation in striatal projection- and interneurons in a mouse model of Huntington's disease: neuronal selectivity and potential neuroprotective role of HAP1. Hum Mol Genet. 2005;14(2):179-189.